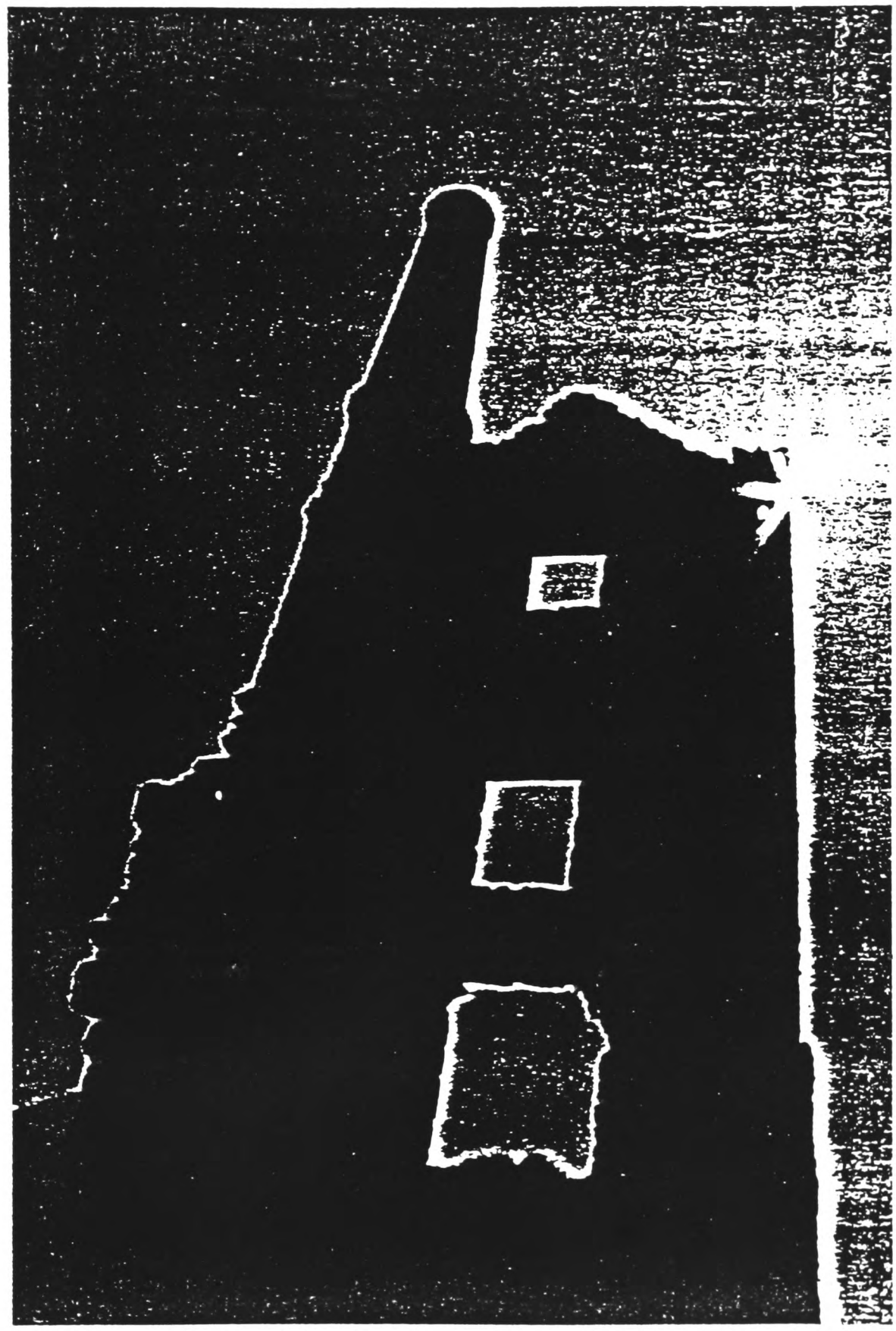


Long Carn Tin Mine, Cornwall

SYNTHESIS AND PROPERTIES OF BIDENTATE COORDINATION COMPOUNDS OF TIN

by

Tonie Louis Stolberg



A Thesis submitted in part fulfilment

of the requirements for the degree of

Doctor of Philosophy

at the

University of Oxford

Balliol College

Oxford

March 1991

To Mum, Dad, Bea, Pam and Michael

SYNTHESIS AND PROPERTIES OF BIDENTATE COORDINATION COMPOUNDS OF TIN

Tonie L. Stolberg
Balliol College

Doctor of Philosophy
Hilary Term 1991

ABSTRACT

This Thesis describes the synthesis, structural characterization and properties of some tin(II) and tin(IV) compounds containing bidentate ligands.

Chapter 1 describes the main spectroscopic techniques used in the identification of tin(II) compounds; infra-red, ^{119}Sn Mössbauer and n.m.r spectroscopy are outlined, and relevant examples given. A comprehensive listing is given of the main spectroscopic and structural properties of known tin(II) compounds.

Chapter 2 describes the general synthetic methods employed for the formation of tin(II)-oxygen heterocyclic compounds. A range of catecholate and related complexes of tin(II) were synthesized and the role of the substituent investigated with regard to their physical properties, especially their solubilities. The use of 4-nitrocatechol leads to a soluble product, $\{Sn[O\text{-}4\text{-}NO_2\text{-}C_6H_3O][OC_4H_8]\}_n$, which enabled it to be studied spectroscopically and its solid state structure to be determined. The nature of the bonding in $\{Sn[O\text{-}4\text{-}NO_2\text{-}C_6H_3O][OC_4H_8]\}_n$ was investigated using Extended Hückel molecular orbital calculations.

Chapter 3 describes the chemical reactivity of the novel, soluble, tin(II)-oxygen heterocycle $\{Sn[O\text{-}4\text{-}NO_2\text{-}C_6H_3O][OC_4H_8]\}_n$. Reaction with iodine gives $SnI_2[O\text{-}4\text{-}NO_2\text{-}C_6H_3O][OC_4H_8]_2$. Reaction with the Lewis base such as 1,2-diaminopropane gives $Sn[NH_2CH_2CH(Me)H_2N][O\text{-}4\text{-}NO_2\text{-}C_6H_3O][OC_4H_8]$, whilst benzyltriethylammonium chloride gives $\{[Et_3BzN][SnCl(O\text{-}4\text{-}NO_2\text{-}C_6H_3O)]\}_n$. The solid-state structure of the compound consists of polymeric chains of $[SnCl(O\text{-}4\text{-}NO_2\text{-}C_6H_3O)]^-$ and associated $[Et_3BzN]^+$ cations. Reaction with $BF_3.Et_2O$ gives the adduct $F_3B.Sn[O\text{-}4\text{-}NO_2\text{-}C_6H_3O][OC_4H_8]$. Reaction with $W(CO)_5$thf gives $\{(OC)_3W.Sn[(O\text{-}4\text{-}NO_2\text{-}C_6H_3O)(OC_4H_8)]\}_2$ in which the tungsten atoms are believed to be bound η^6 to the aromatic rings. Reaction with bis(triphenylphosphine)platinum-ethylene or tris(triphenylphosphine)platinum gives $\{PtH[PPh_3]_3\}\{[\mu_2\text{-}O][\mu_2\text{-}OH][Sn(O\text{-}4\text{-}NO_2\text{-}C_6H_3O)]_2\}$, the anion containing tin(II) and tin(IV) centres. Reaction with $RhCl[CNC_8H_9]_3$ gives $\{RhCl[CNC_8H_9]_3[\mu_2\text{-}Sn(O\text{-}4\text{-}NO_2\text{-}C_6H_3O)]\}_2$. Reaction with Ph_3PAuCl gives the cluster $Au_4(PPh_3)_4(\mu_2\text{-}SnCl_3)_2$, which is the first known example of a compound containing a $\mu_2\text{-}SnX_3$ fragment. In comparison with $SnCl_2$, $\{Sn[O\text{-}4\text{-}NO_2\text{-}C_6H_3O][OC_4H_8]\}_n$ only weakly inserts into the platinum-chlorine bonds of $PtCl_2$(dppe). Two molar equivalents of $SnCl_2$ reacts with $PtCl_2$(dppe) to give Pt(dppe)$(SnCl_3)_2$. Addition of a further equivalent of $SnCl_2$ in the presence of tetraethylammonium chloride gives $[Et_4N][Pt(dppe)(SnCl_3)_3]$. The platinum centre in this ion has a distorted trigonal bipyramidal geometry.

Chapter 4 describes the synthesis of a number of tin(II)-sulphur heterocycles. The reaction between $Sn[SC_6H_4S]$ and TMEDA gives a soluble adduct, $Sn[SC_6H_4S]$TMEDA. A number of tin(II)-nitogen heterocycles were also synthesized. Their intense colours and their instability towards air oxidation indicated that they were monomeric in the solid-state.

Chapter 5 outlines the basis for non-linear optical properties, especially their SHG effects. A wide range of tris(catecholato)tin(IV) compounds were synthesized and tested for SHG activity. A number were found to have a significant SHG effect, especially $[(O\text{-}4\text{-}NO_2\text{-}C_6H_3O)_3Sn][NHEt_3]_2$, which has an SHG effect 1.33 x urea.

The work described in this Thesis was carried out in the Inorganic Chemistry Laboratory of the University of Oxford from September 1987 to February 1991 under the supervision of Dr. D. Michael P. Mingos. All the work is my own, unless stated to the contrary, and it has not previously been submitted for a degree at this or any other University.

Signature removed from this digital version of the thesis

Tonie L. Stolberg

Acknowledgments

I am greatly indebted to Dr. Mike Mingos for his help, encouragement and support over the past four years.

Many thanks must also go to Profs. Malcolm Green and Frank Glockling for their advice and encouragement during my time in Oxford.

To Dr. Peter Smith and all his colleagues at ITRI, especially Dr. Paul Cusack, my sincere thanks for their help and the interest they have shown in this work, during my visits to ITRI and through their financial support of my CASE award.

I would also like to thank those who have helped me with the work described in this Thesis. Drs. Jonathon Machell, Harry Powell, Holm Fleischer and Roy Copley for their amazing strutcture-solving abilities. Curt Lamberth and Dr. Yan-Yong Yang for the SHG measurements. Dr. R. V. Parish for coming to the rescue with a timely Mössbauer spectrum.

To those poor souls who had the misfortune to endure bad jokes and impersonations must go special wishes. Particular thanks to Andy Burrows, Roy Copley, Curt Lamberth and Paul Lyne for proof reading. My thanks to Andy, Andrea, Philip, Carmella and Mild Bill, and all other past and present members of the Green group. Millie Delgado. The Mingos group who were so much fun to be with in and out of work; Osayi, J.J, Mike, Jane, Jenny, Dave, Don, Andy B, Chris, Curt, Javier, Tom, Zhenyang, Andy R., Holm, Sabine, Jonathon, Roy, Big Andy, Harry, and Gavin.

Last and by no means least, my love and thanks to The Gang who made Oxford such a wonderful place.

Abbreviations

ad	adeninate
aden	adenosinate
bipy	2,2'-bipyridyl
bipybim	2,2'-bipyridyl-4-benzimidazole
^{t}Bu	tertiary-butyl
"^{t}Bu-S_4"$^{2-}$	1,2-bis[3,5-di(*tert*-butyl)-2-mercaptophenylthio]ethane(2-)
"^{t}Bu-S_2"$^{2-}$	3,5-di(*tert*-butyl)benzene-1,2-dithiolate(2-)
Bz	benzyl
CNC_8H_9	2,6-dimethylphenyl isocyanide
COD	cyclo-octa-1,5-diene
Cp	cyclopentadienyl
CPMAS	cross-polarised magic-angle spinning
decomp.	decomposed
dist. tet	distorted tetrahedral
dmso	dimethylsulphoxide
dmf	dimethylformamide
dppe	1,2-bis(diphenylphosphino)ethane
dppm	bis(diphenylphosphino)methane
dppp	1,3-bis(diphenylphosphino)propane
edta	ethylenediaminetetraacetic acid
en	ethylenediamine
Et	ethyl
HOMO	highest occupied molecular orbital
Hput	purine-6-thiol
intra.	intramolecular
l.p.	lone pair
L1210	L1210 lymphocyteleukemia
LUMO	lowest unoccupied molecular orbital
Me	methyl
MeO	methoxy
M.pt.	melting point
NOBA	*m*-nitrobenzylalcohol
N. m. r.	nuclear magnetic resonance
P388	P388 lymphocyteleukemia
phen	1,10-phenanthroline
py	pyridine

Infrared data:

br	broad
m	medium
s	strong
sh	shoulder
vs	very strong
w	weak

N. m. r. data:

arom.	aromatic
d	doublet
dd	doublet of doublets
m	multiplet
p.p.m	parts per million
q	quartet
s	singlet
t	triplet
$\{^1H\}$	broad-band proton decoupled
^nJ	coupling constant over n bonds
δ	chemical shift

Contents

Chapter 1 Tin (II) Chemistry 1

1.1 Introduction 1
1.2 Spectroscopic Techniques 1
1.2.1 Infra-red Spectroscopy 2
1.2.2 Mössbauer Spectroscopy 4
1.2.2.1 Mössbauer Spectral Parameters 5
1.2.2.2 The Recoil-free Fraction 8
1.2.2.3 The Isomer Shift 8
1.2.2.4 The Quadrupole Splitting 10
1.2.3 Nuclear Magnetic Resonance 11
1.2.3.1 Solution Studies 11
1.2.3.2 Solid-state Studies 12
1.3 Structure and Bonding 13
1.3.1 Bonding in Tin(II) Compounds 13
1.3.2 The Structures of Tin(II) Compounds 14
1.3.2.1 Tin(II) Compounds With Group VII -Tin Bonds 16
1.3.2.2 Tin(II) Compounds With Group VI-Tin Bonds 18
1.3.2.3 Tin(II) Compounds With Group V-Tin Bonds 25
1.3.2.4 Tin(II) Compounds With Group IV-Tin Bonds 28
1.3.2.5 Tin(II) Compounds-Mixed Ligand Systems 31
1.3.2.6 Tin(II) Compounds-Miscellaneous 32
1.4 Summary 33
1.5 References 33

Chapter 2 Synthesis of Tin(II)-Oxygen Heterocyclic Compounds 44

2.1 Introduction 44
2.2 Synthesis of Tin(II)-Oxygen Heterocyclic Compounds 48
2.3 Preparation of Novel Tin(II)-Oxygen Heterocycles. 51
2.3.1 ^{119}Sn Mössbauer Analysis 53
2.3.2 The Cryoscopic Molecular Weight Determination of $\{Sn[O\text{-}4\text{-}NO_2\text{-}C_6H_3O][OC_4H_8]\}_n$ 55
2.3.3 ^{117}Sn Solution N.M.R Analysis 55
2.3.4 X-ray Crystallographic Analysis of $\{Sn[O\text{-}4\text{-}NO_2\text{-}C_6H_3O][OC_4H_8]\}_n$ 56
2.3.5 A Theoretical Analysis of the Bonding in $\{Sn[O\text{-}4\text{-}NO_2\text{-}C_6H_3O][OC_4H_8]\}_n$ 65

2.3.5.1 Nature of the Bonding in Dihydridotin(II) and Catecholatotin(II) 66
2.3.5.2 Introduction of Nitro Group 69
2.3.5.3 Effect of Coordinated Solvent 71
2.3.5.4 Effect of Polymerization 74
2.3.5.5 Summary of Bonding Analysis of $\{Sn[O\text{-}4\text{-}NO_2\text{-}C_6H_3O][OC_4H_8]\}_n$ 75
2.4 Summary 76
2.5 References 76

Chapter 3 Reactions of the Novel Tin(II) Compounds $\{Sn[O\text{-}4\text{-}NO_2\text{-}C_6H_3O][OC_4H_8]\}_n$ **and** $Sn[OC_6Cl_4O][OC_4H_8]$ 80

3.1 Introduction 80
3.2 Oxidative Addition 80
3.2.1 Synthesis of $SnI_2[O\text{-}4\text{-}NO_2\text{-}C_6H_3O][OC_4H_8]_2$ 81
3.3 Reactions With Lewis Bases 81
3.3.1 Halide Stabilized Tin(II) Compounds 82
3.3.1.1 Synthesis of $\{[Et_3BzN][SnCl(O\text{-}4\text{-}NO_2\text{-}C_6H_3O)]\}_n$ 82
3.3.1.2 X-ray Crystallographic Analysis of $\{[Et_3BzN][SnCl(O\text{-}4\text{-}NO_2\text{-}C_6H_3O)]\}_n$ 82
3.3.1.3 Synthesis of $[Et_3NH][SnCl(O\text{-}C_6Cl_4O)]$ 91
3.3.2 Tin(II) Compounds With Nitrogen-Donor Ligands 92
3.3.2.1 Synthesis of $Sn[NH_2CH_2CH(Me)H_2N][O\text{-}4\text{-}NO_2\text{-}C_6H_3O][OC_4H_8]$ 93
3.4 Reactions As A Lewis Base 93
3.4.1 Synthesis of $F_3B.Sn[O\text{-}4\text{-}NO_2\text{-}C_6H_3O][OC_4H_8]$ 93
3.4.2 Reactions With Unsaturated Transiton Metal Centres 95
3.4.2.1 The Reaction of $\{Sn[O\text{-}4\text{-}NO_2\text{-}C_6H_3O][OC_4H_8]\}_n$ *with* $W[CO]_5[OC_4H_8]$*. Synthesis of* $[Sn(O\text{-}4\text{-}NO_2\text{-}C_6H_3O)]_2[W(CO)_3]_2$ 95
3.4.2.2 Synthesis of $\{[Ph_3P]_3PtH\}\{[\mu_2\text{-}O][\mu_2\text{-}OH][Sn(O\text{-}4\text{-}NO_2\text{-}C_6H_3O)]_2\}$ 99
3.5 Reactions With Transition Metal Halide Complexes 107
3.5.1 The Reaction of $\{Sn[O\text{-}4\text{-}NO_2\text{-}C_6H_3O][OC_4H_8]\}_n$ with $[H_9C_8NC]_3RhCl$. Synthesis of $\{[H_9C_8NC]_3ClRh[\mu_2\text{-}Sn(O\text{-}4\text{-}NO_2\text{-}C_6H_3O)]\}_2$ 107
3.5.2 The Reaction of $\{Sn[O\text{-}4\text{-}NO_2\text{-}C_6H_3O][OC_4H_8]\}_n$ with Ph_3PAuCl. Synthesis of $[Au_4(PPh_3)_4(\mu_2\text{-}SnCl_3)_2]$ 110
3.5.3 X-ray Crystallographic Analysis of $[Au_4(PPh_3)_4(\mu_2\text{-}SnCl_3)_2]$ 110

3.5.4 Insertion Reactions of Tin(II) Chloride and $\{Sn[O\text{-}4\text{-}NO_2\text{-}C_6H_3O][OC_4H_8]\}_n$ into Platinum-Chlorine Bonds 120
3.5.4.1 Synthesis of $[Et_4N][Pt(dppe)(SnCl_3)_3]$ 121
3.5.4.2 X-ray Crystallographic Analysis of $[Et_4N][Pt(dppe)(SnCl_3)_3]$ 121
3.5.4.3 $^{31}P\text{-}\{^1H\}$ Solution N.m.r Studies 127
3.5.4.4 The Reactions of $\{Sn[O\text{-}4\text{-}NO_2\text{-}C_6H_3O][OC_4H_8]\}_n$ and $\{[Et_3BzN][SnCl(O\text{-}4\text{-}NO_2\text{-}C_6H_3O)]\}n$ with $PtCl_2(dppe)$ 134
3.6 Summary 139
3.7 References 140

Chapter 4 Preparation and Properties of Some Novel Tin(II)-Sulphur and Nitrogen Heterocycles 144

4.1 Introduction 144
4.1 Synthesis of Tin(II)-Sulphur Heterocyles 144
4.1.1 Synthesis of $Sn[SC_6H_4S]$ 145
4.1.2 Synthesis of $Sn[SC_6H_4S]$TMEDA. 147
4.2 Attempted Preparation of Bidentate Sulphur Ligands Containing Electron Withdrawing Substituents 147
4.2.1 Synthesis of 3-nitro-4,6-bis(phenylthio)chlorobenzene 149
4.2.2 X-ray Crystallographic Analysis of 3-nitro-4,6-bis(phenylthio)chlorobenzene 150
4.2.4 X-ray Crystallographic Analysis of $[4\text{-}NO_2\text{-}OC_6H_3O][S]P[C_6H_4\text{-}4\text{-}OMe]$ 155
4.3 Preparation of Tin(II)-Nitrogen Heterocyles 161
4.3.1 Synthesis of $Sn[NH\text{-}C_6H_4NH]$ 161
4.3.2 Synthesis of $Sn[NH\text{-}4\text{-}NO_2\text{-}C_6H_3NH]$ 162
4.5 Summary 162
4.6 References 163

Chapter 5 Preparation and Second Harmonic Generation Properties of Tris(catecholato)tin(IV) Compounds 165

5.1 Introduction 165
5.1.1 Second Harmonic Generation 165
5.2 Synthesis of Tris(catecholato)tin(IV) Compounds 168
5.3 Second Harmonic Generation Properties of Tris(catecholato)tin(IV) Compounds 172
5.3.1 X-ray Crystallographic Analysis of $[(O\text{-}4\text{-}NO_2\text{-}C_6H_3O)_3Sn][NHEt_3]_2$ 174

5.4 Summary 181
5.5 References 181

Chapter 6 Experimental Details 183

6.1 General 183
6.2 Experimental Details Relevant to Chapter 2 185
6.3 Experimental Details Relevant to Chapter 3 187
6.4 Experimental Details Relevant to Chapter 4 192
6.5 Experimental Details Relevant to Chapter 5 194
6.6 References 201

Appendices 202

Appendix 1 202
Appendix 2 205
Appendix 3 208
Appendix 4 211
Appendix 5 214
Appendix 7 218

Chapter 1

Tin (II) Chemistry

1.1 Introduction

Tin in its many guises has been of interest to man for thousands of years. Alloyed with copper in bronze, it was one of the first metals to be worked. Its resistance to corrosion, and malleability, gave bronze its durability and thus its usefulness. Today, tin has a wide variety of uses[1] and though the total world consumption of tin is relatively small, (200 000 tonnes per annum compared to 3 million tonnes of copper) it is an integral part of many industrial products and processes[2].

Both inorganic and organometallic tin compounds now constitute an increasingly large proportion of the tin metal consumed, and find use industrially in electroplating, fire retardants, pharmaceutical and agricultural products, plastics and ceramics[3], and many other areas[4,5].

With the upsurge in the use of tin commercially, there has also been a corresponding increase in the study of its compounds[6,7]. The majority of work published has been concerned with tin compounds in which the tin atom can be said formally to be in its quadrivalent state. However, the last twenty five years has seen a blossoming in tin (II) chemistry. As the number of compunds has grown, and their chemistry begun to be explored, their description as heavy carbene analogues[8] can be adjudged.

In this chapter, the techniques used to characterize low oxidation state tin compounds are described, and their reactivities and bonding are explained in terms of their electronic structures.

1.2 Spectroscopic Techniques

Tin compounds are very amenable to spectroscopic study. Tin compounds have distinctive infra-red and Raman spectra, two spin-1/2 n.m.r nuclei in reasonable abundance, a

Mössbauer active nucleide and a characteristic isotope distribution pattern in mass spectrometry, due to the presence of ten stable isotopes.

1.2.1 Infra-red Spectroscopy

The band positions for tin-element stretching vibrations are dominated by the mass effect and decrease to lower frequencies as the element mass increases (see Table 1.1).

Table 1.1 Typical ranges for ν(Sn-X) stretching frequencies[1].

Band	ν(Sn-X) cm^{-1}	Band	ν(Sn-X) cm^{-1}
Sn-H	1820-1920	Sn-P	280-370
Sn-C	440-540	Sn-S	310-380
Sn-Si	310-330	Sn-Se	210-270
Sn-Ge	180-260	Sn-F	340-590
Sn-Sn	100-200	Sn-Cl	320-380
Sn-N	440-610	Sn-Br	220-270
Sn-O	500-600	Sn-I	170-210
Sn-P	280-370	Sn-Metal	150-220

Other effects are also very important, e.g. the nature of the ligand, the substituent at tin or another element, and any involvement in further coordination.

The correct assignment of tin-halide frequencies in the far infra-red presents a difficult problem. This is due to the fact that the asymmetric and symmetric tin-chloride stretching vibrations (see Table 1.2) occur in the same region as that for transition metal-halides and other metal-ligand frequencies.

Table 1.2 Sn-X Frequencies in SnX_3^- and its Complexes (cm^{-1})[9] *

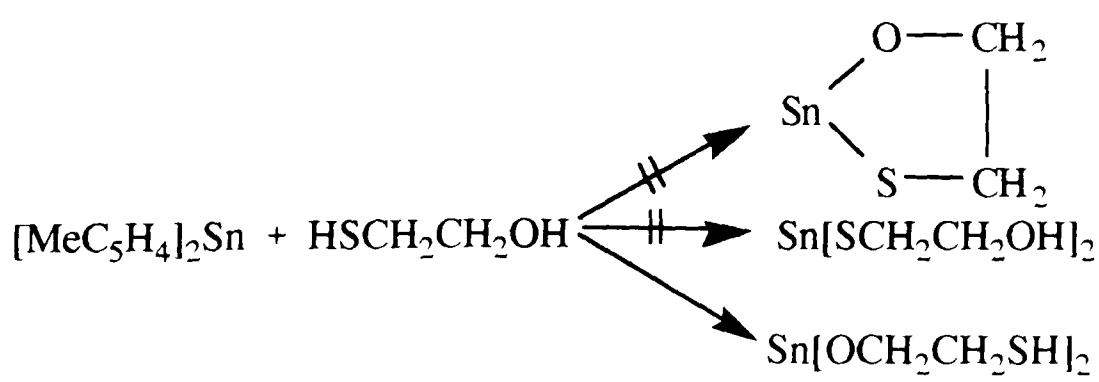
Tin species	ν (A_1)	E	δ (A)	E
$SnCl_3^-$	284-292	247-261	127-130	105-108
$SnBr_3^-$	201-292	176-186	86-97	65-73
M-$SnCl_3$	247-261	284-292	105-108	127-130
M-$SnBr_3$	210-235	240-270		95-112

* The labels A and E refer to the symmetry of the bond stretching (ν) and bond angle bending (δ) modes of the groups indicated in the first column.

In many cases, these bands are not well resolved. The tin-chloride bending and the tin-bromide stretches and bending modes occur at lower frequencies and are often easier to assign, but as they fall below 200 cm^{-1} they have seldom been investigated.

There have been detailed assignments of the vibrational data for only a few tin (II) compounds. The vibrational spectra for tin(II) thiolates, $Sn(SR)_2$, (R= Me, Ph, CH_2Ph) and $Sn[SCH_2CH_2S]$[10] were fully assigned. Their tin-sulphur symmetric and antisymmetric stretching frequencies occur between 299 and 375 cm^{-1}. This careful assignment allowed Harrison to identify the insoluble product of the reaction between 2-thioethanol and di(methyl-cyclopentadienyl)tin.

A very strong, very broad band was observed at 550 cm^{-1}, similar to that exhibited to the tin-oxygen vibration in tin(II) alkoxides, whilst no tin-sulphur stretching vibration was discerned.



In the gas state at high temperatures, tin dihalides such as $SnCl_2$, $SnBr_2$ and SnClBr are monomeric[11], and analysis of the emission spectra showed them to be non-linear[12]. This was confirmed by inspection of the Raman spectra of their vapours[13,14]. Electron diffraction studies established that the valence angle in these molecules is close to 95° [15]. Later, infra-red spectroscopic measurements of the molecules isolated in a low temperature matrix[16,17], suggested that the value of the valence angles in SnX_2 was between 90 and 94°. The vibrational assignments for monomeric tin dihalides are summarized in Table 1.3.

Table 1.3 Vibrational Assignments for Isolated Tin Dihalides (cm^{-1})[18]

Molecule		Argon matrix	N_2 matrix	Gas phase
$SnCl_2$	ν_1	353	341	352
	ν_2	124		120
	ν_3	332	320	
$SnBr_2$	ν_1	244	237	
	ν_2	82	84	
	ν_3	231	223	
SnClBr	$\nu_{(Sn-Cl)}$		328	
	$\nu_{(Sn-Br)}$		228	240
	$\nu_{(ClSnBr)}$			100

1.2.2 Mössbauer Spectroscopy[19-21,23]

When an energy source and an absorbing nucleus have nearly the same characteristic frequencies, the absorbing nucleus will begin to resonate; the absorbed energy allowing excited states to be populated; which then decay via fluorescence of γ-rays. If the energy source is sufficiently "well-tuned", that is the energy of a specific transition within the

nucleide, then the fluorescence observed will be atom specific and all others will be transparent.

In tin compounds, the criteria for the observation of a Mössbauer resonance is fulfilled by the 23.825 KeV (±1/2 ↔ ± 3/2) transition for ^{119}Sn (see Figure 1.1).

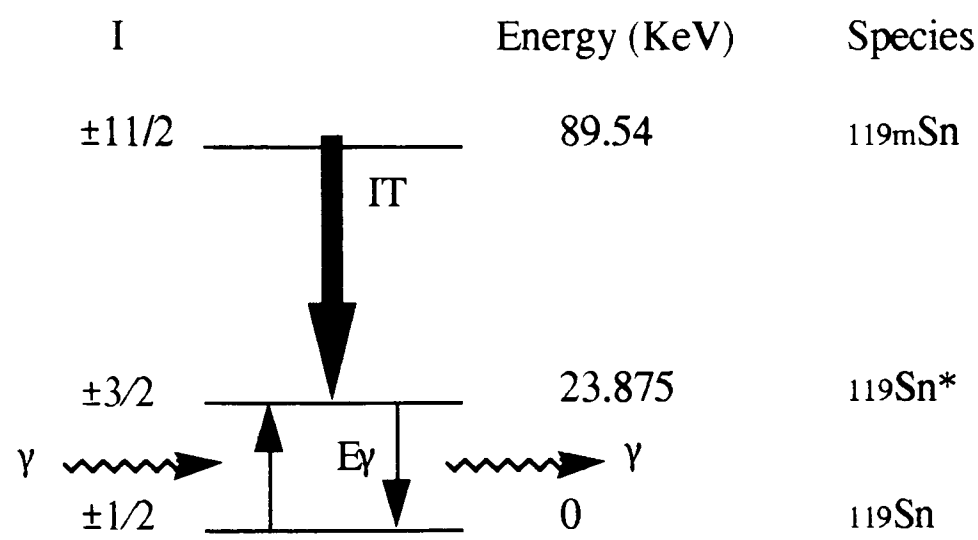


Figure 1.1 The Mössbauer Transitions Resulting From the Nuclear Decay of ^{119}Sn

For resonance of a specific energy level, the γ-source material must be sufficiently "finely-tuned". The half-life $t_{1/2}$ of the ±3/2 excited state has been measured as 17.75 ± 0.12 ns, thus the resonance line width, Γ is 0.325 ± 0.002 mm s^{-1} [22] (mm s^{-1} are the energy units of Doppler Shifts). Thus source materials must have similar linewidths; barium stannate has a line width of 0.33 mm s^{-1} and a half-life of ca. 250 days and is therefore the most frequently used γ-source.

1.2.2.1 Mössbauer Spectral Parameters

The parameters obtained from Mössbauer experiments are briefly summarized below, and are represented diagramatically in Figure 1.2.

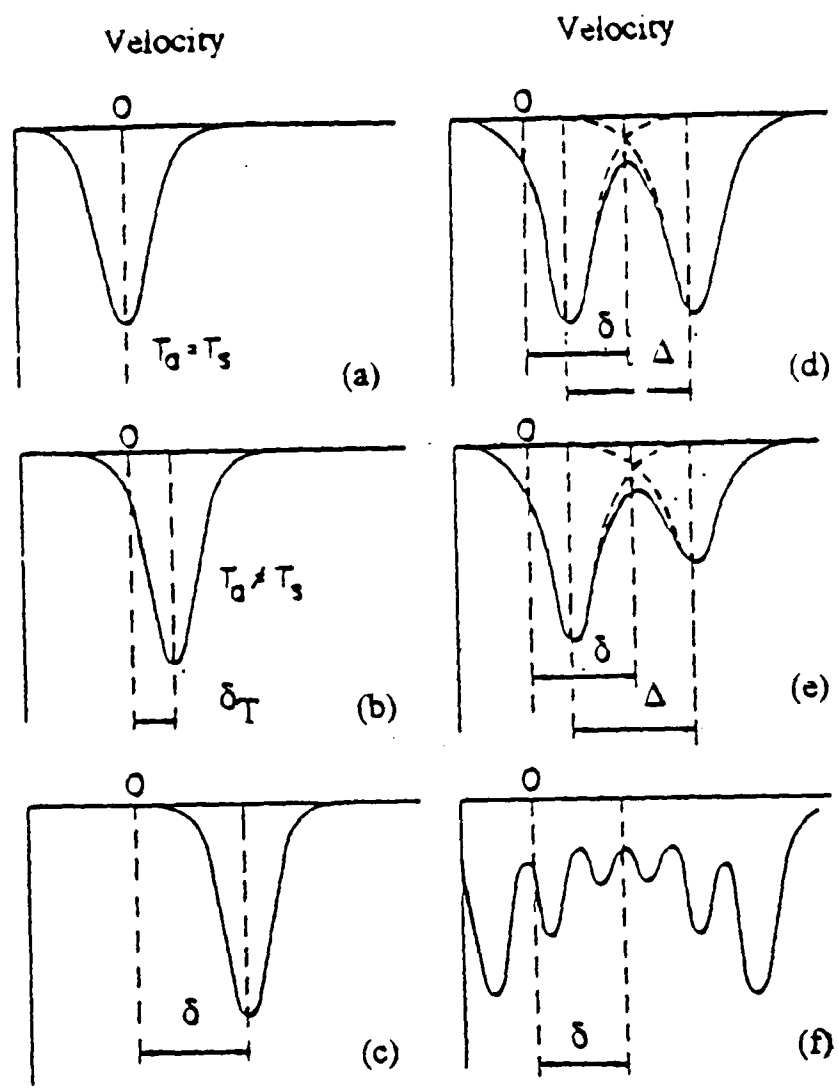


Figure 1.2 Mössbauer Spectral Parameters

(a) Source = Observer The peak area is proportional to the recoil-free fraction f, of the absorber where

$$f = \exp - \frac{4\pi^2 \langle r^2 \rangle}{\lambda^2} \qquad (1.1)$$

and $\langle r^2 \rangle$ is the mean square of the amplitude of atomic displacement, and λ the wavelength of the scattered radiation.

(b) Source = absorber, but the temperatures of the two solids are different. The temperature shift of the resonance lines, δ_T, is given by

$$\delta_T = \frac{E_R \overline{v^2}}{2c^2} \qquad (1.2)$$

where $\overline{v^2}$ is the mean square velocity of the atom in vibrational motion.

(c) Source ≠ absorber. The isomer shift of the resonance line, δ, is given by

$$\delta = \frac{4\pi}{5} Ze^2 R^2 \frac{\Delta R}{R}\left[|\psi(0)|^2_{abs} - |\psi(0)|^2_{source} \right] \qquad (1.3)$$

where the nucleus is of atomic number Z and radius R and ΔR is the change in nuclear radius in decay from the excited isomeric state, and $|\psi(0)|^2$ is the square of the total wave function of the atom defined.

(d) Source ≠ absorber, and the absorber nucleus experiences an electric field gradient, eq, the quadrupole splitting, Δ, is given by

$$\Delta = \frac{e^2 qQ}{4I(2I\text{-}1)}\left[3m^2 - I(I+) \right]\left[1+\eta^2 / 3 \right]^{1/2} \qquad (1.4)$$

where I is the nuclear spin quantum number, m the magnetic quantum number, eQ the quadrupole moment for the nucleus, and η the asymmetry parameter. For the tin nucleus this reduces to

$$\Delta = \frac{e^2 qQ}{2}\left[1+\eta^2 / 3 \right]^{1/2} \qquad (1.5)$$

(e) Source ≠ absorber, the absorber nucleus experiences an electric gradient and the anisotropy of the recoil-free fraction, *f*, these give rise to asymmetries in the line intensities of doublet spectra. This is known as the Goldanskii-Karyagin effect.

(f) Source ≠ absorber, and the absorber experiences a magnetic field, *H*. The resulting nuclear Zeeman splitting is given by

$$\Delta = -\frac{\mu H m}{I}$$

where μ is the magnetic moment of the nucleus and *m* and *I* are the magnetic and spin quantum numbers.

1.2.2.2 The Recoil-free Fraction

From equation (1.1) it is apparent that the recoil-free fraction of tin atoms is directly related to the micro-structure of the lattice. The more tightly it is bound the higher the value of *f*. Only a few tin (II) compounds have had their *f*-values calculated, since many of their Mössbauer readings were measured at low temperature, (usually 77K) and so lattice vibrations were reduced to a minimum. SnO has been studied at room temperature and yielded, $f_{295} = 0.35$[1]. The high value has been attributed to the tin atom being held in a polymeric lattice.

Since there appears to exist no simple functional dependence on *f* equal importance has to be given to the mass of near atoms, coordination of the tin atom and the strength of the inter and intramolecular bonding.

1.2.2.3 The Isomer Shift

The isomer shift, δ, is the displacement of the resonance from zero relative velocity as shown in Figure 1.2 , δ representing the mismatch between the nuclear energy levels of the

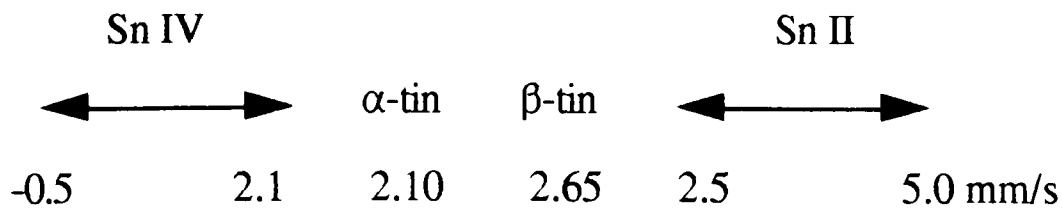
source and the absorber, and is expressed in Doppler shift energy units (mm s^{-1}). The precise value of the energy level separation in each compound is never measured directly. Relative motion of the source-absorber pair toward one another, (assigned a positive velocity) adds energy to the emitted γ−ray, bringing an absorber nucleus with a larger level spacing into resonance. Thus a series of absorbers may be compared with a single defined source. Most Mössbauer data are now measured relative to a barium stannate source, $Ba^{119m}SnO_3$ which is available commercially.

This mismatch of the two sets of nuclear levels arises from the interaction of the two nuclei with their electronic environments (see equation 1.3).

$$\delta = \frac{4\pi}{5} Ze^2 R^2 \frac{\Delta R}{R}\left[\left|\psi(0)\right|^2_{abs} - \left|\psi(0)\right|^2_{source} \right]$$

The effect is called the isomer shift because it depends on the difference in the nuclear radii of the ground and excited isomeric states, ΔR.

The atomic electronic term in the equation may be further simplified. Since, of the types of electrons in the atom, only the s-electrons density does not have a node at the nucleus i.e. $\left[\left|\psi_{ns}(0)\right|^2 \neq 0\right]$. The dominant effect is that of 5s occupation number and electron density at the nucleus[24,25]. If inner s-electron screening and the resultant shrinkage of the tin atom on loss of electrons from the valence shell are ignored, δ can be used to distinguish between the two different oxidation states of tin.



The more positive values associated with tin(II) compounds are due to the lone pair of electrons . This effect is enhanced or reduced by the electronegativity of the groups attached to tin[26].

1.2.2.4 The Quadrupole Splitting

The interaction of the nuclear quadrupole moment, Q with an electric field gradient, lifts the degeneracy of the ±3/2 state, giving rise to a doublet spectrum whose centroid is the isomer shift δ and separation the quadrupole splitting Δ.

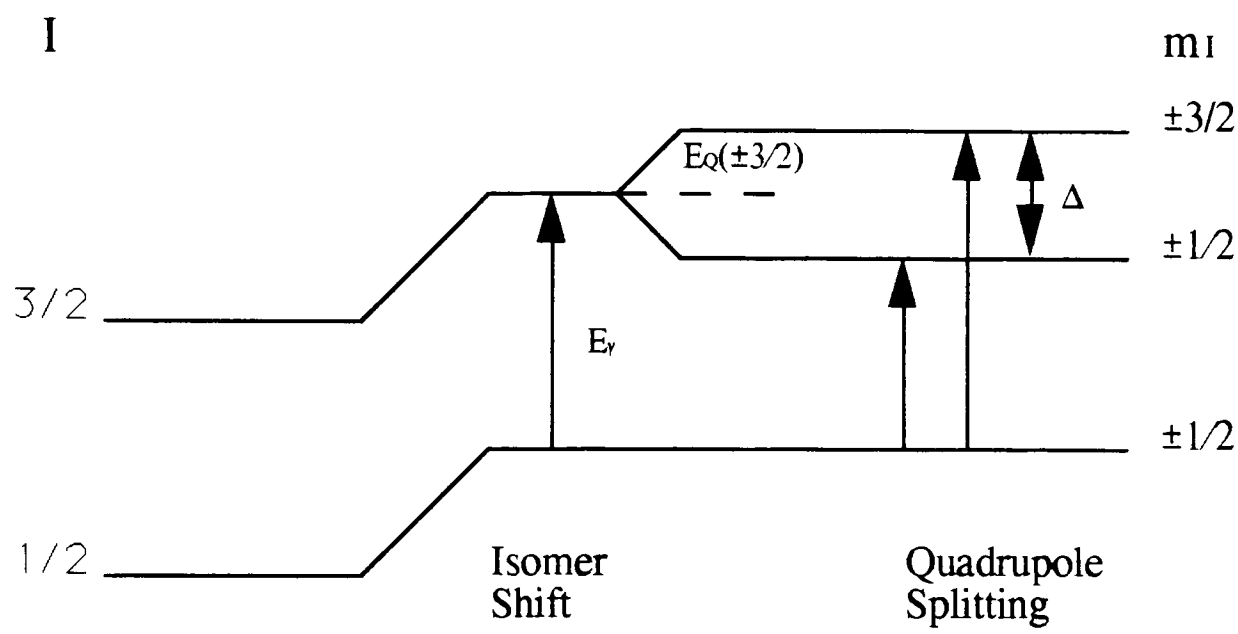


Figure 1.3 The Origin of the Quadrupole Splitting

The presence of a non-zero electric field gradient at the nucleus is determined primarily by the symmetry and the distribution of electrons about the nucleus, which in turn is determined by the symmetry of the bonding of the tin atom in question.

Cubic symmetry (tetrahedral or octahedral arrangement of identical attached atoms) will result in a zero-field gradient. In tin(II) compounds, the dominant contribution to the electric field gradient arises from the p_z electron density in the tin non-bonding orbital, whilst lattice contributions have been found to be of minor importance[27,28]. This is exemplified in the bonding of tin(II) to light atoms such as oxygen and fluorine, whose p-orbitals are sufficently stable to mix with the tin s-electrons. The resulting Sn-O and Sn-F bonds have extra p-character in the non-bonding lone pair, and the imbalance influences the magnitude of the quadrupole splitting.

1.2.3 Nuclear Magnetic Resonance[29,30]

Tin has three isotopes with $I = 1/2$ that are observable by n.m.r. spectroscopy (see Table 1.4).

Table 1.4 Magnetic Properties of Tin Isotopes with $I = 1/2$

($^1H = 100MHz$)

Isotope	Natural abundance, %	N.m.r. resonance frequency, MHz	Receptivity ($^{13}C = 1$)
^{115}Sn	0.35	32.864	0.715
^{117}Sn	7.61	35.626	19.9
^{119}Sn	8.58	37.272	25.6

Two of these, ^{117}Sn and ^{119}Sn have reasonable abundances and are important in the chemical applications of n.m.r. , whilst the other, ^{115}Sn, is of such low abundance that it can be ignored. Due to its slightly higher receptivity, (natural abundance times sensitivity) ^{119}Sn is the isotope more commonly studied.

1.2.3.1 Solution Studies

Tetramethyltin is the universally adopted standard for ^{119}Sn chemical shifts. Negative chemical shift values correspond to resonances upfield from tetramethyltin. ^{119}Sn chemical shifts are affected by a number of factors[30,31], namely, the electronegativity of the groups attached to tin, the coordination number, the concentration and the temperature.

Since the tin atom in tin(II) compounds is usually a centre of high electron density, due to the associated lone pair electrons, most ^{119}Sn chemical shifts are found at low field with respect to tetramethyltin; for example, Cp_2Sn, δ (^{119}Sn) -2199 ppm[32]. If the groups

bound to the tin atom are electron-withdrawing in nature, this generally leads to a decrease in tin shielding, the ^{119}Sn chemical shift moving upfield e.g for $SnCl_2$ δ (^{119}Sn) -236 ppm[33].

When the coordination number at tin is increased, this brings about a dramatic change in chemical shift to high field[34], e.g for $SnCl_2.2H_2O$ δ (^{119}Sn) +341 ppm[33]. The exact reason is unclear, but a major contribution appears to be a reduction in the effective nuclear charge, thus decreasing the paramagnetic contribution to the local tin chemical shift[35-37].

Temperature[38] and solution concentration[39] can also alter the coordination number around the tin atom, thus enabling dynamic processes to be explored. However, chemical shifts are most important in imparting information about the stoichiometry of the complex and chemical environment about the tin atom.

Tin-coupling constants have provided valuable information for tin(II) compounds, mostly their connectivity and relative geometry of the tin atom when bonded to transition metals. These compounds do not fall within the scope of this review, and are extensively covered elsewhere[40-42].

1.2.3.2 Solid-state Studies [43-46]

Like ^{119}Sn Mössbauer spectroscopy, data from solid-state n.m.r. can be correlated directly with structural data obtained by X-ray crystallography, and hence can provide comparisons between solid and solution phase spectra. An elegant example of a tin (II) compound examined in this way has been described by Zilm[47].

Bis[bis(trimethylsilyl)methyl]tin[48] was the first compound known to formally contain a tin-tin double bond. Zilm compared the ^{119}Sn chemical shift in the solid state, obtained using variable-temperature CPMAS with the solution spectra. The results were consistent with the tin-tin double bond being a very weak dative interaction, and in solution. The monomer and dimer exist in equilibrium, with the monomer only being observed at

high temperature, (375K, δ (^{119}Sn) 2315 ppm) whilst at lower temperatures the dimeric species was observed (165K, δ (^{119}Sn) 740 and 725 ppm).

1.3 Structure and Bonding

The use of only two of the valence shell electrons in bonding, means that bivalent tin compounds will contain a completely filled *s* orbital and empty *p* and *d* orbitals, which are available for use in bond formation.

The choice of model used to describe the bonding will vary from compound to compound, and also depends upon the difference in electronegativity between tin and the atoms bound to it. Sanderson[49] has found that the lone pair of electrons significantly reduced the tin electronegativity (Sn^{II} = 1.49, Sn^{IV} = 2.30) by nuclear screening. This results in the higher than otherwise expected bond polarity in tin(II) compounds and their relative stability towards oxidation.

1.3.1 Bonding in Tin(II) Compounds[50-52]

Both covalent[53] and electrostatic[54] arguments have been used to rationalize the bonding. The former, most successfully for high-symmetry structures, (of which there are few) where it is assumed that the non-bonding electrons are in stereochemically inactive orbitals. The latter, when tin is bound to light, electronegative atoms, such as oxygen and fluorine. The weaknesses in these models become apparent by their inability to move away from just describing the tin atom alone, to explain any three-dimensional solid-state effects[55]. These effects can be explained by looking at the bonding energetics of the tin atom, its associated ligands and then finally the overall lattice structure[51,56].

Hall[57] used this approach to analyse the nature of the tin lone pair in decaphenylstannocene, $[\eta^5\text{-}Ph_5C_5]_2Sn$ (Figure 1.4).

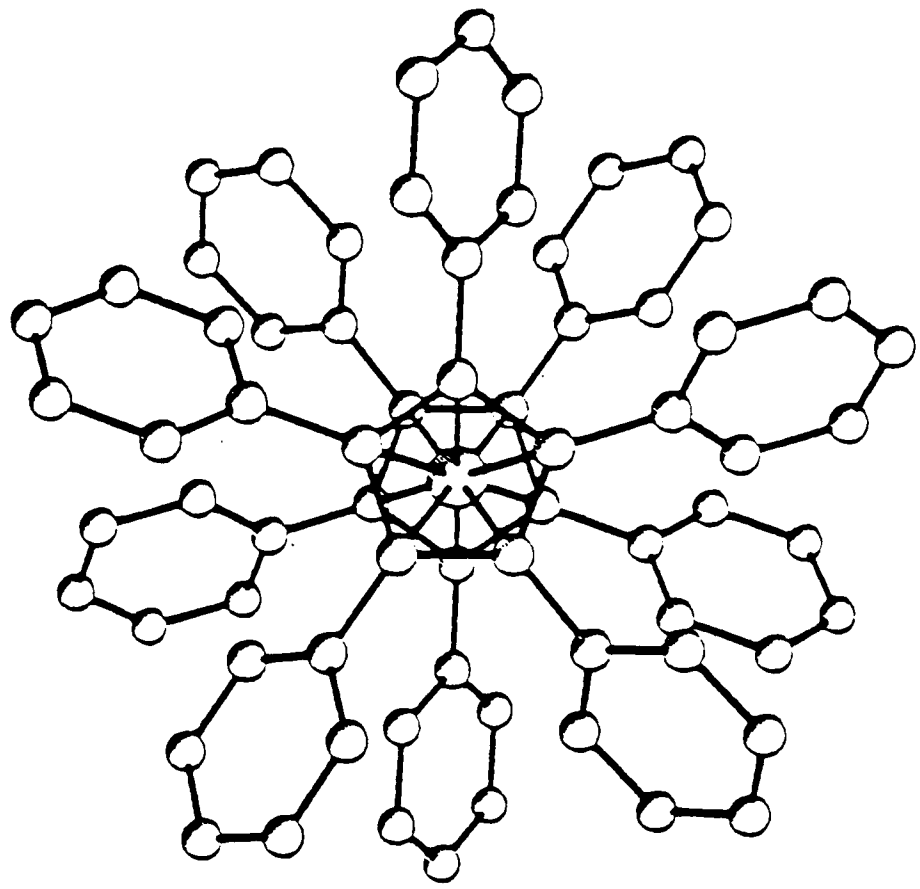


Figure 1.4 X-Ray Structure of Decaphenylstannocene

The X-ray crystal structures of most stannocene derivatives[58,59], reveal a severely bent Cp-Sn-Cp geometry with angles between 143 and 148 degrees. However, in decaphenylstannocene, the cyclopentadienyl rings are exactly parallel[60]. Molecular orbital calculations revealed that the lone pair resides primarily in the tin 5s orbital, and is not delocalized onto the ring system of the ligands as had previously been suggested[60].

1.3.2 The Structures of Tin(II) Compounds

Over the past twenty years tin(II) structures have been collated and their bonding reviewed[1,50,61-68]. The stereochemical effect of the lone pair of electrons at the tin atom greatly influences the observed coordination geometries (see Figure 1.5 and Table 1.5).

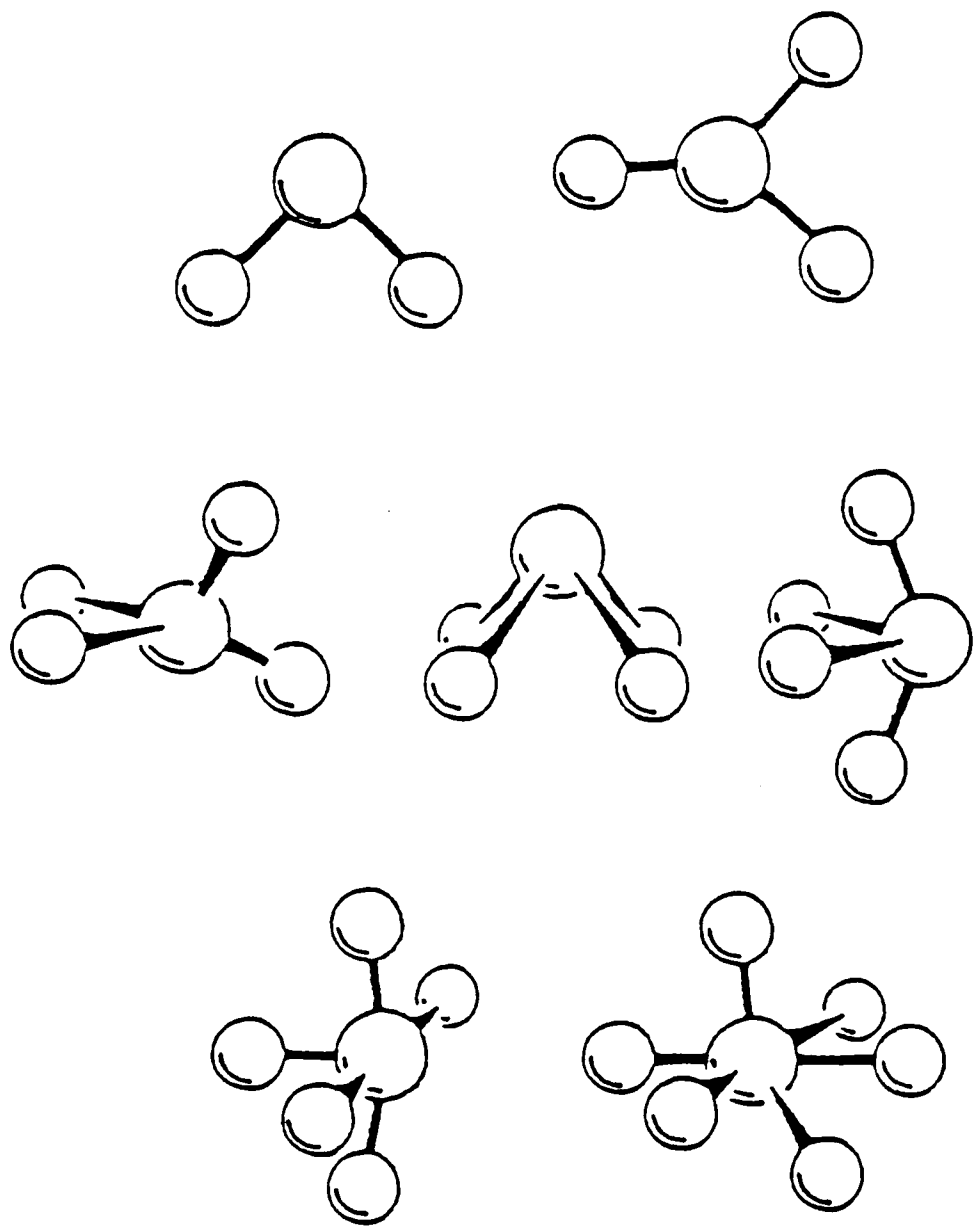


Figure 1.5 Coordination Polyhedra of Tin(II) Atom for Coordination Numbers 2-6

Table 1.5 Coordination Numbers (c.n.) of Important Tin(II)-Ligand Arrangements[64]

c.n.	Coordination Geometry	Angles Found (°)
2	ψ-trigonal planar	73-96
3	trigonal planar	Σ = 360
	trigonal pyramidal	75-95
4	tetragonal pyramidal	70-90
	ψ-trigonal bipyramidal	130-165; 80-95; 4×(60-80)
5	ψ-octahedral	—
6	distorted octahedral	—
9	facially-capped trigonal prism	—

The tin atom is most often found in compounds with coordination numbers higher than two. This is due to extra stability gained either by complexation, chelation or by bridging (see Chapter 2).

1.3.2.1 Tin(II) Compounds With Group VII - Tin Bonds

In this, and in the succeeding sections all important spectroscopic and structural data for known tin(II) compounds are tabulated. More detailed results are given in the individual references and reviews cited.

Table 1.6 Spectroscopic Properties of Tin(II)-X (X = F, Cl, Br, I) Compounds

Compound	^{119}Sn N.M.R. δ (ppm)	^{119}Sn Mössbauer δ	Δ (mms^{-1})	Comments	References
SnF_2	no signal observed	3.46	1.56	monoclinic	69, 70

α-Sn_2F_6		4.10	0.49	mixed valence	69
Sn_3F_8		3.82	1.27	mixed valence	69
Sn_7F_{16}		3.70	1.31	mixed valence	69
$Sn_{10}F_{34}$		4.51	0	mixed valence	69
$SnCl_2$	-236	4.12	0		70, 84-86
$SnCl_2.2H_2O$	+341				70
$SnCl_2$.bipy		3.53	1.16		87
$SnCl_2$.edta	-713				29
$SnBr_2$		3.72	0		96
SnI_2		3.70	0.2		86

Table 1.7 Structural Properties of Tin(II)-X (X = F, Cl, Br, I) Compounds

Compound	**c.n.**	**Sn-X (pm)**	**Sphere, Angle (^{0})**	**Solid Phase**	**References**
SnF_2(monoclinic)	3	211	trig. pyram., 83.3	$[Sn_4F_4]$ rings	71, 72
SnF_2(orthorhombic)	5	228	ψ-trig. bipyram.		73
NH_4SnF_3	3	208	trig. pyram., 82.4	intramol H-bonds	74
$KSnF_3.1/2H_2O$	4	215	ψ-trig. bipyram.	infinite SnF_3^- chains	75
$NaSn_2F_5$	4	223	ψ-trig. bipyram.		76
Sn_3F_8	3	214	trig. pyram., 74.9	octahedral Sn^{IV}	77
$Na_4Sn_3F_{10}$	4	217	ψ-trig. bipyram.		78
SnFCl	4	^{218}SnF ^{252}SnCl	ψ-trig. bipyram.		79
Sn_2F_3Cl	3	215	trig. pyram., 80.3	$[Sn_2F_3]^+$	80
Sn_3F_5Br	3	215	trig. pyram., 81.0	$[Sn_3F_5]^+$	81
$Sn_5F_6Br_4$	4	218	ψ-trig. bipyram.		82

Sn_2F_3I	4	230	ψ-trig. bipyram.	$[Sn_2F_3]^+$ layers	83
$[Sn_2O_2F_4]Sn_2$	4	239	ψ-trig. bipyram.	SnO_2Sn dimer	212
		$^{211}_{SnO}$		sharing O-O edge	
	4	247	dist. tet.		
$SnCl_2$	9	266	trig. prism.	cubic fluorite	15, 88, 89
				lattice	
$SnCl_2$.1,4-dioxan	4	258	ψ-trig. bipyram.	polymeric	92
$[Co(en)_3][SnCl_3]Cl_2$	3	253	trig. pyram., 87.0		93
$[Co(NH_3)_6][SnCl_4]Cl$	4	259	ψ-trig. bipyram.	$[SnCl_4]^{2-}$	94
$[NH_4]_2[SnCl_3]Cl.H_2O$	3	255	trig. pyram., 86.0	weak Cl bridging	94
$CsSnCl_3$	3	252	trig. pyram., 87.0	117^o phase	95
				change to cubic	
$SnBr_2$	9	290	trig. prism.		89
$NH_4SnBr_3.H_2O$	4	272	ψ-trig. bipyram.		94
$CsSnI_3$	6	281	octahedral	double chains.	95
				inactive Sn l.p.	

1.3.2.2 Tin(II) Compounds With Group VI-Tin Bonds

In Tables 1.8 and 1.9 are listed the main spectroscopic and structural data for all bivalent tin compounds containing tin-oxygen, sulphur, selenium and telurium bonds only.

Table 1.8 Spectroscopic Properties of Tin(II)-X (X = O, S, Se, Te)

Compound	**^{119}Sn δ (ppm)** * **^{117}Snδ (ppm)**	**^{119}Sn Mössbauer** δ Δ **(mms^{-1})**	**Comments**	**References**
SnO		2.91 0		86
$Sn[O_3SF]_2$		4.18 0.68		100

$Sn[O_3SCF_3]_2$		4.15 0.84		100
$Sn[edta].2H_2O$		3.38 1.57		101
$(18\text{-crown-6})Sn_2Cl_4$		3.30 0.99		102
		3.89 2.11		
$(18\text{-crown-6})Sn_2(SCN)_4$		3.26 1.70		102
		4.14 1.42		
$(18\text{-crown-6})Sn(ClO_4)_2$		4.45 0.88		102
$[Sn^{II}Sn^{IV}(O_2CC_6H_4NO_2)_4O.OC_4H_8]_2$		3.60 1.82	mixed valence	113
$Sn[OH]_2$		2.83 2.20	ν_{OH} 3390	120
$Sn[O_2CH]_2$		3.15 1.56		1
$Sn[OMe]_2$		3.02 1.97	ν_{SnO} 570	121-123
$Sn[OCOMe]_2$		3.31 1.77		123
$Sn[OCOEt]_2$		3.31 1.89		124
$Sn[OCOCHMe_2]_2$		3.33 1.84		124
$Sn[OCOCMe_3]_2$		3.35 1.88		124
$Sn[OCOCEt_3]_2$		3.34 1.86		124
$Sn[OCOCH_2Cl]_2$		3.20 1.66		124
		3.23 1.69		
$Sn[OCOCCl_3]_2$		3.48 1.64		124
		3.43 1.63		
$Sn[OCOCH_2F]_2$		3.10 1.76		124
		3.17 1.85		
$Sn[OCOCHF_2]_2$		3.25 1.75		124
		3.19 1.78		
$Sn[OCOCF_3]_2$		3.16 1.76		124
$Sn[OCOCHClCH_3]_2$		3.22 1.70		124
$Sn\{OCOCH_2CH_2Cl]_2$		3.27 1.83		124
$Sn[O_2CPh]_2$		3.17 1.69		125
$Sn[O_2CC_6H_4Me\text{-}o]_2$		3.26 1.86	monomer in soln	125

$Sn[O_2CC_6H_4Me\text{-}m]_2$		3.32 1.88	monomer in vap.	125
$Sn[O_2CC_6H_4Me\text{-}p]_2$		3.30 1.85		125
$Sn[O_2CC_6H_4Cl\text{-}o]_2$		3.40 1.91	monomer in vap.	125
$Sn[O_2CC_6H_4Cl\text{-}m]_2$		3.49 1.69		125
$Sn[O_2CC_6H_4Cl\text{-}p]_2$		3.35 1.85		125
$Sn[O_2CC_6H_4Br\text{-}o]_2$		3.38 1.93		125
$Sn[O_2CC_6H_4NH_2\text{-}o]_2$		3.26 1.79		125
$Sn[O_2CC_6H_4NH_2\text{-}p]_2$		3.37 1.89	monomer in vap.	125
$Sn[O_2CC_6H_4{}^tBu\text{-}p]_2$		3.26 2.03	monomer in soln.	125
$Sn[O_2CC_6H_4NO_2\text{-}p]_2$		3.38 2.03	monomer in vap.	125
$Sn[O_2CC_6F_5]_2$		3.46 1.75		125
$Sn[O_2CC_{10}H_7]_2$		3.35 2.00	monomer in soln	125
$Sn[O_3SC_6H_4Me\text{-}p]_2$		3.69 1.69		125
$Sn[O_3SC_6H_4NO_2\text{-}m]_2$		3.25 2.54		125
Sn[OMe]Cl		3.00 2.28		125
Sn[OMe]Br		3.21 1.91		125
Sn[OMe]I		3.66 1.46		125
$Sn[OC(Me)CHCC(OMe)O]_2$		3.07 2.17		126
$Sn[OC(Me)CHC(OEt)O]_2$		3.15 2.19	monomer in soln.	126
$Sn[OC(Me)CHC(O^tBu)O]_2$		3.03 2.14	monomer in soln	126
$Sn[OC(Me)CHC(Ph)O]_2$		3.07 1.98	monomer in soln and vap.	126
$Sn[OC(Ph)CHC(Ph)O]_2$		3.31 1.80	monomer in vap.	126
$Sn[OC_6H_7O]_2$		2.96 2.12		126
$Sn[OC_7H_5O]_2$		2.91 1.95	monomer in soln and vap.	126
$Sn[OC_6H_4Me\text{-}p]_2$		3.21 1.74		127
$Sn[OC_6H_4Cl\text{-}p]_2$		3.20 1.67		127
$Sn[OC_6H_4NH_2\text{-}p]_2$		3.15 1.69		127

$Sn[OC_6H_4NO_2\text{-}p]_2$		3.47 1.47		127
$Sn[OC_6H_4Me\text{-}m]_2$		3.10 1.81		127
$Sn[OC_6H_4NH_2\text{-}m]_2$		3.52 1.85		127
$Sn[OC_6H_4Me\text{-}o]_2$		3.13 1.97		127
$Sn[OC_6H_3Me_2\text{-}2, 6]_2$		3.13 1.97		127
$Sn[OC_6H_3Me_2\text{-}3, 5]_2$		3.14 1.69		127
$Sn[OC_5H_4N\text{-}3]_2$		2.96 1.93		127
$[Sn_2O(OSiMe_3)_2]_x$	-221		dimer in vap.	128
$Sn[O^tBu]_2$	-93.6		dimer in vap.	129, 130
$[^tBuOSnCl]_2$	271			131
$\{CpCo[P(OEt)_2O]_3\}_2Sn$		4.03 1.45		132
$[(15\text{-crown-}5)_2Sn][SnCl_3]_2$		4.59 0	"bare" Sn^{2+} ion	133, 134
[(18-crown-6)SnCl][$SnCl_3$]		3.89 2.11		141
$Sn[OC_6H_4O]$		2.95 1.76		141
$Sn[OC_6H_4\text{-}C_6H_4O]$		3.13 1.98		141
$Sn[O\text{-}3, Me\text{-}C_6H_4O]$		3.09 0.06		141
$Sn[OC_{10}H_6O]$		3.08 1.82		141
$Sn[OCOC_6H_4O]$		3.31 1.80		142
$Sn[OCOCH_2O]$		3.43 1.85		142
$Sn[OC_5NH_3O]$		2.89 2.13		142
Sn[OCOCOO]		3.47 1.59		142
$Sn[OCH(CO_2Et)CH(CO_2Et)O]$	-439 -552		trans-dimer in soln.	143
$\{Sn[O\text{-}4, NO_2\text{-}C_6H_3O]OC_4H_8\}_n$	-452*	3.49 2.33	monomer in soln.	this work
$\{[Et_3NBz][ClSn(O\text{-}4, NO_2\text{-}C_6H_3O)]\}_n$	-294			this work
$Sn[OC_6Cl_4O]$	-333*			this work
$[Et_3NBz][ClSn(OC_6Cl_4O)]$			ν_{SnCl} 389	this work
$Sn[O\text{-}3, MeO\text{-}C_6H_3O]$			ν_{SnO} 544	this work
$Sn[O\text{-}3,5, {}^tBu_2\text{-}C_6H_2O]$			ν_{SnO} 540	this work

Sn[aden]		3.01 2.03		this work
$Sn[ON=CHMe]_2$		3.22 2.26	ν_{NO} 935, 960	123
$Sn[ON=CMe_2]_2$		3.27 2.09	ν_{NO} 915	123
$Sn[ON=CHPh]_2$		3.23 2.14	ν_{NO} 931, 942	123
$Sn[ON=CMeCMeAc]_2$		3.23 1.95	ν_{NO} 905, 915	123
$Sn[ON=CPh_2]_2$		3.30 2.27	ν_{NO} 900, 942	123
$Sn[ON=CMeCMe=NO]_2$		3.30 1.90	ν_{NO} 900, 946	123
$Sn[ON=CHC_6H_4O]$		3.70 2.17	ν_{NO} 914	123
$Sn[ONPhBz]_2$		3.23 2.09	ν_{NO} 905, 920	123
$Sn[ONHBz]_2$		3.37 1.95	ν_{NO} 912	123
$Sn[OCOC_6H_4S]$		3.31 1.99		142
$Sn[OCH_2CH_2S]$		3.08 1.58		142
SnS		3.60 1.13		50
$Sn[SC_7H_{15}]_2$		3.06 1.69		145
$[Ph_4As][Sn(SPh)_3]$	146			146
$[Ph_4As][Sn(SePh)_3]$	208			146
$Sn[SPh]_2$		3.51 1.60		145
$Sn[S_2P(OMe)_2]_2$		3.67 0.97	ν_{SnS} 340	147
$Sn[S_2P(OEt)_2]_2$		3.60 1.11	ν_{SnS} 355	147
$Sn[S_2P(O^iPr)_2]_2$		3.49 1.12	ν_{SnS} 332	147
$Sn[S_2P(OPh)_2]_2$		3.78 1.06	ν_{SnS} 355	147
$Sn[S_2P(0Me)_2]_2$.bipy		3.61 1.07		147
$Sn[S_2P(OEt)_2]_2$.bipy		3.75 1.04		147
$Sn[S_2P(O^iPr)_2]_2$.bipy		3.66 1.03		147
$Sn\{S_2P(OPh)_2]_2$.bipy		3.75 1.15		147
[Sn("^{t}Bu-S_4")]	-274.5		monomer in vap.	148
[Sn("S_4")]	-274.5		monomer in vap.	148
[Sn("^{t}Bu-S_2")]	98.8		monomer in vap.	148

$Sn[SCH_2CH_2S]$		3.10 1.84	ν_{SnS} 299	145
$Sn[S\text{-}5, Me\text{-}C_6H_3S]$		3.36 1.63		142
$Sn[SC_6H_4S]$		3.44 1.72	ν_{SnS} 314	this work
$Sn[SC_6H_4S].tmeda$	-335.4*		ν_{SnS} 319	this work

Table 1.9 Structural Properties of Tin(II)-X (X = O, S, Se, Te) Compounds

Compound	**c.n.**	**Sn-X (pm)**	**Sphere, Angle (°)**	**Solid Phase**	**References**
SnO	4	221	sq. pyram., 75		103
$3SnO.H_2O$				$[Sn_6O_8]$ oligomers	104
α-$SnWO_4$	4	228	ψ-trig. bipyram.		105
β-$SnWO_4$	6	258	dist. octahedral, 82.4		106
$Sn[H_2PO_4]_2$	8	269			107
$SnHPO_4$	8	272		pairs of H-bonded $[HPO_4^{2-}]$	108,109
$SnSO_4$	12			O-Sn-O bridges	110
$SnFPO_3$	3	215	trig. pyram., 90	Sn lies between sheets of $[PO_3F]$	111
$Ca[Sn(O_2CMe)_3]_2$	3	214	trig.pyram., 83.5		112
$[Sn^{II}Sn^{IV}(O_2CC_6H_4NO_2)_4O.OC_4H_8]_2$	6	244	ψ-trig. bipyram.	$[Sn_2^{IV}O_2]$ ring	113, 119
$Sn_2[edta].2H_2O$	7	266	pent. bipyram.	equatorial l.p.	114
$Sn_3O[OH]_2SO_4$	3	213	trig. pyram., 89.6		115
			ψ-trig. bipyram.		
	4	227			
$Sn_3[PO_4]_2$	3	215	trig. pyram., 86.1		116
$Sn_6O_4[OMe]_4$	4	223	sq. pyram., 76	$[Sn_6O_8]$ oligomer	117

$Sn_{10}W_{16}O_{46}$	3	216	trig. pyram., 92		118
			ψ-trig. bipyram.		
	4	224			
$Sn_4^{II}Sn^{IV}O_2[O_2CCF_3]_8$	5	243	ψ-octahedral	mixed valence	119
$Sn[O^tBu]_3Tl$	3	202	ψ-trig. bipyram.	pentaatomic cage	135
$Sn[O^tBu]_3M[O^tBu]_3Sn$	3	206	trig. pyram., 86	two seco-	136
M = Li, Na				norcubane	
				$Sn_2M_2O_3$ units	
$Sn[O_2CH]_2$	4	227	ψ-trig. bipyram.	2-D sheet	137
$Li[\mu\text{-}OAr\text{-}2,6\text{-}Ph_2]_3Sn$	3	215	trig. pyram., 76		138
$\{CpCo[P(OEt)_2O]_3\}_2Sn$	2	253	bent sandwich,	dist. octahedral	132
			149		
$[(15\text{-crown-}5)_2Sn][SnCl_3]_2$	2	289	sandwich	inactive l.p.	134
$Sn[OCHPhCHCMeO]_2$	4	221	ψ-trig. bipyram.		139
$Sn[O^tBu]_2$	3	216	trig. pyram., 76		130
$[^tBuOSnCl]_2$	3	215	trig. pyram., 82	dimer	131
$Sn[OC_6H_2{}^tBu_2Me]_2$	2	200	bent, 80.8	monomer	140
$[(18\text{-crown-}6)SnCl][SnCl_3]$	7	274	ψ-hex. bipyram.	active l.p.	141
$Sn[OCH_2CH_2O]$	3	224	trig. pyram.	3-D network of	144
	4	225	tet. pyram.	linked dimers	
$[Sn(O\text{-}4\text{-}NO_2\text{-}C_6H_3O)OC_4H_8]_n$	5	216	ψ-octahedral	polymer	this work
$\{[Et_3NBz][ClSn(O\text{-}4\text{-}NO_2\text{-}C_6H_3O)]\}_n$	4	214	ψ-trig. bipyram.	polymer	this work
		257_{SnCl}			
α-SnS	3	266	trig. pyram., 90.7	connected zig-zag	149
				chains	
$BaSnS_2$	3	257	trig. pyram., 95	Sn in oct. sites	150
$Sn[SC_6H_2{}^tBu_3\text{-}2,4,6]_2$	2	244	bent, 85.4	monomer	151
$Sn[S_2COMe]_2$	4	271	ψ-trig. bipyram.		152

$Sn[S_2CNEt_2]_2$	4	269	ψ-trig. bipyram.		153, 154
$Sn[S_2P(OPh)_2]_2$	5	291	ψ-octahedral	η^6-Ph/Sn^{II} interaction	147
$[Sn(SC_6H_3{}^iPr_2]_3$	4	271	dist. tet.		151
	3	256	trig. pyram., 90		
$[Sn(SPh)_3]^-$	3	254	trig. pyram., 92		146
$Sn[S\,{}^tBu]_2$	4	278	ψ-trig. bipyram.	polymer	155
SnSe	3	280	trig. pyram., 89	as for SnS	149, 156
$[Sn(SePh)_3]^-$	3	265	trig. pyram., 92		146
SnTe	6	314	ψ-octahedral		149

1.3.2.3 Tin(II) Compounds With Group V-Tin Bonds

In Tables 1.10 and 1.11 the main spectroscopic and structural data for all tin(II) compounds containing tin-nitrogen and phosphorus bonds are listed.

Table 1.10 Spectroscopic Properties of Tin(II)-X (X = N, P)

Compound	^{119}**Sn N.M.R.** δ **(ppm)**	^{119}**Sn Mössbauer** δ	Δ **(mms^{-1})**	**Comments**	**References**
$Sn[NPhCOOC_6H_4\text{-}C_6H_4OCOPhN]$		3.46	1.56	ν_{CO} 1655	157
Sn[phthalocyanine]		2.92	1.24		158
Sn[imidazole]		3.09	2.02		123
Sn[1, 2, 4-triazole]		3.60	2.14		123
$Sn[N(SiMe_3)_2]_2$		2.88	3.52	ν_{SnN} 402	159,160
$\{Sn[N(SiMe_3)C_6H_4(SiMe_3)]OC_4H_8\}$		2.67	2.85	ν_{SnN} 358	159

$\{Sn[N(SiMe_3)C_{10}H_6(SiMe_3)]OC_4H_8\}$		2.70 3.31	ν_{SnN} 365	159
$Sn[NMe_2]_2$		2.80 3.17	dimer in soln.	161
			monomer in vap.	
			ν_{SnN} 440	
$Sn[NCMe_2C_3H_6CMe_2]$		2.92 2.76		162
$Sn[NC_2H_4]_2$		2.72 2.03		162
$Sn[NC_4H_8]_2$		2.58 2.18		162
$Sn[NC_5H_{10}]_2$		2.63 2.12		162
$Sn[NC_{12}H_8]_2[OC_4H_8]_2$		2.94 2.70		162
$Sn[NCOC_2H_4CO]_2$		3.11 2.08		162
$Sn[N(C_5NH_4)]_2$		2.83 2.40		162
$Sn[N^tBu]_2SiMe_2$	638.5			163
$Sn[(N^tBu)_2SiMe_2]_2$	-154			163
$Sn[N^tBu(SiMe_2)_2{}^tBuN]$	760			163
$Sn[N^tBuCH_2SiMe_2]_2$	21			163
$Sn[NH\text{-}C_6H_4NH]$			ν_{SnN} 543	this work
$Sn[NH\text{-}4\text{-}NO_2\text{-}C_6H_3NH]$			ν_{SnN} 549	this work
$Sn[(pz^*)_3BH]_2$	-935		monomer in vap.	164
$SnCl[(pz^*)_3BH]$	-1460		monomer in vap.	164
$Sn[P(CMe_3)_2]_2$	328		dimer in soln.	182
			$^1J_{SnP}$ = 1800,	
			1086 Hz	
$Sn[C(PMe_2)_3]_2$	-258		monomer in vap.	183
			$^1J_{SnP}$ = 776 Hz	
			(+30°C septet,	
			$^1J_{SnP}$ = 551 Hz	
$[Sn(P^tBu_2)_2]_2$	-1310		$^1J_{SnP}$ = 1360 Hz)	184

Table 1.11 Structural Properties of Tin(II)-X (X = N, P) Compounds

Compound	c.n.	Sn-X (pm)	Sphere, Angle (^{0})	Solid Phase	References
Sn[phthalocyanine]	4	225	sq. pyram., 76	monomer	158
$Sn[(pz^*)_3BH]_2$	5	244	ψ-octahedral	monomer	164
$SnCl[(pz^*)_3BH]$	4	234	ψ-trig. bipyram.	monomer	164
		^{263}SnCl			
$Sn[NCMe_2C_2H_6CMe_2]_2$	2	209	bent, 96		165
$Sn[N(SiMe_3)_2]$	2	209	bent, 105	in vap., 96	166
$[Sn(NMe_2)_2]_2$	3	216	trig. pyram., 93	dimer	167
$Sn[N^tBu]_2SiMe_2$	3	224	trig. pyram., 86.5	dimer	168
	2	209	bent, 73.2	monomer	
$Me_2Si[^tBuN]_2SnSnOSnCl_2$	3	231	trig. pyram., 73	cage bonded by O	169
		^{209}SnO		to $SnCl_2$	
	3	^{255}SnCl	trig. pyram., 92		
$Sn_3[N^tBu]_4H_2$	3	223	trig. pyram., 81.3	open seco-	170
				norcubane-like	
				cage	
$Sn_4[N^tBu]_3[OAlMe_3]$	3	222	trig. pyram., 80.5	distorted cube	171, 172
$Sn_2[NMe]_5[SiMe_2]_3$	3	221	trig. pyram., 80	ten atom ring	173
$Sn_4[NMe]_5SiMe_2$	3	222	trig. pyram., 85	edge bridged	173
				Sn_4N_3 cube	
$[SnN_2Me_2]_4$	3	223	trig. pyram., 79	distorted Sn_4N_4	174
				cube	
$[SnO(N^tBu)SiMe_2]_4$	3	209	trig. pyram., 82	tetramer, intra.	175
		^{215}SnO		SnO bonding	
$^tBuH_2NSn(N^tBu)_2SiMe_2$	3	227	trig. pyram., 82.3	intra. NH bonds	176

$Sn_4[N^tBu]_4$	3	221	trig. pyram., 81.4	distorted Sn_4N_4 cube	177
$Sn_3[N^tBu]_2[O^tBu]_2$	3 4	220 $^{223}_{SnO}$	trig. pyram., 83.4 dist. tet.	seven atom "closed" polycycle	178
$[Ph_3PCH_2^+ \ ^-Sn(N^tBu)_2SiMe_2$	3	191 $^{240}_{SnC}$	trig. pyram., 84	phosphor-ylide adduct	179
$Sn_2Si_2[N^tBu]_6$	3	225	trig. pyram., 90	two face-sharing $[Si_2N_2]$ seco-norcubane units	180
$SnClSnO^tBu[N^tBu]_2SiMe_2$	3	234 $^{252}_{SnCl}$ $^{215}_{SnO}$	trig. pyram., 92,8	two edge-sharing four atom rings	181
$Me_2Si[^tBuN]_2Sn_2Cl^+$	3	236 $^{263}_{SnCl}$	trig. pyram., 78	six atom "closed" polycycle	181
$Sn_3Cl_2[N^tBu]_2$	4	223 $^{308}_{SnCl}$	ψ-trig. bipyram.	1-D polymer	181
$Sn[C(PMe_2)_3]_2$	4	270	ψ-trig. bipyram.	monomer	183
$[Sn(P^tBu)_2]_2$	3	278	trig. pyram., 101	dimer	184

1.3.2.4 Tin(II) Compounds With Group IV-Tin Bonds

In Tables 1.12 and 1.13 the main spectroscopic and structural data for all tin(II) compounds containing tin-carbon, silicon and tin bonds are listed.

Table 1.12 Spectrocopic Properties of Tin(II)-X (X = C, Si, Sn) Compounds

Compound	^{119}Sn N.M.R. δ (ppm)	^{119}Sn Mössbauer δ	Δ (mms^{-1})	Comments	References
$Sn[CN]_2$		3.28	2.23		185
$Sn[CH(SiMe_3)_2]_2$	2315	2.16	2.31	monomer in soln.	47, 186
$Sn[C_6H_3(CF_3)_2\text{-}2,6]_2$		3.37	1.93	monomer in soln.	187
$Sn[C_6H_2{}^tBu_3\text{-}2,4,6]_2$		3.28	1.90		187
$SnCl[C_6H_4OMe\text{-}2]$		3.29	1.99		187
$SnCl[C_6H_4{}^iPr\text{-}2]$		3.19	2.12		187
$SnCl[C_6H_2{}^tBu_3\text{-}2,4,6]$		3.25	2.27		187
$SnCl[C_6H_3(NMe_2)_2\text{-}2,6]LiCl$		3.31	1.72		187
$SnCl[C_6H_2(NMe_2)_3\text{-}2,4,6]LiCl$		3.43	2.10		187
$Sn[C_5H_5]_2$	-2199	3.73	0.65		29, 188
$Sn[C_5H_4Me]_2$	-2171	3.83	0.78		189, 190
$Sn[C_5H_4{}^tBu]_2$		3.64	0		191
$Sn[C_5H_4SiMe_3]_2$		3.58	0		191
$Sn[C_5Me_5]_2$	-2129	3.53	0.99		192, 193
$Sn[C_5H_3{}^tBu_2]_2$	-2100				192, 194
$Sn[C_5Ph_5]_2$		3.74	0.58		195
$SnCl[C_5H_5]$		3.71	1.04		196
$SnBr[C_5H_5]$	-1630	3.40	0.99		197
$SnI[C_5H_5]$		3.90	0		197
$Sn[C_5H_5]AlCl_4$		3.73	0		196
$[(Me_5C_5)Sn][CF_3SO_3]$	-2180	3.81	0		192, 198
$[(^tBuC_5H_4)Sn][BF_4]$	-2247	3.67	0		192
$[(^tBu_2C_5H_3)Sn][BF_4]$	-2338				191

$Sn[SiMe_3]_2C_2B_4H_4$	-206	3.25 2.74		199
$SnSiMe_3[Me]C_2B_4H_4$	-171	3.28 2.74		199
$[C_6H_6]Sn[AlCl_4]_2.C_6H_6$		3.93 0		200

Table 1.13 Structural Properties of Tin(II)-X (X = C, Si, Sn) Compounds

Compound	**c.n.**	**Sn-X (pm)**	**Sphere, Angle (°)**	**Solid Phase**	**References**
$Sn[CH(SiMe_3)_2]_2$	3	228 $^{276}_{SnSn}$	trig. pyram., 114	centrosymm. dimer. monomer in vap. bent, 96°	201
$Sn[C_5H_5]_2$	2	$^{241}_{ring}$	bent sandwich, 148	vap. bent, 148°	202
$Sn[C_5H_4Me]_2$	2	$^{240}_{ring}$	bent sandwich	vapour	203
$Sn[C_5Me_5]_2$	2	$^{238}_{ring}$	bent sandwich	vapour	202
$Sn[C_5H_2(SiMe_3)_3]_2$	2	$^{238}_{ring}$	bent sandwich, 162		204
$Sn[C_5Ph_5]_2$	2	240	planar sandwich	S_{10} symmetry	205
$SnCl\{C_5H_5]$	2	$^{230}_{ring}$ $^{268}_{SnCl}$	bent	weakly bonded polymer	206
$[(Me_5C_5)Sn][CF_3SO_4]$		$^{216}_{ring}$	half sandwich	isolated ions	207
$Sn[SiMe_3]C_2B_4H_5$		249	dist. pent. bipyram.		208
$[C_{10}H_8\text{-}N_2]Sn[SiMe_3]_2C_2B_4H_4$		272 $^{250}_{SnN}$	dist. pent. bipyram.	weak SnC interaction	208
$[SnCHP(C_4H_4)(C_6H_5)]_2$	3	229	trig. pyram., 85	$[CH]_2Sn_2$ square	209
$[(C_6H_6)_2SnCl(AlCl_4)]_2$	6	$^{318}_{ring}$	ψ-octahedral	polymer Cl bridges Hexahapto-benzene	210
$\{[(C_6H_6)SnCl][GaCl_4]_2\}_x$	6	$^{327}_{ring}$	ψ-octahedral	polymeric layer lattice	211

$[(Me_3Si)_3Si]_2Sn[\mu\text{-}Cl]Li[OC_4H_8]_3$	3	267 $^{275}_{SnCl}$	trig. pyram., 97	Cl-bridge	212, 213

1.3.2.5 Tin(II) Compounds-Mixed Ligand Systems

In Tables 1.14 and 1.15 the main spectroscopic and structural parameters for tin(II) compounds in which the tin atom is bound to atoms from different Periodic Groups are listed.

Table 1.14 Spectrosopic Properties of Tin(II)-Mixed Ligand Compounds

Compound	**^{119}Sn N.M.R.**	**^{119}Sn Mössbauer**		**Comments**	**References**
	δ (ppm)	**δ**	**Δ (mms^{-1})**		
$Sn[(SCH_2CH_2)_2{}^tBuN]$	140.1	3.09	2.11	monomer in soln.	214
$Sn[(SCH_2CH_2)_2MeN]$	91.2	3.20	1.70	monomer in soln.	214
$Sn[(SCH_2CH_2)_2O]$	82.2	3.22	1.84	monomer in soln.	214
$Sn[(SCH_2CH_2)_2S]$	65.8	3.21	1.90	monomer in soln.	214
$Sn[(N^tBuCH_2CH_2)_2S]$	77.6	2.76	2.45		215
$Sn[(N^iPrCH_2CH_2)_2S]$	79.2				215
$Sn[(SCH_2CH_2)_2PhP]$		3.01	1.69		216
$Sn[(NMeCH_2CH_2)_2MeN]$		2.68	1.98	dimer in soln	216
$Sn[(OCH_2CH_2)_2MeN]$	-303				216
$Sn[(OCH_2CH_2)_2{}^tBu]$		2.87	1.73	dimer in soln.	216
$Sn[OCH_2CH_2Me_2N]_2$	104.2				216
$Sn[SCH_2CH_2Me_2N]_2$	-307				216
$SnCl[N(CHCO^tBu)]_2$	-378.1				219
$SnCl[C_6H_3(CH_2NMe_2)_2\text{-}2,6]$	-208.7				220

Table 1.15 Structural Properties of Tin(II)-Mixed Ligand Compounds

Compound	c.n.	Sn-X (pm)	Sphere, Angle (°)	Solid Phase	References
$Sn[(SCH_2CH_2)_2{}^tBuN]$	4	$^{264}_{SnN}$ $^{284}_{SnS}$	ψ-trig. bipyram.	two dimeric forms via intramol. SnS bonds	224
	4	$^{275}_{SnN}$ $^{271}_{SnS}$			
$Sn[(SCH_2CH_2)_2PhP]$	4	$^{261}_{SnP}$ $^{331}_{SnS}$	ψ-trig. bipyram.	parallel infinite spiral chains	217
$Sn[C_6H_4CH_2NMe_2\text{-}o]_2$	4	$^{259}_{SnN}$ $^{222}_{SnC}$	ψ-trig. bipyram.		218
$SnCl[NCHCO^tBu_2]_2$	4	$^{250}_{SnCl}$ $^{235}_{SnO}$ $^{229}_{SnN}$	ψ-trig. bipyram.	weak intermol. SnCl interaction. zig-zag chains	219
$SnCl[C_6H_5(CH_2NMe_2\text{-}2,6)]$	4	$^{256}_{SnN}$ $^{216}_{SnC}$ $^{249}_{SnCl}$	ψ-trig. bipyram.		220

1.3.2.6 Tin(II) Compounds-Miscellaneous

The structural properties of those tin(II) compounds which do not fall into the catagories outlined above are listed in Table 1.16.

Table 1.16 Structural Properties of Tin(II) (Miscellaneous) Compounds

Compound	c.n.	Sn-X (pm)	Sphere, Angle (^{0})	Solid Phase	References
$[Sn^{II}(NO_3)_2Ph_3Sn^{IV}]_2$	5	$^{258}_{SnO}$ $^{248}_{SnSn}$	dist. tet.	mixed valence bidentate nitrates	221
$[Sn^{II}(\mu\text{-}NO_3)(AsPh_3)Ph_3Sn^{IV}]$	5	$^{261}_{SnO}$ $^{252}_{SnSn(As)}$	dist. tet.	mixed valence nitrate bridging Sn^{II}	222
$Sn[Ta_2Cl_4]_2$	8	$^{292}_{SnCl}$	sq. antiprism	space gp. $P6_{22}$ S_8 coordination	223

1.4 Summary

Tin(II) chemistry has expanded dramatically in the last twenty five years. Most work has concentrated upon their synthesis and chemical similarity to carbenes. The main spectroscopic techniques used in the identification of tin(II) compounds; infra-red, ^{119}Sn Mössbauer and n.m.r spectroscopy are outlined, and relevant examples given. A comprehensive listing is given of the main spectroscopic and structural properties of known tin(II) compounds.

1.5 References

1. *Chemistry of Tin*, ed. P. G. Harrison, Blackie, London 1989.
2. B. T. K. Barry and C. J. Thwaites, *Tin and its Alloys and Compounds*, Ellis Harwood, Chichester 1983.
3. *Tin Chemicals for Success, Publication No. 681*, International Tin Research Institute, Uxbridge.

4. M. Pereyre, J-P. Quintard and A. Rahm, *Tin in Organic Synthesis*, Butterworth, London 1987.

5. K. D. Boss, J. D. Donaldson, D. V. Sanghani and P. J. Smith, *Tin(II) Compounds as Reducing Agents in Organic and Inorganic Chemistry, Publication No. 642*, International Tin Research Institute, Uxbridge.

6. W. P. Neumann, *Die Organishe Chemie des Zinns*, F. Enke, Stuttgart 1967.

7. A. G. Davies and P. J. Smith, *Comprehensive Organometallic Chemistry, Chapter 11*, ed. G. Wilkinson, Pergamon 1982.

8. M. N. Manakov and O. M. Nefedov, *Angew. Chem. Int. Ed. Engl.*, 1966, **5**, 1021.

9. M. S. Holt, J. H. Nelson and W. L. Wilson, *Chem. Rev.*, 1989, **89**, 11.

10. P. G. Harrison and S. R. Stobart, *Inorg. Chim. Acta,* 1973, 7, 306.

11. H. Bilitz and V. Meyer, *Z. Phys. Chem.*, 1988, **2**, 184.

12. R. K. Asundi, M. Karim and R. Samuel, *Proc. Phys. Soc.*, 1938, **50**, 581.

13. R. O. Perry, *J. Chem. Soc., Chem. Commun.*, 1969, 886.

14. I. R. Beattie and R. O. Perry, *J. Chem. Soc. (A),* 1970, 2429.

15. M. W. Lister and L. E. Sutton, *Trans. Faraday Soc.*, 1941, **37**, 406.

16. L. Andrews and D. L. Frederick, *J. Am. Chem. Soc.*, 1970, **92**, 775.

17. J. W. Hastie, R. H. Hauge and S. L. Margrave, *J. Mol. Spec.*, 1973, **45**, 420.

18. G. A. Ozin and A. Vander Voet, *J. Chem. Phys.*,1972, **56**, 4769.

19. N. N. Greenwood and T. C. Gibb, *Mössbauer Spectroscopy,* Chapman and Hall, London 1968.

20. T. C. Gibb, *Principles of Mössbauer Spectroscopy,* McGraw-Hill, London 1973.

21. G. M. Bancroft, *MössbauerSpectroscopy,* McGraw-Hill, London 1976.

22. N. Benezer-Keller and T. Fink, *Nuclear Phys. (A),* 1971, **161**, 123.

23. J. J. Zuckerman, *Adv. Organomet. Chem.*, 1970, **9**, 21.

24. N. N. Greenwood, P. G. Perkins and D. H. Wall, *Symp. Faraday Soc.*, 1968, **1**, 51.

25. N. N. Greenwood, P. G. Perkins and D. H. Wall, *Phys. Lett.*, 1968, **28A**, 339.

26. P. G. Harrison and J. J. Zuckerman, *Inorg. Chim. Acta*, 1977, **21**, L3.

27. J. D. Donaldson, D. C. Puxley and M. J. Trucker, *Inorg. Nucl. Chem. Lett.*, 1972, **8**,

845.

28. J. Barrett, S. R. A. Bird, J. D. Donaldson and J. Silver, *J. Chem. Soc., Dalton Trans.*, 1971, 3105.

29. R. K. Harris, J. D. Kennedy and W. McFarlane, *Multinuclear N.m.r.*, p. 305, ed. J. Mason, Plenum, New York 1987.

30. L. Smith and P. J. Smith, *Inorg. Chim. Acta Rev.*, 1973, **7**, 11.

31. J. Otera, *J. Organomet. Chem.*, 1981, **221**, 57.

32. R. K. Harris and B. E. Mann, *N. m. r. and the Periodic Table*, p. 351, Academic Press, New York 1978.

33. J. J. Burke and P. C. Lauterbar, *J. Am. Chem. Soc.*, 1961, **83**, 326.

34. S. J. Blunden, P. A. Cusack, D. G. Giles and P. J. Smith, *Inorg. Chim. Acta*, 1984, **84**, 35.

35. D. J. Kennedy and W. McFarlane, *Rev. Si. Ge. Tin and Lead Compd.*, 1973, **1**, 235.

36. P. J. Smith and A. P. Tupiauskas, *Ann. Rep. NMR Spectrosc.*, 1978, **8**, 291.

37. H. S. Gutowsky and C. J. Jameson, *J. Chem. Phys.*, 1964, **40**, 1714.

38. A. Appelt, H. H. Karsch and G. Müller, *Organometallics*, 1987, **6**, 1679.

39. R. A. Geanangel and H-M. M. Yeh, *Inorg. Chim. Acta*, 1981, **52**, 113.

40. E. W. Abel, *Comprehensive Inorganic Chemistry*, Vol. 2, p. 1043, Pergamon, Oxford 1973.

41. W. Petz, *Chem. Rev.*, 1986, **86**, 1019.

42. M. S. Holt, J. H. Nelson and W. L. Wilson, *Chem. Rev.*, 1989, **89**, 11.

43. M. A. Alla, G. Engelhardt, E. Lippmaa and T. J. Penk, *J. Am. Chem. Soc.*, 1978, **100**, 1929.

44. A. K. Cheetham, C. M. Dobson, C. P. Grey and R. K. B. Jakeman, *Nature (London)*, 1987, **328**, 706.

45. R. K. Harris and A. Sebald, *J. Organomet. Chem.*, 1987, **331**, C9.

46. N. J. Clayden, C. M. Dobson and A. Fern, *J. Chem. Soc., Dalton Trans.*, 1989, 843.

47. G. A. Lawless, R. M. Merrill, J. M. Millar, G. G. Webb and K. W. Zilm, *J. Am. Chem. Soc.*, 1987, **109**, 7236.

48. P. J. Davidson and M. F. Lappert, *J. Chem. Soc., Chem. Commun.*, 1973, 317.

49. R. T. Sanderson, *Inorg. Chem.*, 1986, **25**, 1856.

50. J. D. Donaldson, *Prog. Inorg. Chem.*, 1967, **8**, 287.

51. J. D. Donaldson and S. M. Grimes, *Rev. Si. Ge. Tin and Lead Cmpd.*, 1984, **8**, 1.

52. S-W. Ng and J. J. Zuckerman, *Adv. Inorg. Radiochem.* 1985, **29**, 297.

53. D. G. Urch, *J. Chem. Soc.*, 1964, 5775.

54. L. F. Orgel, *J. Chem. Soc.*, 1959, 3815.

55. Reference 1, p. 177.

56. J. D. Donaldson and S. M. Grimes, *J. Chem. Soc., Dalton Trans.*, 1984, 1301.

57. M. B. Hall and R. L. Williamson, *Organometallics,* 1986, **5**, 2142.

58. J. L. Atwood, A. H. Cowley, W. E. Hunter and C. A. Stewart, *J. Chem. Soc., Chem. Commun.*, 1981, 925.

59. P. Hofmann, P. Jutzi, F. Kohl, C. Krüger and Y. Tsay, *Chem. Ber.*, 1980, **113**, 757.

60. M. J. Heeg, C. Janiak and J. J. Zuckerman, *J. Am. Chem. Soc.*, 1984, **106**, 4259.

61. P. A. Cusack, J. D. Donaldson, S. M. Grimes and P. J. Smith, *Publication No. 588,* International Tin Research Institute, Uxbridge.

62. B. Y. K. Ho and J. J. Zuckerman, *J. Organomet. Chem.*, 1973, **49**, 1.

63. P. G. Harrison, *Coord. Chem. Rev.*, 1976, **20**, 1.

64. M. Veith, *Topics in Current Chemistry,* Vol. 104, p.1, Springer-Verlag 1982.

65. Y. F. Mironov and V. I. Shiryaev, *Russ. Chem. Rev.*, 1983, **52**, 184.

66. M. Veith, *Angew. Chem. Int. Ed. Engl.*,1987, **26**, 1.

67. M. Veith, *Chem. Rev.*, 1990, **90**, 3.

68. P. Jutzi, *Adv. Organomet. Chem.*, 1985, **26**, 267.

69. J. Fournes, J. Grannes, P. Hagenmuller and Y. Pontin, *Solid State Chem.*, 1986, **59**, 833.

70. J. J. Burke and P. C. Lauterbeur, *J. Am. Chem. Soc.*, 1961, **83**, 326.

71. K. Eriks, H-K. Hau and R. C. McDonald, *Inorg. Chem.*, 1976, **15**, 762.

72. J. W. Hastie, R. H. Hauge and J. L. Margrave, *J. Mol. Spect.*, 1973, **45**, 420.

73. G. Denes, *J. Solid State Chem.*, 1979, **30**, 335.

74. G. Bergerhoff and L. Goost, *Acta Cryst.*, 1978, **B34**, 699.

75. G. Bergerhoff, L. Goost and E. Schultze-Rhonhof, *Acta Cryst.*, 1968, **B24**, 803.

76. D. T. Cromer, A. C. Larson and R. R. McDonald, *Acta Cryst.*, 1964, **17**, 1104.

77. M. F. A. Dove, R. King and T. J. King, *J. Chem. Soc., Chem. Commun.*,1973, 944.

78. G. Bergerhoff and L. Goost, *Acta Cryst.*, 1970, **B26**, 19.

79. L. Cot, C. Geneys and S. Vilminot, *Acta Cryst.*, 1976, **B32**, 3199.

80. J. D. Donaldson, D. R. Laughlin and D. C. Rixley, *J. Chem. Soc., Dalton Trans.*, 1977, 865.

81. L. Cot, W. Granier and S. Vilminot, *Acta Cryst.*, 1978, **B34**, 35.

82. C. Geneys and S. Vilminot, *Rev. Chim. Miner.*, 1977, **14**, 395.

83. S. Vilminot, *Acta Cryst.*, 1978, **B34**, 3308.

84. A. J. F. Boyle, D. St. P. Bunbury and C. Edwards, *Proc. Phys. Soc.*, 1962, **79**, 416.

85. M. Cordey-Hayes, *J. Inorg. Nucl. Chem.*, 1964, **26**, 915.

86. J. D. Donaldson and B. J. Senior, *J. Chem. Soc. (A)*, 1966, 1798.

87. N. N. Greenwood and A. Timmick, *J. Chem. Soc. (A)*, 1971, 676.

88. I. Naray-Szabo, *Inorg. Cryst. Chem., Akad. Kiado, Budapest,* 1969, 215.

89. J. M. van den Berg, *Acta Cryst.*, 1961, **14**, 1002.

90. D. Grdenic and N. Kamenar, *J. Chem. Soc.*, 1961, 3954.

91. H. Kiriyama, R. Kiriyama, K. Kitahama and O. Nakamura, *Bull. Chem. Soc. Jpn.*, 1973, **46**, 1389.

92. E. Hough and D. G. Nicolson, *J. Chem. Soc., Dalton Trans.*, 1976, 1782.

93. H. S. Haupt, F. Huber and H. Preut, *Z. Anorg. Allg. Chem.*, 1976, **97**, 255.

94. P. G. Harrison, B. J. Haylett and T. J. King, *Inorg. Chim. Acta,* 1983, **75**, 265.

95. F. R. Poulsen and S. E. Rasmussen, *Acta Chem. Scand.*, 1970, **24**, 150.

96. P. A. Flinn and J. Lees, *Phys. Lett.*, 1965, **19**, 186.

97. J. Andersson, *Acta Chem. Scand.*, 1972, **26**, 1730.

98. J. Andersson, *Acta Chem. Scand.*, 1972, **26**, 3813.

99. J. Andersson, *Acta Chem. Scand.*, 1972, **26**, 2543.

100. F. Aubke, K. Lee, S. P. Mallela, J. R. Sams and S. T. Tomic, *Inorg. Chem.*, 1986, **25**,

2939.

101. C. Curran and M. A. Doskey, *Inorg. Chim. Acta,* 1969, **3**, 169.

102. R. H. Herber and A. E. Smelkinson, *Inorg. Chem.,* 1978, **17**, 1023.

103. H. J. Haupt, F. Huber and H. Preut, *Z. Anorg. Chem.,* 1974, **408**, 209.

104. R. A. Howie and W. Moser, *Nature (London),* 1968, **219**, 372.

105. W. Jeitschko and A. W. Sleight, *Acta Cryst.,* 1974, **B30**, 2088.

106. W. Jeitschko and A. W. Sleight, *Acta Cryst.,* 1972, **B28**, 3174.

107. R. Herak, *J. Chem. Soc., Dalton Trans.,* 1978, 566.

108. K. Eriks and R. C. McDonald, *Inorg. Chem.,* 1980, **19**, 1237.

109. A. F. Berndt and J. Lamberg, *Acta Cryst.,* 1971, **B27**, 1092.

110. J. D. Donaldson and D. C. Puxley, *Acta Cryst.,* 1972, **B28**, 864.

111. A. F. Berndt, *Acta Cryst.,* 1974, **B30**, 529.

112. J. C. Dewan, *J. Chem. Soc., Dalton Trans.,* 1977, 2319.

113. P. F. R. Ewings, P. G. Harrison, T. J. King and A. Morris, *J. Chem. Soc., Dalton Trans,* 1976, 1602.

114. F. P. van Remoortere, *Inorg. Chem.,* 1971, **10**, 1511.

115. C. G. Davies, *J. Chem. Soc., Dalton Trans.,* 1975, 2241.

116. T. H. Jordan, M. Mathew and M. Schroeder, *Acta Cryst.,* 1977, **B33**, 1812.

117. P. G. Harrison, B. J. Haylett and T. J. King, *J. Chem. Soc., Chem Commun.,* 1978, 112.

118. M. Goreaud, P. Labbé and B. Raveau, *Acta Cryst.,* 1980, **B36**, 15.

119. T. Burchall, R. Faggiani, C. J. L. Lock and V. Manivannan, *J. Chem. Soc., Dalton Trans.,* 1987, 1675.

120. W. W. du Mont and B. Neudert, *Angew. Chem. Int. Ed. Engl.,* 1980, **19**, 7.

121. H. M. Haendler and J. S. Morrison, *J. Inorg. Nucl. Chem.,* 1967, **29**, 393.

122. P. G. Harrison and J. J. Zuckerman, *J. Chem. Soc., Chem. Commun.,* 1969, 321.

123. P. G. Harrison and S. R. Stobart, *J. Chem. Soc., Dalton Trans.,* 1973, 940.

124. J. D. Donaldson and A. Jelen, *J. Chem. Soc. (A),* 1968, 1448.

125. P. F. R. Ewings and P. G. Harrison, *J. Chem. Soc., Dalton Trans.,* 1975, 1717.

126. A. B. Cornwell and P. G. Harrison, *J. Chem. Soc., Dalton Trans.*, 1975, 1722.

127. P. F. R. Ewings and P. G. Harrison, *J. Chem. Soc., Dalton Trans.*, 1975, 2015.

128. M. Grenz and W. W. du Mont, *Z. Naturforsch.*, 1983, **38b**, 113.

129. F. Töllner and M. Veith, *J. Organomet. Chem.*, 1983, **246**, 219.

130. T. Fjeldberg, P. B. Hitchcock, M. F. Lappert, S. J. Smith and A. J. Thorne, *J. Chem. Soc., Chem. Commun.*, 1985, 938.

131. G. Müller and C. Zybill, *Z. Naturforsch.*, 1988, **43b**, 45.

132. E. M. Holt, W. Kläui and J. J. Zuckerman, *J. Organomet. Chem.*, 1987, **335**, 29.

133. G. Carasquillo and R. H. Herber, *Inorg. Chem.*, 1981, **20**, 3693.

134. E. Hough, D. G. Nicholson and A. K. Vasudevan, *J. Chem. Soc., Dalton Trans.*, 1989, 2155.

135. R. Rösler and M. Veith, *Angew. Chem. Int. Ed. Engl.*, 1982, ***21***, 11.

136. R. Rösler and M. Veith, *Z. Naturforsch.*, 1986, **41b**, 1071.

137. P. G. Harrison and E. W. Thornton, *J. Chem. Soc., Dalton Trans.*, 1978, 1274.

138. P. E. Fanwick, I. P. Rothwell and G. D. Smith, *Inorg. Chem.*, 1989, **28**, 618.

139. P. F. R. Ewings, P. G. Harrison and T. J. King, *J. Chem. Soc., Dalton Trans.*, 1975, 1454.

140. J. L. Atwood, B. Cetinkaya, I. Gürnrücü, M. F. Lappert, R. D. Rogers and M. J. Zaworotko, *J. Am. Chem. Soc.*, 1980, **102**, 2088.

141. A. J. Bearden, H. S. Marsh and J. J. Zuckerman, *Inorg. Chem.*, 1966, **5**, 1260.

142. W. D. Honnick and J. J. Zuckerman, *Inorg. Chem.*, 1978, **17**, 1978.

143. J. Augé and G. Bourleaux, *J. Organomet. Chem.*, 1989, **377**, 205.

144. R. Nesper and H. G. von Schnering, *Z. Naturforsch.*, 1982, **37b**, 1144.

145. P. G. Harrison and S. R. Stobart, *Inorg. Chim. Acta*, 1973, **7**, 306.

146. P. A. W. Dean, N. C. Payne and J. J. Vital, *Can. J. Chem.*, 1985, **63**, 394.

147. D. van der Helm, M. B. Hossain, J. L. Lefferts, K. C. Molloy and J. J. Zuckerman, *Inorg. Chem.*, 1982, **21**, 1410.

148. G. Freyberger, M. Moll and D. Sellmann, *Z. Naturforsch.*, 1989, **44b**, 1015.

149. D. H. Olsen and R. E. Rundle, *Inorg. Chem.*, 1964, **3**, 596.

150. J. E. Iglesias and H. Steinfink, *Acta Cryst.*, 1973, **B29**, 1480.

151. P. B. Hitchcock, M. F. Lappert, B. J. Samways and E. L. Weinberg, *J. Chem. Soc., Chem. Commun.*, 1983, 1492.

152. P. F. R. Ewings, P. G. Harrison and T. J. King, *J. Chem. Soc., Dalton Trans.*, 1976, 1399.

153. D. Mastropaola and J. Potenza, *Acta Cryst.*, 1973, **B29**, 1830.

154. B. F. Hoskins, R. L. Martin and N. M. Rohde, *Austral. J. Chem.*, 1976, **29**, 213.

155. P. Hobein, R. Rösler and M. Veith, *Z. Naturforsch.*, 1989, **44b**, 1067.

156. A. Okazaki and I. Ueda, *J. Phys. Soc. Jpn.*, 1956, **11**, 470.

157. P. G. Harrison and J. J. Zuckerman, *Inorg. Chem. Nucl. Lett.*, 1969, **5**, 545.

158. M. K. Friedel, B. F. Hoskins, R. L. Martin and S. A. Mason, *J. Chem. Soc., Chem. Commun.*, 1970, 400.

159. C. D. Schaeffer and J. J. Zuckerman, *J. Am. Chem. Soc.*, 1974, **96**, 7160.

160. D. H. Harris and M. F. Lappert, *J. Chem. Soc., Chem. Commun.*, 1974, 894.

161. P. Foley and M. Zeldin, *Inorg. Chem.*, 1975, **14**, 2264.

162. P. J. Corvan and J. J. Zuckerman, *Inorg. Chim. Acta,* 1979, **34**, L255.

163. C. Stader and B. Wrackmeyer, *Z. Naturforsch.*, 1988, **43b**, 706.

164. C. J. Carrano, A. H. Cowley, R. L. Geerts and C. M. Nunn, *J. Organomet. Chem.*, 1988, **341**, C27.

165. M. F. Lappert, P. P. Power and M. J. Slade, *J. Chem. Soc., Chem. Commun.*, 1979, 368.

166. T. Fjeldberg, H. Hope, M. F. Lappert, P. P. Power and A. J. Thorne, *J. Chem. Soc., Chem. Commun.*, 1983, 368.

167. M. M. Olmstead and P. P. Power, *Inorg. Chem.*, 1984, **23**, 413.

168. M. Veith, *Z. Naturforsch.*, 1978, **33b**, 1.

169. M. Veith, *Chem. Ber.*, 1978, **111**, 2536.

170. M. Veith, *Z. Naturforsch.*, 1980, **35b**, 20.

171. H. Lange and M. Veith, *Angew. Chem. Int. Ed. Engl.*, 1980, **19**, 401.

172. O. Recktenwald and M. Veith, *Z. Naturforsch.*, 1981, **36b**, 144.

173. M. Grosser, O. Recktenwald and M. Veith, *J. Organomet. Chem.*, 1981, **216**, 27.

174. G. Schlemmer and M. Veith, *Chem. Ber.*, 1982, **115**, 2141.

175. M. Grosser and M. Veith, *J. Organomet. Chem.*, 1982, **229**, 247.

176. G. Schlemmer, M. L. Sommer and M. Veith, *Z. Anorg. Allg. Chem.*, 1983, **497**, 157.

177. O. Recktenwald and M. Veith, *Z. Naturforsch.*, 1983, **38b**, 1054.

178. W. Frank and M. Veith, *Angew. Chem. Int. Ed. Engl.*, 1984, **23**, 158.

179. V. Huch and M. Veith, *J. Organomet. Chem.*, 1985, **293**, 161.

180. R. Lisowsky and M. Veith, *Angew. Chem. Int. Ed. Engl.*, 1988, **27**, 1087.

181. P. Hobein, V. Huch, R. Lisowsky and M. Veith, *Z. Anorg. Allg. Chem.*, 1989, **503**, 569.

182. H-J. Knoth and W. W. du Mont, *Angew. Chem. Int. Ed. Engl.*, 1977, **16**, 792.

183. A. Appelt, H. H. Karsch and G. Müller, *Angew. Chem. Int. Ed. Engl.*, 1985, **24**, 402.

184. A. M. Arif, A. H. Cowley, R. A. Jones and J. M. Power, *J. Chem. Soc., Chem. Commun.*, 1986, 1446.

185. P. G. Harrison, *J. Chem. Soc., Chem. Commun.*, 1972, 644.

186. J. D. Cotton, P. J. Davidson, J. D. Donaldson, M. F. Lappert and J. Silver, *J. Chem. Soc., Dalton Trans.*, 1976, 2286.

187. M. P. Bigwood, P. J. Corvan, And J. J. Zuckerman, *J. Am. Chem. Soc.*, 1981, **103**, 7643.

188. P. G. Harrison and J. J. Zuckerman, *J. Am. Chem. Soc.*, 1969, **91**, 6885.

189. A. Bonny, A. D. McMaster and S. R. Stobart, *Inorg. Chem.*, 1978, **17**, 935.

190. S. G. Baxter, A. H. Cowley, J. G. Lasch, M. Lattman, W. P. Sharum and C. A. Stewart, *J. Am. Chem. Soc.*, 1982, **104**, 4064.

191. R. A. Geanangel and R. Hani, *J. Organomet. Chem.*, 1985, **293**, 197.

192. B. Hielscher and P. Jutzi, *Organometallics*, 1986, **5**, 1201.

193. R. Dickbreder and P. Jutzi, *Chem. Ber.*, 1986, **119**, 1750.

194. R. Dickbreder and P. Jutzi, *J. Organomet. Chem.*, 1989, **373**, 301.

195. M. B. Hall and R. L. Williamson, *Organometallics*, 1986, **5**, 2142.

196. P. G. Harrison and J. A. Richards, *J. Organomet. Chem.*, 1976, **108**, 35.

197. J. W. Connelly and C. Hoff, *Adv. Organomet. Chem.,* 1981, **19**, 123.

198. T. S. Dory and J. J. Zuckerman, *J. Organomet. Chem.,* 1984, **264**, 295.

199. R. H. Herber, N. S. Hosmane and N. N. Sirmokadam, *Organomet.allics,* 1984, **3**, 1665.

200. E. L. Amma, T. Auel and P. F. Rodesiler, *J. Am. Chem. Soc.,* 1975, **97**, 7405.

201. D. E. Goldberg, D. H. Harris, M. F. Lappert and K. M. Thomas, *J. Chem. Soc., Chem. Commun.,* 1976, 261.

202. A. Almenningen, A. Haaland and T. Motzfeld, *J. Organomet. Chem.,* 1967, **7**, 97.

203. J. Almlöf, L. Fernholt, K. Faegri, A. Haaland, B. E. R. Schilling, R. Seip and K. Taugbøl, *Acta Chem. Scand.,* 1983, **A37**, 131.

204. A. H. Cowley, P. Jutzi, F. X. Kohl, J. G. Lasch, N. C. Norman and E. Schlüter, *Angew. Chem.,* 1984, **96**, 603.

205. M. J. Heeg, C. Janiak and J. J. Zuckerman, *J. Am. Chem. Soc.,* 1984, **106**, 4259.

206. K. D. Bos, E. J. Bulten and J. G. Noltes, *J. Organomet. Chem.,* 1975, **99**, 71.

207. M. B. Hursthouse, F. X. Kohl, P. Jutzi, E. Schlüter and N. P. C. Walker, *J. Organomet. Chem.,* 1984, **271**, 2789.

208. S. S. C. Chu, R. H. Herber, N. S. Hosmane, N. N. Maldar, P. de Meester and S. B. Potts, *Organometallics,* 1986, **5**, 772.

209. V. Huch and M. Veith, *J. Organomet. Chem., 1986, 308*, 263.

210. B. Huber, G. Müller, T. Probst, H. Schmidbaur and O. Steigelmann, *Organometallics,* 1989, **8**, 1567.

211. W. Frank, *Chem. Ber.,* 1990, **123**, 1233.

212. P. B. Darriet and J. Galy, *Acta Cryst.,* 1977, **B33**, 1489.

213. A. M. Arif, A. H. Cowley and T. M. Elkins, *J. Organomet. Chem.,* 1987, **325**, C11.

214. K. Jurkschat, C. Mügge, M. Scheer, A. Tzschach and A. Zschunke, *Z. Anorg. Allg. Chem.,* 1983, **502**, 158.

215. K. Jurkschat, M. Scheer and A. Tzschach, *Z. Anorg. Allg. Chem.,* 1984, **515**, 147.

216. K. Jurkschat and A. Tzschach, *Rev. Si. Ge. Tin and Lead Cmpds.,* 1986, **9**, 263.

217. U. Baumeister, H. Hartung, K. Jurkschat and A. Tzschach, *J. Organomet. Chem.,*

1986, **304**, 107.

218. K. Angermund, K. Jonas, C. Krüger, J. L. Latten and Y-H. Tsay, *J. Organomet. Chem.,* 1988, **353**, 17.

219. A. J. Arduengo and G. Bettermann, *J. Am. Chem. Soc.*, 1988, **110**, 877.

220. J. Boersma, D. Heijdenrijk, J. T. B. H. Jastrzebski, G van Koten and P. A. van der Schaaf, *Organometallics,* 1989, *8*, 1373.

221. M. Nardelli, C. Pelizzi and G. Pelizzi, *J. Organomet. Chem.,* 1975, **85**, C43.

222. C. Pelizzi, G. Pelizzi and P. Tarasconi, *J. Chem. Soc., Dalton Trans.,* 1977, 1935.

223. F. A. Cotton, E. B. Kibala, L. R. Falvello, and M. Shang, *Inorg. Chem.,* 1990, **29**, 2591.

224. M. van Meerssche, J. Meunier-Piret, K. Jurkschat, M. Scheer and A. Tzschach, *J. Organomet. Chem.,* 1985, **281**, 173.

Chapter 2

Synthesis of Tin(II)-Oxygen Heterocyclic Compounds

2.1 Introduction

The development of platinum(II) antitumour drugs such as *cis*-platin ($Pt(NH_3)_2Cl_2$) has been a major growth area in inorganic chemistry and these compounds are now routinely used in the treatment of testicular and ovarian cancer, as well as for teratoma (tumours in foetuses). In addition, a considerable amount of research has been directed towards the mode of action of these drugs[1-6]. The platinum compounds are thought to act by inhibiting DNA replication- while the transcriptional activity (RNA synthesis) and the translational activity (protein synthesis) are relatively unaffected. The main reaction involves the loss of two chloride ions and binding of platinum to the N7 atoms of adjacent guanine bases on the same strand. The success of these drugs has stimulated the study of compounds of other metals as possible antitumour reagents[7]. As part of these investigations it has been established that the tin(IV) compounds listed in Table 2.1 are effective against a range of tumours.

Table 2.1 Active Antitumour Tin(IV) Compounds[7,12-15]

Compound	Tumour System	Ref.
Et_2SnCl_2.phen	P388	16
Et_2SnCl_2.dmso	P388	17
Et_2SnCl_2.bipybim	Renal adenocarcinoma	18
Ph_2SnCl_2.2py	P388	15
Ph_2SnCl_2.tmphen	Renal adenocarcinoma	18
$Et_2Sn(smes)_2$	P388	19
$^nBu_2Sn(ad)_2$	P388	20

$^{n}Bu_2Sn$.pyrid	L1210	14
$^{n}Bu_2Sn(put)_2$	P388	21
2'-3'-*o*-Di-*n*-butylstannyl-5-fluorouridine	P388	22
$(Et^{n}BuClSn)_2O$	P388	23
$(o\text{-}Tol_2ClSn)_2O$	P388	24

Since both platinum and tin compounds exhibit significant antitumour activity, it was of interest to synthesize a range of platinum-tin compounds in order to establish whether there are any important synergic effects. A number of classes of platinum-tin compounds have been characterized and reported in the literature[8-11] . The most important compounds are those based on $SnCl_3^-$ and some of these compounds are listed in Table 2.2. These compounds are readily isolated from the insertion of SnX_2 into platinum-chlorine bonds.

Table 2.2 Compounds Containing Pt-SnX_2Cl

Compound	**Ref.**
X = Cl	
$[PtCl_2(SnCl_3)_2]^{2-}$	23, 25
$[PtCl(SnCl_3)_3]^{2-}$	23, 25
$[Pt(SnCl_3)_4]^{2-}$	23, 25
$[Pt(SnCl_3)_5]^{3-}$	24
$[Pt(COD)(SnCl_3)_3]^{-}$	26
$[Pt(SnCl_3)_3(AsMe_3)_2]^{-}$	29

$[Pt(CO)Cl(SnCl_3)_2]^-$	27
$Pt(CO)(SnCl_3)_2(PPh_3)_2$	28
$Pt(CO)(SnCl_3)_2(PPh_3)_2(EtOH)$	27
trans-$PtCl(SnCl_3)(PEt_3)_2$	28
trans-$Pt(SnCl_3)_2(P(OPh)_3)_2$	29
trans-$Pt(SnCl_3)(PEt_3)_2(COPh)$	30
trans-$PtH(SnCl_3)(PPh_3)_2$	31
trans-$PtH(SnCl_3)(SnCl_2.OCMe_2)(PPh_3)_2$	31
cis-$Pt(SnCl_3)(C_2H_5)(dppp)$	32
cis-$Pt(SnCl_3)(COC_2H_5)(dppp)$	32
trans-$Pt(SnCl_3)_2L_2$ L = 4-methylpyridine	33
$[Pt_2(SnCl_3)_2(\mu\text{-dppm})_2]$	34
[*cis*-$Pt_2(SnCl_3)_2(\mu\text{-Cl})_2(PMe_2Ph)_2$]	35
$Pt_3(SnCl_3)_2(COD)_3$ **X = $CH(SiMe_3)_2$**	36
$PtCl(SnClX_2)(SnX_2)(PEt_3)$	37

The initial aim of this project was to synthesize tin(II) compounds which would also insert into platinum-chlorine bonds, but simultaneously incorporate some of the factors associated with the tin compounds listed in Table 2.1, which have shown antitumour activity.

Veith[38] has proposed two general aspects which appear to be important in the bonding of tin(II) compounds (see Figure 2.1).

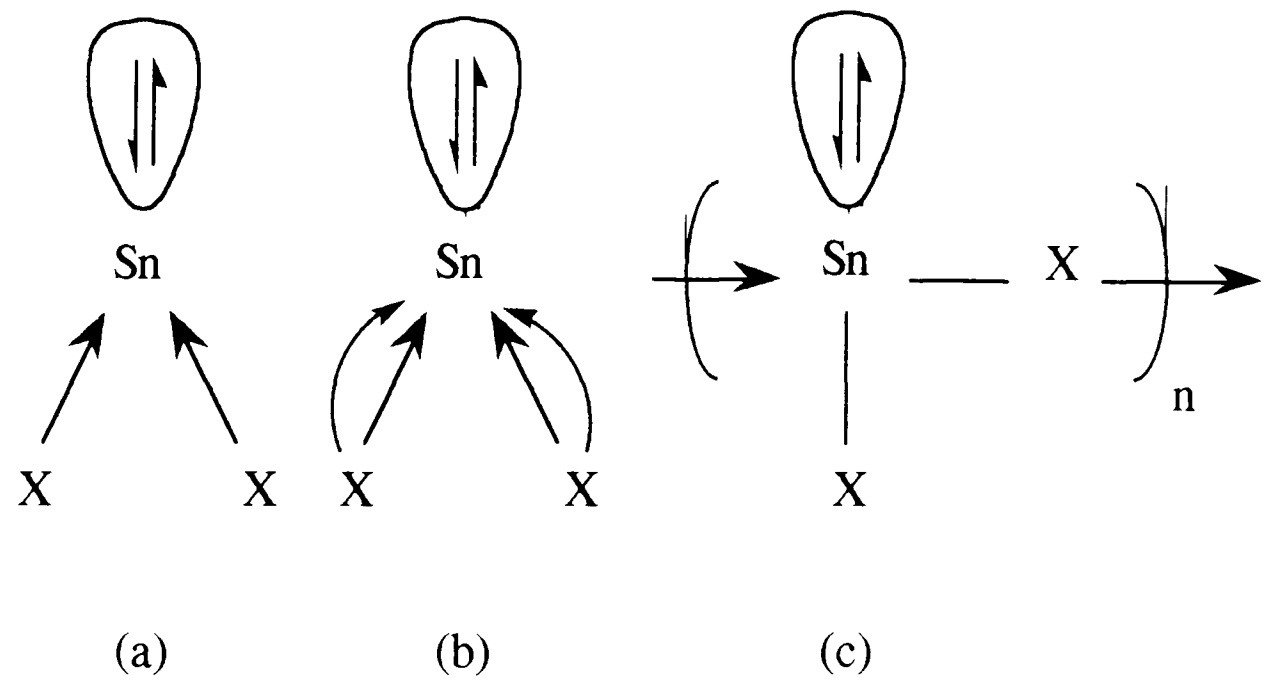
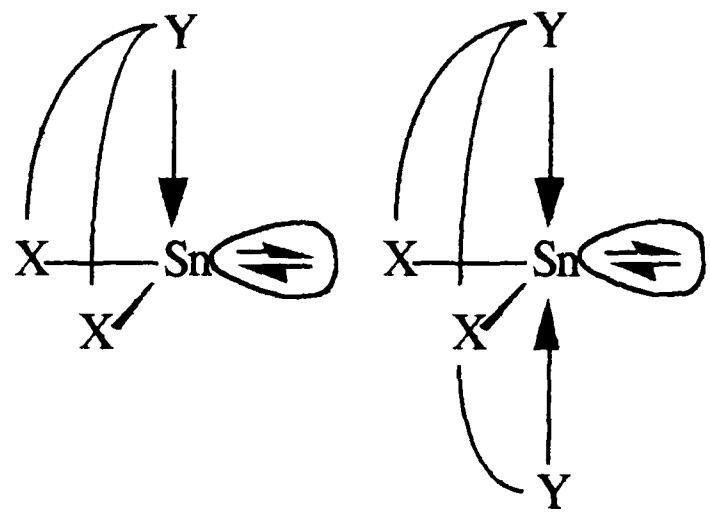


Figure 2.1

1. The relative deficiency of electron pairs at the tin atom has to be compensated for by electron releasing groups, via a simple inductive σ-effect, or via a mesomeric π-effect, or via both (see (a) and (b) in Figure 2.1).

2. The steric requirements of the groups X should be demanding to prevent the polymerization process shown in Figure 2.1(c).

The use of bulky groups has been most effective in stabilizing monomeric tin(II) centres[36-41], whilst Jurkschat[42] and others[43,44] have prevented polymerization by the use of intramolecular Lewis acid-base interactions(see Figure 2.2).



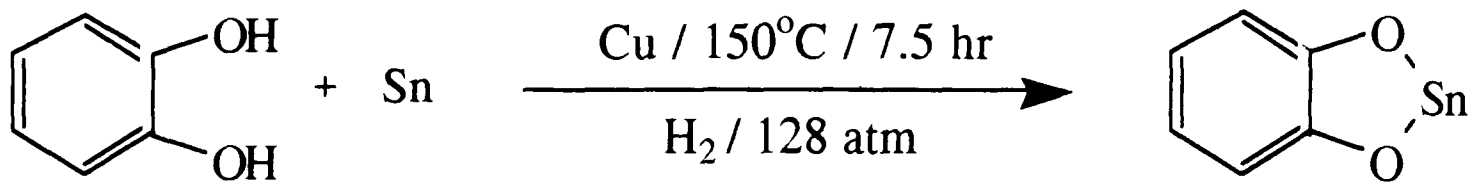
X, Y = O, S, N, P

Figure 2.2

Nefedov[45] has suggested that the use of bulky groups usually leads to an increase in the valence angle at tin e.g $[Sn(NMe_2)_2]_2$ [46] which has an angle of 93°, whilst $Sn[N(SiMe_3)_2]$ [40] has an angle of 105°, signifying an increase in energy in the σ-bond formed due to the large steric volume of the substituents. The p-orbitals on tin, which are responsible for the reactivity of the molecule are left relatively unaffected. It is therefore their further interaction with the ligands that is important. Hence $Sn[N(SiMe_3)_2]$ is a monomer and $[Sn(NMe_2)_2]_2$ is a dimer. In $[Sn(NMe_2)_2]_2$ the vacant tin p-orbitals are close in energy to the π−molecular orbitals associated with the nitrogen atom of another molecule. In $Sn[N(SiMe_3)_2]$ such Lewis acid-base interactions are shielded by the energetically raised σ-bond molecular orbitals. The tin p-orbitals instead being closer in energy to the π^*-molecular orbitals.

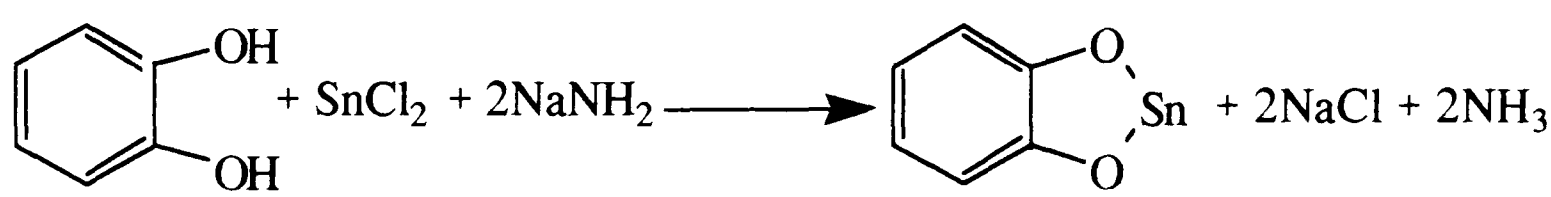
2.2 Synthesis of Tin(II)-Oxygen Heterocyclic Compounds

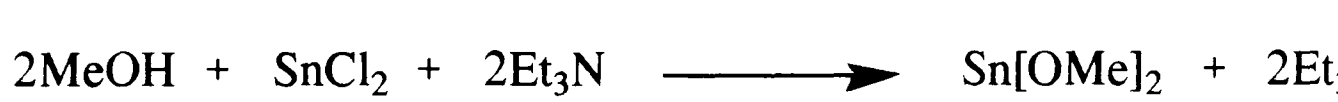
The tin(II)-oxygen heterocycles so far synthesized are listed in section 1.3.2.2. They are mostly polymeric and insoluble, and so not very useful for subsequent insertion reactions. The preparative methods employed have used their chemical inertness as a means of isolation. The early work of Zuckerman[47] used the rather unusual method of heating diphenols with tin metal in the presence of a copper catalyst, under a hydrogen atmosphere.



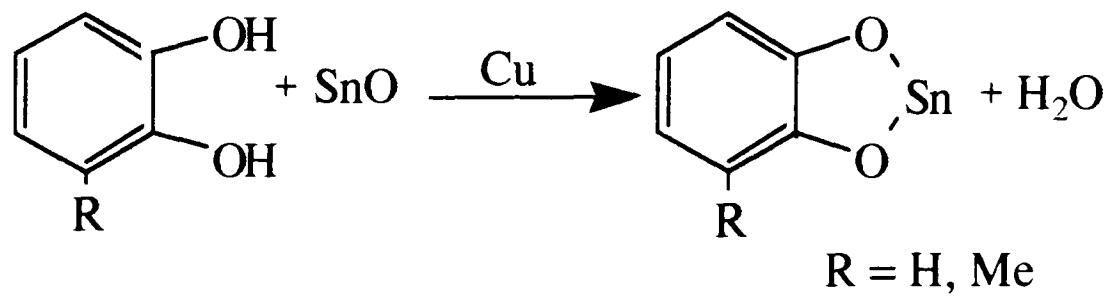
The reaction conditions and the method of purification (sublimation at 300°C *in vacuo*) indicated a high degree of thermal and chemical stability. The products, however are very insoluble in organic solvents.

Subsequent methods were less severe, and relied upon salt elimination, combined with the removal of the acidic phenolic protons by bases[48,49] e.g.

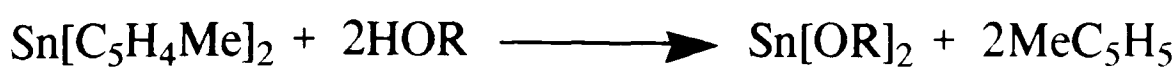


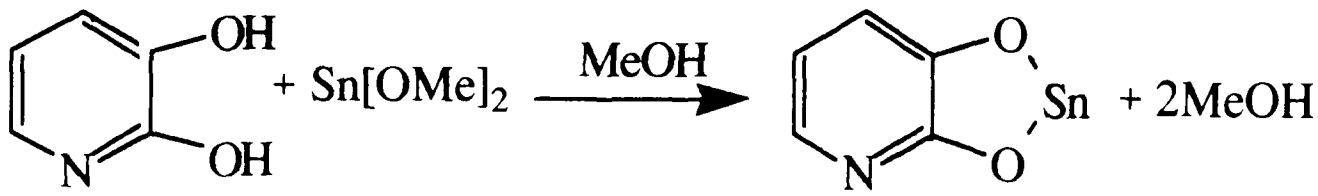


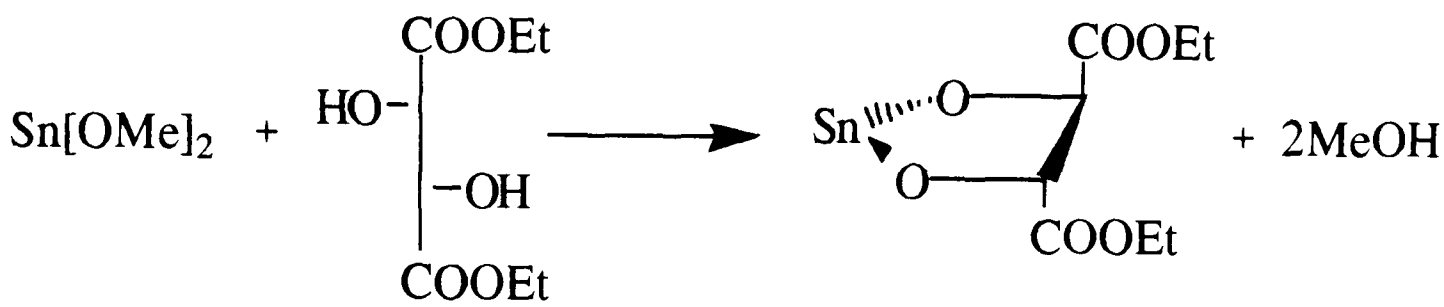
Heterocycles have also been prepared by the direct melting of stannous oxide with the diol[50,51] e.g.

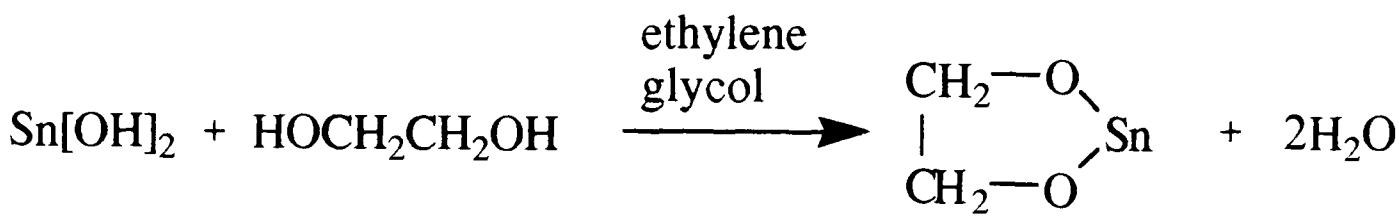


In hydrogen-transfer reactions, the leaving group at the tin(II) centre has been cyclopentadiene[52], methanol[53,54] or in one case, water[55] e.g.

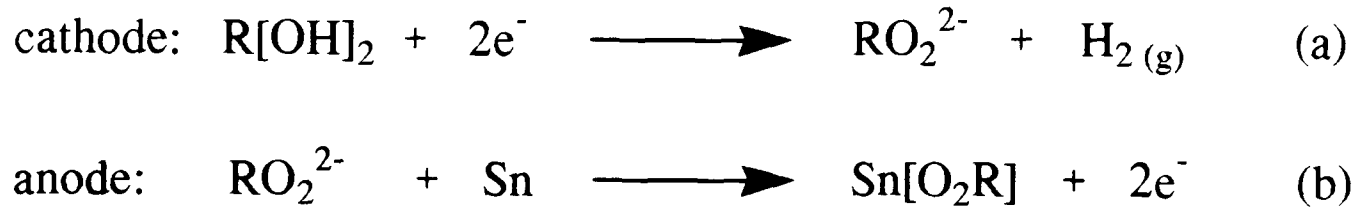




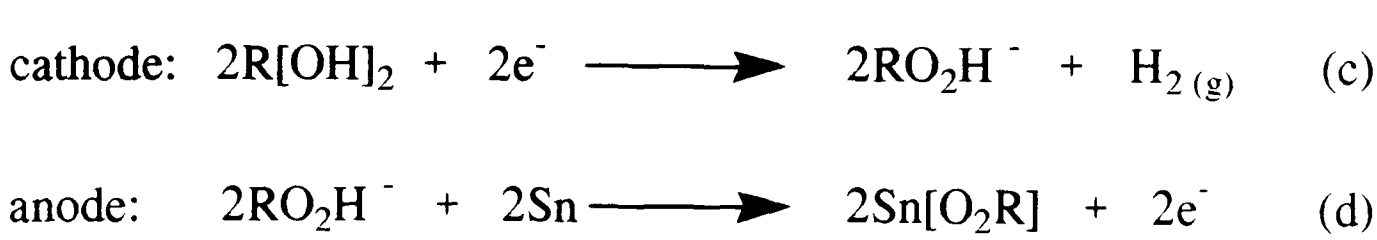




Recently the direct electrochemical synthesis of tin(II)-oxygen heterocycles was reported[56]. The tin anode being oxidised in the presence of the ligand in organic solvents. Tuck proposed two possible reaction sequences.



Sequence (a) and (b) involves the current being carried by a catecholate dianion, whilst the alternative sequence, (c) and (d), involves the loss of only one hydrogen atom, with the resultant monoanions migrating and eventually reacting at the anode in pairs.



2.3 Preparation of Novel Tin(II)-Oxygen Heterocycles.

In order to generate more attractive tin(II) reagents it was decided to investigate the effect of substituents on the catechol ligands on the properties of their compounds. This study was encouraged by the following factors.

1. The availability of a wide range of 1, 2-diols with either bulky, electron-donating or electron-withdrawing substituents.
2. The possibility of π-interactions between the substituents, and the empty p-orbitals on the tin centre reducing the degree of polymerization.

The ligands used incorporate all the factors discussed above. They include the sterically demanding tertiary-butyl, the electron-donating methoxy and electon-withdrawing groups such as chlorine and nitro. (-)-Adenosine is also used as an example of an optically-active, naturally occuring vicinal diol containing system, as a test for the possible incorporation of important antitumour agents based upon the carbocyclic analogues of adenosine, such as (-)-aristeromycin and (-)-neplanocin[62,63].

The novel tin(II)-oxygen heterocyclic compounds were prepared by the addition of a tetrahydrofuran solution of the reagent to an equimolar amount of freshly prepared tin(II) methoxide. The hydrogen transfer reaction was immediate at room temperature. Depending upon their solubilities, the products were either washed and isolated as an insoluble solid, or in the case of $\{Sn[O\text{-}4\text{-}NO_2\text{-}C_6H_3O][OC_4H_8]\}_n$ recrystallized from tetrahydrofuran. The results are summarized in Table 2.3.

Table 2.3 Physical Properties of Novel Tin(II)-Oxygen Heterocycles

Reagent	Product	Colour	Yield (%)	M.pt. (^{o}C)	Solubility
3,5-Di-*tert*-butylcatechol	$Sn[O\text{-}3,5\text{-}^{t}Bu_2\text{-}C_6H_2O]$	white	95	>300	insoluble
(-)adenosine	Sn[aden]	off-white	87	210 (decomp.)	insoluble
3-Methoxycatechol	$Sn[O\text{-}3\text{-}MeO\text{-}C_6H_3O]$	white	96	240 (decomp.)	sparingly soluble in dimethyl sulphoxide
Tetrachloro-*o*-benzoquinone	$Sn[OC_6Cl_4O][OC_4H_8]$	pale yellow	93	192 (decomp.)	soluble in dimethylformamide
4-Nitrocatechol	$\{Sn[O\text{-}4\text{-}NO_2\text{-}C_6H_3O][OC_4H_8]\}_n$	bright yellow	76	178 (decomp.)	soluble in all polar solvents

The stoichiometry of the compounds were confirmed by elemental analyses, and the oxidation state of the tin atom was determined by ^{119}Sn Mössbauer spectroscopy (see section 2.3.1). Infra-red spectroscopy revealed the loss of the oxygen-hydrogen stretch associated with the vicinal diol ligand, and the appearance of a very strong, broad signal between 500 and 550 cm^{-1}, which was attributed to the tin-oxygen stretch (see Table 1.1).

From these results, the introduction of bulky substituents did little to reduce the strength of the intermolecular interaction, resulting in the low solubility and high thermal stability of $Sn[O\text{-}3,5\text{-}^{t}Bu_2\text{-}C_6H_2O]$. What was also apparent was the pronounced effect substituents with significant electron-donating (methoxy) or electron-withdrawing (chloride and nitro) capabilities had in reducing thermal stability and increasing solubility, indicating a change in the intermolecular interactions. It would be expected that best results would be with the electron-donating methoxy group, since the electron-withdrawing chlorides or nitro groups would interact unfavourably with the electron deficient tin centre. However, this is not

the case, as Sn[O-3-MeO-C_6H_3O] is only sparingly soluble in dimethylsulphoxide, whilst Sn[OC_6Cl_4O][OC_4H_8] and $\{Sn[O\text{-}4\text{-}NO_2\text{-}C_6H_3O][OC_4H_8]\}_n$ are soluble in donor solvents allowing their stuctures to be more fully characterized.

The successful reaction of (-)-adenosine yielding Sn[aden], the first example of tin(II) compound incorporating a biologically important ligand shows the wide applicability of the reaction scheme for use with all vicinal diol systems.

2.3.1 ^{119}Sn Mössbauer Analysis

The ^{119}Sn Mössbauer spectra for the tin(II)-oxygen heterocyclic compounds, Sn[aden] and $\{Sn[O\text{-}4\text{-}NO_2\text{-}C_6H_3O][OC_4H_8]\}_n$ show their isomer shifts lie in the range expected for the tin(II) oxidation state (see section 1.2.2.3). The isomer shift for Sn[aden] was 3.09 mms^{-1} and 3.49 mms^{-1} for $\{Sn[O\text{-}4\text{-}NO_2\text{-}C_6H_3O][OC_4H_8]\}_n$ (see Figure 2.3). The isomer shift for $\{Sn[O\text{-}4\text{-}NO_2\text{-}C_6H_3O][OC_4H_8]\}_n$ is in accordance with Harrrison's observation that tin(II)-oxygen bonded compounds with an isomer shift in excess of 3.15 mms^{-1} are composed of molecules held together by only weak intermolecular interactions[64]. This is seen in the increased solubility of $\{Sn[O\text{-}4\text{-}NO_2\text{-}C_6H_3O][OC_4H_8]\}_n$ compared with Sn[aden], which has an isomer shift below 3.15 mms^{-1} and so is attributed with stronger intermolecular interactions.

The quadrupole splittings for Sn[aden] and $\{Sn[O\text{-}4\text{-}NO_2\text{-}C_6H_3O][OC_4H_8]\}_n$ are 2.03 mms^{-1} and 2.33 mms^{-1} respectively. The size of the splittings are indicative of a large departure from cubic symmetry.

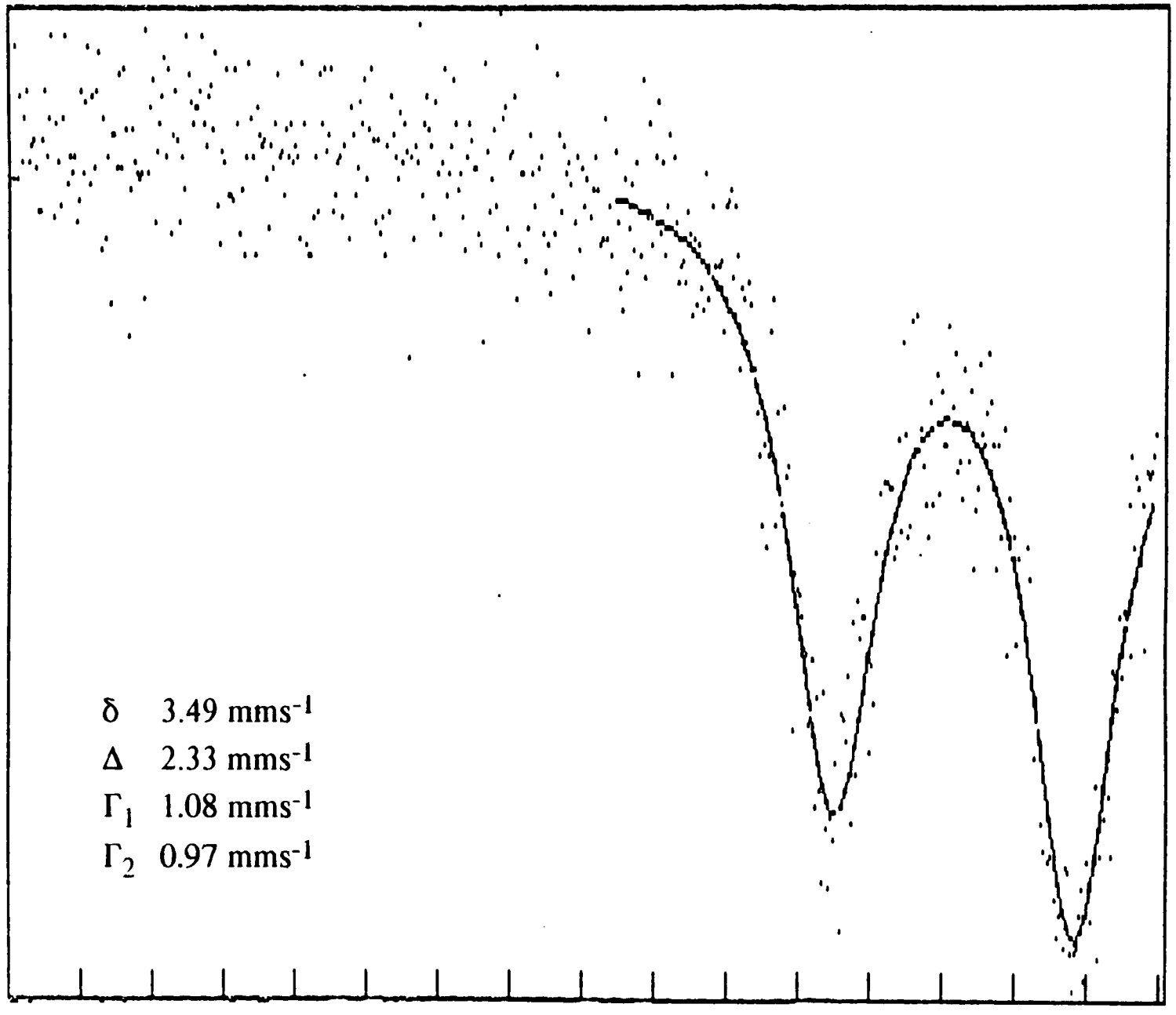


Figure 2.3 ^{119}Sn Mössbauer Spectrum of $\{Sn[O\text{-}4\text{-}NO_2\text{-}C_6H_3O][OC_4H_8]\}_n$

2.3.2 The Cryoscopic Molecular Weight Determination of $\{Sn[O\text{-}4\text{-}NO_2\text{-}C_6H_3O][OC_4H_8]\}_n$

The cryoscopic molecular weight determination of $\{Sn[O\text{-}4\text{-}NO_2\text{-}C_6H_3O][OC_4H_8]\}_n$ was carried out in dimethyl sulphoxide. The results indicated that the polymeric chain is broken down and the compound is monomeric in dimethyl sulphoxide, M_{meas} 298. This value is slightly higher than that for the unsolvated monomer, $Sn[O\text{-}4\text{-}NO_2\text{-}C_6H_3O]$, M_{calc} 272. The possibility of measuring the molecular weight in a non-donor solvent was excluded by the solubility properties of the compounds.

2.3.3 ^{117}Sn Solution N.M.R Analysis

Only $Sn[OC_6Cl_4O][OC_4H_8]$ and $\{Sn[O\text{-}4\text{-}NO_2\text{-}C_6H_3O][OC_4H_8]\}_n$ were sufficiently soluble in organic solvents for spectroscopic studies. From its cryoscopic molecular weight determination, $\{Sn[O\text{-}4\text{-}NO_2\text{-}C_6H_3O][OC_4H_8]\}_n$ was known to be monomeric in solution, (see section 2.3.2) and it was therefore reasonable to assume that $Sn[OC_6Cl_4O][OC_4H_8]$ would have only a low degree of oligomerization in dimethylformamide, the only solvent in which it dissolves.

The n.m.r. spectrum of the compounds were recorded using the ^{117}Sn resonance, because the ^{119}Sn spectrum was subject to local radio frequency interference effects. The factors influencing the position of the ^{117}Sn resonance are the same as those for ^{119}Sn n.m.r. discussed in section 1.2.3.

The ^{117}Sn n.m.r chemical shifts for $Sn[OC_6Cl_4O][OC_4H_8]$ and $\{Sn[O\text{-}4\text{-}NO_2\text{-}C_6H_3O][OC_4H_8]\}_n$ were found at low field with respect to tetramethyltin, at -333 and -452 p.p.m respectively. These values are consistent with a tin(II) atom bound to electronegative ligands. The disparity between the two chemical shifts could be due to the much greater electron-withdrawing capacity of the nitro group in $\{Sn[O\text{-}4\text{-}NO_2\text{-}C_6H_3O][OC_4H_8]\}_n$ compared to the four chlorine atoms in $Sn[OC_6Cl_4O][OC_4H_8]$, reducing the deshielding ability of the oxygen atoms bound to the tin centre. The uncertainty regarding the coordination

about the two tin centres in solution and the use of two different solvents, suggest that such conclusions should be treated with caution.

2.3.4 X-ray Crystallographic Analysis of $\{Sn[O\text{-}4\text{-}NO_2\text{-}C_6H_3O][OC_4H_8]\}_n$

Single crystals suitable for study by X-ray diffraction of $\{Sn[O\text{-}4\text{-}NO_2\text{-}C_6H_3O][OC_4H_8]\}_n$ were grown by slow diffusion of hexane into a tetrahydrofuran solution. The data collection and structure solution were carried out by Dr. Jonathan C. Machell of this laboratory.

A single crystal of dimensions 0.8 x 0.4 x 0.2 mm was mounted in a glass capillary under nitrogen and solvent vapour and transferred to the goniometer head of an Enraf-Nonius CAD4 diffractometer. Final unit cell dimensions, calculated from a least-squares treatment of the angles of 24 accurately centered reflections are given in Table 2.4. 2458 reflections were collected by $\omega/2\vartheta$ scans (scan width $1.00 \pm 0.35\tan\vartheta$) using graphite monochromated Mo-K_α radiation, of which 1621 were considered unique and observed ($I \geq 3\sigma(I)$, R_{merg}= 0.0161). These were corrected for Lorentz and polarization effects and an empirical absorption correction was applied (min/max correction 1.00/1.22).

The structure was solved by routine Patterson, direct methods (SHELXS), Fourier methods and full-matrix, least-squares refinement of all non-hydrogen atoms. After converting all of the atoms to anisotropic thermal parameters, the hydrogens on the catechol ligand were located from a difference map and those on the tetrahydrofuran were generated geometrically. On application of a Chebyshev weighting scheme (coefficients 8.496, -12.144, 7.170, -2.962), the model converged at $R = 0.0375$, $R_w = 0.0391$.

Table 2.5 and Appendix 1 contain the structural data for $\{Sn[O\text{-}4\text{-}NO_2\text{-}C_6H_3O][OC_4H_8]\}_n$, whilst Figures 2.4 to 2.8 show the main structural features.

Table 2.4 Structural Details for $\{Sn[O\text{-}4\text{-}NO_2\text{-}C_6H_3O][OC_4H_8]\}_n$

Compound	$[Sn_1O_5C_{10}H_{11}N_1]_n$		
Molecular Weight	343.89		
Space Group	P $\bar{1}$		
Cell Dimensions	a 6.121(3)Å	α	107.39(2)°
	b 9.295(3)Å	β	98.28(3)°
	c 11.073(2)Å	γ	98.28(4)°
Cell Volume	583 Å^3		
Z	2		
Density	1.96 g cm^{-3}		
Linear Absorption Coefficient	22.06 cm^{-1}		
Radiation	Mo-K_α (λ = 0.71069Å)		
Standard Reflections	1 0 4, 3 -2 -1, 2 -2 3		
Decay of Standards	5%		
2ϑ Range	2-50°		
Number of Parameters Varied	157		
R	0.0375		
R_w	0.0396		
Goodness of Fit	1.13		
F(000)	336		
Residual Electron Density	14.7		

Table 2.5 Selected Bond Lengths (Å) and Angles (°) for $\{Sn[O\text{-}4\text{-}NO_2\text{-}C_6H_3O][OC_4H_8]\}_n$

Distances and Angles Around Sn

Atoms	Distance	Atoms	Distance
Sn-O(1)	2.208(4)	Sn-O(1')	2.430(5)
Sn-O(2)	2.112(4)	Sn-O(2")	2.607(4)
Sn-O(5)	2.535(6)		

Atoms	Angle	Atoms	Angle
O(1)-Sn-O(1')	74.7(2)	O(1)-Sn-O(2)	75.6(2)
O(1)-Sn-O(2")	138.1(2)	O(1)-Sn-O(5)	78.7(2)
O(1')-Sn-O(2)	93.5(2)	O(1')-Sn-O(2")	94.4(2)
O(1')-Sn-O(5)	153.3(2)	O(2)-Sn-O(2")	64.5(2)
O(2)-Sn-O(5)	78.3(2)	O(2")-Sn-O(5)	104.5(2)

Other Bond Lengths and Angles

Atoms	Distance	Atoms	Distance
C(1)-C(2)	1.407(9)	C(1)-C(6)	1.391(9)
C(2)-C(3)	1.381(9)	C(2)-O(2)	1.351(7)
C(3)-C(4)	1.39(1)	C(3)-H(31)	1.00(1)
C(4)-C(5)	1.37(1)	C(4)-H(41)	1.11(1)
C(5)-C(6)	1.400(9)	C(5)-N(1)	1.465(8)
C(6)-H(61)	1.13(1)	C(7)-C(8)	1.49(1)
C(7)-O(5)	1.43(1)	C(8)-C(9)	1.36(2)
C(9)-C(10)	1.42(1)	C(10)-O(5)	1.39(1)
O(3)-N(1)	1.215(8)	O(4)-N(1)	1.221(9)

Atoms	Angle	Atoms	Angle
O(1)-C(1)-C(2)	117.7(6)	O(1)-C(1)-C(6)	122.2(6)
C(3)-C(2)-C(1)	120.1(6)	O(2)-C(2)-C(1)	116.9(6)
O(2)-C(2)-C(3)	122.9(6)	C(4)-C(3)-C(2)	120.9(6)
H(31)-C(3)-C(2)	122.8(10)	H(31)-C(3)-C(4)	116.2(10)
C(5)-C(4)-C(3)	118.0(6)	H(41)-C(4)-C(3)	126.6(4)
H(41)-C(4)-C(5)	115.4(4)	C(6)-C(5)-C(4)	123.7(6)
N(1)-C(5)-C(4)	118.1(6)	N(1)-C(5)-C(6)	118.2(6)
C(5)-C(6)-C(1)	117.3(6)	H(61)-C(6)-C(1)	118.6(9)
H(61)-C(6)-C(5)	123.8.(8)	O(5)-C(7)-C(8)	105.2(8)
C(9)-C(8)-C(7)	107.0(10)	C(10)-C(9)-C(8)	110.5(11)
O(5)-C(10)-C(9)	107.7(9)	Sn-O(1)-Sn	105.3(2)
C(1)-O(1)-Sn	110.8(4)	C(1)-O(1)-Sn	106.5(4)
C(2)-O(2)-Sn	115.0(4)	C(1)-O(5)-C(7)	109.4(7)
O(3)-N(1)-C(5)	119.4(7)	O(4)-N(1)-C(5)	118.0(6)
C(6)-C(1)-C(2)	120.0(6)		

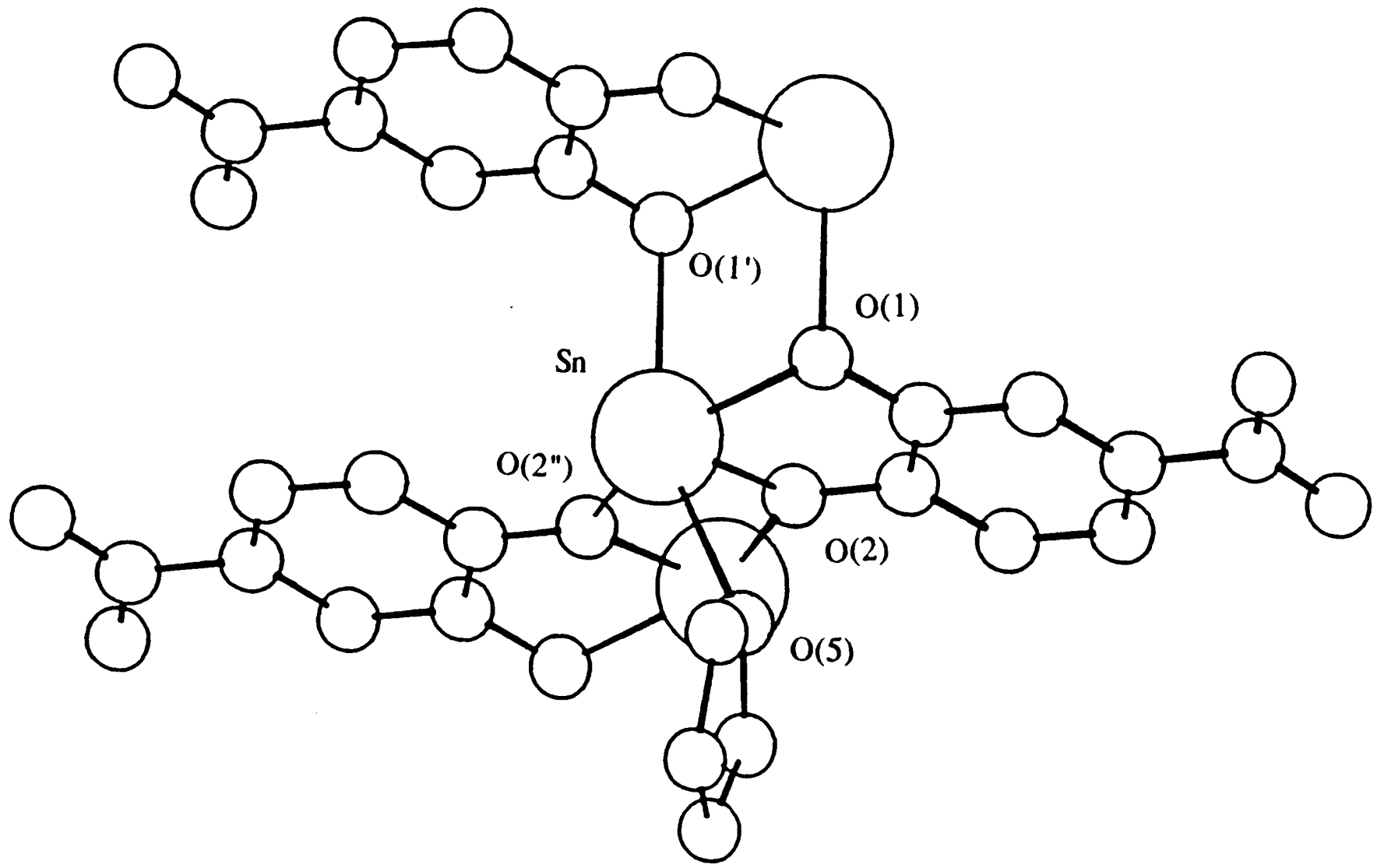


Figure 2.4 The Molecular Structure of $\{Sn[O\text{-}4\text{-}NO_2\text{-}C_6H_3O][OC_4H_8]\}_n$

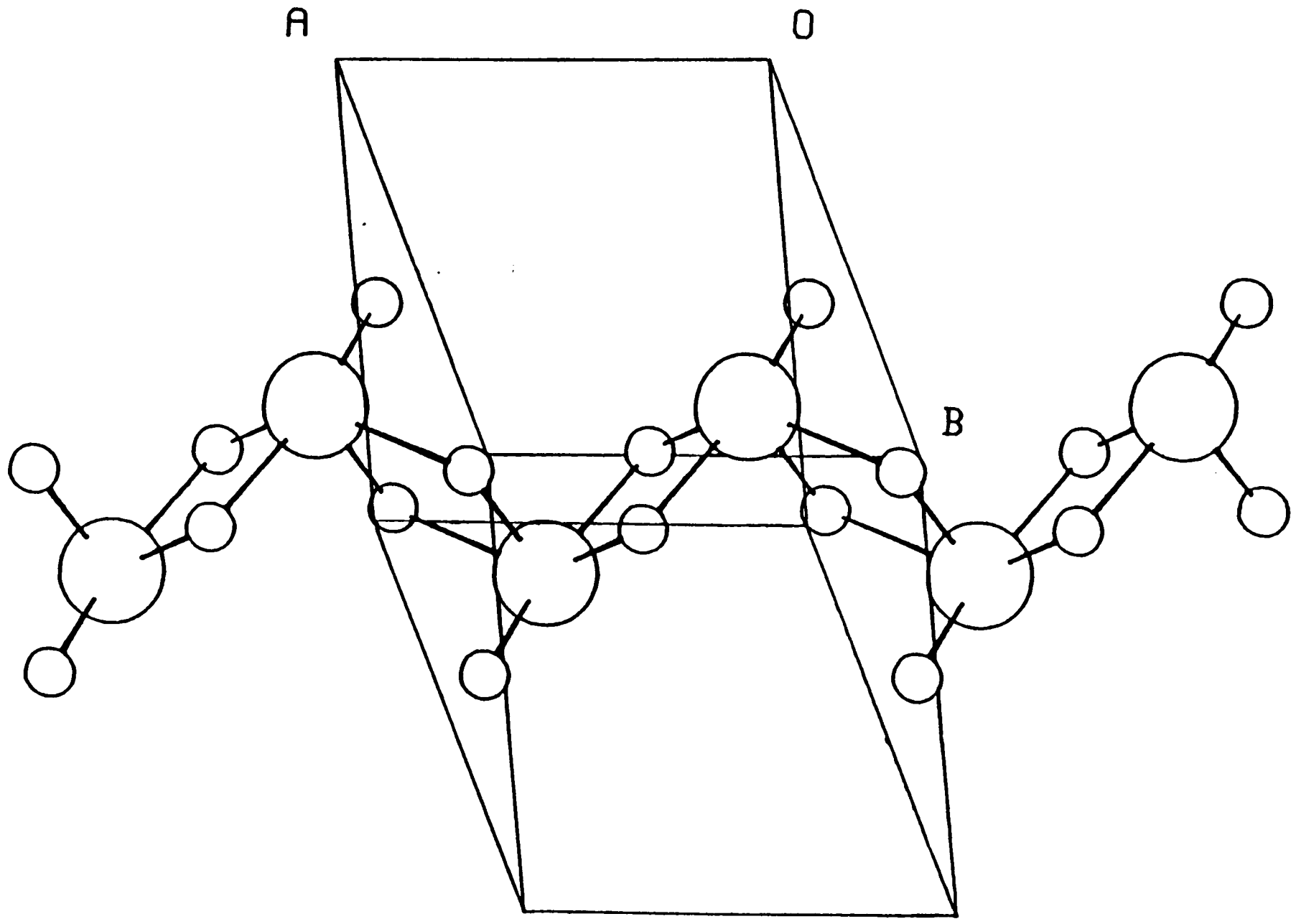


Figure 2.5 Polymeric Chain in $\{Sn[O\text{-}4\text{-}NO_2\text{-}C_6H_3O][OC_4H_8]\}_n$

(carbon atoms and nitro groups omitted for clarity)

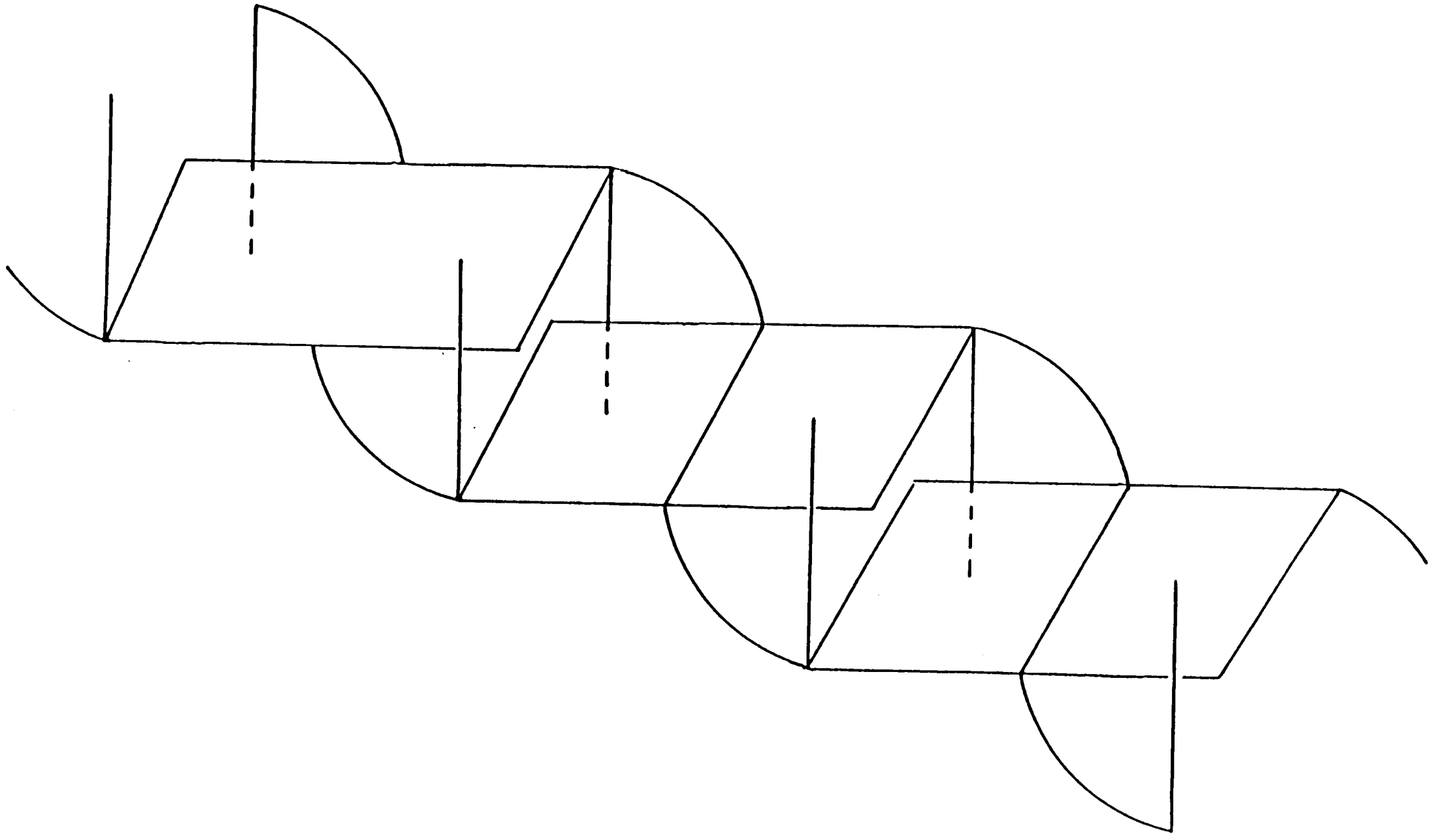


Figure 2.6 Idealized Representation of the Polymeric Chain in $\{Sn[O\text{-}4\text{-}NO_2\text{-}C_6H_3O][OC_4H_8]\}_n$

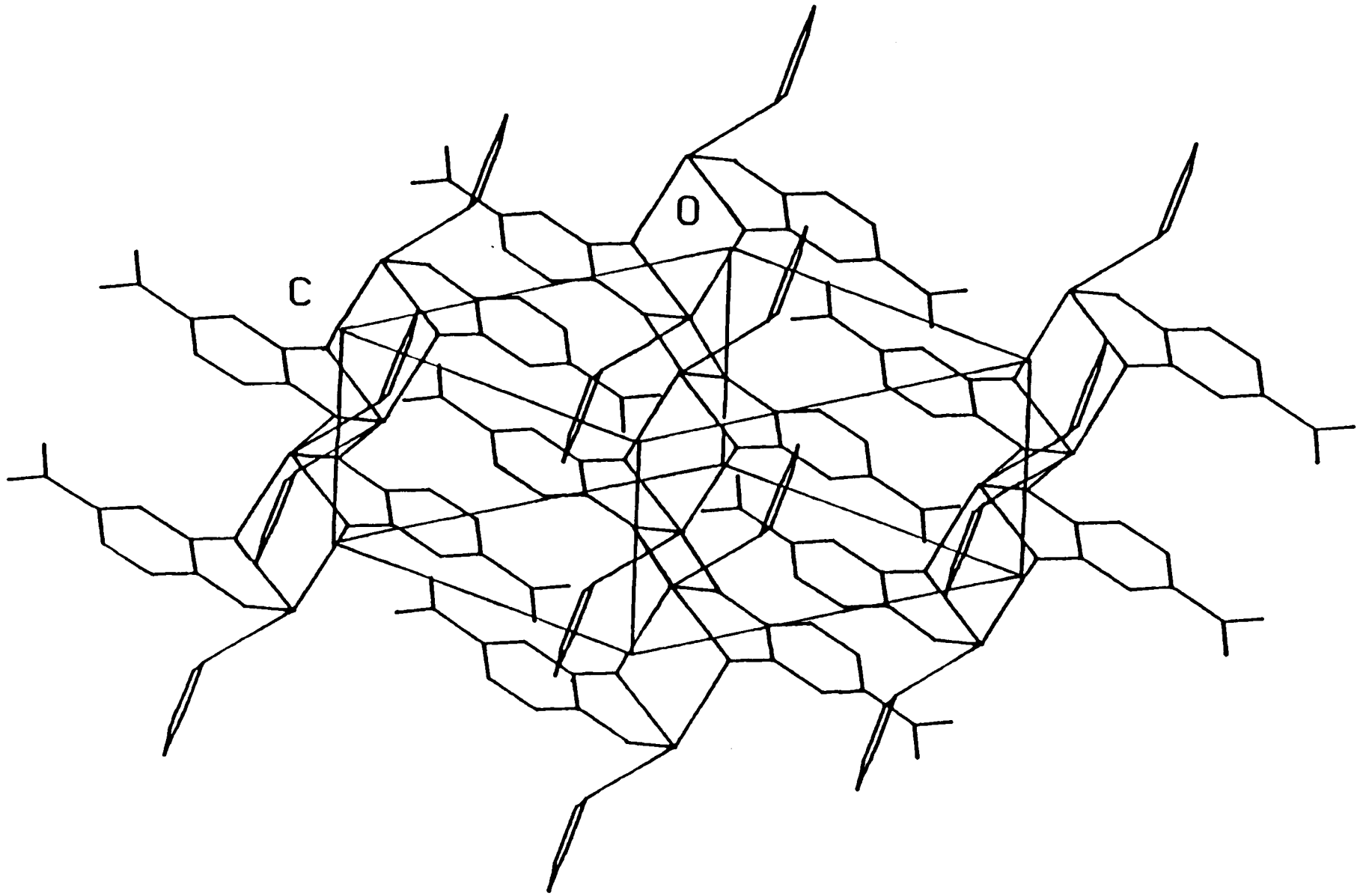


Figure 2.7 Crystal Packing in $\{Sn[O\text{-}4\text{-}NO_2\text{-}C_6H_3O][OC_4H_8]\}_n$

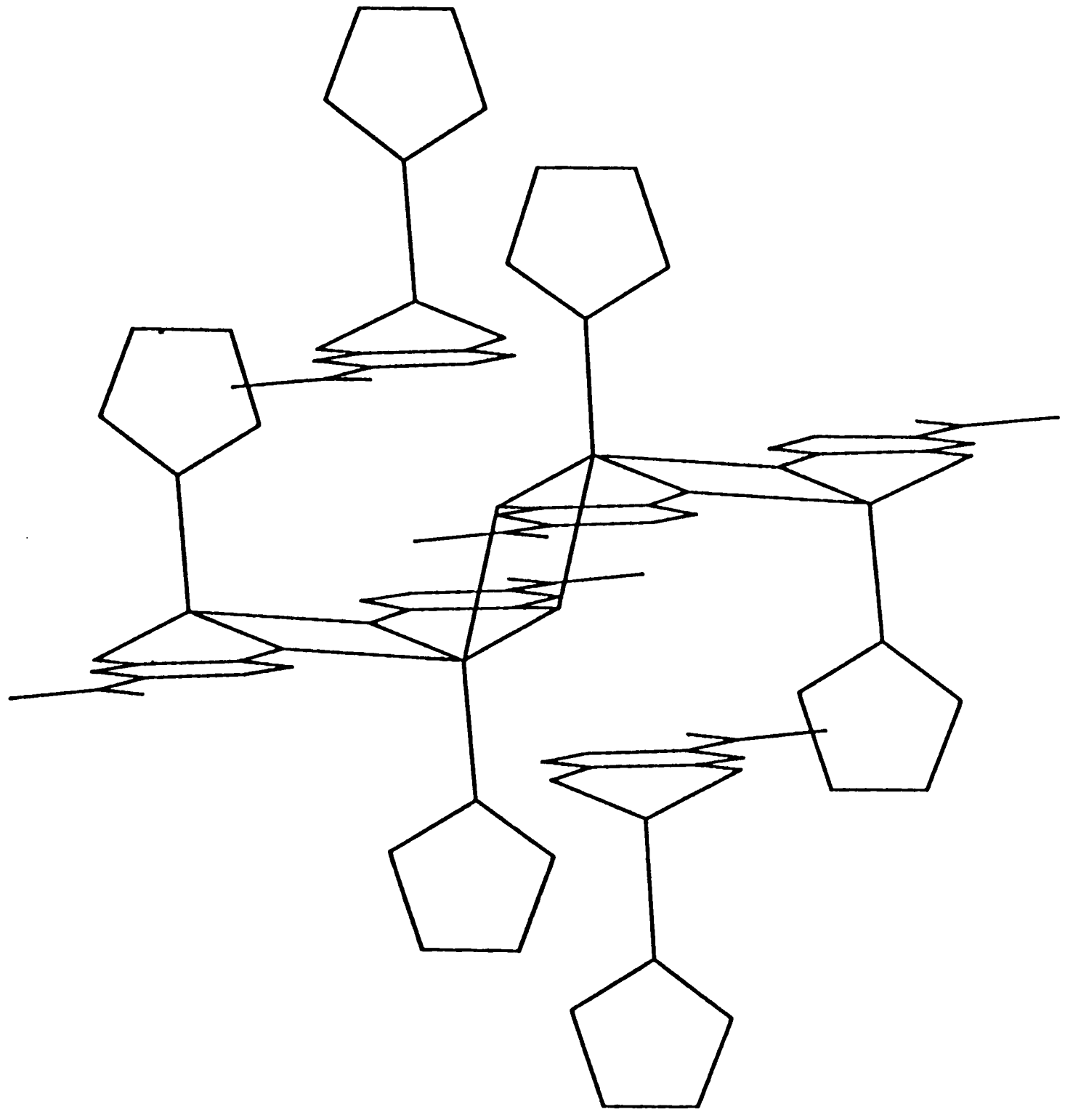


Figure 2.8 Close-up of the Packing of the Chains in $\{Sn[O\text{-}4\text{-}NO_2\text{-}C_6H_3O][OC_4H_8]\}_n$

The structure, shown in Figures 2.3 and 2.4, consists of polymeric chains of $\{Sn[O\text{-}4\text{-}NO_2\text{-}C_6H_3O][OC_4H_8]\}_n$, the monomeric units being linked by oxygen bridges from the catechol ligands and belongs to the space group P $\bar{1}$. This use of oxygen bridging is very common in tin(IV) chemistry, and has been postulated by Harrison[52] from ^{119}Sn Mössbauer data as the likely interaction between tin(II) bis(phenoxide) units. There are only two structurally characterized examples of this type of bonding between tin(II) and oxygen.

The four monomeric units making up $[SnO(N^tBu)SiMe_2]_4$[57], interact forming a ring (see Figure 2.9).

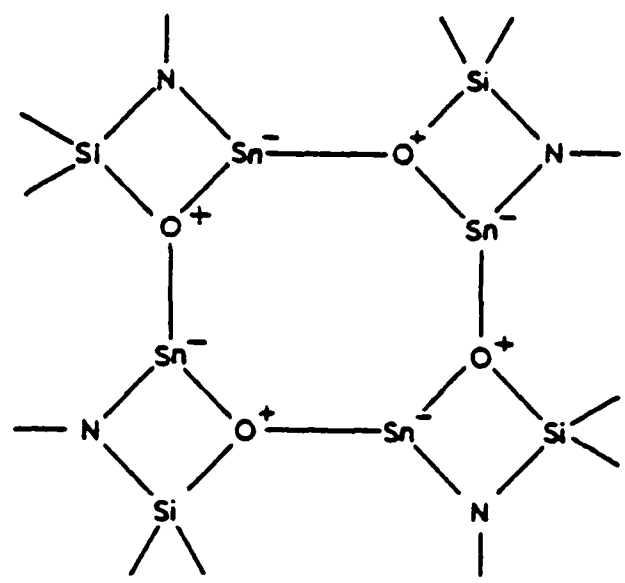


Figure 2.9 The Intramolecular Tin(II)-Oxygen Bonding in $[SnO(N^tBu)SiMe_2]_4$

Whilst the polymer, $\{Sn[OC_2H_4O]\}_n$[55] which crystallizes in a rhombohedral point group, and has a cross-linked arrangement of tin-oxygen rings about a three-fold symmetry axis.

The coordination around each tin(II) atom in $\{Sn[O\text{-}4\text{-}NO_2\text{-}C_6H_3O][OC_4H_8]\}_n$ may be described as very distorted square pyramidal. The tin-oxygen bonds for the catechol ligands, at 2.208(4)Å and 2.112(4)Å, are significantly shorter than the bond to the tetrahydrofuran oxygen O(5) at 2.535(4)Å. The tin-oxygen bond *para* to the nitro group is shorter than the other tin-oxygen catechol bond. As expected, the tin-oxygen bond lengths are longer than those found in tin(IV) catechol complexes, which fall in the range 1.995(8)Å to 2.10(1)Å [21].

The monomeric units of $\{Sn[O\text{-}4\text{-}NO_2\text{-}C_6H_3O][OC_4H_8]\}_n$ are linked together by long tin-oxygen bonds, Sn-O(1') 2.430(4)Å and Sn-O(2") 2.607(4)Å to generate infinite polymeric chains. These long intermolecular bonds must contribute to the ease of dissociation of the polymeric chain in donor solvents. The square pyramid is severely distorted as a result of the small bite angle of the catechol ligand and the stereochemical consequences of the lone pair on tin(II). The O(1)-Sn-O(2) angle is 75.6(2)°. This maybe compared with O-Sn(IV)-O in tin(IV) catechol compounds which lie between 81.4(2)° [58] and 83.6(3)°.

The basal plane of the distorted square pyramid in $\{Sn[O\text{-}4\text{-}NO_2\text{-}C_6H_3O][OC_4H_8]\}_n$ defined by O(1), O(1'), O(2") and O(5) has two angles which deviate a large amount from the ideal 180° [O(1)-Sn-O(2") 138.1(2)° and O(1')-Sn-O(5) 153.3(2)°]. The apex of the square pyramid is defined by O(2) and the remaining angles which ideally should be 90° vary from 64.5(2)° to 104.5(2)°. The manner in which the pyramidal units are linked to form the polymeric chains is represented in an idealized fashion in Figure 2.5. Pairs of square pyramids are linked by basal oxygen atoms O(1) and O(1') in a centrosymmetric fashion about a crystallographically imposed centre of symmetry at the midpoint of the common edge. The monomeric units are also linked by apical-basal bridges, about a second centre of symmetry, via O(2) and O(2"). Since each tin is in a chiral environment, this packing mode requires an alternation of the enantiomeric forms of the asymmetric unit along the chain.

2.3.5 A Theoretical Analysis of the Bonding in $\{Sn[O\text{-}4\text{-}NO_2\text{-}C_6H_3O][OC_4H_8]\}_n$

In order to explain the structural features, and the physical properties of $\{Sn[O\text{-}4\text{-}NO_2\text{-}C_6H_3O][OC_4H_8]\}_n$, an analysis of the bonding in $\{Sn[O\text{-}4\text{-}NO_2\text{-}C_6H_3O][OC_4H_8]\}_n$was performed. The main points of interest were as follows.

Firstly, the nature of the bonding involved between the catecholate dianion and tin(II). Model fragments of catecholatotin(II) and dihydridotin(II) were compared, noting what (if any) is the significance in the change of ligand upon bonding and the tin lone pair. Secondly, the effect of adding the nitro-group to the aromatic ring was investigated. Thirdly, the role played by the coordinated solvent molecule was examined. In the model compounds the

tetrahydrofuran was modelled by a water molecule. Finally, the effect of polymerization on the bonding was considered. The compound was considered to consist of three fragments, the central tin atom coordinated to tetrahydrofuran, whilst the outer tin atoms were bound to water molecules.

Extended Hückel calculations were employed[59]. This is a semi-empirical method and the Hamiltonian elements, H_{ij}, are not evaluated explicitly, but calculated from experimental parameters. It provides an estimate of the relative energies and the approximate forms of the π-molecular orbitals.

2.3.5.1 Nature of the Bonding in Dihydridotin(II) and Catecholatotin(II)

The molecular orbitals of the following two model systems were compared (Figure 2.10). The atoms in these and in subsequent model compounds all lie in the xy-plane, the x-axis bisecting the X-Sn-X angle.

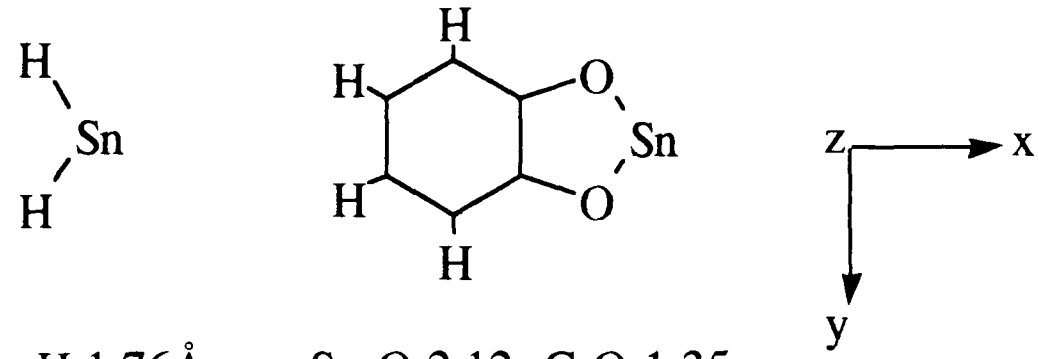
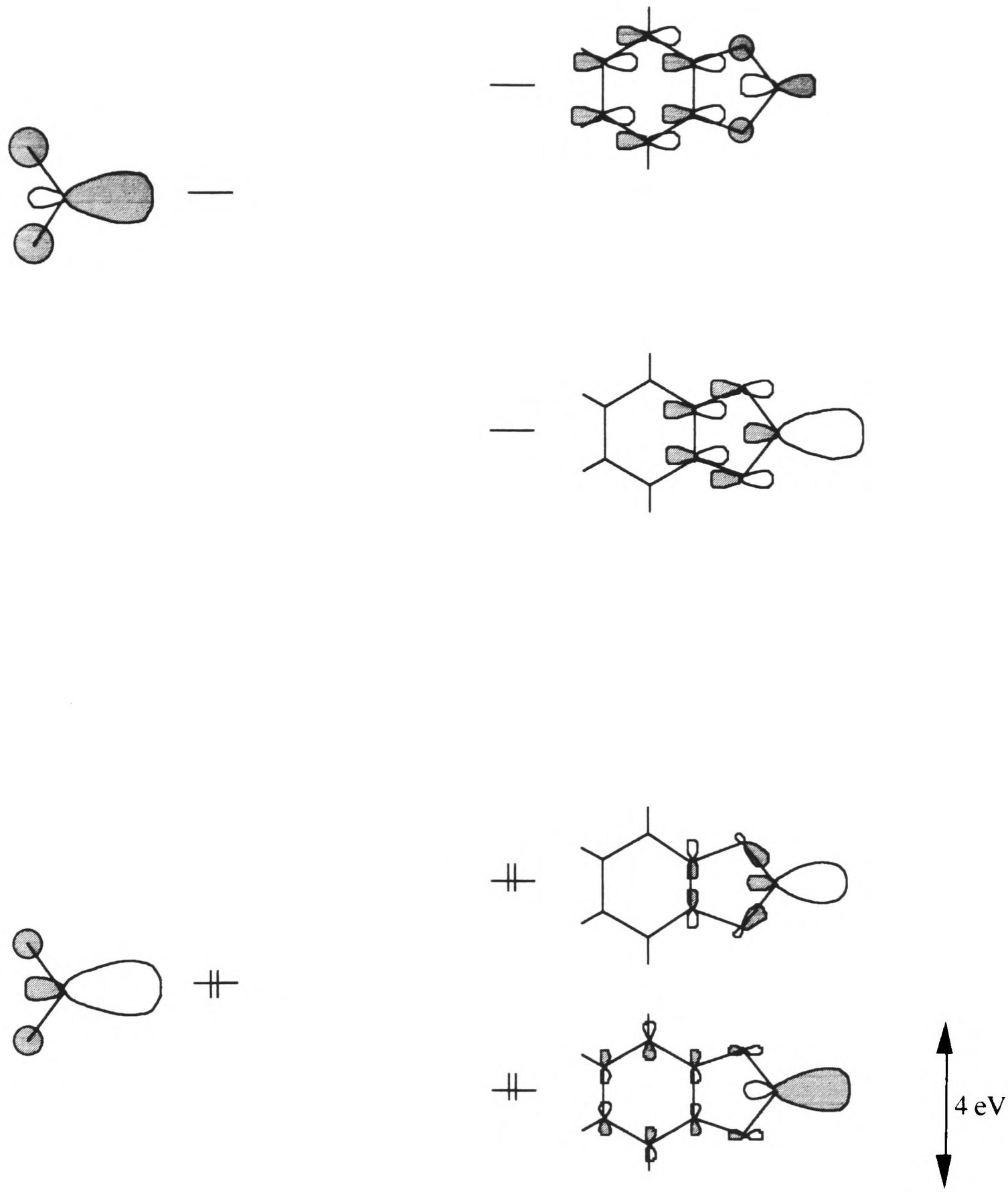


Figure 2.10 Models of Tin(II) Dihydride and Catecholatotin(II)

The bond lengths and angles of SnH_2 were those obtained from geometrically optimised *ab initio* molecular orbital calculations for the singlet state[60,61].

It was found that the tin-oxygen bond has only a small covalent component, whilst analysis of the atomic net charges shows that it is largely ionic in character. The LUMO and HOMO of catecholatotin(II) are mainly localized on the aromatic ring. On the left hand side of Figure 2.11 the molecular orbital which can be associated with the tin "lone pair" is

illustrated. It is the HOMO of the molecule. The related Sn-H antibonding orbital is also shown. The corresponding orbitals in catecholatotin(II) are illustrated on the right hand side of the figure. The tin lone pair is stabilized (with respect to SnH_2) by mixing of the tin p_x and oxygen p_x and p_y atomic orbitals, increasing the s-character of the lone-pair, but delocalizing it into two pairs of molecular orbitals (see Figure 2.11).



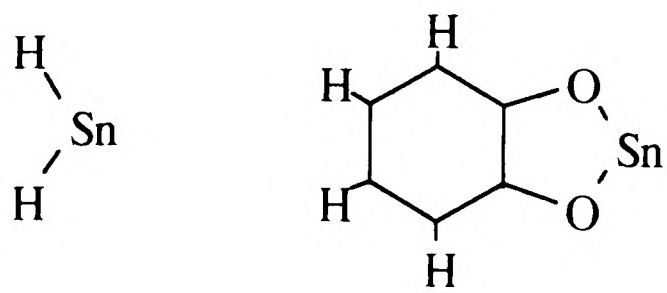
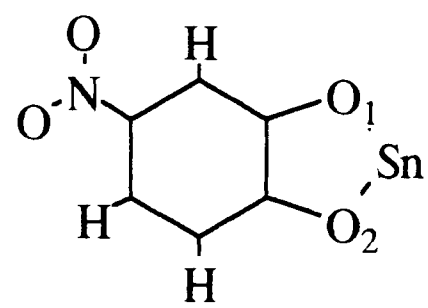


Figure 2.11 Effect of Catecholate Upon Tin Lone Pair

2.3.5.2 Introduction of Nitro Group

The introduction of the nitro group, to generate the molecule shown in Figure 2.12 does not effect the strength of the covalent bonds between tin and oxygen, but the net charge on the oxygen *para* to the nitro group, O_2 is reduced, from -1.10 to -1.08, whilst the net charge for O_1 remains unaltered at -1.10.

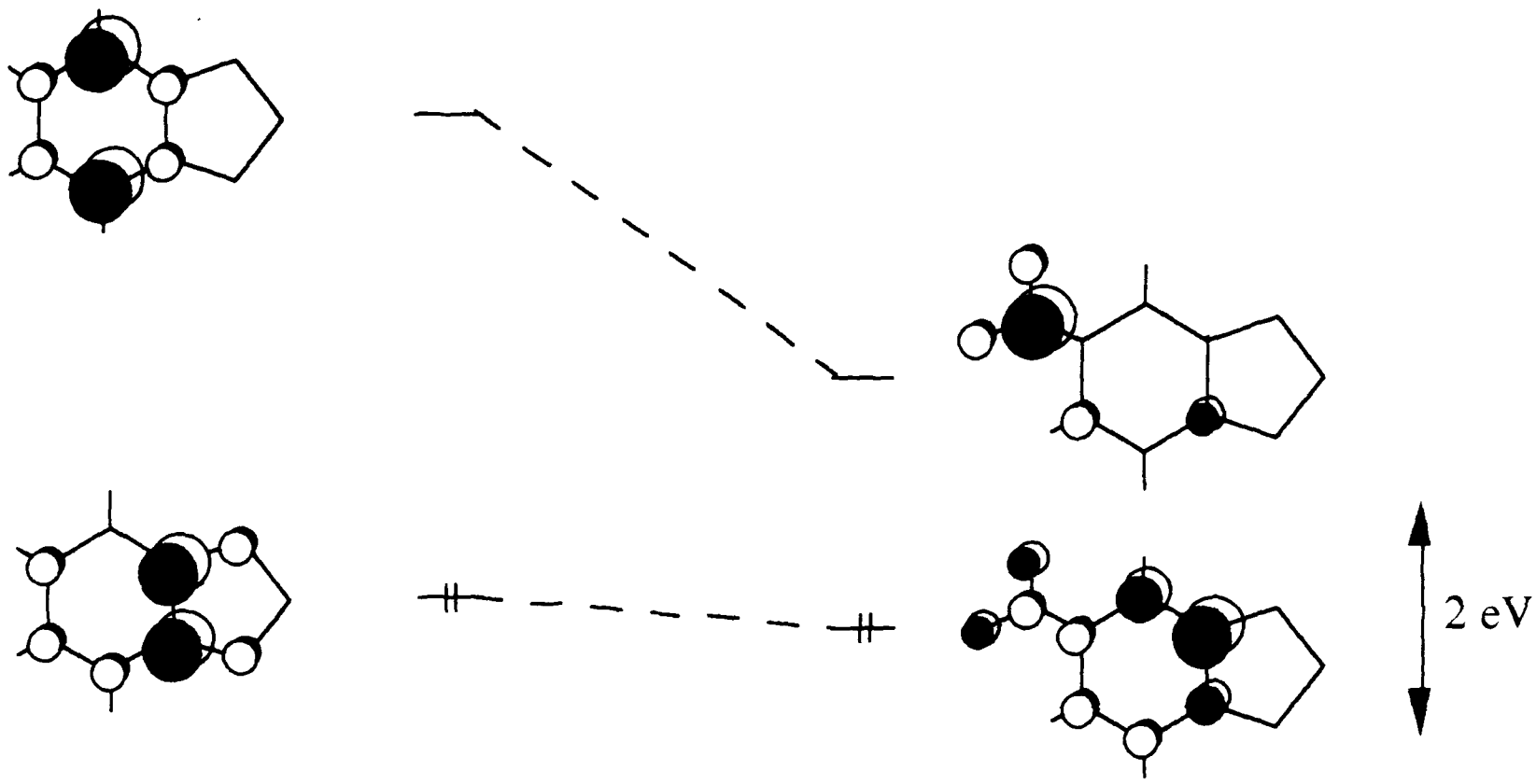


N-C 1.20, N-O 1.21Å

Figure 2.12 The Model Fragment 4-Nitrocatecholatotin(II)

This weakening of the ionic interaction between O_2 and tin is not reflected in the observed bond lengths in $\{Sn[O\text{-}4\text{-}NO_2\text{-}C_6H_3O][OC_4H_8]\}_n$, in fact quite the reverse, since Sn-O_2 is 0.096Å shorter than Sn-O_1.

Since there is no change in the covalent interaction between the oxygens, O_1, O_2 and tin, there is no change in the molecular orbitals describing the tin lone pair, the nitro-group interacting predominantly with the LUMO and HOMO (Figure 2.13).



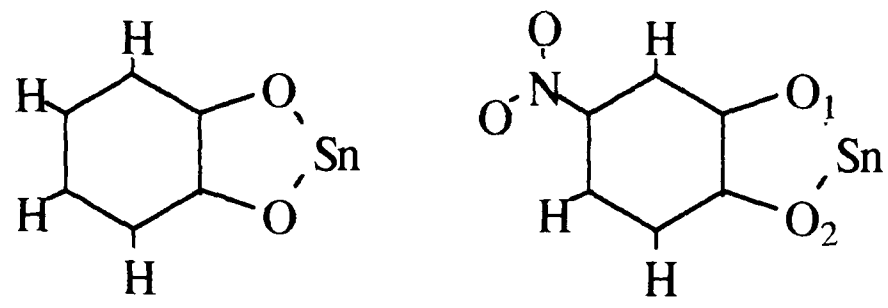
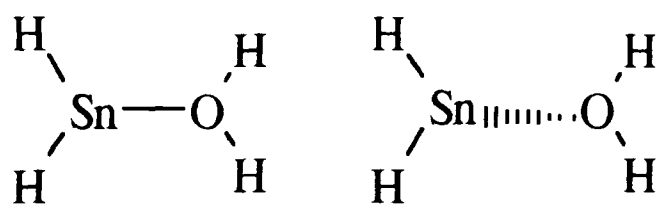


Figure 2.13 Effect of Nitro-group upon LUMO and HOMO

2.3.5.3 Effect of Coordinated Solvent

The effect of the solvent molecule was first studied in isolation by considering the interaction of dihydridotin(II) and water. The water was placed in the xy-plane (a), or perpendicular to tin (b), as shown in Figure 2.14.



(a) (b)

Sn-O 2.10, O-H 1.00Å
H-O-H 104°

Figure 2.14 Models Used to Study the Effect of Water upon Tin(II) Dihydride

In both cases there is only a weak covalent interaction between tin and the water molecule, the main interaction again being ionic. The net charge on tin is reduced from 0.70 to 0.46 in (b) whilst in (a) the change is considerable, leaving tin with a net charge of only 0.06. This is due to interaction with the tin lone pair. The compound with water perpendicular to the SnH_2 plane is the much more stable arrangement, by 4.3 eV. In this geometry there is a much stronger donor-acceptor interaction with the p_z orbital perpendicular to the SnH_2 plane (see Figure 2.15).

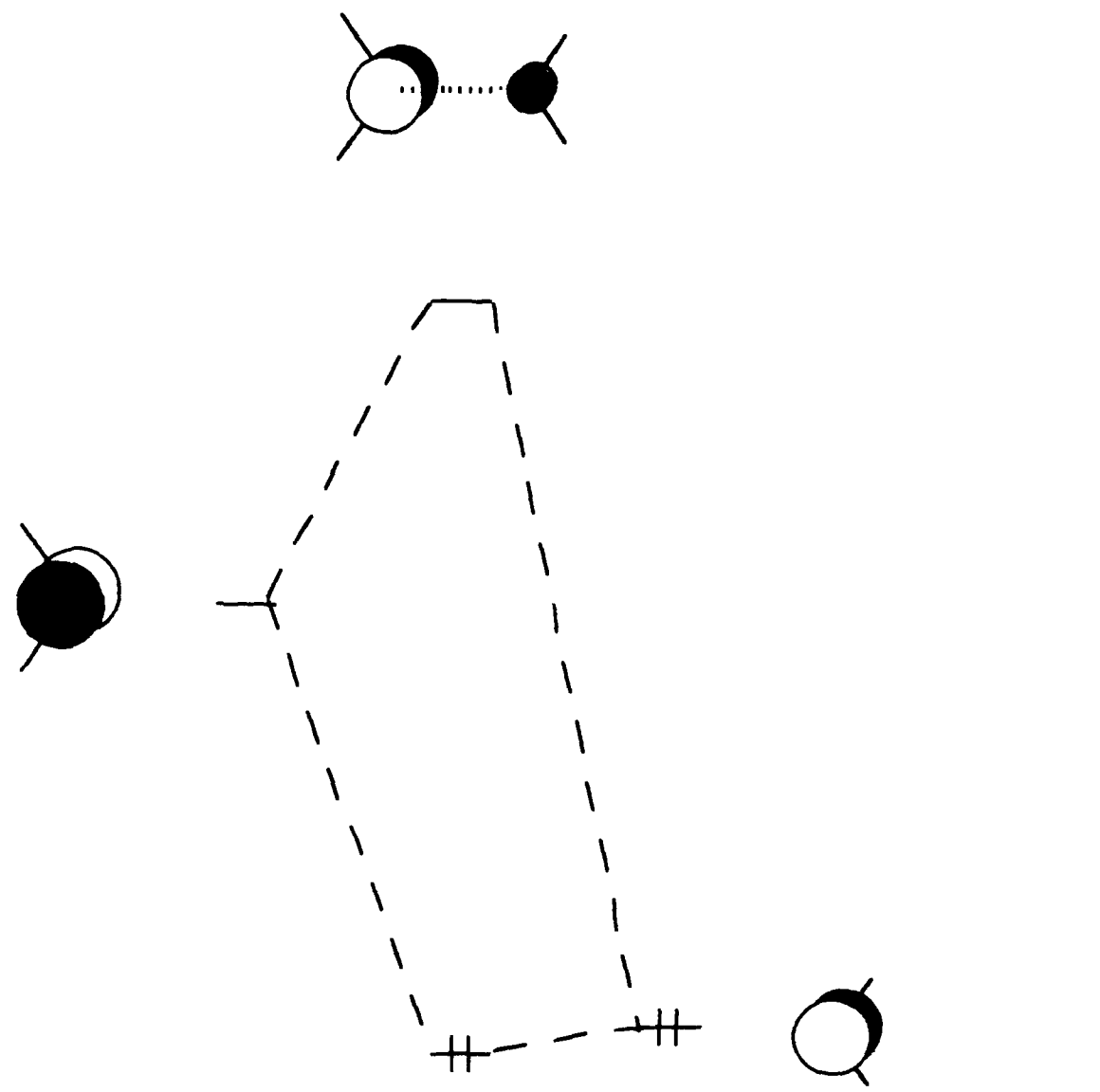
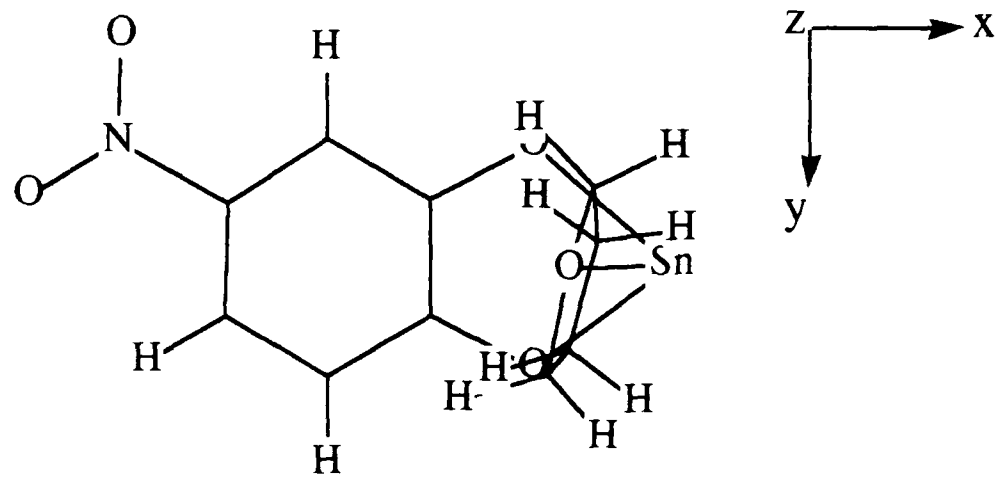


Figure 2.15 Molecular Orbitals Showing Enhanced Stability of Model (b) Fragment

From the above analysis we see that donor solvents would tend to bind perpendicularly to the tin centre. In $\{Sn[O\text{-}4\text{-}NO_2\text{-}C_6H_3O][OC_4H_8]\}_n$ this is indeed the case, with tetrahydrofuran taking up a position above the catecholatotin(II) plane, at an angle of 79°.

A model compound, $Sn[O\text{-}4\text{-}NO_2\text{-}C_6H_3O][OC_4H_8]$ was then analysed with the tetrahydrofuran placed at the distace and orientation found in the polymer $\{Sn[O\text{-}4\text{-}NO_2\text{-}C_6H_3O][OC_4H_8]\}_n$ (see Figure 2.16).



Sn-O(thf) 2.54Å

O_1-Sn-O(thf) 78.7, O_2-Sn-O(thf) 78.3°

Figure 2.16 Model Fragment $Sn[O\text{-}4\text{-}NO_2\text{-}C_6H_3O][OC_4H_8]$

Due to the large increase in the distance between the donor oxygen molecule, O(thf), and the tin atom, the covalent interaction is very weak. Furthermore the donor-acceptor interaction described in section 2.3.5.3 is now very small and there is no interaction with the tin lone pair. Since the tetrahydrofuran does not adopt a mean position along the x-axis, but lies closer to O_2 (O_2-O(thf) 2.95Å) than O_1 (O_1-O(thf) 3.02Å), the symmetry up to now observed in the interactions between O_1, O_2 and tin (the nitro-group as we have shown having no effect) is broken, whilst the interaction between O_2 and tin is enhanced. The Sn-O(2) overlap population increasing from 0.27 to 0.28, whilst the Sn-O(1) overlap population decreases, from 0.27 to 0.23.

The introduction of the terahydrofuran also leads to increased electron density at both O_1 (from -1.10 to -1.14) and O_2 (from -1.08 to -1.09). The disparity between the charges on O(1) and O(2) increasing due to the greater covalent character of the Sn-O_2 bond.

2.3.5.4 Effect of Polymerization

The fragment used to model the polmeric chain is shown in figure 2.17. It consists of a chain of three catecholatotin(II) monomers, the outer tin atoms bound to water molecules, whilst the central tin is bound to tetrahydofuran. The intramonomer bond lengths and angles are those of $\{Sn[O\text{-}4\text{-}NO_2\text{-}C_6H_3O][OC_4H_8]\}_n$, and can be found in section 2.3.4.

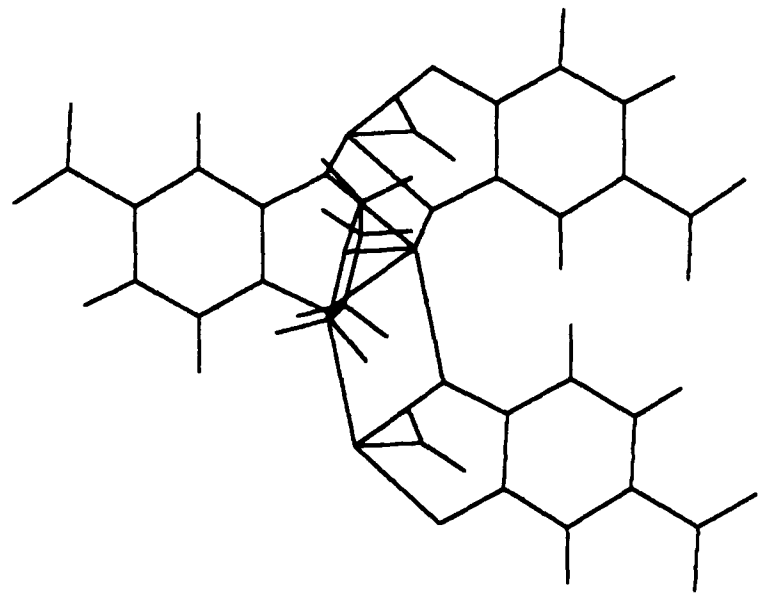


Figure 2.17 The Polymer Model Fragment

The covalent interaction upon polymerization is very small, the overlap populations between Sn_1 and O_1, and O_2" are 0.09 and 0.05 respectively. These interactions (involving the tin p_y and p_z and oxygen p_y and p_z atomic orbitals) are significant enough to raise in energy the molecular orbitals describing the lone pair (an average increase of 0.05eV), allowing the one of highest energy to become the HOMO The increase in bond order on polymerization significantly changes the charge populations of O_1, O_2, O(thf) and Sn (see Table2.6).

Table 2.6 Net Charges for O_1, O_2, O(thf) and Sn in Monomer and Polymer

	Net Charges	
	Monomer	**Polymer**
O_1	-1.14	-1.07
O_2	-1.09	-1.03
O(thf)	-0.72	-0.76
Sn	1.42	1.33

The change is most pronounced for O_1 and accounts for the difference in the strength of the intramolecular tin-oxygen bonds in $\{Sn[O\text{-}4\text{-}NO_2\text{-}C_6H_3O][OC_4H_8]\}_n$. The bond length for Sn-O(2") is 2.607Å, whilst Sn-O(1') is only 2.430Å, a difference of 0.177Å. This reduction in net charge cancels out the contribution of the tetrahydrofuran. The difference in net charge between O_1 and O_2 is restored to its value before the introduction of the tetrahydrofuran (see section 2.3.5.3), but significantly at an overall reduced level . The slip of the tetrahydrofuran from a mean position now becomes even more significant. The overlap population between O_1 and Sn is reduced still further, from 0.23 in the monomer to 0.20 in the polymer, whilst the value for Sn-O_2 remains at 0.28. The overlap between Sn and O_2 must now be significant enough to outweigh the charge imbalance, resulting in the Sn-O(1) and Sn-O(2) bond lengths in $\{Sn[O\text{-}4\text{-}NO_2\text{-}C_6H_3O][OC_4H_8]\}_n$.

2.3.5.5 Summary of Bonding Analysis of $\{Sn[O\text{-}4\text{-}NO_2\text{-}C_6H_3O][OC_4H_8]\}_n$

The bonding between 4-nitrocatecholate and tin is mainly ionic in character. The tin lone pair is based upon the tin 5s atomic orbital. Upon mixing with oxygen p_x and p_y orbitals, the lone pair is delocalized into two molecular orbitals one becoming the HOMO upon polymerization.

The nitro group interacts strongly with the catecholate ligand, but has little effect upon the tin lone pair. Since the LUMO and HOMO of the monomeric unit are predominantly based upon the interaction of the nitro group with the catecholate ligand, on polymerization the

intermonomer interactions are much weaker resulting in the increased solubility of the polymer.

The tetrahydrofuran sits in the energetically more stable position above the catecholatotin(II) plane, via a weak donor-acceptor interaction with the empty p_z tin atomic orbital. The asymmetric position adopted by the terahydrofuran molecule is the cause of the increase in overlap population between tin and O(2) and the resulting shortening of the Sn-O(1) bond.

2.4 Summary

The general synthetic methods employed for the formation of tin(II)-oxygen heterocycles was outlined. A range of catecholate and related complexes of tin(II) were synthesized and the role of the substituent was investigated with regard to their physical properties, especially their solubilities. The use of 4-nitrocatechol leads to a soluble product, $\{Sn[O\text{-}4\text{-}NO_2\text{-}C_6H_3O][OC_4H_8]\}_n$, which enabled it to be studied spectroscopically and its solid state structure to be determined. The nature of the bonding in $\{Sn[O\text{-}4\text{-}NO_2\text{-}C_6H_3O][OC_4H_8]\}_n$ and the effect of the nitro group and solvent were investigated using Extended Hückel molecular analysis.

2.5 References

1. J. Reedjik, *Struct. Bonding,* 1987, **67**, 53.
2. S. J. Lippard and A. L. Pinto, *Biochim. Biophys. Acta,* 1985, **780**, 167.
3. S. G. de Almeida, N. P. Farrell and K. A. Skov, *J. Am. Chem. Soc.,* 1988, **110**, 5018.
4. D. Gibson, S. J. Lippard, S. E. Sherman and A. H. -J. Wang, *J. Am. Chem. Soc.*, 1988, **110**, 7368.
5. K. J. Ahmed, B. E. Bowler, L. S. Hollis, S. J. Lippard, W. I. Sundquist and E. E. Whang, *J. Am. Chem. Soc.*, 1989, **111**, 1299.

6. N. M. Kostic, *Comments Inorg. Chem.,* 1988, **8**, 137.

7. I. Haiduc and C. Silvestru, *Coord. Chem. Rev.,* 1990, **99**, 253.

8. P. B. Hitchcock, M. F. Lappert and M. C. Misra, *J. Chem. Soc., Chem. Commun.,* 1985, 863.

9. W. Petz, *Chem. Rev.,* 1986, **86**, 1019.

10 M. S. Holt, J. H. Nelson and W. L. Wilson, *Chem. Rev.,* 1989, **89**, 11.

11. *Chemistry of Tin*, ed. P. G. Harrison, Blackie, London 1989.

12 N. F. Cardarelli, *Si. Ge. Tin and Lead Compds.,* 1986, **9**, 307.

13. A. J. Crowe, *Drugs for the Future,* 1987, **12**, 255.

14. M. Gielen, E. Joosen, T. Mancilla, J. Ramharter and R. Willem, *Si. Ge. Tin and Lead Compds.,* 1986, **9**, 349.

15. F. Huber and A. K. Saxena, *Coord. Chem. Rev.,* 1989, **95**, 109.

16. G. Atassi, A. J. Crowe and P. J. Smith, *Chem.-Biol. Interact.,* 1980, **32**, 171.

17. G. Atassi, A. J. Crowe and P. J. Smith, *Inorg. Chim. Acta,* 1984, **93**, 179.

18. G. Atassi, *Revs. Si. Ge. Tin and Lead Compounds,* 1985, **2-3**, 219.

19. G. Alonzo, G. Atassi, R. Barbieri, L. Carl, F. Di Bianca, S. Filippeschi, F. Huber, E. Rivarola, G. Roge, G. Ruisi, A. Silvestri and F. Spreafico, *J. Chem. Soc., Dalton Trans.,*1985, 523.

20. G. Atassi, R. Barbieri, F. Huber, L. Pellerito, M. T. Lo Giudice and G. Ruisi, *Inorg. Chim. Acta,* 1982, **66**, 39.

21. S. Ozaki and H. Sakai, *Jpn. Pat.,*1975, 76100089.

22. H. A. Budding, E. J. Bulten, A. M. J. Liebregts and H. A. Meinema, *Revs. Si. Ge. Tin and Lead Compounds,* 1985, **2-3**, 157.

23. V. Cooper, J. H. Nelson and R. W. Rudolph, *J. Inorg. Nucl. Chem.,* 1980, **16**, 263.

24. N. W. Alcock and J. H. Nelson, *Inorg. Chem.,* 1982, **21**, 1196.

25. P. G. Antonov, F. K. Egorov, Y. P. Kosticov, Y. N. Kukushkin and V. G. Shtrele, *Zh. Neorg. Khim.,* 1982, **27**, 3130.

26. A. Albinati, P. S. Pregosin and H. Rüegger, *Angew. Chem. Int. Ed. Engl.,* 1984, **23**, 78.

27. J. V. Kingston and G. R. Scollary, *J. Chem. Soc.A*, 1971, 3765.

28. J. V. Kingston and G. R. Scollary, *J. Chem. Soc.D*, 1970, 362.

29. A. Albinati, P. S. Pregosin and H. Rüegger, *Inorg. Chem.*, 1984, **23**, 3223.

30. A. Albinati, P. S. Pregosin, H. J. Rüegger and U. Von Gunten, *J. Organomet. Chem.*, 1985, **295**, 239.

31. V. L. Bogdashkina, A. B. Permin, V. S. Petrosyan, O. A. Reutov and Y. E. Zubarev, *Isv. Akad. Nauk. SSSR, Ser. Khim.*, 1980, **12**, 2840.

32. A. Berton, C. Botteghi, A. Scrivanti and L. Toniolo, *J. Organomet. Chem.*, 1988, **344**, 261.

33. K. R. Koch, *S. Afr. J. Chem.*, 1983, **36**, 89.

34. M. C. Grossel, R. P. Moulding and K. R. Seddon, *Inorg. Chim. Acta*, 1982, **64**, L275.

35. P. S. Pregosin and H. Rüegger, *Inorg. Chem.*, 1987, **26**, 2912.

36. R. V. Lindsey, G. W. Parshall and U. G. Stolberg, *Inorg. Chem.*, 1966, **5**, 109.

37. J. D. Cotton, P. J. Davidson and M. F. Lappert, *J. Chem. Soc., Dalton Trans*, 1976, 2275.

38. O. Rectenwald and M. Veith, *Topics in Current Chemistry*, **104**, 1, Springer-Verlag 1982.

39. M. Veith, *Z. Naturforsch*, 1978, **33b**, 7.

40. M. F. Lappert, P. P. Power and M. J. Slade, *J. Chem. Soc., Chem. Commun.*, 1979, 368.

41. B. Chetinkaya, *J. Am. Chem. Soc.*, 1980, **102**, 2088.

42. K. Jurkschat and A. Tzschach, *Rev. Si. Ge. Tin and Lead Compds.*, 1986, **9**, 263.

43. P. F. R. Ewings and P. G. Harrison, *J. Chem. Soc., Dalton Trans.*, 1975, 1717.

44. A. B. Cornwell and P. G. Harrison, *J. Chem. Soc., Dalton Trans.*, 1975, 1722.

45. A. I. Ioffe and O. M. Nefedov, *Mendeleev Chem. J.*, 1979, **24**, 475.

46. M. M. Olmstead and P. P. Power, *Inorg. Chem.*, 1984, **23**, 413.

47. J. J. Zuckerman, *J. Chem. Soc.*, 1963, 1322.

48. H. J. Emeléus and J. J. Zuckerman, *J. Organomet. Chem.*, 1964, **1**, 328.

49. H. M. Haendler and J. S. Morrison, *J. Inorg. Nucl. Chem.*, 1967, **29**, 393.

50. G. T. Cocks and J. J. Zuckerman, *Inorg. Chem.*, 1965, **4**, 592.

51. D. E. Fenton, R. R. Gould, P. G. Harrison, K. C-T. Sze and J. J. Zuckerman, *Inorg. Chim. Acta.*, 1970, *4*, 234.

52. P. F. R. Ewings and P. G. Harrison, *J. Chem. Soc., Dalton Trans.*, 1975, 2015.

53. W. D. Honnick and J. J. Zuckerman, *Inorg. Chem.*, 1978, **17**, 501.

54. J. Augé and G. Bourleaux, *J. Organomet. Chem.*, 1989, **377**, 205.

55. R. Nesper and H. G. von Schnering, *Z. Naturforsch.*, 1982, **37b**, 1144.

56. H. E. Mabrouk and D. G. Tuck, *J. Chem. Soc., Dalton Trans.*, 1988, 2539.

57. M. Grosser and M. Veith, *J. Organomet. Chem.*, 1982, **229**, 247.

58. This work, Chapter 5.

59. The Extended Hückel programmes at Oxford were run on the TRIBBLE system on the VAX cluster. The calculation programme used was FMO80.

60. G. Olbrich, *Chem. Phys. Lett.*, 1980, **73**, 110.

61. T. Fjeldberg, A. Haaland, M. F. Lappert, B. E. R. Schilling and A. J. Thorne., *J. Chem. Soc., Dalton Trans.*, 1986, 1551.

62. J. A. Montgomery, *J. Med. Chem.*, 1982, **25**, 626.

63. G. V. B. Madhaven and J. C. Martin, *J. Org. Chem.*, 1986, **51**, 1287.

64. P. G. Harrison and S. R. Stobart, *J. Chem. Soc., Dalton Trans.*, 1973, 940.

Chapter 3

Reactions of the Novel Tin(II) Compounds $\{Sn[O\text{-}4\text{-}NO_2\text{-}C_6H_3O][OC_4H_8]\}_n$ and $Sn[OC_6Cl_4O][OC_4H_8]$

3.1 Introduction

The insolubility of previously prepared tin(II)-oxygen heterocycles has severely restricted the study of their chemistries. The enhanced solubilities of $Sn[OC_6Cl_4O][OC_4H_8]$ and $\{Sn[O\text{-}4\text{-}NO_2\text{-}C_6H_3O][OC_4H_8]\}_n$ has made it possible to investigate their chemical properties. The reduction in the degree of polymerization has meant that $Sn[OC_6Cl_4O][OC_4H_8]$ is soluble in dimethylformamide and $\{Sn[O\text{-}4\text{-}NO_2\text{-}C_6H_3O][OC_4H_8]\}_n$ in a range of donor solvents.

The reactions associated with tin(II) chemistry[1,2] fall into several distinct categories and are based upon one, or a combination of the following electronic characteristics. The low-oxidation state unsaturated tin atom, the non-bonding electron pair, the polarity of the tin-ligand bond, the Lewis-base properties of the ligand and the inherent reactivity of the ligand. It is within these distinct categories that the chemical reactivity of $\{Sn[O\text{-}4\text{-}NO_2\text{-}C_6H_3O][OC_4H_8]\}_n$ is described.

3.2 Oxidative Addition

The reaction of tin(II) compounds with oxidising agents has been widely explored[1,2] and can best be described as the insertion of a six-electron system into a two-electron bond, the bond could be a single σ-bond such as C-X, C-M, M-M, X-X or S-S (where X is H or halogen), or a π-bond as found in unsaturated organic molecules, or in dioxygen.

The stability of $\{Sn[O\text{-}4\text{-}NO_2\text{-}C_6H_3O][OC_4H_8]\}_n$ with respect to oxidation appears to be high, since it shows no reactions with iodomethane, dihydrogen and substituted buta-1,3-dienes. Stronger oxidizing agents were required, and reactions were observed with

dioxygen, hydrogen peroxide, chlorine and bromine; unfortunately the products isolated did not lend themselves to unambiguous identification.

3.2.1 Synthesis of $SnI_2[O\text{-}4\text{-}NO_2\text{-}C_6H_3O][OC_4H_8]_2$

An unambiguous product was isolated from the reaction of $\{Sn[O\text{-}4\text{-}NO_2\text{-}C_6H_3O][OC_4H_8]\}_n$ with iodine. The addition of a solution of iodine in tetrahydrofuran to $\{Sn[O\text{-}4\text{-}NO_2\text{-}C_6H_3O][OC_4H_8]\}_n$ brought about an immediate reaction, which afforded after recrystallization, bright orange-brown crystals of the tin(IV)-diiodo compound, $SnI_2[O\text{-}4\text{-}NO_2\text{-}C_6H_3O][OC_4H_8]_2$ in good yield (71%).

The change in oxidation state of tin was confirmed by ^{119}Sn Mössbauer, which shows the chemical shift for $SnI_2[O\text{-}4\text{-}NO_2\text{-}C_6H_3O][OC_4H_8]_2$ is in the range expected for tin(IV). This is also reflected in its solution ^{119}Sn n.m.r. spectrum which shows a significant shift in the tin resonance to high field (+26.05 p.p.m), with respect to $\{Sn[O\text{-}4\text{-}NO_2\text{-}C_6H_3O][OC_4H_8]\}_n$, due to the loss of electron density at the tin atom, which accompanies the change in oxidation state.

Elemental analyses and solution ^1H n.m.r, both suggested that two tetrahydrofuran molecules are coordinated to the tin atom. Similar six coordinate tin(IV) compounds, viz $SnI_2[O_2R]$bipy have been synthesized by Tuck[3,4] when tin(II) catecholates prepared electrochemically were oxidised by iodine in the presence of a bidentate ligand such as 2, 2'-dipyridyl.

3.3 Reactions With Lewis Bases

The tendency for tin(II) compounds to act as Lewis acids is due to their coordinative unsaturation. Thus stability is gained by bonding covalently to a suitable donor molecule. This could be another tin(II) monomeric unit, via the tin lone-pair resulting in a tin-tin double bond, or via the ligand bound to the tin centre resulting in polymerization.

Alternatively, tin(II) compounds can form simple adducts with bases, which often stabilize the tin compound in solution (see Chapter 2).

Since $Sn[OC_6Cl_4O][OC_4H_8]$ and $\{Sn[O\text{-}4\text{-}NO_2\text{-}C_6H_3O][OC_4H_8]\}_n$ already contain weakly coordinated tetrahydrofuran, displacement was achieved by reacting them with stronger Lewis bases such as halide, or bidentate nitrogen-donor ligands.

3.3.1 Halide Stabilized Tin(II) Compounds

3.3.1.1 Synthesis of $\{[Et_3BzN][SnCl(O\text{-}4\text{-}NO_2\text{-}C_6H_3O)]\}_n$

The reaction of equimolar amounts of benzyltriethylammonium chloride and $\{Sn[O\text{-}4\text{-}NO_2\text{-}C_6H_3O][OC_4H_8]\}_n$ in tetrahydrofuran gave after crystallization an orange solid. Elemental analyses and solution n.m.r. studies confirmed the following stoichiometry, $[Et_3BzN][SnCl(O\text{-}4\text{-}NO_2\text{-}C_6H_3O)]$. The tin-chlorine stretching mode at 389 cm^{-1} in the infra-red confirmed adduct formation and the increase in coordination at the tin centre was reflected in the upfield shift in the solution ^{119}Sn n.m.r. resonance with respect to $\{Sn[O\text{-}4\text{-}NO_2\text{-}C_6H_3O][OC_4H_8]\}_n$, to -294.3 p.p.m.

3.3.1.2 X-ray Crystallographic Analysis of $\{[Et_3BzN][SnCl(O\text{-}4\text{-}NO_2\text{-}C_6H_3O)]\}_n$

Single crystals of $\{[Et_3BzN][SnCl(O\text{-}4\text{-}NO_2\text{-}C_6H_3O)]\}_n$ suitable for study by X-ray diffraction were grown by slow diffusion of diethyl ether into a methanol solution of the compound. The data collection and structure solution were carried out by Dr. Jonathan C. Machell of this laboratory.

A single crystal of dimensions 0.6 x 0.2 x 0.1 mm was mounted in a glass capillary and transferred to an Enraf-Nonius CAD4 diffractometer. Final unit cell dimensions, calculated from a least-squares treatment of the angles of 24 accurately centered reflections are given in Table 3.1. 4397 reflections were collected using $\omega/2\vartheta$ scans (scan width $0.80 + 0.35\tan\vartheta$) using graphite monochromated Mo-K_α radiation, of which 2057 were considered

unique and observed ($I \geq 3\sigma(I)$, R_{merg}= 0.0263). These were corrected for Lorentz and polarization effects and an absorption correction was applied (min/max correction 1.00/1.13).

The structure was solved by routine Patterson, direct methods (SHELXS), Fourier methods and full-matrix, least squares refinement of all the non-hydrogen atoms, followed by DIFABS and spherical absorption corrections. After converting all of the atoms to anisotropic thermal parameters, the hydrogens were located from a difference map. On application of a Cebyshev weighting scheme (coefficients 4.742, -6.002, 3.429, -1.748), the model converged at R = 0.0300, R_w= 0.0314.

Table 3.2 and Appendix 2 contain the structural data for $\{[Et_3BzN][SnCl(O\text{-}4\text{-}NO_2C_6H_3O)]\}_n$ whilst Figures 3.1 to 3.4 show the main structural features.

Table 3.1 Structural Details for $\{[Et_3BzN][SnCl(O\text{-}4\text{-}NO_2\text{-}C_6H_3O)]\}_n$

Compound	$[Sn_1C_{19}ClN_2O_4H_{25}]_n$
Molecular Weight	499.56
Space Group	$P2_1/n$
Cell Dimensions	a 17.254(4)Å α 90°
	b 7.689(6)Å β 112.71(2)°
	c 16.740(3)Å γ 90°
Cell Volume	2049 Å^3
Z	4
Density	1.62 g cm^{-3}
Linear Absorption Coefficient	14.07 cm^{-1}
Radiation	Mo-K_α ($\lambda = 0.71069$Å)
Standard Reflections	12 1 -2; -1 -1 11
Decay of Standards	< 1%
2ϑ Range	2-50°
Number of Parameters Varied	244
R	0.0300
R_w	0.0314
Goodness of Fit	1.15
F(000)	1008

Table 3.2 Selected Bond Lengths (Å) and Angles (°) for $\{[Et_3BzN][SnCl(O\text{-}4\text{-}NO_2\text{-}C_6H_3O)]\}_n$

Distances and Angles Around Sn

Atoms	Distance	Atoms	Distance
Sn-O(1)	2.162(3)	Sn-O(1')	2.697(4)
Sn-O(2)	2.121(4)	Sn-O(2")	3.095(4)
Sn-Cl(1)	2.571(1)	Sn-Cl(1')	3.574(2)

Atoms	Angle	Atoms	Angle
O(1)-Sn-O(1')	144.67(8)	O(1)-Sn-O(2)	76.8(1)
O(1)-Sn-O(2")	60.95(11)	O(1)-Sn-Cl(1)	88.6(1)
O(1')-Sn-O(2)	69.45(12)	O(1')-Sn-O(2")	153.50(10)
O(1')-Sn-Cl(1)	80.66(8)	O(2)-Sn-O(2")	130.4511)
O(2)-Sn-Cl(1)	88.80(1)	O(2")-Sn-Cl(1)	1113.24(7)
O(1)-Sn-Cl(1")	67.90(10)	O(1')-Sn-Cl(1")	116.56(8)
O(2)-Sn-Cl(1")	82.96(10)	O(2")-Sn-Cl(1")	58.76(7)
Cl(1)-Sn-Cl(1")	156.27(3)		

Other Bond Lengths and Angles

Atoms	Distance	Atoms	Distance
C(1)-O(1)	1.338(6)	O(2)-C(6)	1.326(6)

Atoms	Angle	Atoms	Angle
Sn(1')-O(1')-Sn(1)	110.11(14)	Sn(1")-Cl(1")-Sn(1)	79.26(4)
Sn(1")-O(2")-Sn(1)	98.23(12)	C(1)-O(1)Sn(1)	113.4(3)
C(6)-O(2)-Sn(1)	114.60(3)		

Figure 3.1 Molecular Structure of $\{[Et_3BzN][SnCl(O\text{-}4\text{-}NO_2\text{-}C_6H_3O)]\}_n$

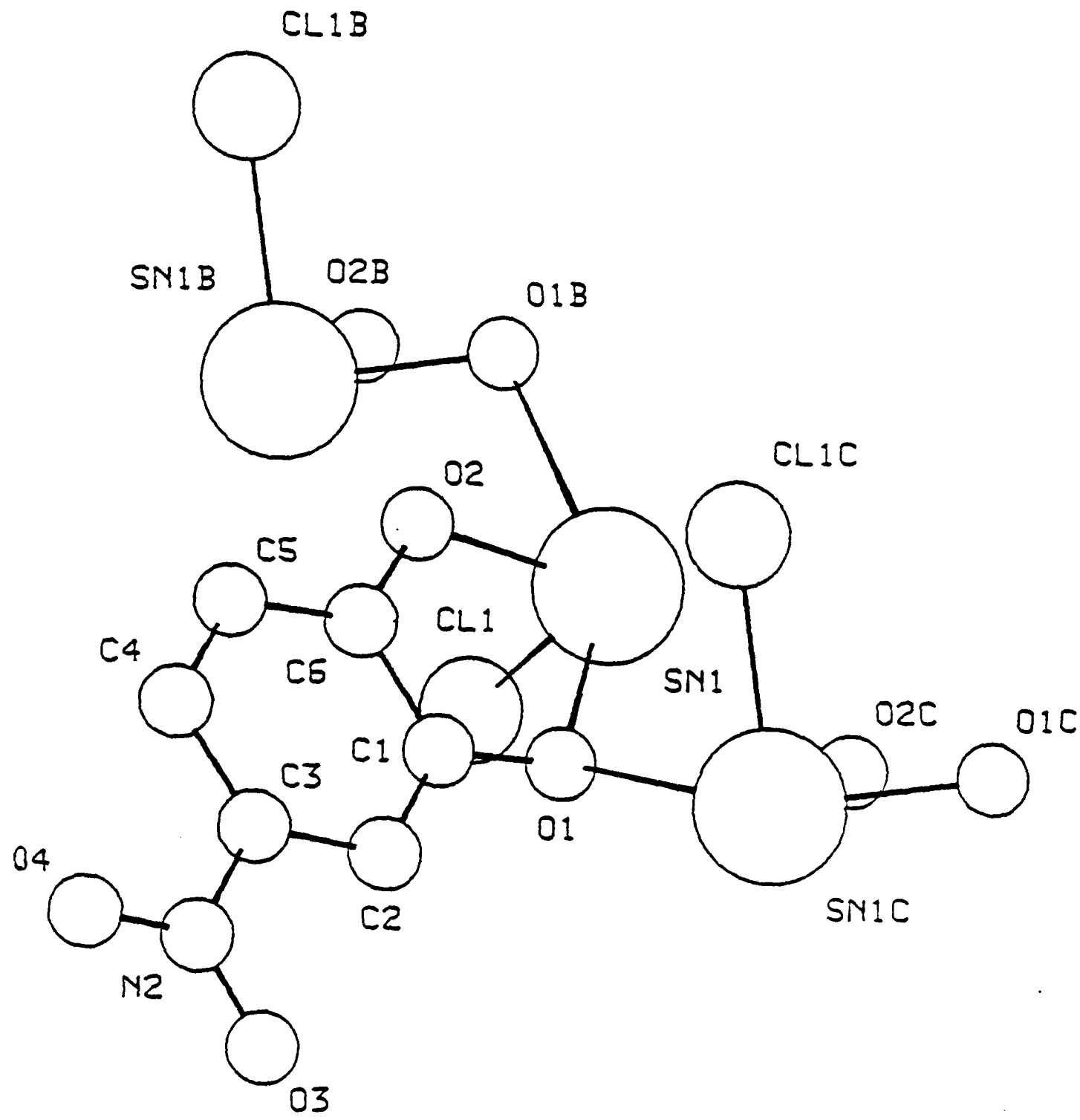


Figure 3.2 Polymeric Anionic Chain in $\{[Et_3BzN][SnCl(O\text{-}4\text{-}NO_2\text{-}C_6H_3O)]\}_n$

(carbon atoms and nitro groups omitted for clarity)

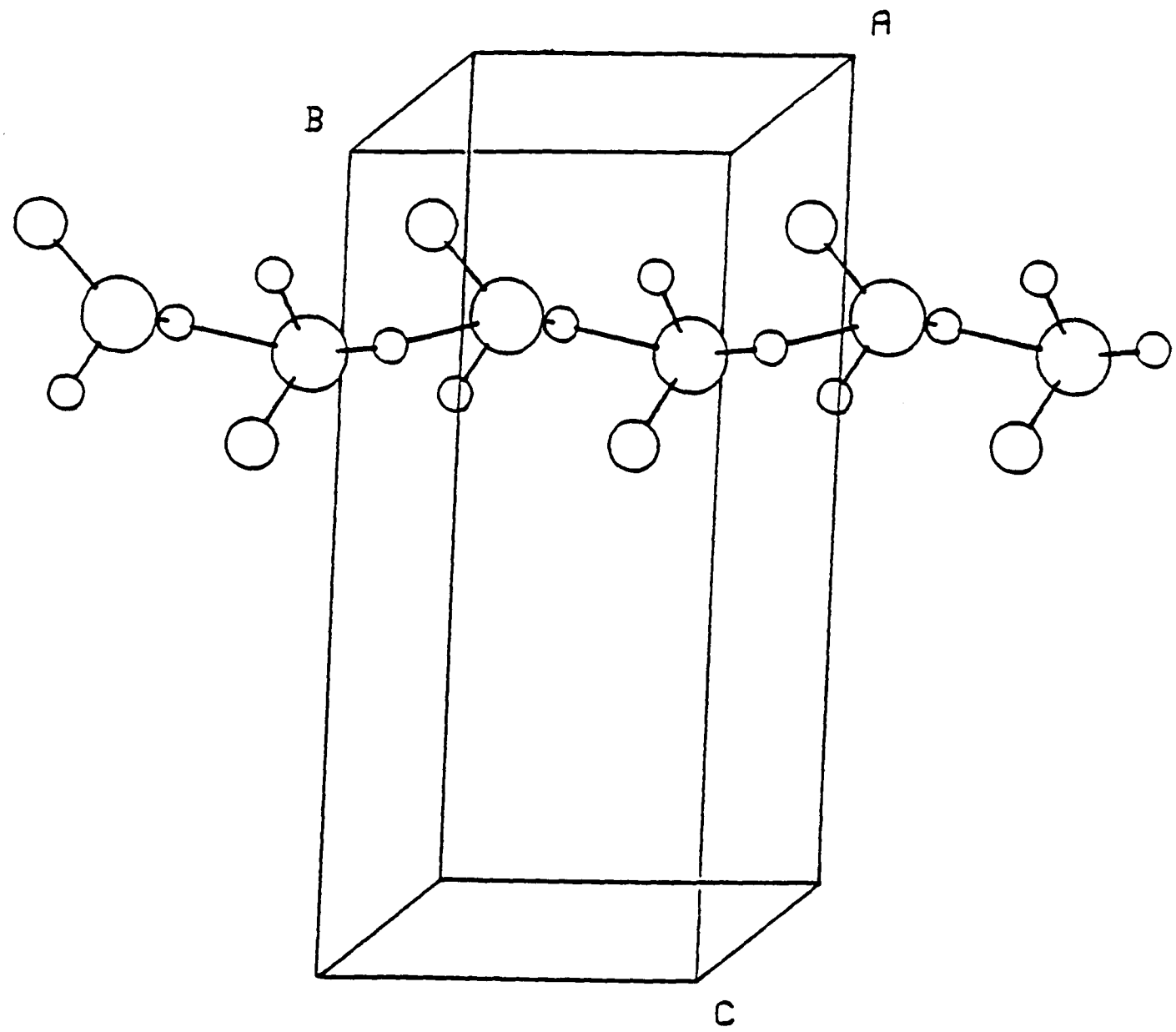
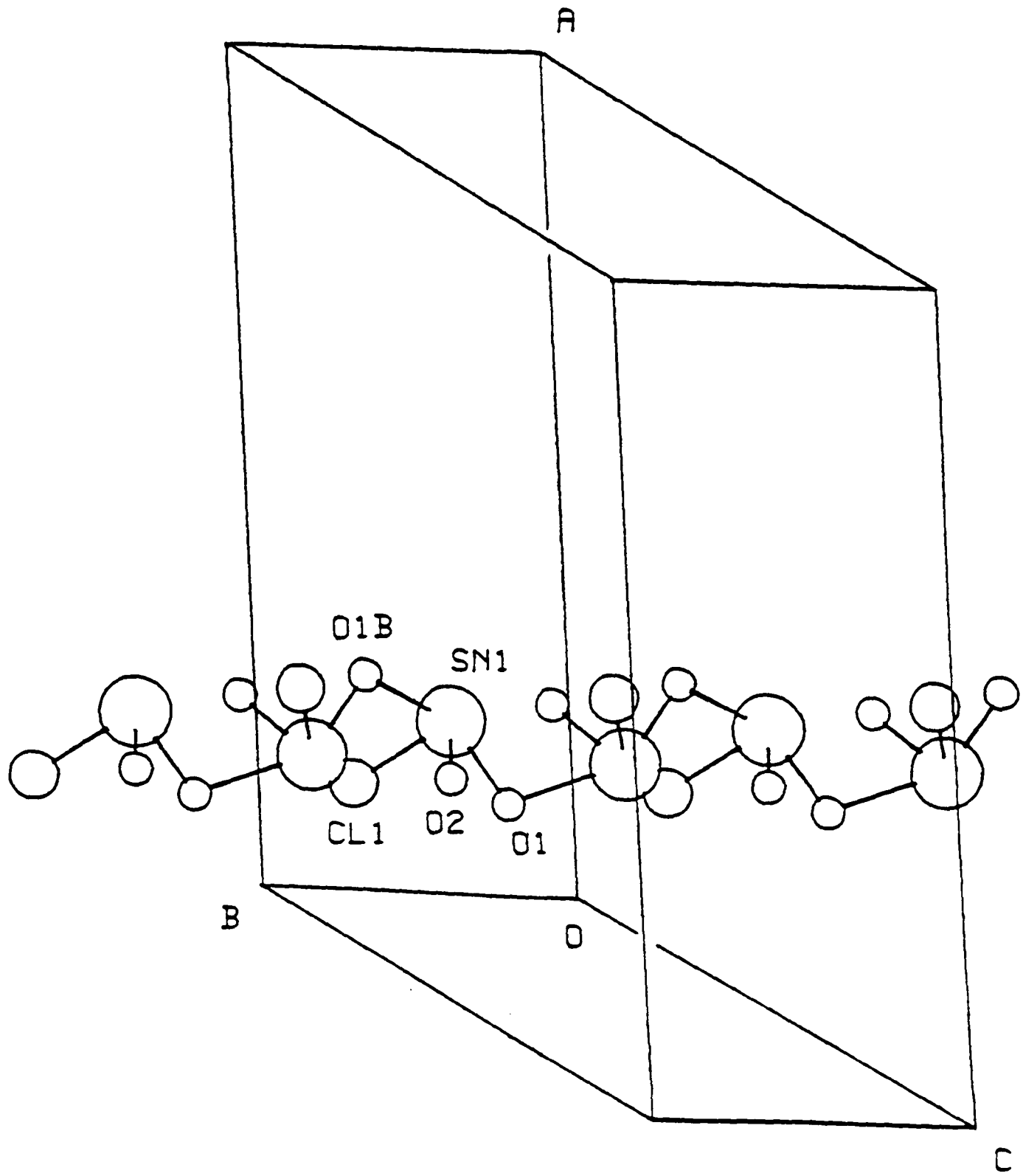


Figure 3.3 Polymeric Anionic Chain in $\{[Et_3BzN][SnCl(O\text{-}4\text{-}NO_2\text{-}C_6H_3O)]\}_n$

(carbon atoms and nitro groups omitted for clarity)



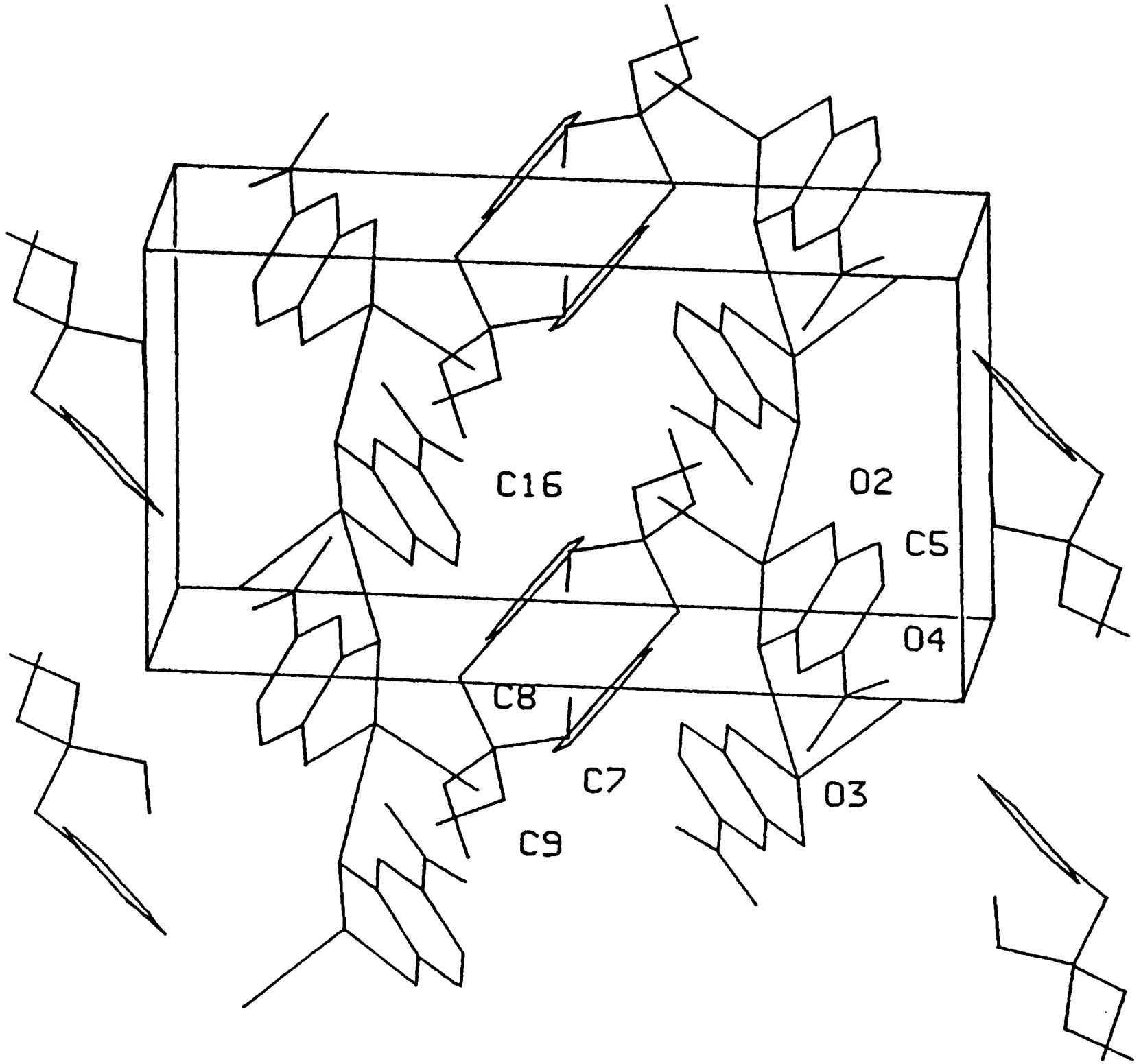


Figure 3.4 Crystal Packing in $\{[Et_3BzN][SnCl(O\text{-}4\text{-}NO_2\text{-}C_6H_3O)]\}_n$

The compound crystallizes in the space group $P2_1/n$ and the structure consists of polymeric chains of $[ClSn(O\text{-}4\text{-}NO_2\text{-}C_6H_3O)]^-$ and associated $[Et_3BzN]^+$ cations. The cations are well separated from the anionic chains.

The coordination around each tin(II) atom (as shown in Figure 3.1) may be described as distorted trigonal bipyramidal with one of the equatorial ligands replaced by a lone pair of electrons. The distortion may be rationalized on the basis of the small bite angle of the catechol ligand and the stereochemical consequences of the lone pair on tin. The oxygen atoms, O(1) and O(1') take up axial positions about the tin centre, O(1') is the catechol oxygen from an adjacent monomeric unit, the O(1)-Sn-O(1') angle is 144.67(8)°. The equatorial positions are occupied by O(2) and Cl(1), making an angle of 88.8(1)° at the tin atom. The angles between axial and equatorial atoms fall in the range 69.4(1)-88.6(1)° The angle O(1)-Sn-O(2) is 76.8(1)°, compared to 75.6(2)° in $\{Sn[O\text{-}4\text{-}NO_2\text{-}C_6H_3O][OC_4H_8]\}_n$ and is a consequence of the shortening of Sn(1)-O(1) and O(2) bonds, (Sn(1)-O(1) 2.162(3)Å and Sn(1)-O(2) 2.121(4)Å) compared to those of $\{Sn[O\text{-}4\text{-}NO_2\text{-}C_6H_3O][OC_4H_8]\}_n$ (Sn(1)-O(1) 2.208(4)Å and Sn(1)-O(2) 2.112(4)Å). It should be noted that the Sn-O bond *para* to the nitro group is still shorter, and an explanation in terms of the bonding scheme outlined for $\{Sn[O\text{-}4\text{-}NO_2\text{-}C_6H_3O][OC_4H_8]\}_n$ in Section 2.3.5 will be discussed later

The Sn-Cl(1) bond in $\{Sn[O\text{-}4\text{-}NO_2\text{-}C_6H_3O][OC_4H_8]\}_n$ of 2.571(1)Å is in good agreement with tin-chlorine bonds found in $SnCl_3^-$ containing tin(II) compounds (see Table 1.7).

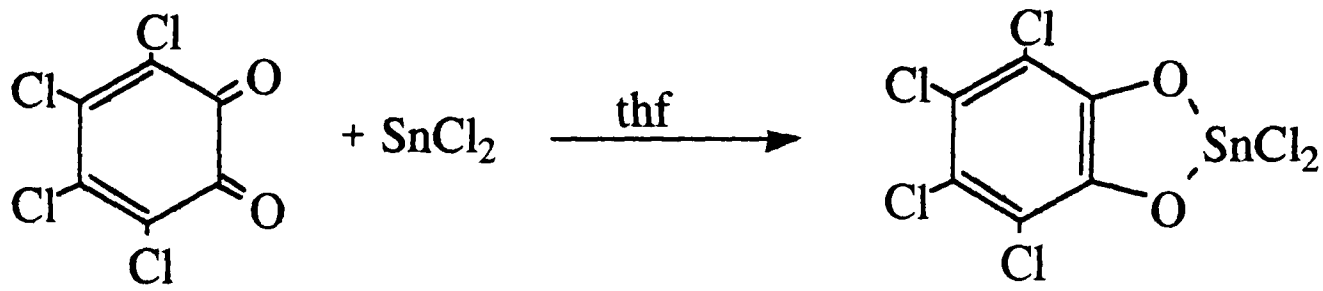
The polymeric chains are formed via Sn-O-Sn linkages from one of the catechol oxygen atoms O(1), with a Sn(1)-O(1') distance of 2.697(4)Å, and Sn(1)-O(1)-Sn(1') angle of 110.1(1)°. The other short intermolecular contacts Sn(1)-O(2") at 3.095(4)Å and Sn(1)-Cl(1") at 3.574(2)Å, are too long to be considered to invole significant bonding. The manner in which the monomeric units are linked is shown in Figures 3.2, 3.3 and 3.4. In $\{Sn[O\text{-}4\text{-}NO_2\text{-}C_6H_3O][OC_4H_8]\}_n$, there is an alternation of enantiomeric forms of the monomeric unit along the polymeric chains. In $\{[Et_3BzN][SnCl(O\text{-}4\text{-}NO_2\text{-}C_6H_3O)]\}_n$, each anionic chain contains only one enantiomeric form of the monomeric unit, the

crystallographic centres of inversion lying between the chains. The long intermolecular bonds in both $\{Sn[O\text{-}4\text{-}NO_2\text{-}C_6H_3O][OC_4H_8]\}_n$ and $\{[Et_3BzN][ClSn(O\text{-}4\text{-}NO_2\text{-}C_6H_3O)]\}_n$ are reflected in their increased solubilities and the breakdown of their polymeric chains in solution. The further degree of weakening in the intermolecular bonding in $\{[Et_3BzN][SnCl(O\text{-}4\text{-}NO_2\text{-}C_6H_3O)]\}_n$ may be ascribed to the negative charge associated with the monomeric units of the polymeric chain which must increase the strength of the electrostatic repulsive forces. Tuck[3] observed that conductivity values for the anionic complexes $[SnX(O_2R)]^-$ (X = Br or I) were sometimes lower than normally expected, due to a degree of association in solution. A similar situation might exist for $\{[Et_3BzN][SnCl(O\text{-}4\text{-}NO_2\text{-}C_6H_3O)]\}_n$.

The replacement of the tetrahydrofuran molecule in $\{Sn[O\text{-}4\text{-}NO_2\text{-}C_6H_3O][OC_4H_8]\}_n$ by the stronger Lewis base appears to have only a small effect upon the observed bonding. The bonding analysis applied to $\{Sn[O\text{-}4\text{-}NO_2\text{-}C_6H_3O][OC_4H_8]\}_n$ in Section 2.3.5 still seems applicable. The chlorine atom takes up a very similar position to the tetrahydrofuran and is closer to O(2) (O(2)-Cl(1) 3.299Å) than O(1) (O(1)-Cl(1) 3.319Å). This is probably the cause of the strengthening of the Sn-O(2) covalent interaction, and the lack of further bonding by O(2) with other monomeric units. The introduction of the chlorine atom also increases the ionic character of the molecule and is reflected in the general shortening of the Sn(1)-O(1) and Sn-O(2) distances compared to those found in $\{Sn[O\text{-}4\text{-}NO_2\text{-}C_6H_3O][OC_4H_8]\}_n$.

3.3.1.3 Synthesis of $[Et_3NH][SnCl(O\text{-}C_6Cl_4O)]$

No reaction was observed between benzyltriethylammonium chloride and $Sn[OC_6Cl_4O][OC_4H_8]$. To form the compound analogous to $\{[Et_3BzN][SnCl(O\text{-}4\text{-}NO_2\text{-}C_6H_3O)]\}_n$, the tin(IV) compound, $SnCl_2[OC_6Cl_4O]$ was first synthesized by the addition of tetrachloro-*o*-benzoquinone to tin(II) chloride.



Addition of two equivalents of triethylamine and a slight excess of methanol gave the desired product, $[Et_3NH][SnCl(O\text{-}C_6Cl_4O)]$ in relatively low yield (57%), after crystallization from tetrahydrofuran-diethyl ether as cream solid. A tin-chlorine stretching mode at 395 cm^{-1} was observed in the infra-red spectrum. The stoichiometry of the product was confirmed by elemental analyses and ^1H solution n.m.r. studies.

3.3.2 Tin(II) Compounds With Nitrogen-Donor Ligands

The formation of tin(II) complex compounds with nitrogen-donor ligands is well documented[3,5-9]. Adducts of stoichiometry 1:1 and 1:2 have been formed with unidentate donors, and 1:1 aducts with bidentate donors. An investigation into the reactivity of $\{Sn[O\text{-}4\text{-}NO_2\text{-}C_6H_3O][OC_4H_8]\}_n$ with nitrogen-donor ligands was considered worthwhile due to the importance of such groups in biological systems. The compounds formed upon complexation of such groups by tin and other metals appear to be promising agents for the stimulation antitumour and antimicrobial activity[10-14].

Since the majority of tin(II) adducts so far isolated contain two nitrogen donor atoms per tin, the bidentate ligands, 1,2-diaminopropane, teramethylethylenediamine and 2,2'-dipyridyl were used assources of two nitrogen donor atoms. Chelation also aided the displacement of the tetrahydrofuran in $\{Sn[O\text{-}4\text{-}NO_2\text{-}C_6H_3O][OC_4H_8]\}_n$ and reduced the likelyhood of polymerization. Analogous compounds were obtained when all three ligands were reacted with $\{Sn[O\text{-}4\text{-}NO_2\text{-}C_6H_3O][OC_4H_8]\}_n$. The reaction of 1,2-diaminopropane and the properties of the resulting adduct is given as an example.

3.3.2.1 Synthesis of $Sn[NH_2CH_2CH(Me)H_2N][O\text{-}4\text{-}NO_2\text{-}C_6H_3O][OC_4H_8]$

The addition of a tetrahydrofuran solution of 1,2-diaminopropane to an equimolar amount of $\{Sn[O\text{-}4\text{-}NO_2\text{-}C_6H_3O][OC_4H_8]\}_n$ in tetrahydrofuran gave an immediate reaction. The polymer, which is not totally soluble in tetrahydrofuran at room temperature is rapidly taken up into solution, an indication of the breaking down of the polymeric chain upon adduct formation. Crystallization from tetrahydrofuran-diethyl ether afforded the adduct $Sn[NH_2CH_2CH(Me)H_2N][O\text{-}4\text{-}NO_2\text{-}C_6H_3O][OC_4H_8]$ as an orange microcrystalline solid in high yield (82%). $Sn[NH_2CH_2CH(Me)H_2N][O\text{-}4\text{-}NO_2\text{-}C_6H_3O][OC_4H_8]$ is much more soluble than its parent compound, indicating a reduction in the strength of the intermolecular interactions in the solid state. The stoichiometry was confirmed by elemental analyses and solution ^1H n.m.r. studies.

3.4 Reactions As A Lewis Base

The reaction of the non-bonding electron pair in tin(II) compounds with stronger electron pair acceptors, such as Group 13 trihalides[15-24] , or as a ligand to a transition metal centre[25-27] has been intensively studied, and so the reactions of $\{Sn[O\text{-}4\text{-}NO_2\text{-}C_6H_3O][OC_4H_8]\}_n$ as a Lewis base source were investigated.

3.4.1 Synthesis of $F_3B.Sn[O\text{-}4\text{-}NO_2\text{-}C_6H_3O][OC_4H_8]$

The addition of a solution of boron trifluoride etherate to an equimolar amount of $\{Sn[O\text{-}4\text{-}NO_2\text{-}C_6H_3O][OC_4H_8]\}_n$ produced an immediate reaction. $\{Sn[O\text{-}4\text{-}NO_2\text{-}C_6H_3O][OC_4H_8]\}_n$, which is only sparingly soluble in tetrahydrofuran at room temperature, is quickly consumed in the reaction and a clear solution formed. This implied that the intermolecular bonds holding the polymeric chain together have been broken upon the addition of the Lewis acid. Subsequent work-up and recrystallization resulted in a pale yellow crystalline solid which was found to be highly solvent sensitve, stable only in

tetrahydrofuran and rapidly decomposed upon exposure to any other solvent. Elemental analyses, FABMS and solution ^{1}H n.m.r confirmed the formation of a 1:1 adduct.

There has been much uncertainty surrounding the role the tin lone pair plays in the reaction of tin(II) compounds with main group Lewis acids. Zuckerman[17] found that the compound originally formulated as $Cp_2Sn.BF_3$ was in fact $[(\mu\text{-}Cp)_2Sn(\mu\text{-}CpSn)(OC_4H_8)][BF_4]$[23]. The presence of other Lewis base sources as possible coordination sites must also be considered. Geanangle[21-22] has shown that BF_3 can bind to tin or nitrogen or both in $Sn[NMe_2]_2$, depending upon the molar ratio used. He found that at low molar ratios of BF_3 to $Sn[NMe_2]_2$, the BF_3 is initially bound to the tin atom. Since $\{Sn[O\text{-}4\text{-}NO_2\text{-}C_6H_3O][OC_4H_8]\}_n$ contains a number of possible donor centres, such as the oxygen atoms of the nitro, catecholate and tetrahydrofuran, further studies were undertaken to try and ascertain the bonding involved.

Adduct formation between BF_3 and the nitro-group was easily eliminated, since this was unlikely to result in the apparent loss of oligomerization observed. Furthermore, no changes were observed in the bands assigned to N-O stretching modes in the infra-red.

^{11}B and ^{19}F solution n.m.r. confirmed a change in bonding had taken place at boron. A weak interaction was indicated due to the small shifts in the resonances observed ($^{11}B\text{-}\{^{1}H\}$ δ 0.05 p.p.m. ($F_3B.OEt_2$ δ 0.00 p.p.m.) and $^{19}F\text{-}\{^{1}H\}$ δ -148.9 p.p.m. ($F_3B.OEt_2$ δ -131.0 p.p.m)) and a broadening in the resonances rather than any discernible tin coupling. The small shift in the $^{11}B\text{-}\{^{1}H\}$ resonance might be rationalized on the basis of an exchange process between free BF_3 and the adduct in solution. However, no change in the $^{11}B\text{-}\{^{1}H\}$ resonance was observed upon warming the sample.

The most compelling evidence for coordination of the BF_3 to the tin atom came from analysis of the ^{117}Sn solution n.m.r. The ^{117}Sn n.m.r. resonance is very susceptible to any change in coordination about the tin centre (see Section 1.2.3). The dramatic change in the position of the ^{117}Sn resonance from $^{117}Sn\text{-}\{^{1}H\}$ δ -452.3 p.p.m for $\{Sn[O\text{-}4\text{-}NO_2\text{-}C_6H_3O][OC_4H_8]\}_n$, to a value of -727.1 p.p.m. is indicative of a change in the environment about tin. The broadness of the resonance (1393 Hz at half-height) is also an indication of coordination to a nucleus with a large degree of quadrupolar coupling such as boron.

3.4.2 Reactions With Unsaturated Transiton Metal Centres

3.4.2.1 The Reaction of $\{Sn[O\text{-}4\text{-}NO_2\text{-}C_6H_3O][OC_4H_8]\}_n$ with $W[CO]_5[OC_4H_8]$. Synthesis of $[Sn(O\text{-}4\text{-}NO_2\text{-}C_6H_3O)]_2[W(CO)_3]_2$

Many of the Lewis acid-base reactions involving transition metals have utilized the ability of tin(II) compounds to displace (either photolytically or thermally) labile ligands from transition metal carbonyl compounds giving a range of mono or disubstituted compounds[1,2].

Refluxing equimolar quantities of $\{Sn[O\text{-}4\text{-}NO_2\text{-}C_6H_3O][OC_4H_8]\}_n$ and freshly prepared $W[CO]_5[OC_4H_8]$ in tetrahydrofuran for three hours, a colour change from yellow to red-orange was observed. Work-up of the reaction afforded a white crystalline solid identified as $W[CO]_6$ (30% with respect to starting material) and a red-orange microcrystalline solid which elemental analyses showed contained tin and tungsten in a 1:1 ratio. ^1H solution n.m.r. revealed that the only proton containing species present were tetrahydrofuran and the 4-nitrocatecholate anion, also in a 1:1 ratio.

The $^{117}Sn\text{-}\{^1H\}$ solution n.m.r. spectrum also showed a shift upfield to -166.0 p.p.m., a movement of 286 p.p.m. from $\{Sn[O\text{-}4\text{-}NO_2\text{-}C_6H_3O][OC_4H_8]\}_n$ indicating an increase in coordination at the tin centre. No tungsten coupling was observed, suggesting that there is no direct tin-tungsten bond.

The $^{13}C\text{-}\{^1H\}$ solution n.m.r spectrum showed only one carbonyl resonance with a $^1J_{CW}$ of 128 Hz. This implies that all the carbonyl groups attached to tungsten are equivalent in solution, and precludes the presence of the expected $W[CO]_5$ moiety, which would show two resonances in a 4:1 ratio. The resonances attributed to the aromatic carbons of 4-nitrocatecholate showed a shift to high field (δ 115.8-109.7 p.p.m.) with respect to $\{Sn[O\text{-}4\text{-}NO_2\text{-}C_6H_3O][OC_4H_8]\}_n$ (δ 116.5-110.2 p.p.m.) implying a reduction in ring electron density[35].

The infra-red spectrum in tetrahydrofuran solution shown in Figure 3.5 shows only terminal carbonyl groups.

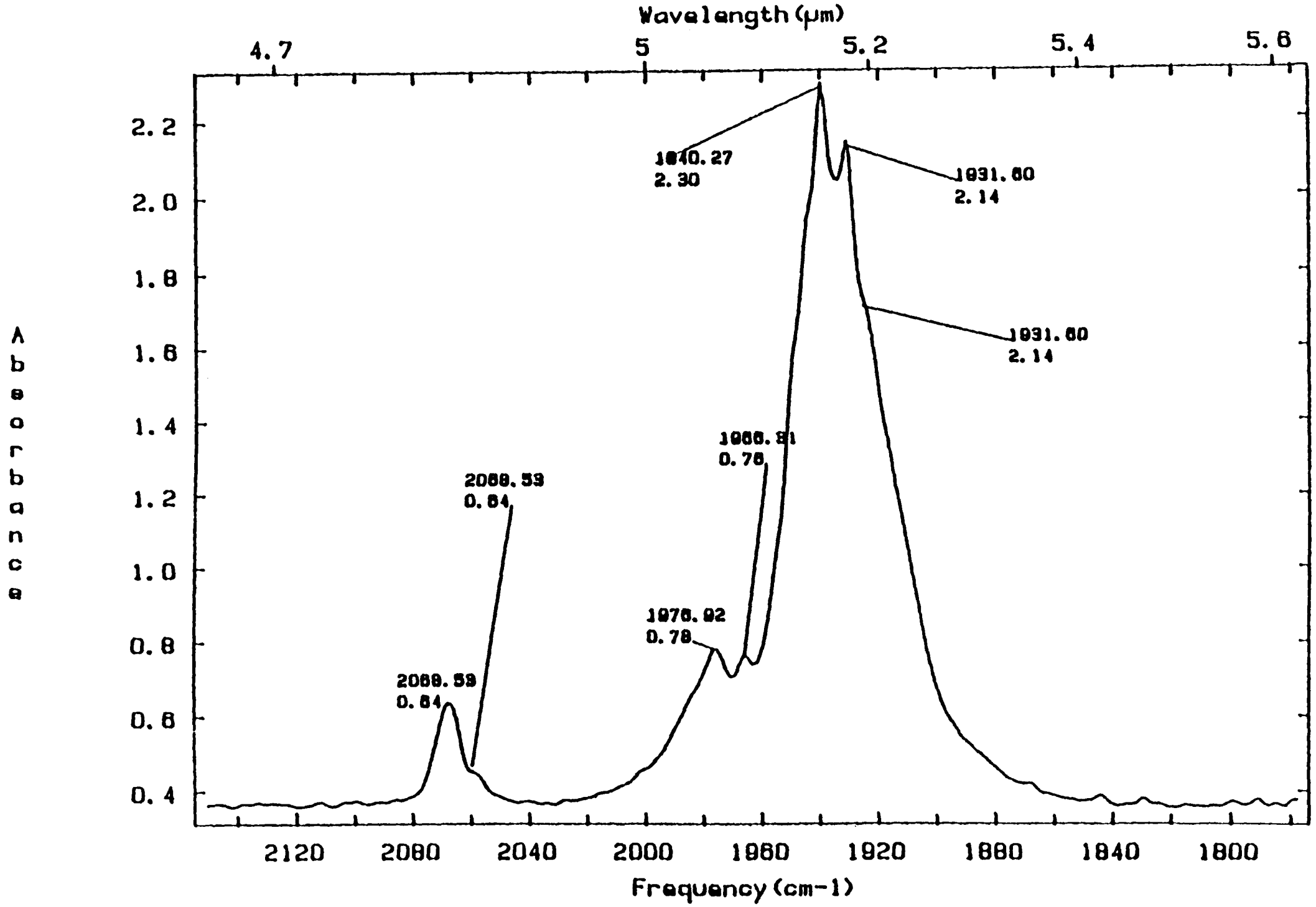


Figure 3.5 Carbonyl Stretches of a Terahydrofuran Solution of $[Sn(O\text{-}4\text{-}NO_2\text{-}C_6H_3O)]_2[W(CO)_3]_2$ in a 1 mm KBr Cell

At least four bands are shown, two of very strong intensity at 1940 and 1932 cm^{-1} and two lower intensity bands at 2069 and 1976 cm^{-1}. The number of bands shows the product does not have a high symmetry structure.

The stoichiometry of the product was obtained from its FABMS spectrum (see Table 3.3).

Table 3.3 Details of the Positive Ion FABMS of the Reaction Product of $\{Sn[O\text{-}4\text{-}NO_2\text{-}C_6H_3O][OC_4H_8]\}_n$ and $W[CO]_5[OC_4H_8]$

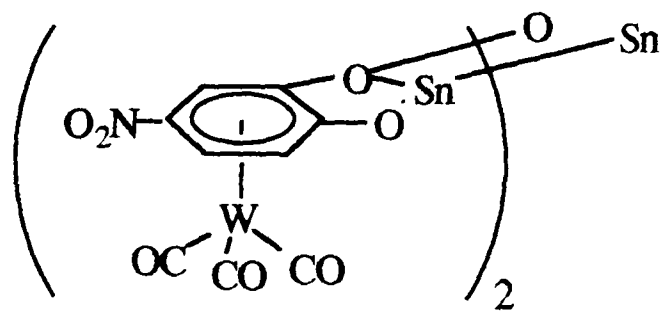
m/z	Assignment	Relative abundance (%)
1080	$\{[Sn(O\text{-}4\text{-}NO_2\text{-}C_6H_3O)]_2[W(CO)_3]_2\}^+$ $\{M\}^+$	60
1048	$\{M\text{-}2O\}^+$	24
1017	$\{M\text{-}2NO\}^+$	20
989	$\{M\text{-}2NO\text{-}CO\}^+$	29
961	$\{M\text{-}2NO\text{-}2CO\}^+$	21
812	$\{M\text{-}W\text{-}3CO\}^+$	23
691	$\{M\text{-}W\text{-}3CO\text{-}C_6H_3NO_2\}^+$	46
675	$\{M\text{-}W\text{-}3CO\text{-}OC_6H_3NO_2\}^+$	31
544	$\{[Sn(O\text{-}4\text{-}NO_2\text{-}C_6H_3O)]_2\}^+$	23
268	$\{W[CO]_3\}^+$	7
240	$\{W[CO]_2\}^+$	6
136	$\{SnO\}^+$ or $\{OC_6H_3NO_2\}^+$	100

The positive ion FAB mass spectrum shows a molecular ion peak at m/z = 1080 which is equivalent to a compound composed of two 4-nitrocatecholatotin(II) units and two $W[CO]_3$ units. Analysis of the fragmentation pattern reveals the presence of a 4-nitrochatecholatotin(II) dimer (m/z = 544), and low abundance peaks which were assigned as $W[CO]_3$ (m/z = 268) and $W[CO]_2$ (m/z = 240). This composition is corroborated by the

product's elemental analyses, if one equivalent of tetrahydrofuran, as solvent of crystallization is included.

Since the ^{13}C-{^{1}H} solution n.m.r. spectrum shows the carbonyl ligands to be equivalent in solution and the solution infra-red reveals no bridging carbonyl ligands, this implies that the local symmetry of the $W[CO]_3$ group is pyramidal. The lack of tungsten coupling in the ^{117}Sn-{^{1}H} n.m.r spectrum suggests that the tin lone pair is not used to stabilize the electron deficient tungsten centre. The only other electron sources available are tetrahydrofuran, the catecholate oxygens and the aromatic ring. No coordinated tetrahydrofuran was observed and so can be discounted. The use of the aromatic ring electrons, perhaps in association with the catecholate oxygen atoms would appear to be the most satisfactory explanation of the available data (see Figure 3.6). The η-bonded "piano stool" configuration is well known for many aromatic-$W[CO]_3$ systems[28] and would account for the asymmetry observed in the carbonyl infra-red stretching modes and the shift in the aromatic carbon resonances in the solution ^{13}C-{^{1}H} n.m.r. The molecular weight obtained from FABMS could be due to dimerization via intramolecular Sn-O bonds, similar to that found in $\{Sn[O\text{-}4\text{-}NO_2\text{-}C_6H_3O][OC_4H_8]\}_n$.

Figure 3.6 Proposed Structure of $[Sn(O\text{-}4\text{-}NO_2\text{-}C_6H_3O)]_2[W(CO)_3]_2$



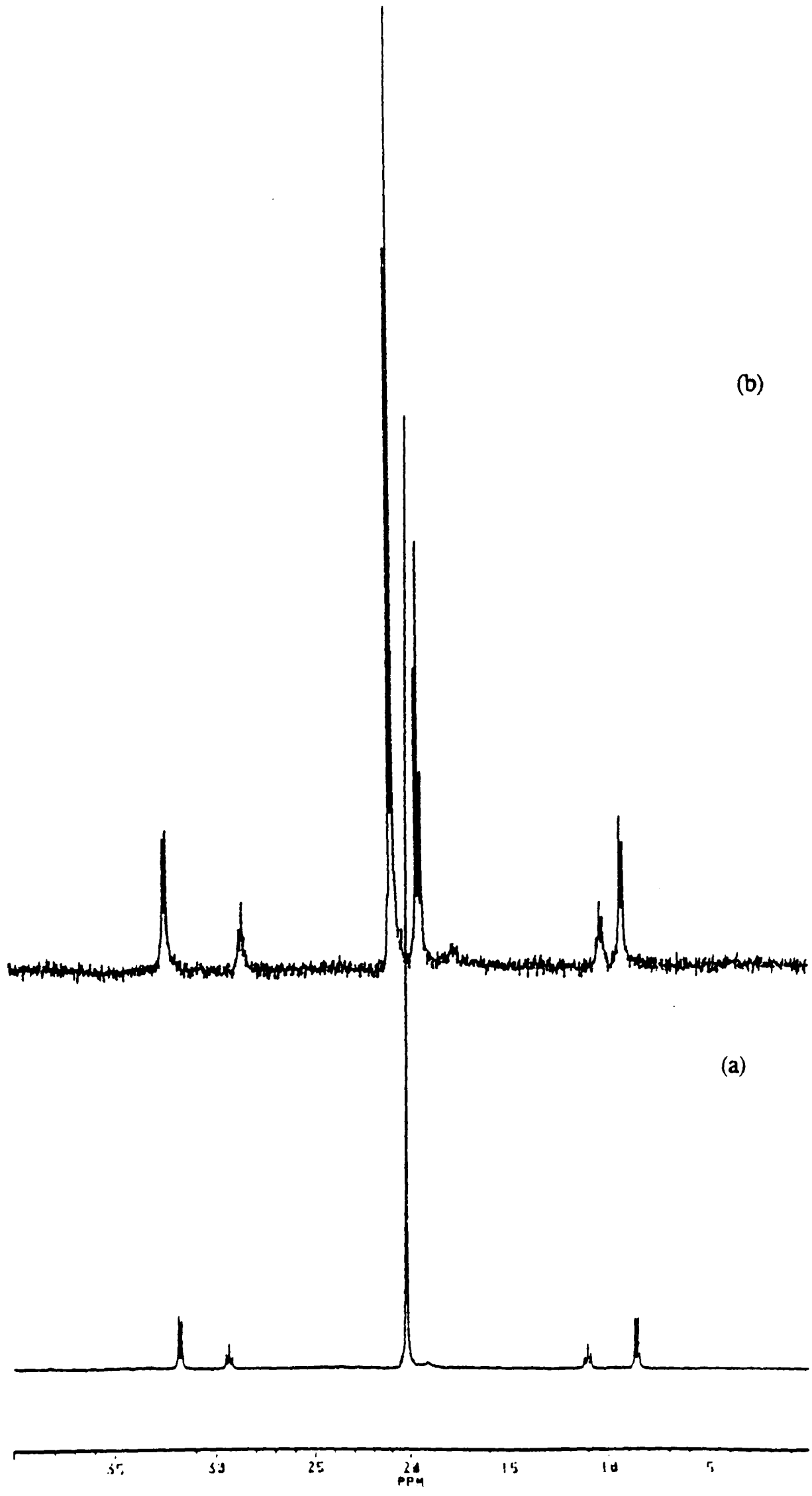
3.4.2.2 Synthesis of $\{[Ph_3P]_3PtH\}\{[\mu_2\text{-}O][\mu_2\text{-}OH][Sn(O\text{-}4\text{-}NO_2\text{-}C_6H_3O)]_2\}$

In transition metal complexes, the displacement of phosphines[16,29], cyclo-octa-1,5-diene[30], norbornadiene[16,29] and ethylene[16,31] ligands by tin(II) compounds has been observed, leading to the formation of non-carbonyl containing tin-transition metal bonds.

The reactions between molar equivalent quantities of $\{Sn[O\text{-}4\text{-}NO_2\text{-}C_6H_3O][OC_4H_8]\}_n$ and (ethylene)bis(triphenylphosphine)platinum or tris(triphenylphosphine)platinum in tetrahydrofuran were rapid, the reaction mixture changing from bright yellow to dark red. Work-up and crystallization from tetrahydrofuran-hexane afforded a dark-red microcrystalline solid. Elemental analyses revealed the product has a platinum:tin ratio of 1:2.

The solution $^{31}P\text{-}\{^1H\}$ n.m.r at room temperature (Figure 3.7a) showed only a single central resonance at 20.2 p.p.m. Two sets of ^{195}Pt satellites are observed, one set a doublet to one phosphorus ($^2J_{PP}$ 18Hz, $^1J_{PPt}$ 2822Hz), the other a triplet to two equivalent phosphorus atoms ($^2J_{PP}$ 18Hz, $^1J_{PPt}$ 2228Hz). The inequivalence of the phosphine ligands with respect to the central resonance only becomes apparent upon cooling the sample, thus freezing out the rapid rotation of the phosphine ligands about the platinum centre (Figure 3.7b), resolving the central resonance into the doublet ($^2J_{PP}$ 19Hz, $^1J_{PPt}$ 2819Hz) and triplet ($^2J_{PP}$ 19Hz, $^1J_{PPt}$ 2218Hz) expected for a AB_2B' spin system (coalescence at 288K).

Figure 3.7 ^{31}P-{^{1}H} Solution N.m.r. Spectra for {$[Ph_3P]_3PtH$}{$[\mu_2$-O][μ_2-OH][Sn(O-4-NO_2-$C_6H_3O)]_2$} at (a) Room Temperature (298K) and (b) 218K



The solution ^{1}H n.m.r. spectrum revealed resonances attributable to a hydride ligand at high field. The hydride resonances at room temperature (Figure 3.8a) shows a doublet of doublets ($^{2}J_{HP(cis)}$ 12.6Hz, $^{2}J_{HP(trans)}$ 164Hz), whilst the platinum satellites appear as pairs of triplets ($^{2}J_{HP(cis)}$ 12.6Hz, $^{2}J_{HP(trans)}$ 160Hz). The phosphorus decoupled solution $^{1}H-\{^{31}P\}$ n.m.r. spectrum (Figure 3.8b), shows a hydride resonance at -5.71 p.p.m. with a $^{1}J_{HPt}$ 777Hz.

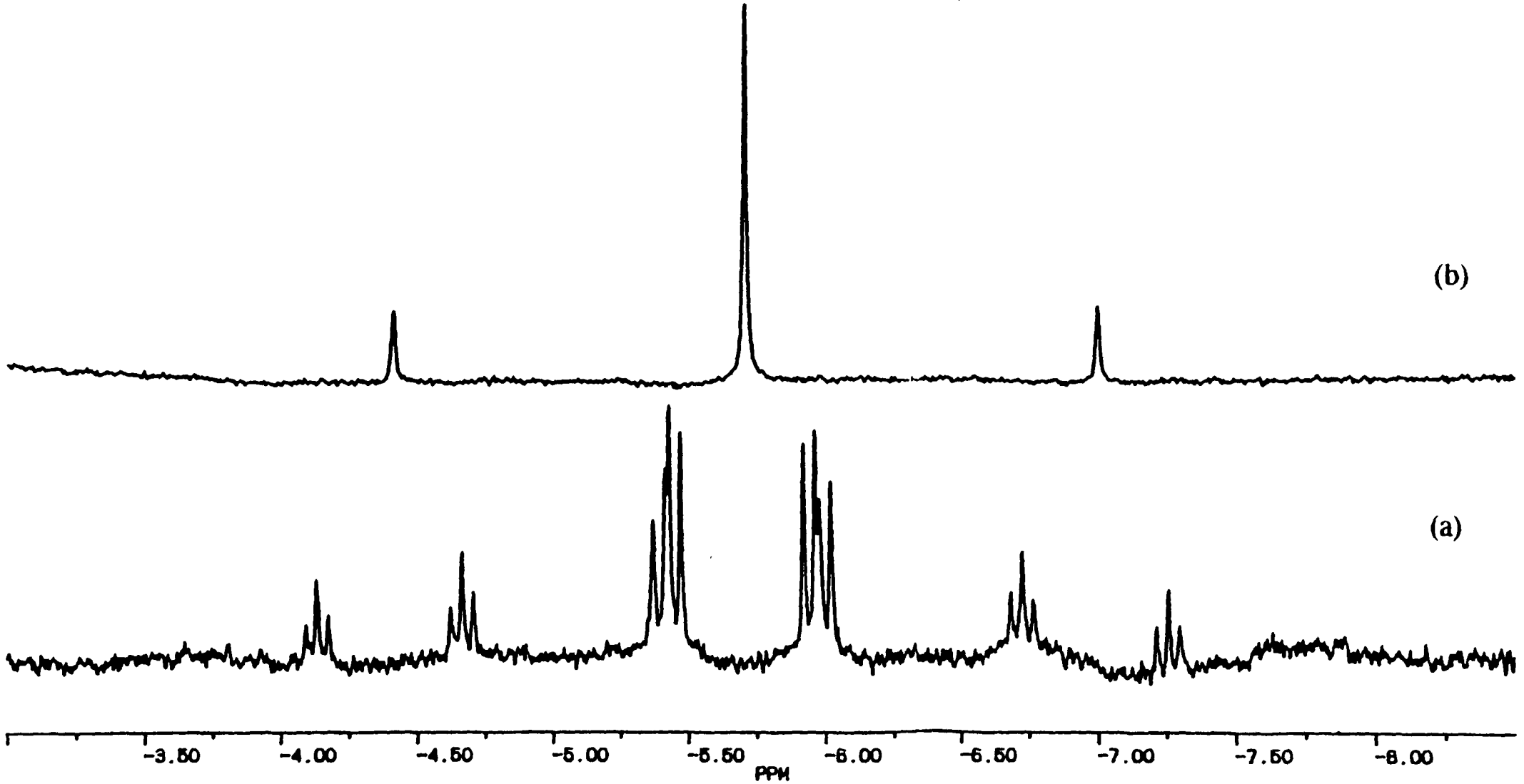


Figure 3.8 Hydride Region of the ^{1}H Solution N.m.r. Spectra for $\{[Ph_3P]_3PtH\}\{[\mu_2\text{-}O][\mu_2\text{-}OH][Sn(O\text{-}4\text{-}NO_2\text{-}C_6H_3O)]_2\}$ at Room Temperature with (a) No Decoupling and (b) ^{31}P Decoupled

The presence of a $[(Ph_3P)_3PtH]^+$ was confirmed by positive ion FABMS of the product (Table 3.4) which shows $[(Ph_3P)_3PtH]^+$ as the molecular ion.

Table 3.4 Details of the Positive Ion FABMS of $\{[Ph_3P]_3PtH\}\{[\mu_2\text{-}O][\mu_2\text{-}OH][Sn(O\text{-}4\text{-}NO_2\text{-}C_6H_3O)]_2\}$

m/z	Assignment	Relative abundance (%)
982	$\{Pt(PPh_3)_3H\}^+$ $\{M\}^+$	71
905	$\{M\text{-}Ph\}^+$	6
827	$\{M\text{-}2Ph\text{-}H\}^+$	12
751	$\{M\text{-}3Ph)^+$	4
719	$\{M\text{-}PPh_3\text{-}H\}^+$	100
642	$\{M\text{-}PPh_3\text{-}Ph\text{-}H\}^+$	13
565	$\{M\text{-}PPh_3\text{-}2Ph\text{-}H\}^+$	3
488	$\{M\text{-}PPh_3\text{-}3Ph\text{-}H\}^+$	7
457	$\{M\text{-}2PPh_3\text{-}H\}^+$	18
380	$\{M\text{-}2PPh_3\text{-}Ph\text{-}H\}^+$	19
262	$\{M\text{-}2PPh_3\text{-}Pt\text{-}H\}^+$	19

Previous examples of hydridotris(tertiary phosphine)platinum(1+) compounds are all white crystalline salts[32-34], whereas $\{[Ph_3P]_3PtH\}\{[\mu_2\text{-}O][\mu_2\text{-}OH][Sn(O\text{-}4\text{-}NO_2\text{-}C_6H_3O)]_2\}$ is dark red in colour. Simulating the hydride resonances of $[(Ph_3P)_3PtH][(CF_3COO)_2H]$, Roundhill[34] found that the AB_2XM spin system for a square planar $[Ph_3P]_3PtH^+$, exactly modelled the eight central resonances. The simplification observed for the platinum satellites due to the difference in the chemical shifts of the cis and trans phosphorus nuclei.

The solution $^{117}Sn\text{-}\{^1H\}$ n.m.r spectrum shows a single resonance at -455 p.p.m. little changed from that observed for $\{Sn[O\text{-}4\text{-}NO_2\text{-}C_6H_3O][OC_4H_8]\}_n$ at -452 p.p.m. and there is no sign of any coupling to either platinum or phosphorus.

The ^{119}Sn Mössbauer spectrum, shows two distinct resonances, at 0.37 and 2.55 mms^{-1} (see Figure 3.9). The lower velocity line is consistent with a tin(IV) centre, whilst the higher velocity line falls in the range ascribed to tin(II) species (see Section 1.2.2.3). No quadrupole splitting was observed for either resonance. The tin(II) resonance is however broad, with a line width of 1.38 mms^{-1} suggesting a departure from a regular geometry.

Similar mixed valence tin compounds have been reported in the literature[36-39]. With example, octakis-μ-(*o*-nitrobenzoato)-di-μ_3-oxo-bis(tetrahydrofuran)ditin(II)-ditin(IV)[37], the ^{119}Sn Mössbauer spectrum shows resonances at 3.597 and 0.068 mms^{-1}, which were assigned to tin(II) and tin(IV) centres respectively.

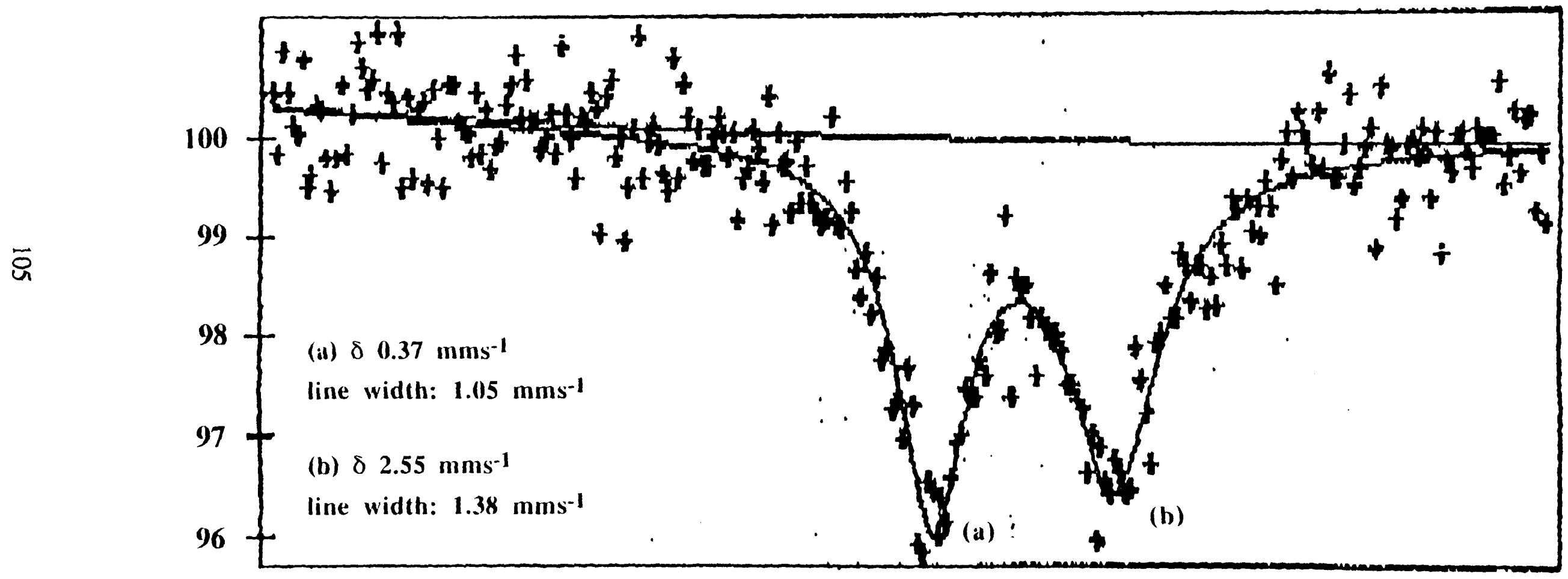


Figure 3.9 ^{119}Sn Mössbauer Spectrum of $\{[Ph_3P]_3PtH\}\{[\mu_2\text{-}O][\mu_2\text{-}OH][Sn(O\text{-}4\text{-}NO_2\text{-}C_6H_3O)]_2\}$

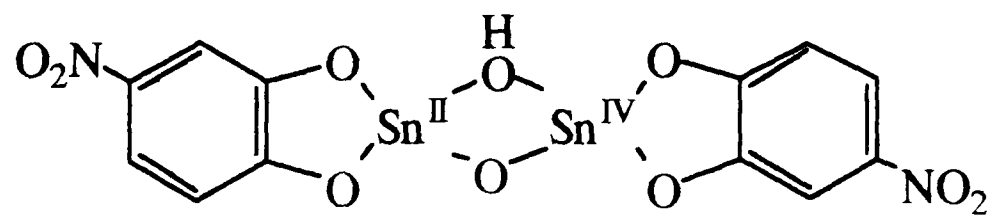
To try and determine the stoichiometery of the anion, negative ion FABMS was employed. The molecular ion (see Table 3.5) of m/z 577 was assigned to the species $\{[\mu_2\text{-}O][\mu_2\text{-}OH][Sn(O\text{-}4\text{-}NO_2\text{-}C_6H_3O)]_2\}^-$, the fragment ion peaks showing the subsequent loss of Sn, SnO and SnO_2.

Table 3.5 Details of the Negative Ion FABMS of $\{[Ph_3P]_3PtH\}\{[\mu_2\text{-}O][\mu_2\text{-}OH][Sn(O\text{-}4\text{-}NO_2\text{-}C_6H_3O)]_2\}$

m/z	Assignment	Relative abundance (%)
577	$\{[\mu_2\text{-}O][\mu_2\text{-}OH][Sn(O\text{-}4\text{-}NO_2\text{-}C_6H_3O)]_2\}^-$ $\{M\}^-$	56
459	$\{M\text{-}Sn\}^-$	29
443	$\{M\text{-}Sn\text{-}O\}^-$	100
427	$\{M\text{-}Sn\text{-}2O\}^-$	98

The proposed structrure of the anion is shown in Figure 3.10. The two tin atoms are bridged μ_2 by an oxygen atom and a hydroxyl group. The formal oxidation states of tin(II) and tin(IV) resulting in a one minus charge on the anion.

Figure 3.10 Proposed Structure for the Anion $\{[\mu_2\text{-}O][\mu_2\text{-}OH][Sn(O\text{-}4\text{-}NO_2\text{-}C_6H_3O)]_2\}^-$



Bridging oxygen atoms are found in both tin(II) and tin(IV) chemistry and an example of a bridging hydroxyl-group has been reported. The crystal structure of $C_2H_5Sn(OH)Cl_2.H_2O$[40] shows it to be dimeric via bridging hydroxyl-groups.

3.5 Reactions With Transition Metal Halide Complexes

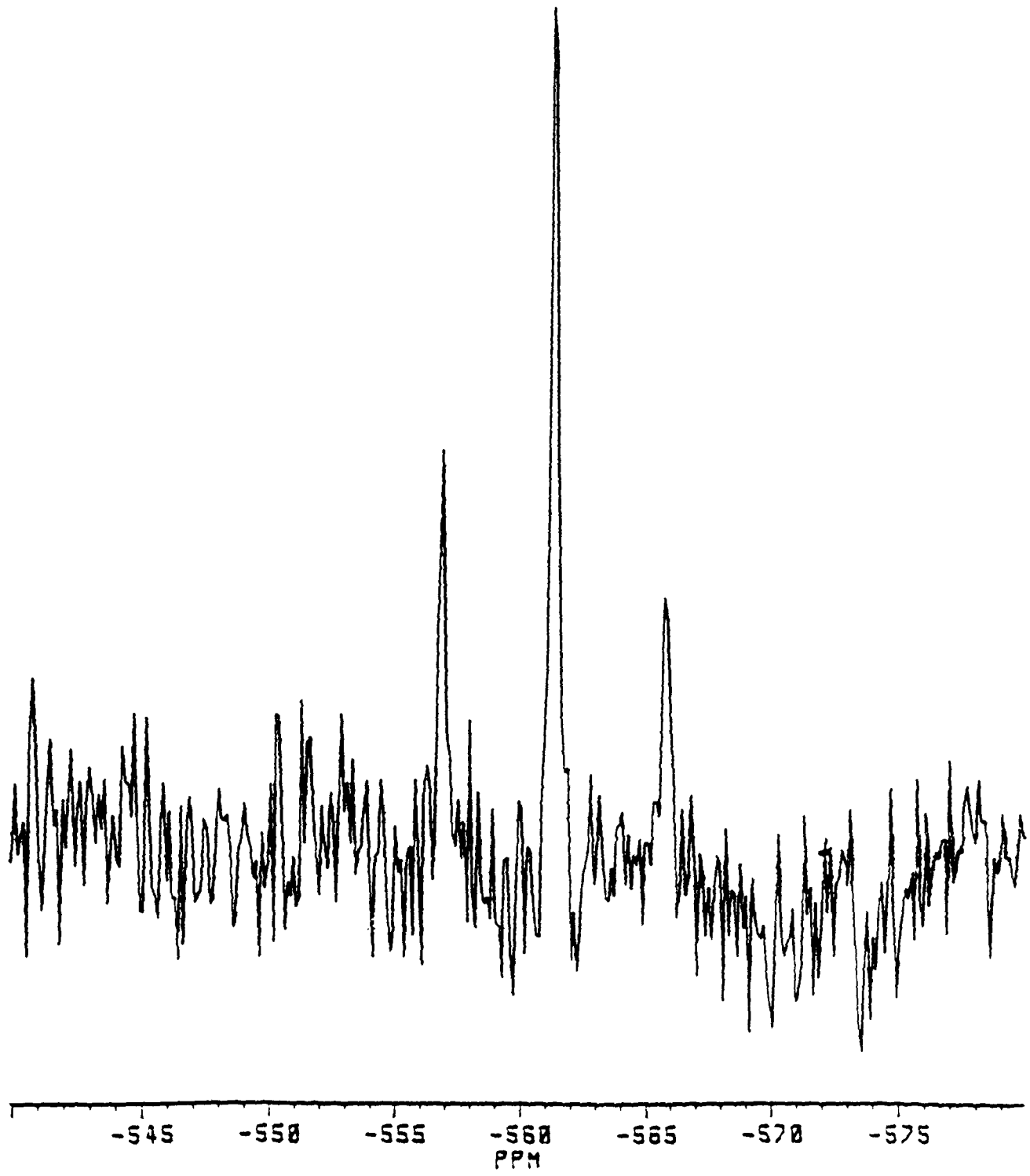
The reactions between tin(II) compounds and a wide variety of transition metal halide compounds have been reported[25-27]. Since one of the main aims of this work was the formation of novel tin-transition metal complexes (especially platinum-tin complexes), via insertion of tin(II) compounds into the metal-halide bonds, the reactivity of $\{Sn[O\text{-}4\text{-}NO_2\text{-}C_6H_3O][OC_4H_8]\}_n$ with such complexes was investigated.

3.5.1 The Reaction of $\{Sn[O\text{-}4\text{-}NO_2\text{-}C_6H_3O][OC_4H_8]\}_n$ with $[H_9C_8NC]_3RhCl$. Synthesis of $\{[H_9C_8NC]_3ClRh[\mu_2\text{-}Sn(O\text{-}4\text{-}NO_2\text{-}C_6H_3O)]\}_2$

The addition of a pale yellow tetrahydrofuran solution of $[H_9C_8NC]_3RhCl$ (H_9C_8NC = 2,6-dimethylphenyl isocyanide) to $\{Sn[O\text{-}4\text{-}NO_2\text{-}C_6H_3O][OC_4H_8]\}_n$ in tetrahydrofuran resulted in a rapid reaction which was accompanied by a dramatic colour change. The intense red-green dichroic solution afforded dark red crystals upon crystallization from tetrahydrofuran-diethyl ether. The infra-red spectrum showed the presence of terminal isocyanide ligands, ν(CN) at 2170 and 2144 cm^{-1} and a metal-chloride stretching mode at 305 cm^{-1}.

The solution ^1H n.m.r spectrum showed two isocyanide environments in a ratio of 2:1. In each environment further splittings are observed, as the two methyl groups of the xylyl ring are now inequivalent due to the asymmetry of the product. The expected singlet has split into two signals. The bonding adopted by the 4-nitrocatecholatotin(II) was solved by analysis of the product's $^{117}Sn\text{-}\{^1H\}$ solution n.m.r spectrum (see Figure 3.11).

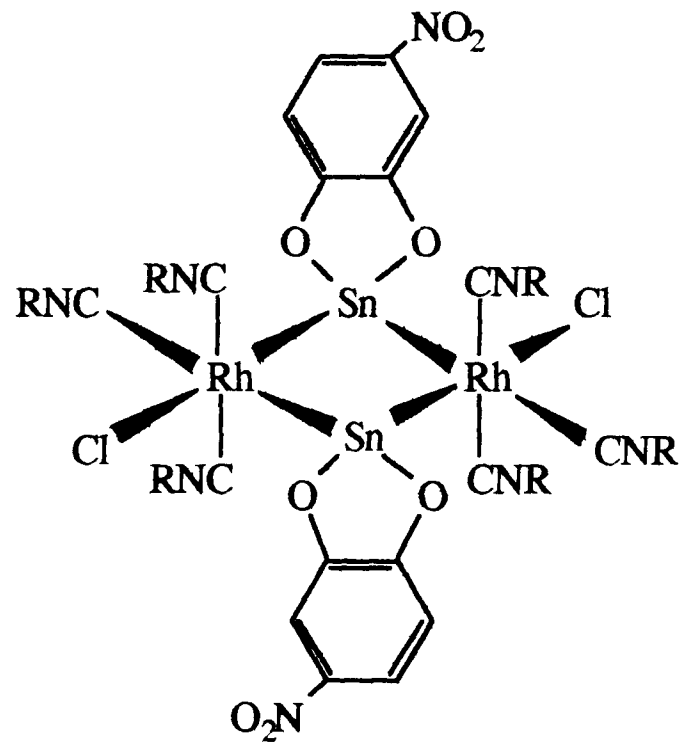
Figure 3.11 The ^{117}Sn-{^{1}H} Solution N.m.r Spectrum of $\{[H_9C_8NC]_3ClRh[\mu_2\text{-}Sn(O\text{-}4\text{-}NO_2\text{-}C_6H_3O)]\}_2$



Instead of the doublet expected due to insertion into the rhodium-chlorine bond, a 1:2:1 triplet is observed due to the tin coupling to two equivalent spin 1/2 ^{103}Rh nuclei (100% abundance). The $^{1}J_{SnRh}$ coupling constant of 472Hz is comparable to that observed for other rhodium-tin compounds[41-44].

Elemental analyses showed the presence of one chlorine and two isocyanides per rhodium. This implies that the compound consists of two $[H_9C_8NC]_3RhCl$ fragments bridged by two 4-nitrocatecholatotin units (see Figure 3.12).

Figure 3.12 Proposed Coordination Geometry of $\{[H_9C_8NC]_3ClRh[\mu_2\text{-}Sn(O\text{-}4\text{-}NO_2\text{-}C_6H_3O)]\}_2$ (R = C_8H_9)



An example of a compound with this coordination geometry, i.e two edge-sharing octahedral rhodium complexes with the octahedra linked by two bridging tin groups has recently been reported by this laboratory[45]. The addition of tin(II) chloride to $[H_9C_8NC]_3RhCl$ gave dark green insoluble crystals of *mer*-$[Rh(CNC_8H_9)(SnCl_3)(\mu_2\text{-}SnCl_2)]_2$. An X-ray diffraction study revealed a coordination geometry very similar to that proposed for $\{[H_9C_8NC]_3ClRh[\mu_2\text{-}Sn(O\text{-}4\text{-}NO_2\text{-}C_6H_3O)]\}_2$.

3.5.2 The Reaction of $\{Sn[O\text{-}4\text{-}NO_2\text{-}C_6H_3O][OC_4H_8]\}_n$ with Ph_3PAuCl. Synthesis of $[Au_4(PPh_3)_4(\mu_2\text{-}SnCl_3)_2]$

After refluxing $\{Sn[O\text{-}4\text{-}NO_2\text{-}C_6H_3O][OC_4H_8]\}_n$ and Ph_3PAuCl in tetrahydrofuran for three hours, extraction of the reaction residue with acetone and addition of toluene afforded a small number of golden-yellow octahedral crystals.

The infra-red spectrum showed a metal-chlorine stretching mode at 312 cm^{-1} and the $^{31}P\text{-}\{^1H\}$ solution n.m.r spectrum showed a single peak at 56.9 p.p.m. No phosphorus-tin coupling was observed. This may be due to the low signal to noise ratio of the spectrum on account of the small amount of compound available for analysis. In order to determine the structure of this compound, a single crystal X-ray diffraction study was undertaken.

3.5.3 X-ray Crystallographic Analysis of $[Au_4(PPh_3)_4(\mu_2\text{-}SnCl_3)_2]$

Golden yellow octahedral crystals of $[Au_4(PPh_3)_4(\mu_2\text{-}SnCl_3)_2]$ were grown by slow diffusion of toluene into an acetone solution of the compound. The data collection and stucture solution were carried out by Dr. Harry Powell of this laboratory.

A single crystal of dimensions 0.16 x 0.16 x 0.16 mm was mounted on a glass fibre and transferred to an Enraf-Nonius CAD4. Final unit cell dimensions, calculated from a least-squares treatment of the angles of 24 accurately centered reflections are given in Table 3.6. 6911 reflections were collected using $\omega/2\vartheta$ scans (scan width 1.00 + 0.35tanϑ) using graphite monochromated Mo-K_α radiation, of which 4231 were considered unique and observed ($I \geq 3\sigma(I)$, R_{merg}= 0.0226). These were corrected for Lorentz and polarization effects and an absorption correction was applied (min/max correction 2.36/3.26).

The coordinates of the two gold atoms and tin atom were deduced from interpretation of a Patterson synthesis. All remaining non-hydrogen atoms were located from a difference Fourier synthesis. Hydrogen atoms were included in geometrically idealized positions. All non-hydrogen atoms were refined with anisotropic temperature factors in the final cycles of full matrix least-squares refinement. The hydrogen atoms were

assigned a common isotropic temperature factor which was refined to a final value of 0.11Å^2. Refinement converged with R = 0.0316 and R_w = 0.0328.

Table 3.7 and Appendix 3 contain the structural data for $[Au_4(PPh_3)_4(\mu_2\text{-}SnCl_3)_2]$, whilst Figures 3.13 and 3.14 show the main structural features.

Table 3.6 Structural Details for $[Au_4(PPh_3)_4(\mu_2\text{-}SnCl_3)_2]$

Compound	$C_{72}H_{60}Au_4Cl_6P_4Sn_2.0.5(C_6H_5CH_3)$
Molecular Weight	2333.20
Space Group	C2/c
Cell Dimensions	a 19.858(4)Å α 90°
	b 19.877(6)Å β 97.06(2)°
	c 20.127(3)Å γ 90°
Cell Volume	7884.44 Å^3
Z	4
Density	1.968 g cm^{-3}
Linear Absorption Coefficient	83.632 cm^{-1}
Radiation	Mo-K_α ($\lambda = 0.71069$Å)
Min., Max. h, k, l	-23, 23; -1, 23; -1, 23
Decay of Standards	< 1%
2ϑ Range	0-50°
Number of Parameters Varied	388
R	0.0316
R_w	0.0328

Table 3.7 Selected Bond Lengths (Å) and Angles (°) for $[Au_4(PPh_3)_4(\mu_2\text{-}SnCl_3)_2]$

Distances and Angles for Metal Cage

Atoms	Distance	Atoms	Distance
Au(2)-Au(2)	2.773(6)	Au(2)-Au(3)	2.634(5)
Au(2)-Au(3)	2.813(5)	Au(2)-Sn(1)	2.973(8)
Au(3)-Au(3)	2.766(6)	Au(3)-Sn(1)	2.815(7)

Atoms	Angle	Atoms	Angle
Au(3)-Au(3)-Au(2)	62.63(1)	Au(3)-Au(3)-Au(2)	56.27(1)
Au(3)-Au(2)-Au(3)	60.94(2)	Sn(1)-Au(2)-Au(2)	116.80(2)
Sn(1)-Au(2)-Au(3)	59.92(2)	Sn(1)-Au(2)-Au(3)	111.06(2)
Au(2)-Au(3)-Au(2)	61.10(1)	Au(3)-Au(3)-Au(2)	62.72(1)
Au(3)-Au(3)-Au(2)	56.34(1)	Sn(1)-Au(3)-Au(2)	66.02(2)
Sn(1)-Au(3)-Au(2)	120.86(2)	Sn(1)-Au(3)-Au(3)	117.45(2)
Au(3)-Sn(1)-Au(2)	54.06(1)		

Metal-Ligand Bond Lengths and Angles

Atoms	Distance	Atoms	Distance
Au(2)-P(2)	2.315(2)	Au(3)-P(3)	2.321(2)
Sn(1)-Cl(1)	2.384(4)	Sn(1)-Cl(2)	2.366(3)
Sn(1)-Cl(3)	2.387(3)		

Atoms	Angle	Atoms	Angle
P(2)-Au(2)-Au(2)	115.07(6)	P(2)-Au(2)-Au(3)	177.34(6)
P(2)-Au(2)-Au(3)	116.85(6)	P(2)-Au(2)-Sn(1)	122.74(6)
P(3)-Au(3)-Au(2)	175.15(6)	P(3)-Au(3)-Au(2)	114.40(6)
P(3)-Au(3)-Au(3)	113.63(6)	P(3)-Au(3)-Sn(1)	118.81(6)
Cl(1)-Sn(1)-Au(2)	90.40(1)	Cl(1)-Sn(1)-Au(3)	144.20(1)
Cl(2)-Sn(1)-Au(2)	134.6(1)	Cl(2)-Sn(1)-Au(3)	105.25(9)
Cl(2)-Sn(1)-Cl(1)	96.60(1)	Cl(3)-Sn(1)-Au(2)	127.50(1)
Cl(3)-Sn(1)-Au(3)	108.90(1)	Cl(3)-Sn(1)-Cl(1)	96.20(1)
Cl(3)-Sn(1)-Cl(2)	96.30(1)		

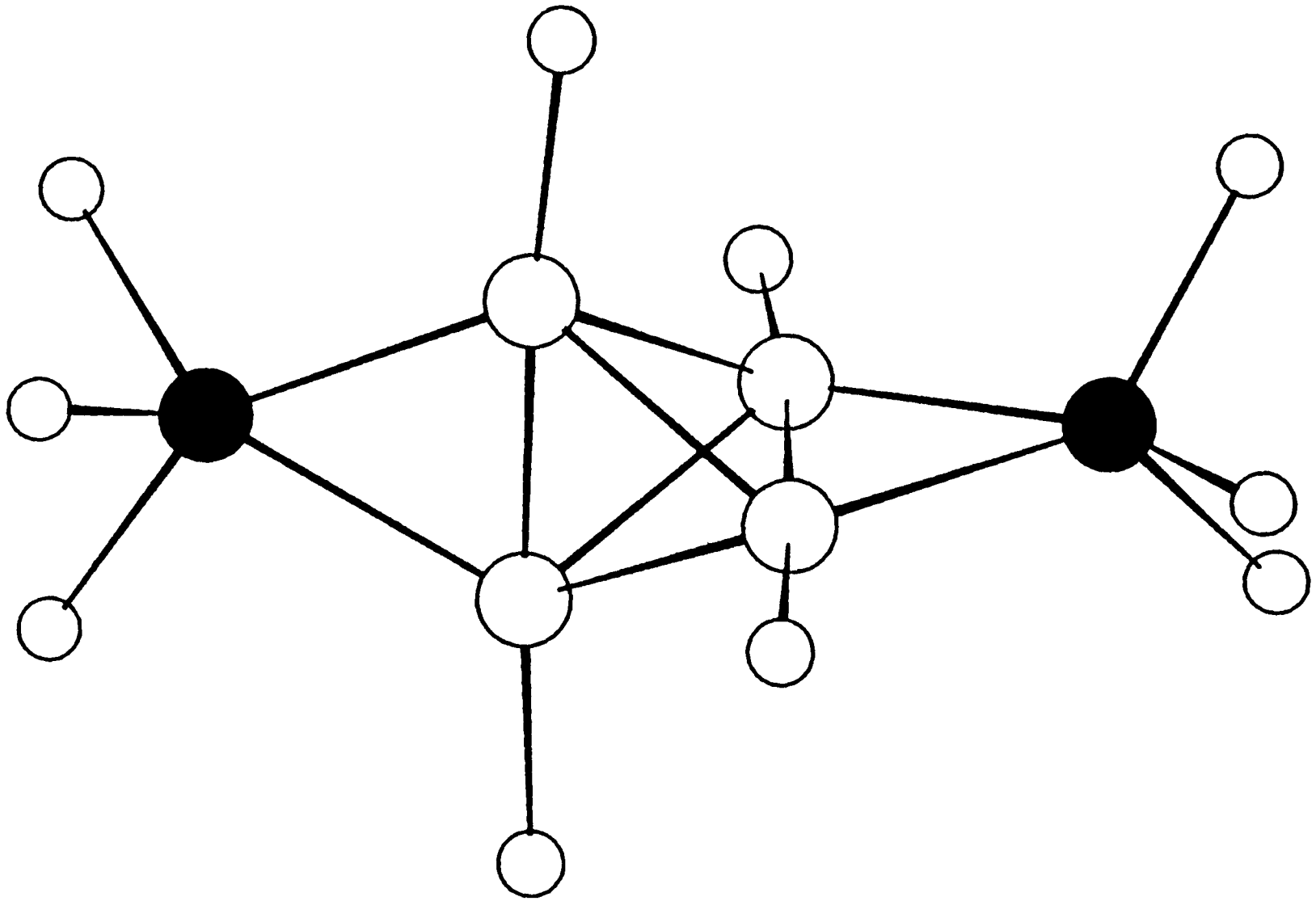
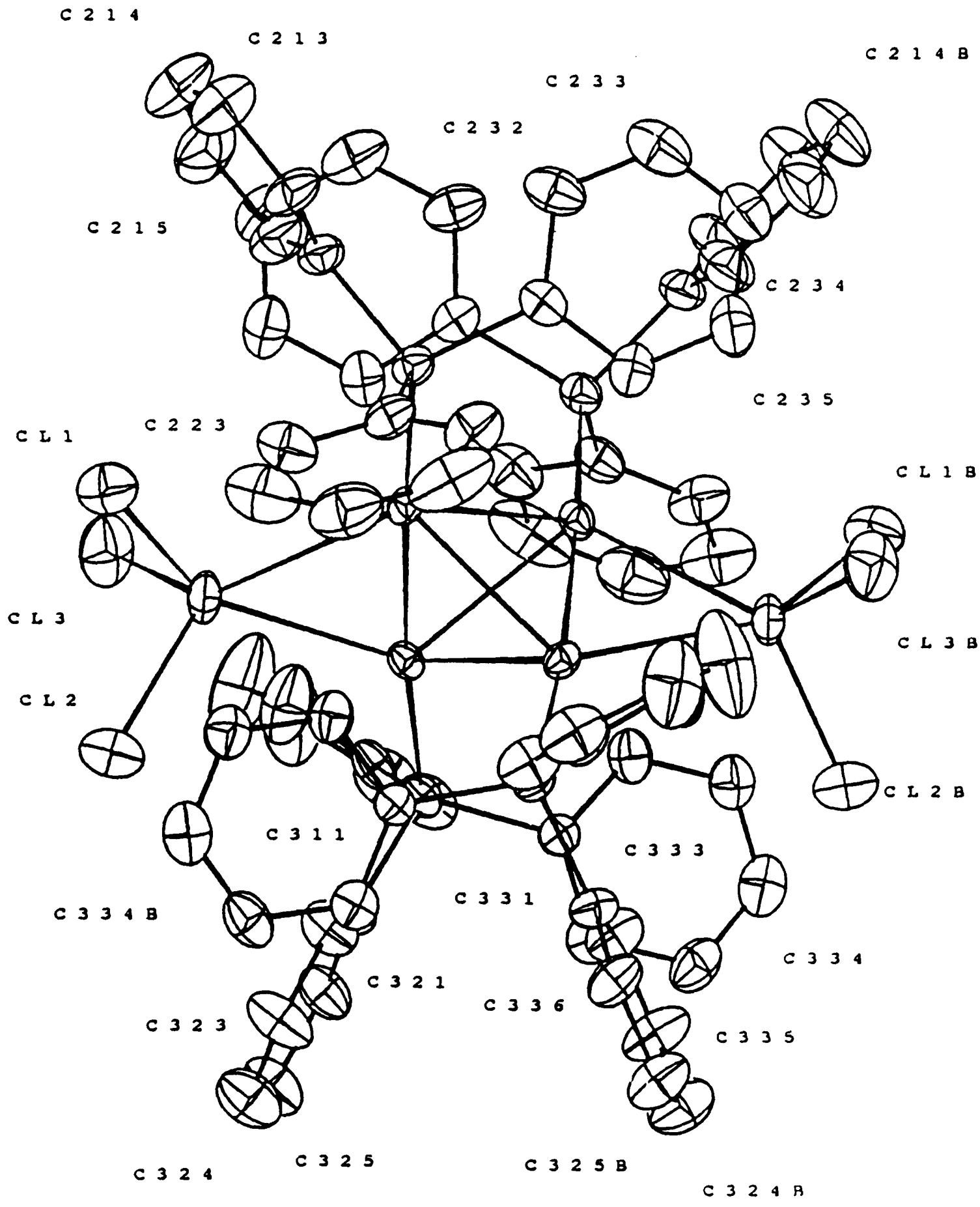


Figure 3.13 The Inner Coordination Geometry of $[Au_4(PPh_3)_4(\mu_2\text{-}SnCl_3)_2]$

Figure 3.14 The Molecular Structure of $[Au_4(PPh_3)_4(\mu_2\text{-}SnCl_3)_2]$



The crystallographic determination showed the presence of the neutral 54 valence electron gold cluster $[Au_4(PPh_3)_4(\mu_2\text{-}SnCl_3)_2]$. It consists of a tetrahedral gold core, with two opposite edge bridging $SnCl_3$ groups. The molecule has a crystallographically imposed c_2 symmetry axis.

The gold-gold bond lengths range from 2.6341(5)Å to 2.8128(5)Å, with the shorter bonds between those of the gold atoms edge bridged by the $SnCl_3$ groups. This is also observed in $[Au_4I_2(PPh_3)_4]$[47,48] which has gold-gold bond lengths in the range 2.659(1)Å to 2.828(1)Å, with the shorter bonds between those gold atoms bridged by the iodides. The Au-Au-Au bond angles for $[Au_4(PPh_3)_4(\mu_2\text{-}SnCl_3)_2]$ range from 56.34(1)° to 62.72(1)° showing the slight departure from a regular tetrahedral geometry. The distortion from the regular tetrahedron is also seen in the positions adopted by the triphenylphosphine ligands. The Au-Au-P bond angles at 175.16(6) and 177.34(6)° must mainly be attributed to reducing the steric interaction, but MO calculations[46] performed upon the isostrucural and isoelectronic compound, $[Au_4I_2(PPh_3)_4]$[47,48] have shown that this structure is also stabilized by interaction of the b_2 component of the t_2 set of $Au_4(PPh_3)_4^{2+}$ (see Figure 3.15) with the two iodide ligands. The distortion of the triphenylphosphine ligands causes a localization of the p_σ contribution in the b_2 orbital, accounting for its stabilization, whilst the e set becomes essentially pure p_π in character and is therefore destabilized (Figure 3.16).

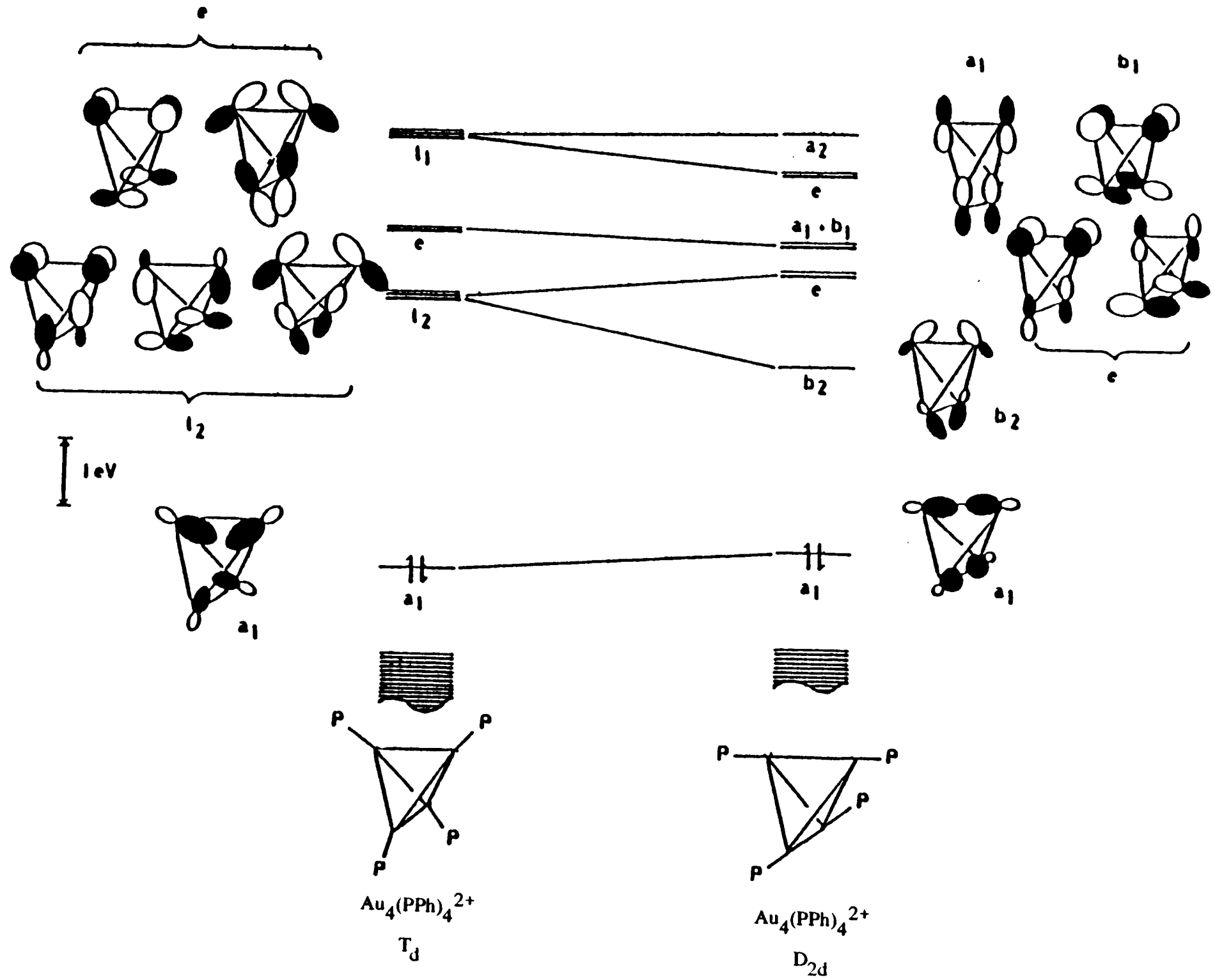


Figure 3.15 The Effect of Lowering the Symmetry to D_{2d} on the MO's of the $Au_4(PPh_3)_4^{2+}$ Tetrahedron

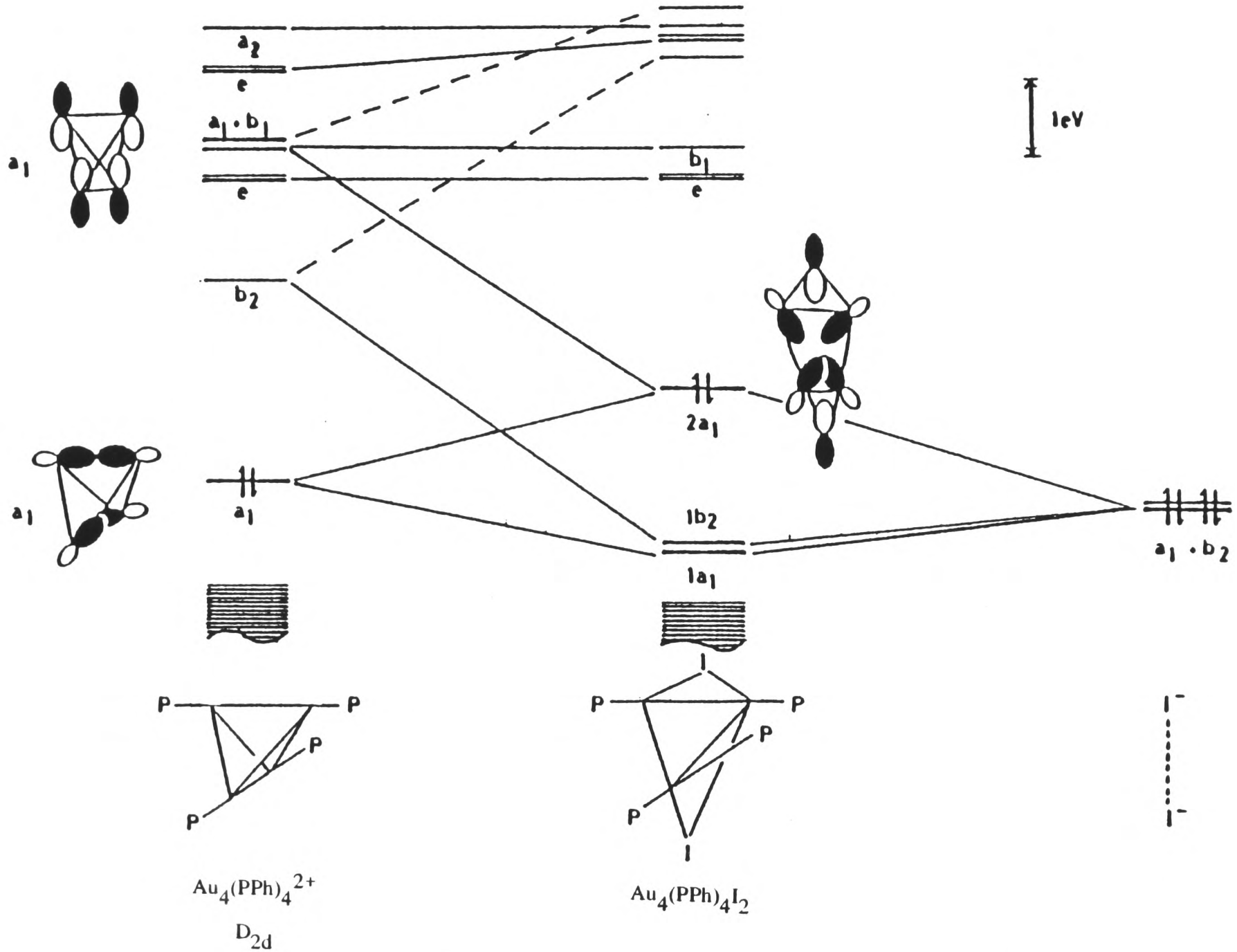


Figure 3.16 The MO Interaction Diagram for $Au_4(PPh_3)_4^{2+}$ with Two Bridging Iodide Ligands

The differences observed in the gold-gold bond lengths can also be primarily attributed to the bonding contribution of the cluster b_2 molecular orbital, which is more strongly bonding along the two bridged edges.

The gold-tin bond lengths in $[Au_4(PPh_3)_4(\mu_2\text{-}SnCl_3)_2]$ of 2.8150(7) and 2.9725(8)Å are long and imply a weak interaction between $SnCl_3^-$ and the gold cage. There are only two other structurally characterized gold-tin bonded compounds, both containing terminally bound $SnCl_3$ groups. $(Me_2PhP)_2AuSnCl_3$[49] contains a long gold-tin distance of 2.881Å, whilst in $[Au_8(PPh_3)_7(SnCl_3)]_2[SnCl_6]$[50], the distance is much shorter at 2.625(3)Å.

$[Au_4(PPh_3)_4(\mu_2\text{-}SnCl_3)_2]$ is the first example of a SnX_3 group bridging two metal centres. Nearly all compounds so far studied have had the ligand terminally bound to the metal centre, although examples of μ_3 coordinated SnX_3 groups have been reported recently[51-53]. The coordination geometry about the five coordinate tin atom is pseudo-trigonal bipyramidal. The distorted geometry is mainly due to the weakness of the interaction between $SnCl_3$ and the gold cage, resulting in a small Au-Sn-Au bond angle ((54.06(1)°) and the maintenance of the bonding and coordination found in free trichlorostannate. The mean tin-chlorine bond length and Cl-Sn-Cl bond angle in $Au_4(PPh_3)_4(\mu_2\text{-}SnCl_3)_2$ are 2.379Å and 96.4° respectively, values intermediate between those found in compounds containing the free anion (e.g $[Co(en)_3][SnCl_3]Cl_2$[54], Sn-Cl 2.53Å, Cl-Sn-Cl 87°) and trichlorostannate bound to a single metal centre (e.g $[OC]_5MnSnCl_3$[55], Sn-Cl 2.34Å, Cl-Sn-Cl 100°).

The isolation of $[Au_4(PPh_3)_4(\mu_2\text{-}SnCl_3)_2]$ from the reaction between $\{Sn[O\text{-}4\text{-}NO_2\text{-}C_6H_3O][OC_4H_8]\}_n$ and Ph_3PAuCl was unexpected, and attempts to increase the yield of $[Au_4(PPh_3)_4(\mu_2\text{-}SnCl_3)_2]$ by increasing the amount $\{Sn[O\text{-}4\text{-}NO_2\text{-}C_6H_3O][OC_4H_8]\}_n$ used, or by the addition of Cl^- or $SnCl_3^-$ ions into the reaction mixture were unsuccessful.

The overall reaction leading to the formation of $[Au_4(PPh_3)_4(\mu_2\text{-}SnCl_3)_2]$ may be represented by:

$$6Ph_3PAuCl + 3Sn(O\text{-}4\text{-}NO_2\text{-}C_6H_3O) \longrightarrow 2[Ph_3PAu]^+ + [Sn(O\text{-}4\text{-}NO_2\text{-}C_6H_3O)_3]^{2-} + [Au_4(PPh_3)_4(\mu_2\text{-}SnCl_3)_2]$$

In the presence of Ph_3PAuCl, $\{Sn[O\text{-}4\text{-}NO_2\text{-}C_6H_3O][OC_4H_8]\}_n$ acts as a mild reducing agent, forming the tetrahedral gold species, $[Au_4(PPh_3)_4]^{2+}$. From other work described in this Thesis (see Chapter 5), the tris(catecholato)tin(IV) dianion, $[Sn(O\text{-}4\text{-}NO_2\text{-}C_6H_3O)_3]^{2-}$ can be synthesized, and is the most likely oxidation product of $\{Sn[O\text{-}4\text{-}NO_2\text{-}C_6H_3O][OC_4H_8]\}_n$. The redistribution of catecholate ligands allows the formation of the $SnCl_3^-$ groups, by reaction with excess Ph_3PAuCl. The $SnCl_3^-$ groups can then react with $[Au_4(PPh_3)_4]^{2+}$ to give the neutral cluster $[Au_4(PPh_3)_4(\mu_2\text{-}SnCl_3)_2]$.

3.5.4 Insertion Reactions of Tin(II) Chloride and $\{Sn[O\text{-}4\text{-}NO_2\text{-}C_6H_3O][OC_4H_8]\}_n$ into Platinum-Chlorine Bonds

As outlined in Section 2.1, the mode of action of the platinum(II) antitumour drugs involves the loss of two chloride ions before binding to the DNA bases. Since all known active platinum(II) agents are based upon a *cis* configuration of chlorine atoms about the platinum centre, it was therefore felt important to retain this *cis* configuration in any platinum-tin compounds formed, thus enhancing the prospect of any synergic antitumour activity.

The strong π-acceptor nature of the SnX_2Cl^- group usually leads to the formation of strong platinum-tin bonds with considerable s-character, thus giving rise to a strong *trans* influence. Since platinum(II) antitumour drugs usually contain nitrogen-donor ligands, which are weak *trans* influencing ligands, to ensure insertion of two tin(II) species *cis* to each other, bidentate donor ligands were used to restrict the coordination about the platinum centre. To enable the reaction mechanisms to be studied in greater detail, the bidentate phosphine ligand 1,2-bis(diphenylphosphino)ethane (dppe) was chosen. Due to the presence of 100% spin-1/2 ^{31}P nuclei, identification of any product would be made simpler by the relatively low concentrations and collection times required for ^{31}P solution n.m.r, compared to ^{195}Pt and ^{117}Sn n.m.r. As a comparative study, the ability of tin(II) chloride to insert into the platinum-chlorine bonds of the model system was also investigated.

3.5.4.1 Synthesis of $[Et_4N][Pt(dppe)(SnCl_3)_3]$

The addition of two molar equivalents of anhydrous tin(II) chloride to a solution of $PtCl_2$(dppe) in dichloromethane brought about an immediate reaction. The pale yellow solid formed was only very sparingly soluble in dichloromethane, and insoluble in all other common solvents. Infra-red spectra showed the presence of tin-chlorine stretching modes at 355(br) and 286(br) cm^{-1}, whilst elemental analyses confirmed that the compound was the desired product $Pt(SnCl_3)_2$(dppe). To try and enhace solubility, a molar equivalent of tetraethylammonium chloride, and a further molar equivalent of tin(II) chloride were added. This further reaction yielded a bright red-orange solution. If the product was left in solution over a period of time (3-4 hours), decomposition was observed giving white crystalline $PtCl_2$(dppe) (by ^{31}P-$\{^1H\}$ solution n.m.r). Crystallization from dichloromethane-acetonitrile at -20°C afforded red-orange plates. Infra-red showed tin-chlorine stretching modes at 359, 287 and 266 cm^{-1}. Due to the unstable nature of the product in solution a series of ^{31}P-$\{^1H\}$ n.m.r experiments were undertaken and are described in detail in section 3.5.4.3. In order to determine the solid-state structure of the compound, a single crystal X-ray diffraction study was undertaken.

3.5.4.2 X-ray Crystallographic Analysis of $[Et_4N][Pt(dppe)(SnCl_3)_3]$

Red-orange plates of $[Et_4N][Pt(dppe)(SnCl_3)_3]$, were grown by slow diffusion of acetonitrile into a dichloromethane solution of the compound. The data collection and stucture solution were carried out by Dr. Jonathan Machell of this laboratory.

A single crystal of dimensions 0.5 x 0.5 x 0.5 mm was mounted in a glass capillary and transferred to an Enraf-Nonius CAD4 diffractometer. Final unit cell dimensions, calculated from a least-squares treatment of the angles of 24 accurately centred reflections are given in Table 3.8. 5559 reflections were collected using $\omega/2\vartheta$ scans (scan width 0.70 + 0.35tanϑ) using graphite monochromated Mo-K_α radiation, of which 2111 were considered unique and observed ($I \geq 3\sigma(I)$, R_{merg}= 0.0606). These were corrected for Lorentz and

polarization effects and an absorption correction was applied (min/max correction 1.00/1.94).

The structure was solved by routine Patterson, direct methods (SHELXS), Fourier methods and full-matrix, least squares refinement of all the non-hydrogen atoms, followed by DIFABS and spherical absorption corrections. Platinum, tin, phosphorus and non-solvent chlorine atoms were converted to having anisotropic thermal perameters, whilst all hydrogen atoms were generated geometrically. On application of a Cebyshev weighting scheme (coefficients 7.417, -5.031, 5.551), the model converged at $R = 0.0488$, $R_w = 0.0541$.

Table 3.9 and Appendix 4 contain the structural data for $[Et_4N][Pt(dppe)(SnCl_3)_3]$ whilst Figures 3.17 to 3.18 show the main structural features.

Table 3.8 Structural Details for $[Et_4N][Pt(dppe)(SnCl_3)_3]$

Compound	$C_{34}H_{34}Cl_9N_1P_2Pt_1Sn_3.3/2(CH_2Cl_2)$
Molecular Weight	1526.31
Space Group	Pbca
Cell Dimensions	a 16.364(8)Å α 90°
	b 18.323(9)Å β 90°
	c 36.800(2)Å γ 90°
Cell Volume	11033 Å^3
Z	8
Density	1.84 g cm^{-3}
Linear Absorption Coefficient	45.74 cm^{-1}
Radiation	Mo-K_α ($\lambda = 0.71069$Å)
Standard Reflections	-6 -1 4; 4 -8 -4; -1 5 11
Decay of Standards	5%
2ϑ Range	2-36°
Number of Parameters Varied	300
R	0.0488
R_w	0.0541
Goodness of Fit	1.06
F(000)	5832

Table 3.9 Selected Bond Lengths (Å) and Angles (°) for $[Et_4N][Pt(dppe)(SnCl_3)_3]$

Atoms	Distance	Atoms	Distance
Pt(1)-Sn(1)	2.600(3)	Pt(1)-Sn(2)	2.679(2)
Pt(1)-Sn(3)	2.613(3)	Pt(1)-P(1)	2.324(8)
Pt(1)-P(2)	2.314(8)	Sn(1)-Cl(1)	2.337(9)
Sn(1)-Cl(2)	2.340(1)	Sn(1)-Cl(3)	2.330(1)
Sn(2)-Cl(4)	2.380(9)	Sn(2)-Cl(5)	2.381(8)
Sn(2)-Cl(6)	2.389(9)	Sn(3)-Cl(7)	2.338(9)
Sn(3)-Cl(8)	2.343(9)	Sn(3)-Cl(9)	2.367(9)

Atoms	Angle	Atoms	Angle
Sn(2)-Pt(1)-Sn(1)	91.8(8)	Sn(3)-Pt(1)-Sn(1)	86.6(9)
Sn(3)-Pt(1)-Sn(2)	106.4(8)	P(1)-Pt(1)-Sn(1)	91.40(2)
P(1)-Pt(1)-Sn(2)	108.4(2)	P(1)-Pt(1)-Sn(3)	145.2(2)
P(2)-Pt(1)-Sn(1)	107.8(2)	P(2)-Pt(1)-Sn(2)	97.3(2)
P(2)-Pt(1)-Sn(3)	91.8(2)	P(2)-Pt(1)-P(1)	84.7(3)
Cl(1)-Sn(1)-Pt(1)	118.6(3)	Cl(2)-Sn(1)-Pt(1)	119.3(3)
Cl(2)-Sn(1)-Cl(1)	96.2(4)	Cl(3)-Sn(1)-Pt(1)	122.6(3)
Cl(3)-Sn(1)-Cl(1)	96.6(4)	Cl(3)-Sn(1)-Cl(2)	97.9(4)
Cl(4)-Sn(2)-Pt(1)	119.5(2)	Cl(5)-Sn(2)-Pt(1)	113.8(2)
Cl(5)-Sn(2)-Cl(4)	97.9(3)	Cl(6)-Sn(2)-Pt(1)	128.9(2)
Cl(6)-Sn(2)-Cl(4)	94.3(3)	Cl(6)-Sn(2)-Cl(5)	96.2(3)
Cl(7)-Sn(3)-Pt(1)	119.5(3)	Cl(8)-Sn(3)-Pt(1)	122.8(2)
Cl(8)-Sn(3)-Cl(7)	93.6(4)	Cl(9)-Sn(3)-Pt(1)	118.9(2)
Cl(9)-Sn(3)-Cl(7)	99.5(3)	Cl(9)-Sn(3)-Cl(8)	96.9(3)

Figure 3.17 The Inner Coordination Geometry of $[Et_4N][Pt(dppe)(SnCl_3)_3]$

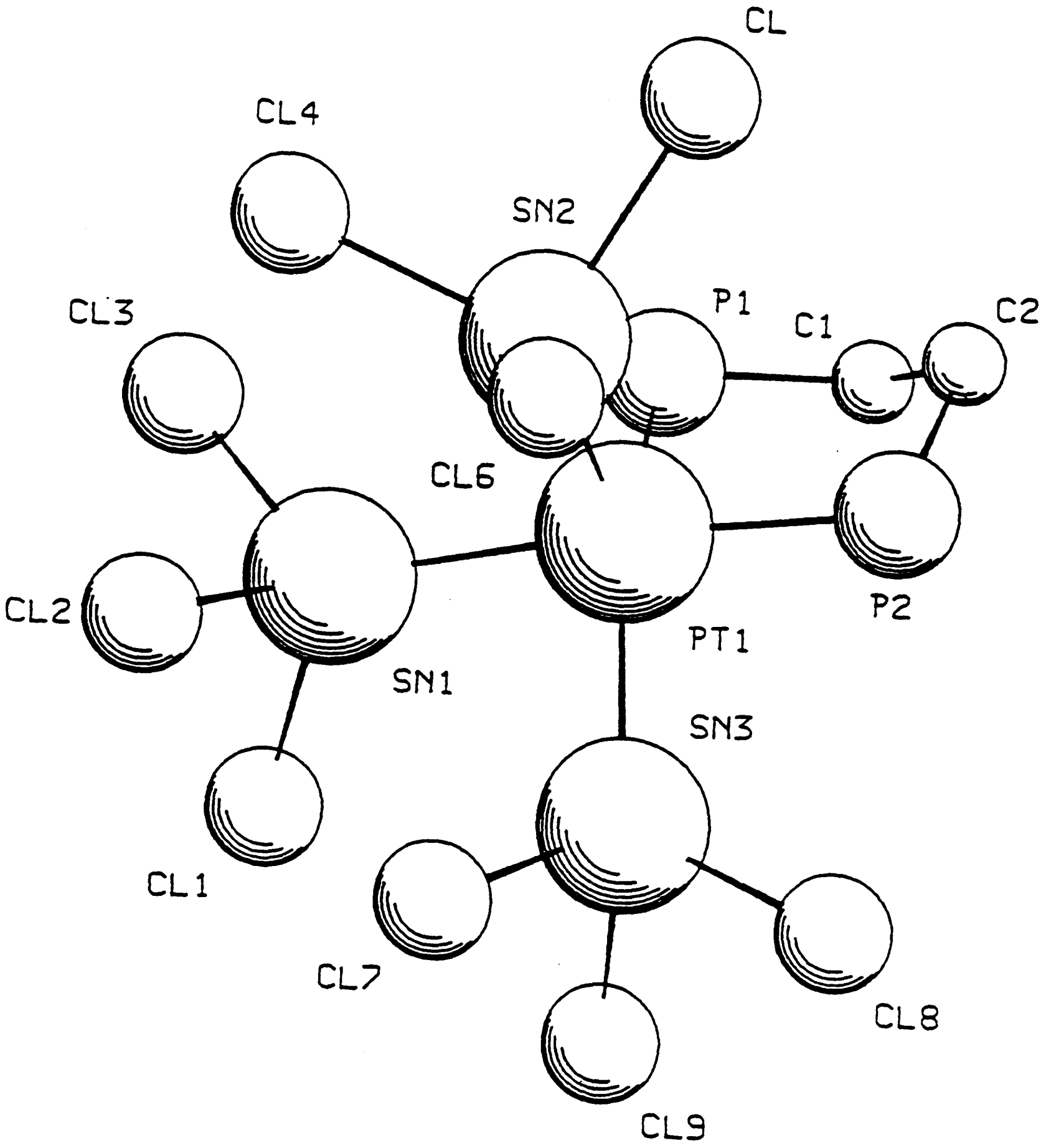
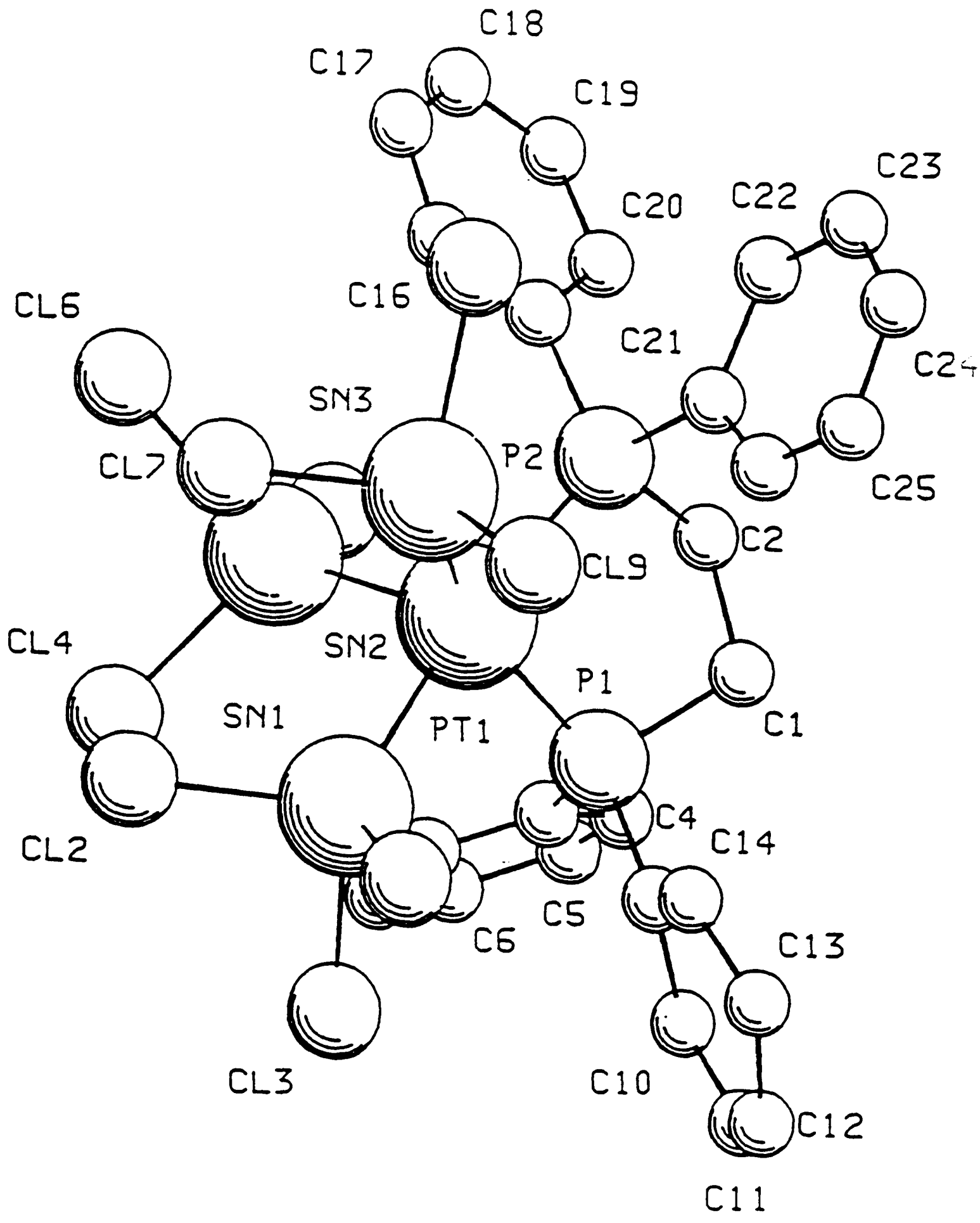


Figure 3.18 The Molecular Structure of $[Et_4N][Pt(dppe)(SnCl_3)_3]$



The structure consists of well separated anions of $[Pt(dppe)(SnCl_3)_3]^-$ and cations of $[Et_4N]^+$ together with areas of electron density best modelled as one full-occupancy dichloromethane molecule and one partial occupancy dichloromethane molecule. The compound crystallizes in the space group Pbca without disorder except in one of the solvent molecules.

There have been a number of compounds isolated which have been identified as five-coordinate complexes of Pt(II) with trichlorostannate (see Table 2.2). Only three have been structurally characterized and has revealed a range of coordination geometries. The platinum-tin bond lengths in $[Pt(dppe)(SnCl_3)_3]^-$ (2.600(3)-2.679(2)Å) straddles the range of bond lengths (2.546(2)-2.643(2)Å) previously observed for the five-coordinate, Pt-$SnCl_3$ containing complexes $[Pt(SnCl_3)_5][AsPh_4]$[56], $[Ph_3PCH_3]_3[Pt(COD)(SnCl_3)_3]$[57], and $[(PPh_3)_2N][Pt(SnCl_3)_3(AsMe_3)_2]$[58].

In $[Pt(dppe)(SnCl_3)_3]^-$ the bond angles deviate significantly from those for ideal trigonal bipyramidal or square pyramidal geometries, but they more closely approximate to trigonal bipyramidal as shown in Figure 3.17. There are six bond angles lying between 84.7(3) and 97.3(2)°, three bond angles lying between 106.4(8) and 145.2(2)° and one bond angle equal to 170.8(2)°. The ion should be described as distorted trigonal bipyramidal, with P(2) and Sn(1) occupying the axial positions.

The complex $[Pt(SnCl_3)_5][AsPh_4]$ is said to have a regular trigonal bipyramidal geometry. The average axial platinum-tin bond length is 2.553(7)Å, whilst the equatorial platinum-tin bonds are longer at 2.572(1)Å. The axial platinum-tin bond length in $[Pt(dppe)(SnCl_3)_3]^-$ is 2.600(3)Å, with longer equatorial platinum-tin bonds at 2.679(2) and 2.613(3)Å.

3.5.4.3 ^{31}P-{^1H} Solution N.m.r Studies

As was outlined in Section 3.5.4.1, the reaction of $PtCl_2(dppe)$ with two molar equivalents of $SnCl_2$ yields insoluble $Pt(SnCl_3)_2(dppe)$, which upon addition of $SnCl_3^-$ reacts further to give $[Pt(dppe)(SnCl_3)_3]^-$. Since $[Pt(dppe)(SnCl_3)_3]^-$ is unstable in solution a number of

n.m.r experiments were undertaken to try and ascertain the species involved in the production and subsequent decomposition of $[Pt(dppe)(SnCl_3)_3]^-$.

A series of dichloromethane solutions were prepared of $PtCl_2(dppe)$ with various molar equivalents of $SnCl_2$, Cl^- and/or $SnCl_3^-$. Product formation was followed by $^{31}P-\{^1H\}$ solution n.m.r. spectroscopy. The results from these experiments are shown in Figures 3.19 to 3.21.

Figure 3.19 Room Temperature Time-lapse $^{31}P-\{^{1}H\}$ Solution N.m.r Spectra for the Reaction Between $PtCl_2(dppe)$ and One Molar Equivalent of $SnCl_2$

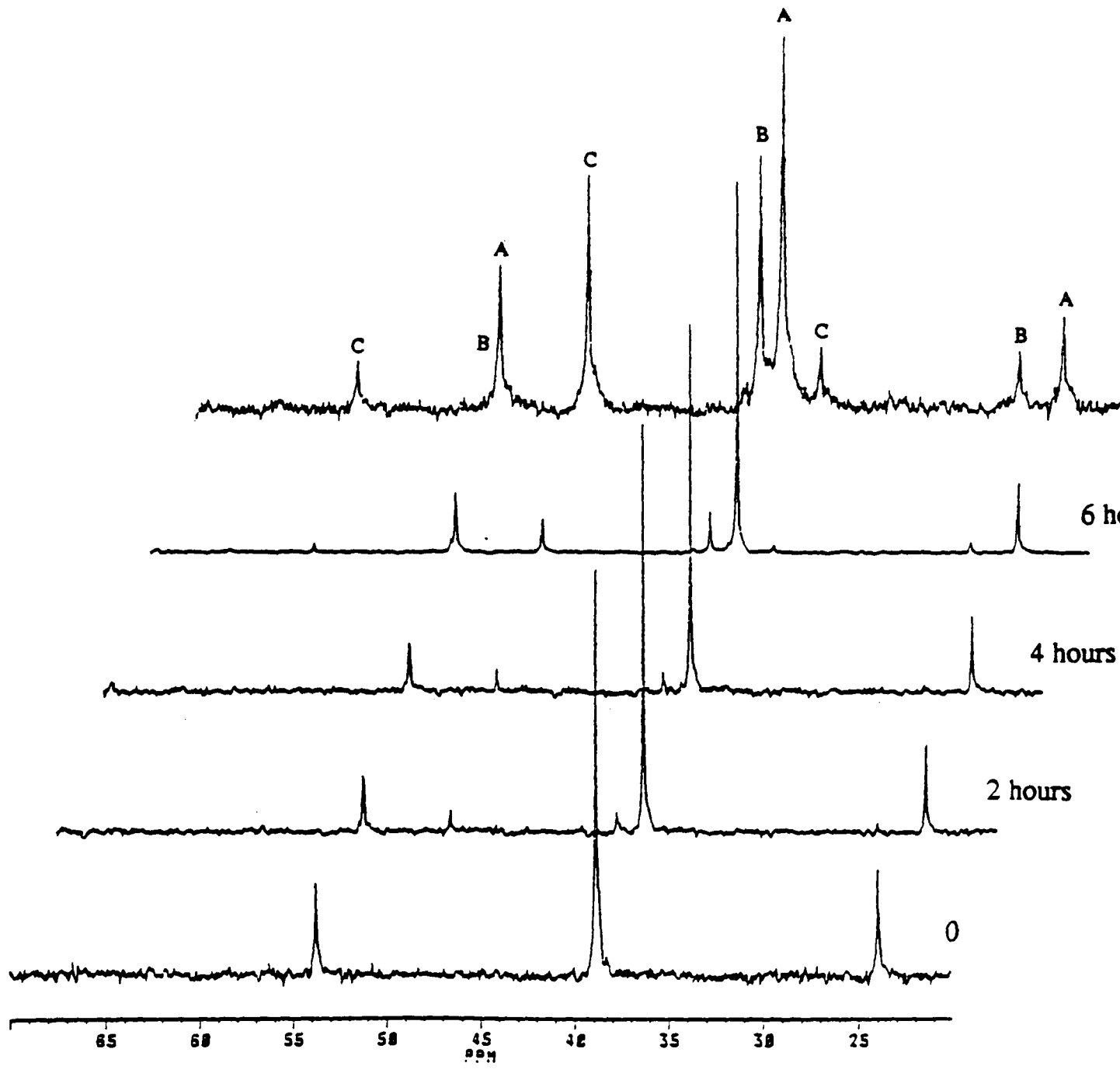


Figure 3.20 Room Temperature Time-lapse $^{31}P-\{^{1}H\}$ Solution N.m.r Spectra for the Reaction Between $PtCl_2$(dppe) and Two Molar Equivalents of $SnCl_2$

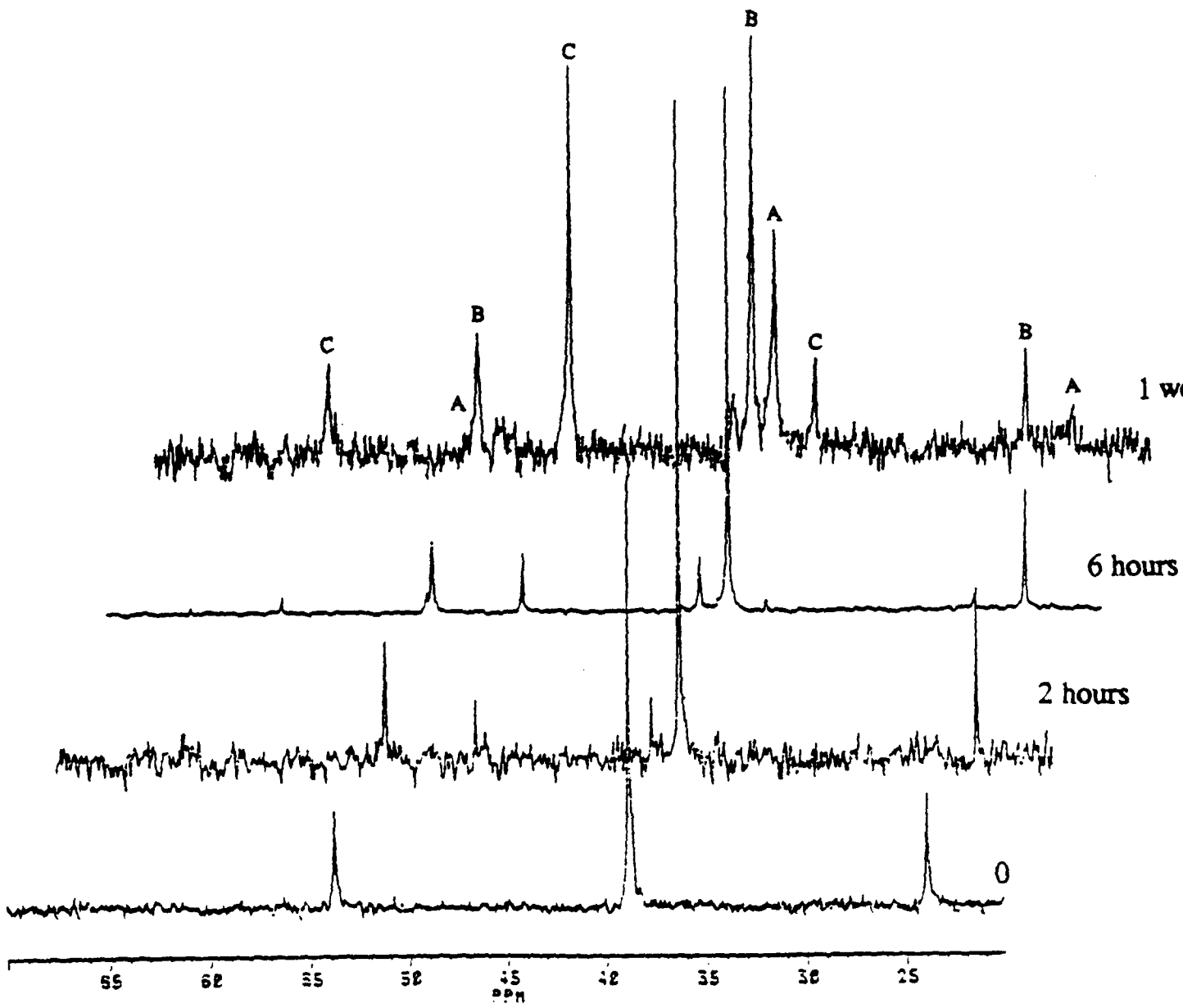
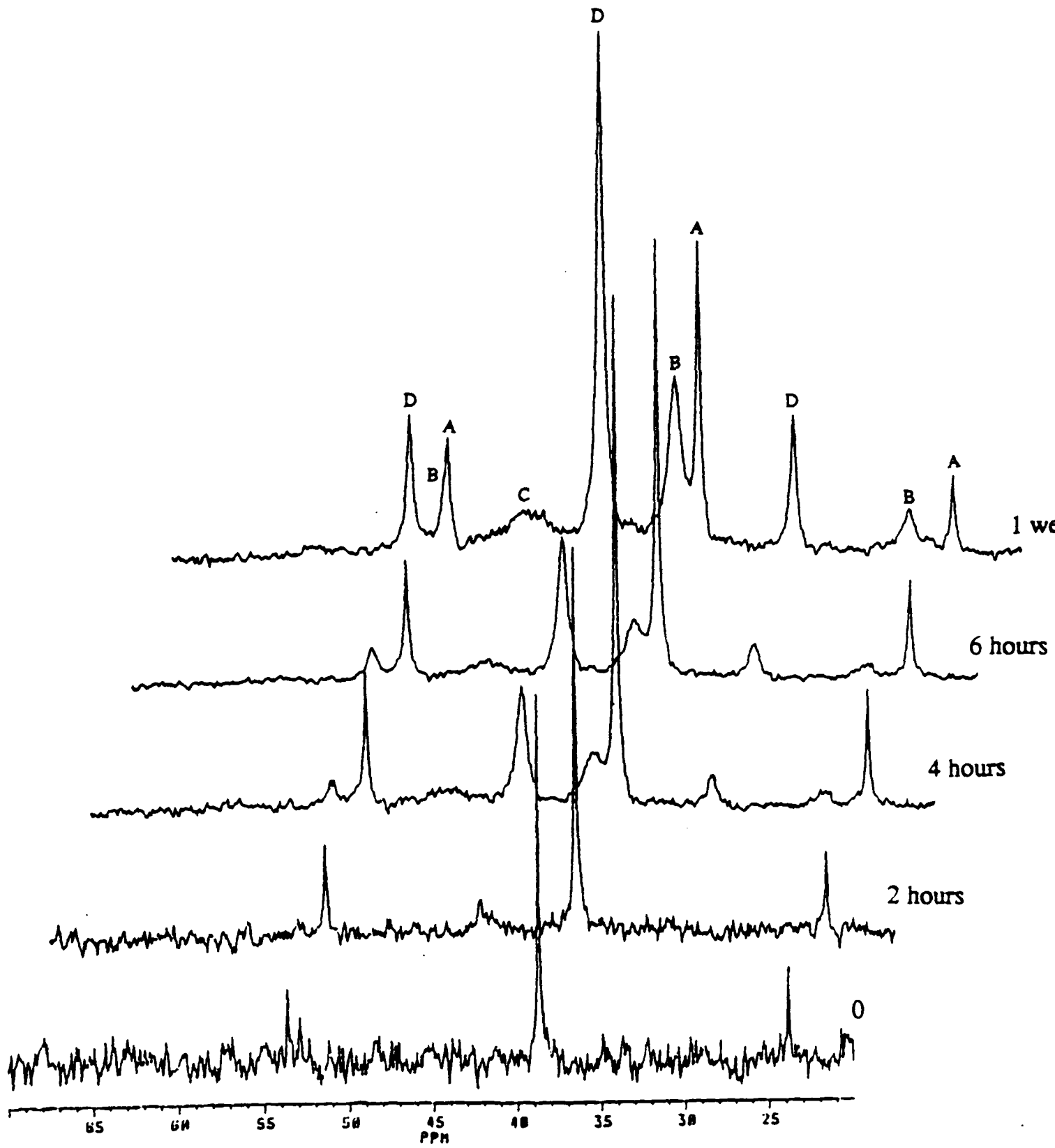
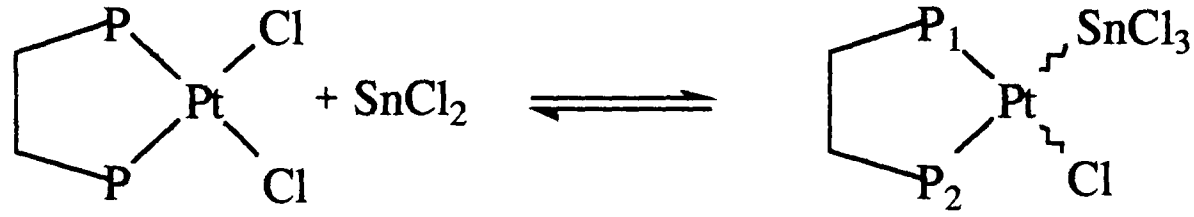


Figure 3.21 Room Temperature Time-lapse $^{31}P-\{^{1}H\}$ Solution N.m.r Spectra for the Reaction Between $PtCl_2(dppe)$, Two Molar Equivalents of $SnCl_2$ and One Molar Equivalent of $SnCl_3^-$



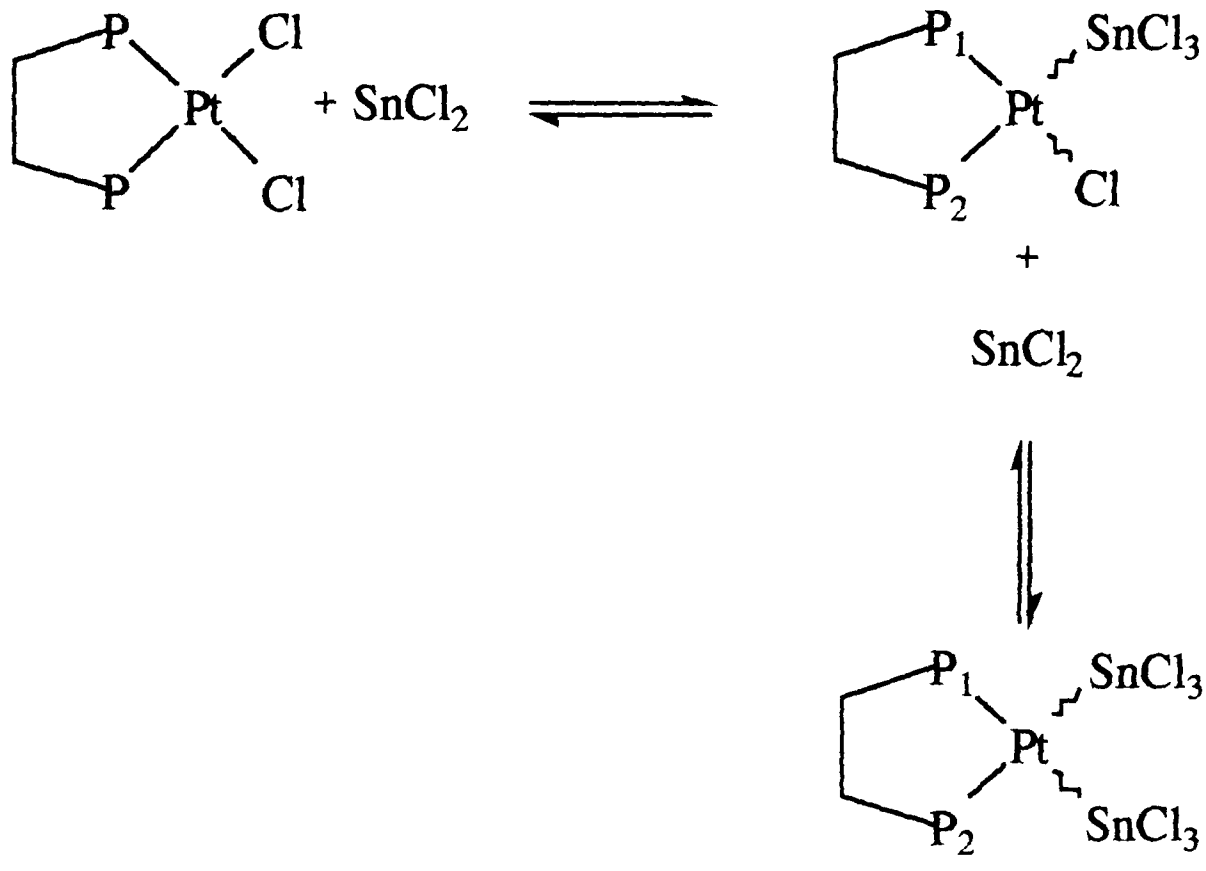
The $^{31}P-\{^{1}H\}$ solution n.m.r spectra for the reactions between $PtCl_2(dppe)$ and one molar equivalent of Cl^- or $SnCl_3^-$ ions only showed the signal of the $PtCl_2(dppe)$ starting material (δ 38.9 p.p.m., $^{1}J_{PPt}$ 3620 Hz). In addition, no change of colour was observed and so it was assumed that no reaction occurs between $PtCl_2(dppe)$ and a molar equivalent of Cl^- or $SnCl_3^-$.

The $^{31}P-\{^{1}H\}$ solution n.m.r spectra for the addition of one molar equivalent of $SnCl_2$ to a dichloromethane solution of $PtCl_2(dppe)$ are shown in Figure 3.19. Immediately after the addition of tin(II) chloride, only the spectrum for $PtCl_2(dppe)$ was observed (**A**). After a short period of time two more phosphorus environments were seen (**B** δ 40.0 p.p.m., $^{1}J_{PPt}$ 3346 Hz and **C** δ 49.1 p.p.m., $^{1}J_{PPt}$ 3060 Hz). Their emergence was simultaneous and and their integrals are equal. Resonances (**B**) and (**C**) are due to the dppe phosphorus atoms becoming magnetically inequivalent (P_1 and P_2) upon insertion of $SnCl_2$ into one of the platinum-chlorine bonds i.e.

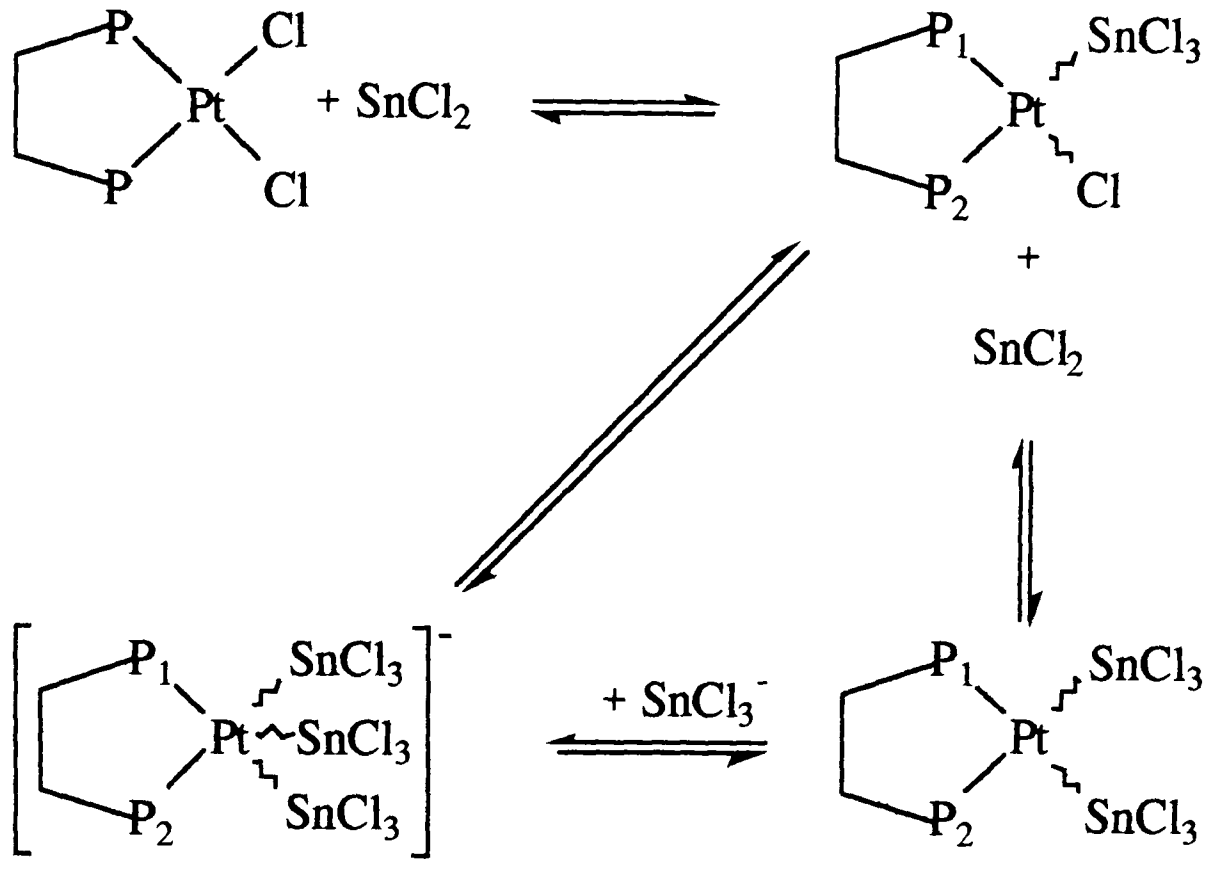


The absence of *cis*- $^{2}J_{PP}$ couplings in the spectrum may be due to their low values. In similar systems[59-61] *cis*- $^{2}J_{PP}$ couplings range from values which are too small to be determined[59], upto a maximum of 35Hz[61].

The $^{31}P-\{^{1}H\}$ solution n.m.r. spectra for the addition of two molar equivalents of $SnCl_2$ to a dichloromethane solution of $PtCl_2(dppe)$ are shown in Figure 3.20. The only products observed are the same as those previously assigned in Figure 3.19. The major difference being that the resonances due to $SnCl_2$ insertion have increased relative to unreacted $PtCl_2(dppe)$, resulting from a shift in the equilibrium position upon the addition of more tin(II) chloride, whilst the highly insoluble $Pt(dppe)(SnCl_3)_2$ was seen to precipitate out of the n.m.r. sample i.e.



The $^{31}P-\{^{1}H\}$ solution n.m.r. spectra for the addition of two molar equivalents of $SnCl_2$ and one molar equvalent of $SnCl_3^-$ ions to a dichloromethane solution of $PtCl_2$(dppe) are shown in Figure 3.21. The first product resonance (**D**) (δ 44.6 p.p.m., $^{1}J_{PPt}$ 2760Hz), was not observed in the previous experiments and must be due to the addition of $SnCl_3^-$. Since there was no reaction between $SnCl_3^-$ and $PtCl_2$(dppe), it is most unlikely to be the complex $[PtCl_2(dppe)(SnCl_3)]^-$. The fact that the only other resonances detected are those previously observed for $PtCl(dppe)(SnCl_3)$, and that resonance (**D**) is the major component even after one week, suggests that this resonance is that of the isolated complex $[Pt(dppe)(SnCl_3)_3]^-$, the intermediate complex, $[PtCl(dppe)(SnCl_3)_2]^-$ being too unstable to be observed i.e.



The $^{1}J_{PPt}$ coupling constant for $[Pt(dppe)(SnCl_3)_3]^-$ of 2760Hz is close to the values obtained for similar complexes[62], which range from 2883 to 4705Hz.

3.5.4.4 The Reactions of $\{Sn[O\text{-}4\text{-}NO_2\text{-}C_6H_3O][OC_4H_8]\}_n$ and $\{[Et_3BzN][SnCl(O\text{-}4\text{-}NO_2\text{-}C_6H_3O)]\}_n$ with $PtCl_2(dppe)$

Upon the addition of $\{Sn[O\text{-}4\text{-}NO_2\text{-}C_6H_3O][OC_4H_8]\}_n$ to a solution of $PtCl_2(dppe)$ in dichloromethane a colour change was observed from yellow to bright orange, indicating a reaction. Unfortunately, after work-up of the reaction mixture, the only phosphorus containing species present was $PtCl_2(dppe)$. Since the products of the reaction between $\{Sn[O\text{-}4\text{-}NO_2\text{-}C_6H_3O][OC_4H_8]\}_n$ and $PtCl_2(dppe)$ appear to be not readily isolatable, a series of n.m.r studies akin to those described in section 3.5.4.3 were undertaken. This involved the recording of the room temperature $^{31}P\text{-}\{^{1}H\}$ solution n.m.r spectra for mixtures of $PtCl_2(dppe)$, $\{Sn[O\text{-}4\text{-}NO_2\text{-}C_6H_3O][OC_4H_8]\}_n$ and/or $\{[Et_3BzN][SnCl(O\text{-}4\text{-}NO_2\text{-}C_6H_3O)]\}_n$ in dichloromethane. The results from these experiments are shown in Figures 3.22 to 3.24.

Figure 3.22 Room Temperature Time-lapse ^{31}P-$\{^{1}H\}$ Solution N.m.r Spectra for the Reaction Between $PtCl_2$(dppe) and One Molar Equivalent of $\{Sn[O\text{-}4\text{-}NO_2\text{-}C_6H_3O][OC_4H_8]\}_n$

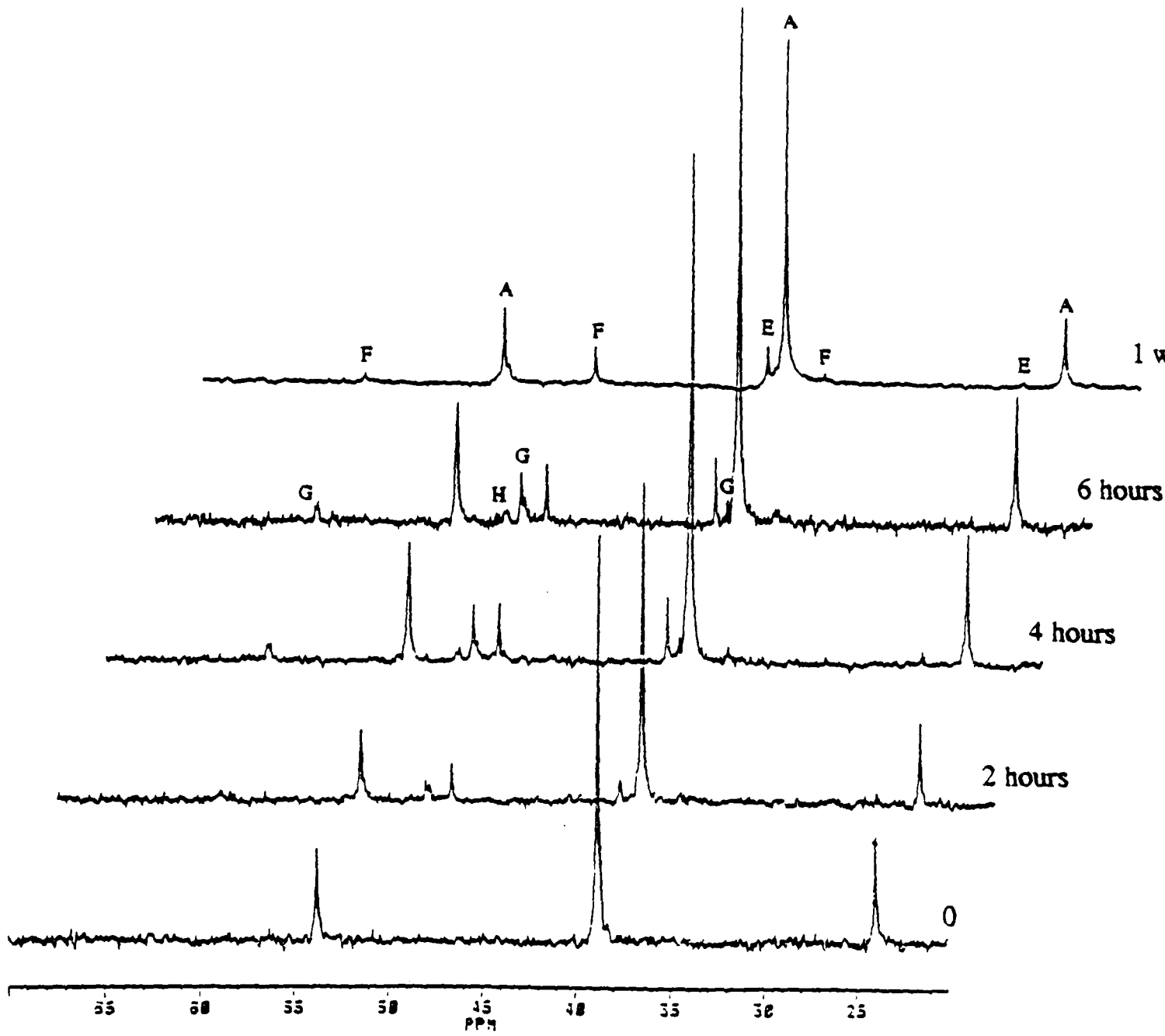


Figure 3.23 Room Temperature Time-lapse ^{31}P-{^{1}H} Solution N.m.r Spectra for the Reaction Between $PtCl_2$(dppe) and Two Molar Equivalents of {Sn[O-4-NO_2-C_6H_3O][OC_4H_8]}$_n$

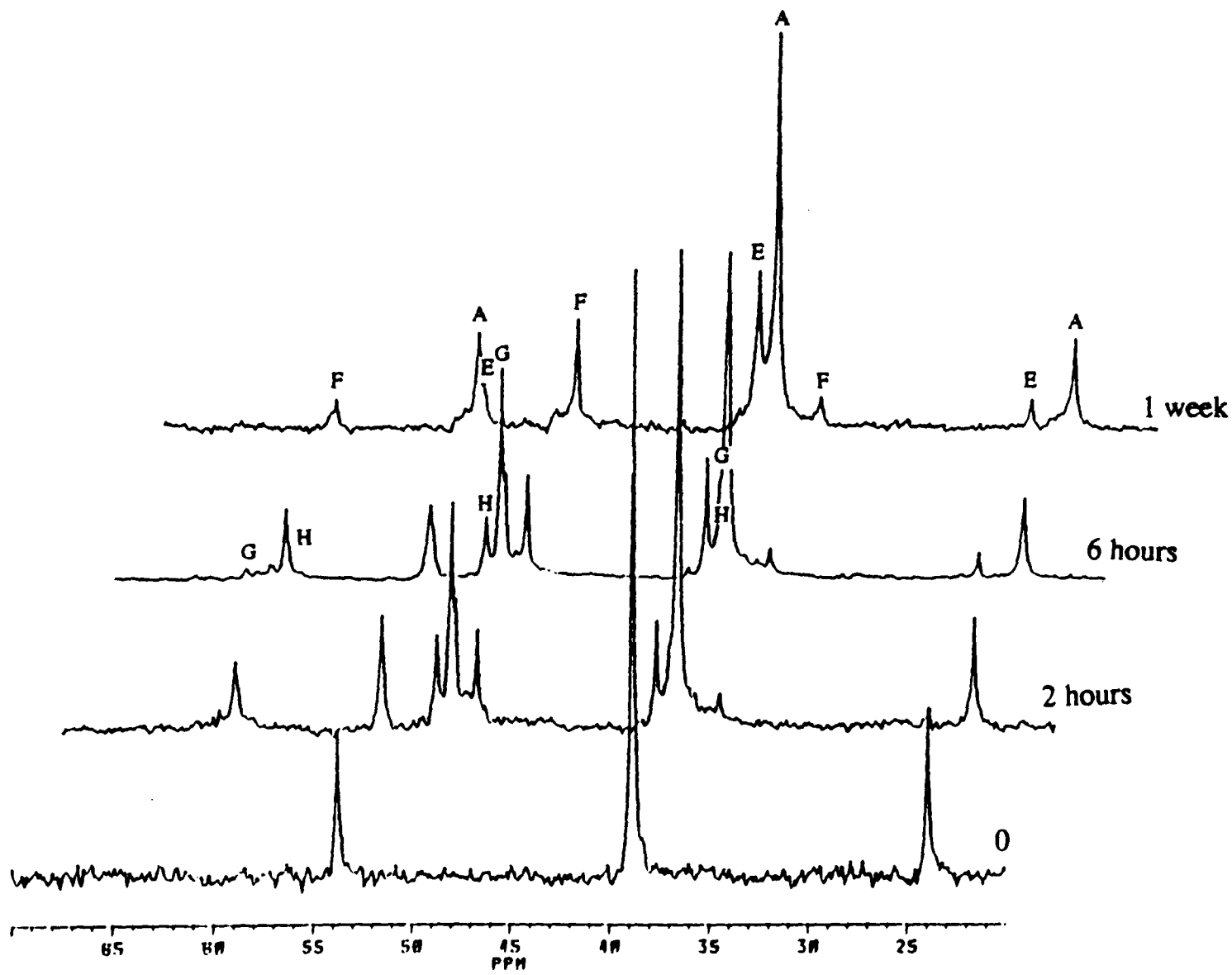
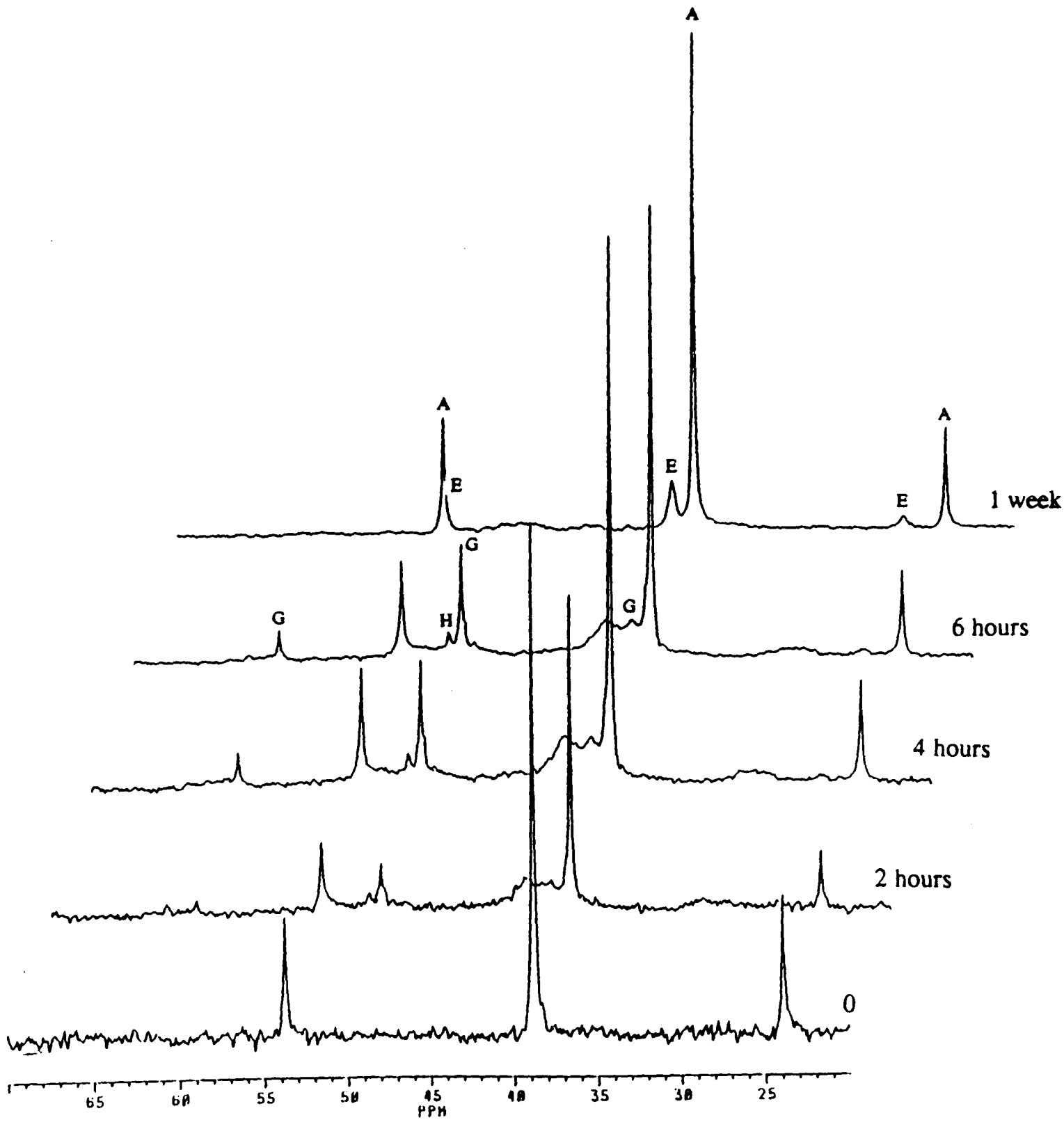


Figure 3.24 Room Temperature Time-lapse ^{31}P-{^{1}H} Solution N.m.r Spectra for the Reaction Between $PtCl_2$(dppe), Two Molar Equivalents of {$Sn[O\text{-}4\text{-}NO_2\text{-}C_6H_3O][OC_4H_8]$}$_n$ and One Molar Equivalent of {$[Et_3BzN][SnCl(O\text{-}4\text{-}NO_2\text{-}C_6H_3O)]$}$_n$



The ^{31}P-$\{^{1}H\}$ solution n.m.r. spectra for the reactions between $PtCl_2$(dppe) and one molar equivalent of $\{[Et_3BzN][SnCl(O\text{-}4\text{-}NO_2\text{-}C_6H_3O)]\}_n$ only showed the signal of the $PtCl_2$(dppe) starting material (δ 38.9 p.p.m., $^{1}J_{PPt}$ 3620 Hz). In addition, no change of colour was observed and it was therefore assumed that there was no reaction.

The ^{31}P-$\{^{1}H\}$ solution n.m.r spectra for the addition of one molar equivalent of $\{Sn[O\text{-}4\text{-}NO_2\text{-}C_6H_3O][OC_4H_8]\}_n$ to a dichloromethane solution of $PtCl_2$(dppe) are shown in Figure 3.22. As well as the signal for $PtCl_2$(dppe) (**A**), two other signals of equal intensity (**E** δ 40.2 p.p.m., $^{1}J_{PPt}$ 3340Hz and **F** δ 49.2 p.p.m., 2962Hz) simultaneously appeared. Due to their similarity to the resonances to (**B**) and (**C**) in section 3.5.4.3, they were assigned to the insertion complex, PtCl[dppe][SnCl(O-4-NO_2-C_6H_3O)]. Their relatively low concentration compared to those for PtCl(dppe)($SnCl_3$) in Figure 3.18 shows the low tendency $\{Sn[O\text{-}4\text{-}NO_2\text{-}C_6H_3O][OC_4H_8]\}_n$ has towards insertion compared with $SnCl_2$.

The ^{31}P-$\{^{1}H\}$ solution n.m.r spectra for the addition of two molar equivalents of $\{Sn[O\text{-}4\text{-}NO_2\text{-}C_6H_3O][OC_4H_8]\}_n$ to a dichloromethane solution of $PtCl_2$(dppe) are shown in Figure 3.23. As was seen in Figure 3.20, the resonances associated with the mono-insertion complex are greater in intensity upon increasing the concentration of $\{Sn[O\text{-}4\text{-}NO_2\text{-}C_6H_3O][OC_4H_8]\}_n$. In Figures 3.22 and 3.23 two other resonances (**G** δ 50.5 p.p.m., $^{1}J_{PPt}$ 2628Hz and **H** δ 51.2 p.p.m., 2672Hz) are observed and these were assigned to the bis-insertion complex Pt[dppe][SnCl(O-4-NO_2-C_6H_3O)]$_2$. Its associated resonances also increase upon the addition of more $\{Sn[O\text{-}4\text{-}NO_2\text{-}C_6H_3O][OC_4H_8]\}_n$, but its stability is much lower than the mono-insertion complex, virtually disappearing after one week.

The ^{31}P-$\{^{1}H\}$ solution n.m.r spectra for the addition of two molar equivalents of $\{Sn[O\text{-}4\text{-}NO_2\text{-}C_6H_3O][OC_4H_8]\}_n$ and one molar equvalent of $\{[Et_3BzN][SnCl(O\text{-}4\text{-}NO_2\text{-}C_6H_3O)]\}_n$ to a dichloromethane solution of $PtCl_2$(dppe) are shown in Figure 3.24. No new resonances were observed, only those of the mono and bis-insertion complexes already identified. This imples that further reaction to form a five-coordinate compound is not favoured, the reaction stopping at the neutral four-coordinate species.

The insertion products of $\{Sn[O\text{-}4\text{-}NO_2\text{-}C_6H_3O][OC_4H_8]\}_n$ and $(dppe)PtCl_2$ are unstable with respect to the starting reagents. However, room temperature time-lapse $^{31}P\text{-}\{^1H\}$ solution n.m.r spectra showed that the mono and bis-insertion compounds are produced.

3.6 Summary

This Chapter described the chemical reactivity of the novel tin(II)-oxygen heterocycles, $Sn[OC_6Cl_4O][OC_4H_8]$ and $\{Sn[O\text{-}4\text{-}NO_2\text{-}C_6H_3O][OC_4H_8]\}_n$. This was possible due to their enhanced solubility compared with other tin(II)-oxygen heterocycles.

$\{Sn[O\text{-}4\text{-}NO_2\text{-}C_6H_3O][OC_4H_8]\}_n$ undergoes oxidative addition reactions. The synthesis and properties of its reaction with iodine giving, $SnI_2[O\text{-}4\text{-}NO_2\text{-}C_6H_3O][OC_4H_8]_2$ was described. $\{Sn[O\text{-}4\text{-}NO_2\text{-}C_6H_3O][OC_4H_8]\}_n$ also reacted with Lewis bases such as 1, 2-diaminopropane giving $Sn[NH_2CH_2CH(Me)H_2N][O\text{-}4\text{-}NO_2\text{-}C_6H_3O][OC_4H_8]$, and benzyltriethylammonium chloride giving $\{[Et_3BzN][SnCl(O\text{-}4\text{-}NO_2\text{-}C_6H_3O)]\}_n$. A single crystal X-ray diffraction study of $\{[Et_3BzN][SnCl(O\text{-}4\text{-}NO_2\text{-}C_6H_3O)]\}_n$ revealed that the solid-state structure consists of polymeric chains of $[SnCl(O\text{-}4\text{-}NO_2\text{-}C_6H_3O)]^-$ and associated $[Et_3BzN]^+$ cations and belongs to the space group $P2_1/n$. Preparation and properties of an analogous compound, $[Et_3NH][SnCl(O\text{-}C_6Cl_4O)]$ was also outlined.

The reaction of $\{Sn[O\text{-}4\text{-}NO_2\text{-}C_6H_3O][OC_4H_8]\}_n$ with the Lewis base, boron trifluoride etherate afforded the adduct $F_3B.Sn[O\text{-}4\text{-}NO_2\text{-}C_6H_3O][OC_4H_8]$. However, with unsaturated transiton metal Lewis bases, the products were not as straightforward. The reaction of $\{Sn[O\text{-}4\text{-}NO_2\text{-}C_6H_3O][OC_4H_8]\}_n$ with $W(CO)_5thf$ afforded the mixed-metal tetramer $\{(OC)_3W.Sn[(O\text{-}4\text{-}NO_2\text{-}C_6H_3O)(OC_4H_8)]\}_2$ in which the tungsten atom is believed to be bound η^6 to the aromatic ring. The reactions between bis(triphenylphosphine)platinum-ethylene or tris(triphenylphosphine)platinum and $\{Sn[O\text{-}4\text{-}NO_2\text{-}C_6H_3O][OC_4H_8]\}_n$ gave $\{[Ph_3P]_3PtH\}\{[\mu_2\text{-}O][\mu_2\text{-}OH][Sn(O\text{-}4\text{-}NO_2\text{-}C_6H_3O)]_2\}$, the anion containing tin(II) and tin(IV) centres.

The reactions between $\{Sn[O\text{-}4\text{-}NO_2\text{-}C_6H_3O][OC_4H_8]\}_n$ and transition metal halide complexes were also studied. The reaction between $\{Sn[O\text{-}4\text{-}NO_2\text{-}C_6H_3O][OC_4H_8]\}_n$ and $[H_9C_8NC]_3RhCl$ yielded $\{[H_9C_8NC]_3ClRh[\mu_2\text{-}Sn(O\text{-}4\text{-}NO_2\text{-}C_6H_3O)]\}_2$. The reaction of $\{Sn[O\text{-}4\text{-}NO_2\text{-}C_6H_3O][OC_4H_8]\}_n$ with Ph_3PAuCl gave the cluster $Au_4(PPh_3)_4(\mu_2\text{-}SnCl_3)_2$ in low yield. A single crystal X-ray diffraction study showed $Au_4(PPh_3)_4(\mu_2\text{-}SnCl_3)_2$ consists of a tetrahedral gold core, with two opposite edge bridging $SnCl_3$ groups. $Au_4(PPh_3)_4(\mu_2\text{-}SnCl_3)_2$ is the first known example of a compound containing a $\mu_2\text{-}SnX_3$ fragment.

$\{Sn[O\text{-}4\text{-}NO_2\text{-}C_6H_3O][OC_4H_8]\}_n$ was shown to only weakly insert into the platinum-chlorine bond of $PtCl_2(dppe)$, compared to $SnCl_2$. Two molar equivalents of $SnCl_2$ were shown to react with $PtCl_2(dppe)$ to give $Pt(SnCl_3)_2(dppe)$. Addition of a further equivalent of $SnCl_2$ in the presence of tetraethylammonium chloride gave $[Et_4N][Pt(dppe)(SnCl_3)_3]$. A single crystal X-ray diffraction study showed that the coordination about the platinum centre in $[Et_4N][Pt(dppe)(SnCl_3)_3]$ to be distorted trigonal bipyramidal.

3.7 References

1. V. F. Mironov and V. I. Shiryaev, *Russ. Chem. Rev.*, 1983, **52**, 184.
2. O. Rectenwald and M. Veith, *Topics in Current Chemistry*, **104**, 1, Springer-Verlag (1982).
3. H. E. Mabrouk and D. G. Tuck, *J. Chem. Soc., Dalton Trans.*, 1988, 2539.
4. T. A. Annan, R. K. Chanda, D. G. Tuck and K. D. Watson, *Can. J. Chem.*, 1987, **65**, 2670.
5. H. M. Haendler and J. S. Morrison, *J. Inorg. Nucl. Chem.*, 1967, **29**, 393.
6. G. W. A. Fowles and I. A. Khan, *J. Less-Common Met.*, 1968, **15**, 209.
7. N. N. Greenwood and A. Timnick, *J. Chem. Soc. A*, 1971, 677.
8. R. A. Geanangel and S. Vasnin, *Inorg. Chim. Acta*, 1989, **160**, 167.
9. M. Veith, *Z. Naturforsch*, 1978, **33b**, 1.

10. E. K. D'yachenko and K. N. Lybomirova, *J. Gen. Chem. U. S. S. R.*, 1981, **51**, 2183.

11. M. A. Porai-Kashits and V. I. Sokol, *Sov. J. Coord. Chem.*, 1979, **5**, 1346.

12. M. Gielen, E. Joosen, T. Mancilla, J. Ramharter and R. Willem, *Si. Ge. Tin and Lead Compds.*, 1986, **9**, 349.

13. F. Huber and A. K. Saxena, *Coord. Chem. Rev.*, 1989, **95**, 109.

14. G. Atassi, *Revs. Si. Ge. Tin and Lead Compounds*, 1985, **2-3**, 219.

15. A. Rodgers and S. Stobart, *Inorg. Chim. Acta*, 1976, **16**, L13.

16. J. D. Cotton, P. J. Davidson and M. F. Lappert, *J. Chem. Soc., Dalton Trans.*, 1976, 2275.

17. P. G. Harrison and J. J. Zuckerman, *J. Am. Chem. Soc.*, 1970, **92**, 2577.

18. T. Birchall, P. A. W. Dean and R. J. Gillespie, *J. Chem. Soc. A*, 1971, 1777.

19. S. Borkett, J. Doe and P. G. Harrison, *J. Organomet. Chem.*, 1973, **52**, 343.

20. P. G. Harrison and J. A. Richards, *J. Organomet. Chem.*, 1976, **108**, 35.

21. R. A. Geanangle and C. Hsu, *Inorg. Chim. Acta*, 1979, **34**, 241.

22. R. A. Geanangle and C. Hsu, *Inorg. Chem.*, 1980, **19**, 110.

23. C. L. Barnes, T. S. Dory and J. J. Zuckerman, *J. Organomet. Chem.*, 1985, **281**, C1.

24. W. Frank and M. Veith, *Angew. Chem. Int. Ed. Engl.*, 1985, **24**, 222.

25. E. W. Abel, *Comprehensive Inorganic Chemistry*, Vol. 2, p. 1043, Pergamon, Oxford 1973.

26. W. Petz, *Chem. Rev.*, 1986, **86**, 1019.

27. M. S. Holt, J. H. Nelson and W. L. Wilson, *Chem. Rev.*, 1989, **89**, 11.

28. *Dictionary of Organometallic Compounds*, ed J. Buckingham, Chapman and Hall (1984).

29. J. D. Cotton, P. J. Davidson, D. E. Goldberg, M. F. Lappert and K. M. Thomas, *J. Chem. Soc., Chem. Commun*, 1974, 893.

30. P. B. Hitchcock, M. F. Lappert and M. C. Misra, *J. Chem. Soc., Chem. Commun.*, 1985, 863.

31. E. T. Brennan, G. W. Bushnell, T. S. Cameron, D. T. Eadie, R. D. Holmes-Smith, A. Pidcock, A. R. Sam and S. R. Stobart, *J. Am. Chem. Soc.*, 1982, **104**, 583.

32. F. Bonati, F. Cariati and R. Ugo, *Inorg. Chem.*, 1966, **5**, 1128.

33. H. C. Clark and K. R. Dixon, *J. Am. Chem. Soc.*, 1969, **91**, 596.

34. J. T. Dumler, C. J. Nyman, B. W. Renoe, D. M. Roundhill and K. Thomas, *Inorg. Chem.*, 1972, **11**, 1795.

35. B. E. Mann, *J. Chem. Soc., Dalton Trans.*, 1973, 2012.

36. M. Nardelli, C. Pelizzi and G. Pelizzi, *J. Organomet. Chem.*, 1975, **85**, C43.

37. P. F. R. Ewings, P. G. Harrison, T. J. King and A. Morris, *J. Chem. Soc., Dalton Trans*, 1976, 1602.

38. C. Pelizzi, G. Pelizzi and P. Tarasconi, *J. Chem. Soc., Dalton Trans.*, 1977, 1935.

39. T. Burchall, R. Faggiani, C. J. L. Lock and V. Manivannan, *J. Chem. Soc., Dalton Trans.*, 1987, 1675.

40. J. Protas, *Acta Cryst.*, 1976, **B32**, 923.

41. T Aoki, H. Moriyama, Y. Saito and S. Shinoda, *J. Chem. Soc., Dalton Trans.*, 1981, 639.

42. M. Kretschmer, P. S. Pregosin and H. Ruegger, *J. Organomet. Chem.*, 1983, **241**, 87.

43. M. Kretschmer, P. S. Pregosin and H. Ruegger, *J. Organomet. Chem.*, 1983, **244**, 175.

44. M. Kretschmer, P. S. Pregosin and H. Ruegger, *Helv. Chim. Acta*, 1981, **64**, 1150.

45. M. J. Watson, *D. Phil Thesis*, University of Oxford (1990).

46. D. G. Evans, *D. Phil Thesis*, University of Oxford (1984).

47. F. Demartin, M. Manassero, L. Naldini, R. Ruggeri and M. Sansoni, *J. Chem. Soc., Chem. Commun.*, 1981, 222.

48. P. T. Beurskens, W. P. Bosman, J. J. Bour, J. A. K. M. Buskes, M. Kolenbrander, J. H. Noordik and J. W. A. van der Velden, *Inorg. Chem.*, 1984, **23**, 146.

49. W. Clegg, *Acta Cryst.*, 1978, **B34**, 278.

50. Z. Demidowicz, R. L. Johnston, J. C. Machell, D. M. P. Mingos and I. D. Williams, *J. Chem. Soc., Dalton Trans.*, 1988, 1751.

51. M. Grassi, S. V. Meille, A. Musco, R. Pontellini and A. Sironi, *J. Chem. Soc., Dalton Trans.*, 1990, 251.

52. G. Douglas, M. C. Jennings, Lj. Manojlovic-Muir and R. J. Puddephatt, *J. Chem. Soc.*,

Chem. Commun., 1989, 159.

53. G. Douglas, M. C. Jennings, Lj. Manojlovic-Muir, K. W. Muir, R. J. Puddephatt, S. Roy and G. Schoettel, *Inorg. Chem.*, in press.
54. H. S. Haupt, F. Huber and H. Preut, *Z. Anorg. Allg. Chem.*, 1976, **97**, 255.
55. S. Onaka, *Bull. Chem. Soc. Jpn.*, 1975, **48**, 319.
56. N. W. Alcock and J. H. Nelson, *Inorg. Chem.*, 1982, **21**, 1196.
57. A. Albinati, P. S. Pregosin and H. Rüegger, *Angew. Chem. Int. Ed. Engl.*, 1984, **23**, 78.
58. A. Albinati, R. Naegeli, P. S. Pregosin and H. Rüegger, *Angew. Chem. Int. Ed. Engl.*, 1982, **21**, 284.
59. J. D. Kennedy, W. McFarlane, R. J. Puddephatt and P. J. Thompson, *J. Chem. Soc., Dalton Trans.*, 1976, 874.
60. M. P. Brown, R. J. Puddephatt, M. Rashidi and K. R. Seddon, *J. Chem. Soc., Dalton Trans.*, 1977, 951.
61. A. Berton, C. Botteghi, A. Scrivanti and L. Toniolo, *J. Organomet. Chem.*, 1988, **344**, 261.
62. A. Albinati, P. S. Pregosin and H. Rüegger, *Inorg. Chem.*, 1984, **23**, 3223.

Chapter 4

Preparation and Properties of Some Novel Tin(II)-Sulphur and Nitrogen Heterocycles

4.1 Introduction

Active antitumour tin compounds with tin bound to sulphur and nitrogen have also been reported (see Table 2.1). This Chapter describes some attempts to synthesize tin(II) heterocycles with the tin atom bound to elements other than oxygen.

4.1 Synthesis of Tin(II)-Sulphur Heterocyles

The tin(II)-sulphur compounds which have been reported in the literature have been summarized in Tables 1.8 and 1.9 in Chapter 1. Of the compounds which have been structurally characterized, those which have tin:sulphur ratios of 1:3 or greater are all monomeric in the solid state. $Sn[S^tBu]_2$[1] with only two sulphurs per monomeric unit is polymeric in the solid state, with a coordination number of four about each tin atom. Polymerization may be avoided by using bulky substituents. For example, $Sn[SC_6H_2{}^tBu_3$-2, 4, 6$]_2$[2] is monomeric in the solid state.

No tin(II)-sulphur heterocycles have been structurally characterized. Those which have so far been synthesized[3-5] are high melting point polymers with a corresponding low reactivity. Only toluene-3,4-dithiolatotin(II)[3] undergoes further oxidation with excess thiol to *spiro*-bis(toluene-3,4-dithiolato)tin(IV). The solubility of tin(II)-sulphur hetrerocycles in strong donor solvents such as dimethyl sulphoxide, suggests that the intermolecular tin-sulphur bonds are much weaker than their tin-oxygen analogues. This results from the lower electronegativity of sulphur compared with oxygen. This suggested that the synthesis of sulphur compounds analagous to those described in Chapter 2 might lead to the formation of soluble and so chemically useful tin(II)-sulphur reagents.

4.1.1 Synthesis of $Sn[SC_6H_4S]$

The reaction between 1,2-benzenedithiol and a molar equivalent of tin(II) methoxide in tetrahydrofuran produced a cream precipitate which was found to be only soluble in dimethyl sulphoxide. An infra-red spectrum showed the presence of a band at 314 cm^{-1}, which was assigned to a tin-sulphur stretching mode. The ^{119}Sn Mössbauer spectrum (see Figure 4.1) of $Sn[SC_6H_4S]$ confirmed the oxidation state of the tin atom. The isomer shift of 3.44 mms^{-1} is in the correct region for tin(II) (see Section 1.2.2.3) and is similar to that measured for other tin(II)-sulphur compounds (see Table 1.8). The similar solubility properties of $Sn[SC_6H_4S]$ compared to the previously reported tin(II)-sulphur heterocycles suggests that the compound is polymeric in the solid state. The compound also appears to maintain a degree of oligomerization in solution. Examination of the ^1H solution n.m.r spectra for $Sn[SC_6H_4S]$ recorded in d_6-dmso, shows a second order spectrum for the aromatic protons of the ring, which would not be the case for a simple monomeric species. $Sn[SC_6H_4S]$ was not sufficiently soluble in dimethyl sulphoxide to allow the observation of a ^{117}Sn n.m.r signal.

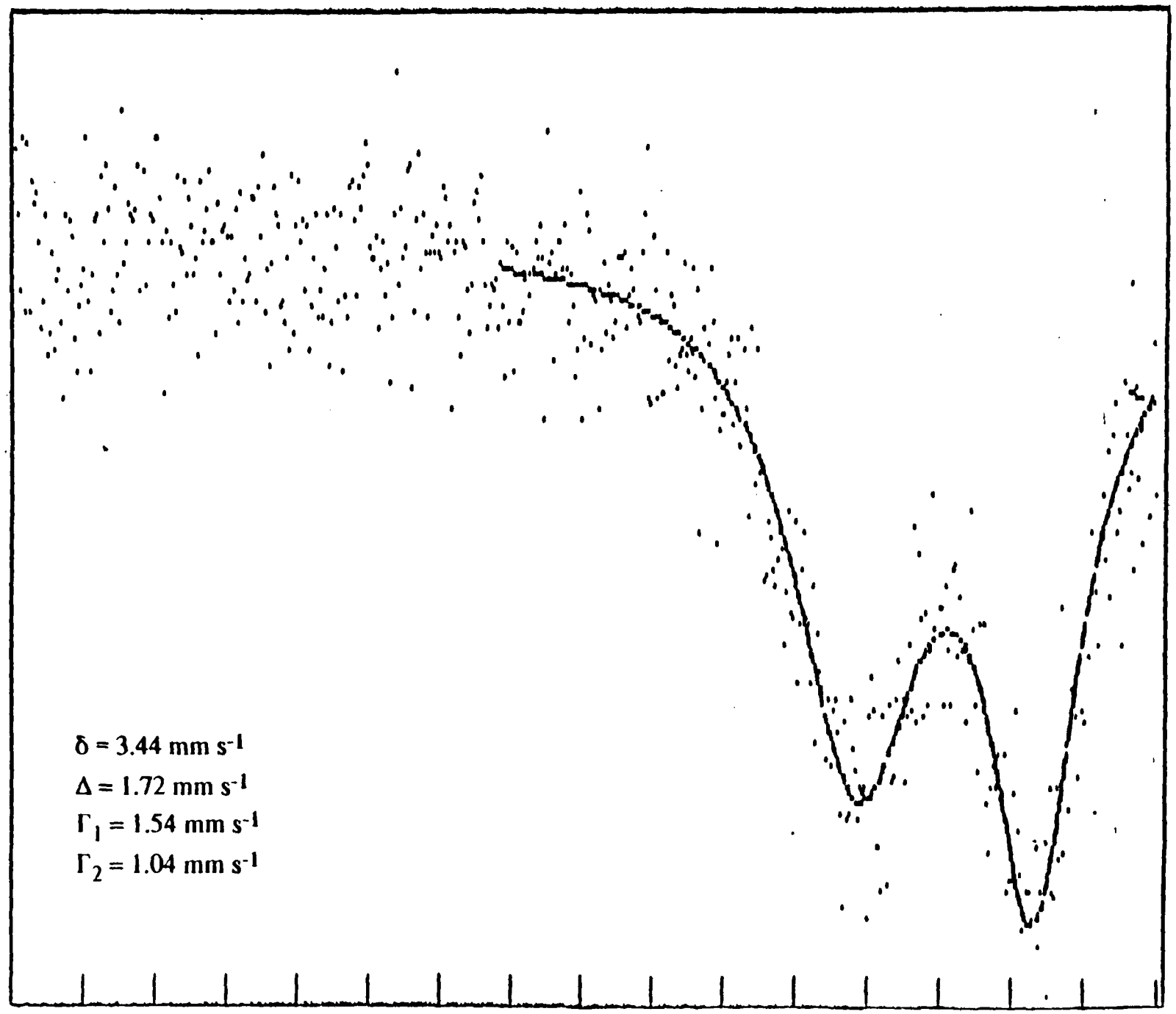


Figure 4.1 ^{119}Sn Mössbauer Spectrum for $Sn[SC_6H_4S]$

4.1.2 Synthesis of $Sn[SC_6H_4S]TMEDA$.

As with other tin(II)-sulphur heterocycles, the reactivity of $Sn[SC_6H_4S]$ is low. No reaction was observed for $Sn[SC_6H_4S]$ with the Lewis acid, boron trifluoride, or with monodentate Lewis bases, such as chloride ions. Reaction with a bidentate base, such as N,N,N',N'-tetramethylethylenediamine (TMEDA) was however, immediate. The adduct, $Sn[SC_6H_4S]TMEDA$ was found to be soluble in tetrahydrofuran, acetone and ethanol. This increase in solubility is due to the coordinately unsaturated tin centre preferentially binding to the diamine, rather than undergoing polymerization. The enhanced solubility of $Sn[SC_6H_4S]TMEDA$ enabled a full spectroscopic analysis of the compound in solution to be undertaken. The monomeric nature of $Sn[SC_6H_4S]TMEDA$ in solution, was indicated by the presence of a first order ^1H n.m.r spectrum, allowing the coupling constants for the aromatic protons to be determined. The $^{117}Sn-\{^1H\}$ solution n.m.r shows a single resonance at -335.4 p.p.m.

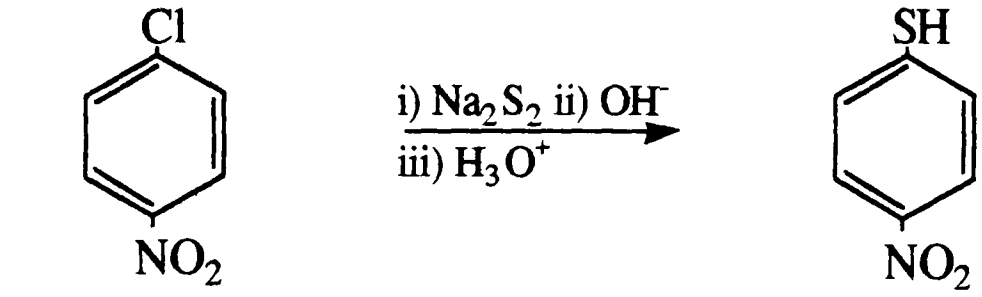
4.2 Attempted Preparation of Bidentate Sulphur Ligands Containing Electron Withdrawing Substituents

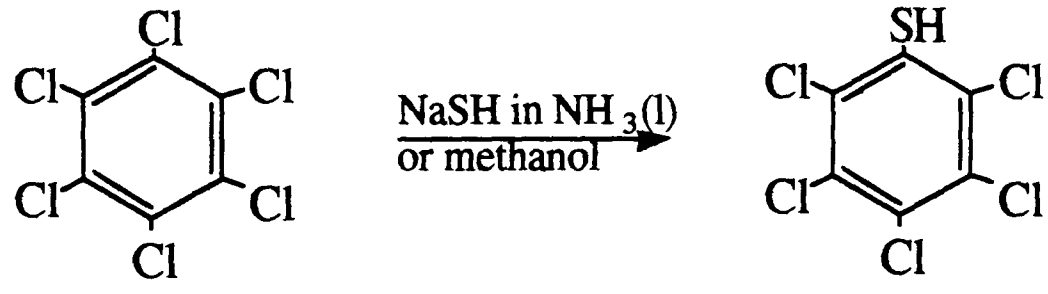
Section 4.1 has shown that the tin(II)-sulphur heterocycles so far synthesized are polymeric in the solid state and are only soluble in strong donor solvents. It is this extra intermolecular bonding that gives tin(II)-sulphur heterocycles their low reactivity. This can be increased by donor ligands (such as TMEDA with $Sn[SC_6H_4S]$) which preferentially bind to the tin centre, reducing the need for polymerization and so increasing the solubility and thus the reactivity of the compound. This is exactly analogous to the chemistry of tin(II)-oxygen heterocycles as described in Chapter 2. In Chapter 2 it was found that the introduction of sterically demanding groups such as *tertiary*-butyl had little effect upon reducing polymerization, whilst the greatest effect was produced upon the introduction of a nitro substituent onto the aromatic ring.

A tin(II)-sulphur heterocycle containing sterically demanding substituents attached to the aromatic ring has recently been reported[5]. 3,5-Di(*t*-butyl)benzene-1,2-dithiolatotin(II) was synthesized by the addition of hydrated tin(II) chloride to a solution of the dithiol and sodium methoxide in methanol. The resulting solid was found to be soluble only in dimethyl sulphoxide and stable towards oxidation. This confirms that the rationale constructed for the stability of tin(II)-oxygen heterocycle also appears to hold for tin(II)-sulphur heterocycles. To test this conclusion it was decided to try and synthesize the sulphur analogue of $\{Sn[O\text{-}4\text{-}NO_2\text{-}C_6H_3O][OC_4H_8]\}_n$ to see if the introduction of the nitro-group would have an equally beneficial effect with regards to solubility. Unfortunately, the range of available vicinal dithiol ligands is limited and no ligands containing electron-withdrawing substituents are commercially available. It was therefore decided to attempt to synthesize a vicinal dithiol ligand containing a nitro group using the standard techniques employed in the preparation of aryl-mercaptans[6].

The reactions of chlorosulphonic acid[7], CuSPh[8], NaSH[9] and 2,4-bis(4-methoxyphenyl)-1,3-dithia-2,4-diphosphetane-2,4-disulphide[10,11] (Lawesson's Reagent) with 4-nitrobezenesulphonyl chloride, 1,2-dichloro-4,5-dinitrobenzene, 3,5-dichloronitrobenzene and 4-nitrocatechol respectively, were all unsuccessful with regards to the production of a nitrated aromatic dithiol.

Nucleophilic substitution reactions between sources of SH^-, such as Na_2S_2 or NaSH, and chloro-aromatic compounds are well known[6,12]. The presence of an electron-withdrawing substituent, such as NO_2 at a position *ortho* or *para* to chlorine is required to activate the ring towards substitution e.g.

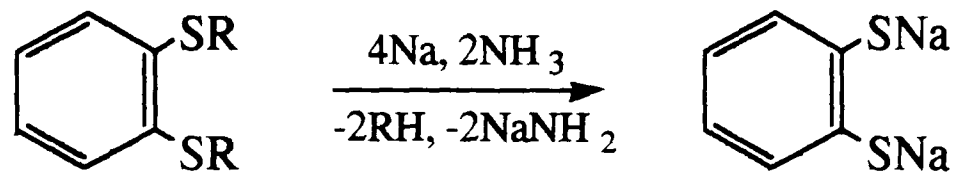


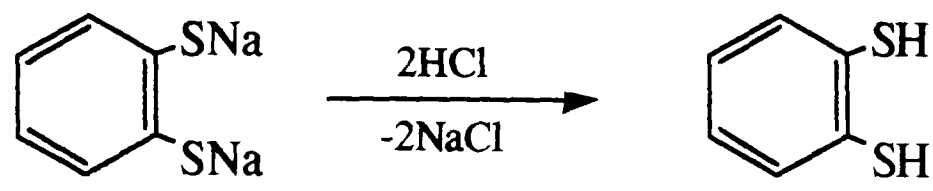


The reactions between 1,2-dichloro-4,5-dinitrobenzene or 3,5-dichloronitrobenzene and NaSH did not lead to replacement of chloride by SH^-, instead reduction of the nitro group occured with formation of the corresponding amine.

4.2.1 Synthesis of 3-nitro-4,6-bis(phenylthio)chlorobenzene

Vicinal dithiols have been synthesized by the action of sodium in liquid ammonia upon dithioethers[8]. Acid work-up of the disodium salt giving the desired dithiol e.g.





Attempts to synthesize a vicinal dithioether precursor containing nitro groups were unsuccessful. The reaction between 1,2-dichloro-4,5-dinitrobenzene and a four-fold excess

of cuprous phenylmercaptide in a pyridine/quinoline solvent system, afforded an orange crystalline solid. Elemental analyses and electron impact mass spectroscopy showed that instead of leading to the substitution of the two chloro groups by PhS^-, addition of cuprous phenylmercaptide leads to the replacement of one nitro-group and one chloro-group. Since spectroscopic studies were unable to definitively characterize the product, a single crystal X-ray diffraction study was undertaken.

4.2.2 X-ray Crystallographic Analysis of 3-nitro-4,6-bis(phenylthio)chlorobenzene

Orange crystals of 3-nitro-4,6-bis(phenylthio)chlorobenzene were grown by slow diffusion of acetone into a toluene solution of the compound. The data collection and stucture solution were carried out by Dr. Holm Fleischer of this laboratory.

A single crystal of dimensions 0.20 x 0.60 x 1.40 mm was mounted in a glass capillary and transferred to the goniometer head of an Enraf-Nonius CAD4. Final unit cell dimensions, calculated from a least-squares treatment of the angles of 24 accurately centered reflections are given in Table 4.1. 2953 reflections were collected by $\omega/2\vartheta$ scans (scan width $1.00 + 0.35\tan\vartheta$) using graphite monochromated Mo-K_α radiation, of which 2508 were considered unique and 1570 were considered observed ($I \geq 3\sigma(I)$, $R_{merg} = 0.0639$). An absorption correction based on azimuthal scans was applied to the data (min/max correction 1.01/1.45).

The coordinates of the sulphur and chlorine atoms were determined by direct methods (SIR). All remaining non-hydrogen atoms were located from a difference Fourier synthesis. Hydrogen atoms were included in geometrically idealized positions. All non-hydrogen atoms were refined with anisotropic temperature factors in the final cycles of full matrix least-squares refinement. All hydrogen atoms were placed in idealized positions. Refinement converged with $R = 0.0422$ and $R_w = 0.0507$.

Table 4.2 and Appendix 5 contain the structural data for 3-nitro-4,6-bis(phenylthio)chlorobenzene whilst Figure 4.2 shows the main structural features.

Table 4.1 Structural Details for 3-nitro-4,6-bis(phenylthio)chlorobenzene

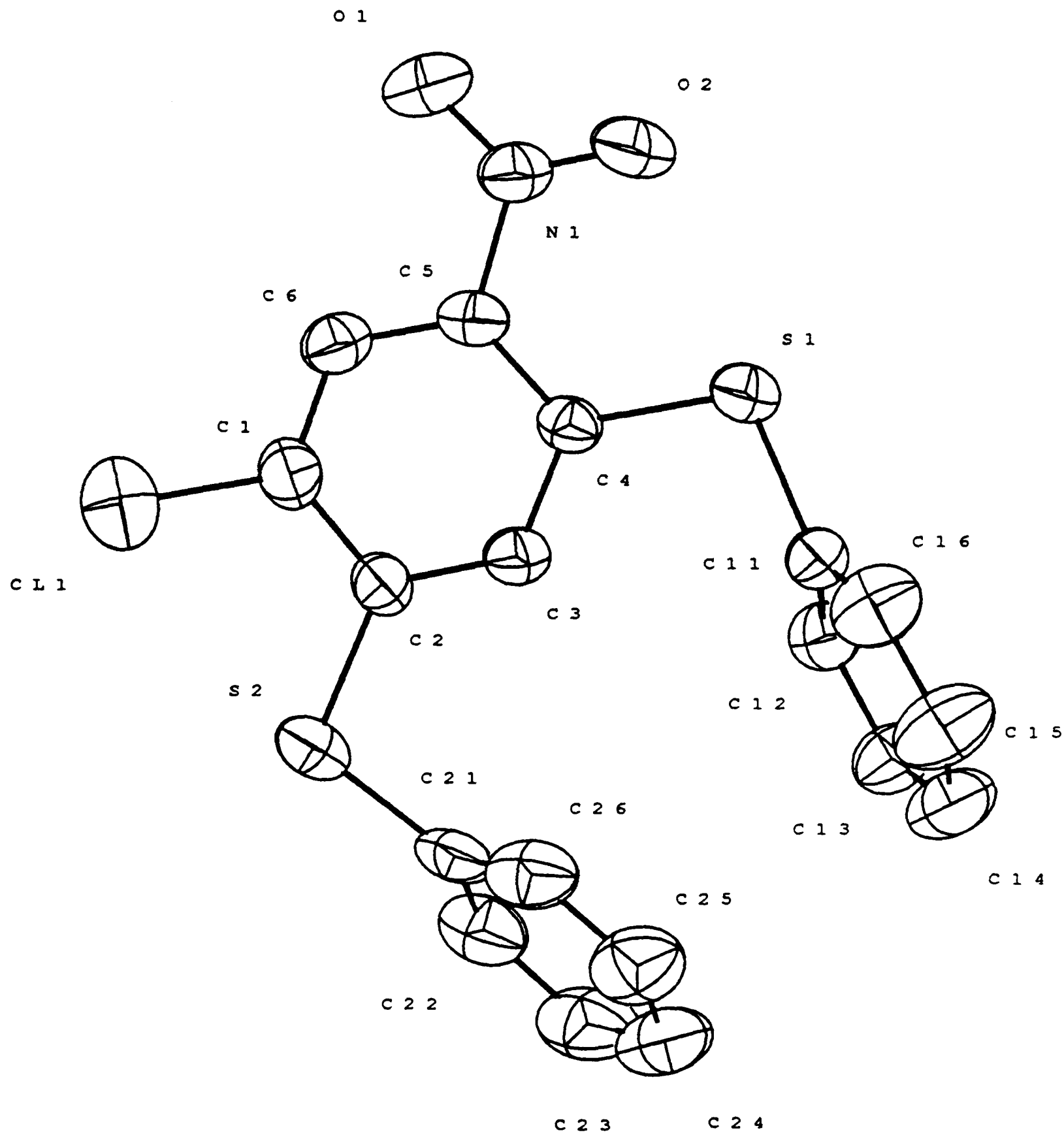
Compound	$C_{18}H_{12}ClNO_2S_2$	
Molecular Weight	343.8	
Space Group	C2/c	
Cell Dimensions	a 22.864(3)Å	α 90°
	b 10.148(1)Å	β 127.66(4)°
	c 18.531(1)Å	γ 90°
Cell Volume	3403 Å^3	
Z	8	
Density	1.459 gcm^3	
Linear Absorption Coefficient	4.675 cm^{-1}	
Radiation	Mo-K_α	
Standard Reflections	-2 22 -2, 9 -17 17	
Decay of Standards	< 1%	
2ϑ Range	0-40°	
Number of Parameters Varied	218	
R	0.0422	
R_w	0.0507	

Table 4.2 Selected Bond Lengths (Å) and Angles (°) for 3-nitro-4,6-bis(phenylthio)chlorobenzene

Atoms	Distance	Atoms	Distance
S(1)-C(4)	1.760(5)	S(1)-C(11)	1.772(5)
S(2)-C(2)	1.762(4)	S(2)-C(21)	1.769(5)
Cl(1)-C(1)	1.698(5)	N(1)-O(1)	1.207(5)
N(1)-O(2)	1.193(5)	N(1)-C(5)	1.476(6)
C(1)-C(2)	1.416(6)	C(1)-C(6)	1.357(6)
C(2)-C(3)	1.371(6)	C(3)-C(4)	1.394(6)
C(4)-C(5)	1.405(6)	C(5)-C(6)	1.381(6)
C(11)-C(12)	1.381(7)	C(11)-C(16)	1.384(7)
C(12)-C(13)	1.377(7)	C(13)-C(14)	1.370(7)
C(14)-C(15)	1.348(8)	C(15)-C(16)	1.365(7)
C(21)-C(22)	1.366(7)	C(21)-C(26)	1.375(7)
C(22)-C(23)	1.383(8)	C(23)-C(24)	1.360(9)
C(24)-C(25)	1.360(8)	C(24)-H(241)	0.950(6)
C(25)-C(26)	1.373(8)		

Atoms	Angle	Atoms	Angle
C(11)-S(1)-C(4)	103.2(2)	C(21)-S(2)-C(2)	103.9(2)
O(2)-N(1)-O(1)	123.9(4)	C(5)-N(1)-O(1)	117.7(5)
C(5)-N(1)-O(2)	118.4(4)	C(2)-C(1)-Cl(1)	120.0(4)
C(6)-C(1)-Cl(1)	120.1(4)	C(6)-C(1)-C(2)	119.9(4)
C(1)-C(2)-S(2)	116.6(3)	C(3)-C(2)-S(2)	125.0(3)
C(3)-C(2)-C(1)	118.4(4)	C(4)-C(3)-C(2)	123.6(2)
C(3)-C(4)-S(1)	122.2(3)	C(5)-C(4)-S(1)	122.4(3)
C(5)-C(4)-C(3)	115.3(4)	C(4)-C(5)-N(1)	120.9(4)
C(6)-C(5)-N(1)	116.6(4)	C(6)-C(5)-C(4)	122.5(4)
C(5)-C(6)-C(1)	120.2(4)	C(12)-C(11)-S(1)	121.1(4)
C(16)-C(11)-S(1)	119.3(4)	C(16)-C(11)-C(12)	119.4(4)
C(13)-C(12)-C(11)	120.3(5)	C(14)-C(13)-C(12)	119.7(4)
C(15)-C(14)-C(13)	119.5(5)	C(16)-C(15)-C(14)	122.4(5)
C(15)-C(16)-C(11)	118.6(5)	C(22)-C(21)-S(2)	119.6(5)
C(26)-C(21)-S(2)	121.4(4)	C(26)-C(21)-C(22)	118.9(5)
C(23)-C(22)-C(21)	120.2(5)	C(24)-C(23)-C(22)	120.4(5)
C(25)-C(24)-C(23)	119.6(5)	C(26)-C(25)-C(24)	120.4(6)
C(25)-C(26)-C(21)	120.5(5)		

Figure 4.2 The Molecular Structure of 3-nitro-4,6-bis(phenylthio)chlorobenzene



3-Nitro-4,6-bis(phenylthio)chlorobenzene crystallizes in the space group C2/c. The structure consists of a central benzene ring substituted at four positions, at C(1) by chlorine, C(5) by nitro and at C(2) and C(4) by phenylthio groups.

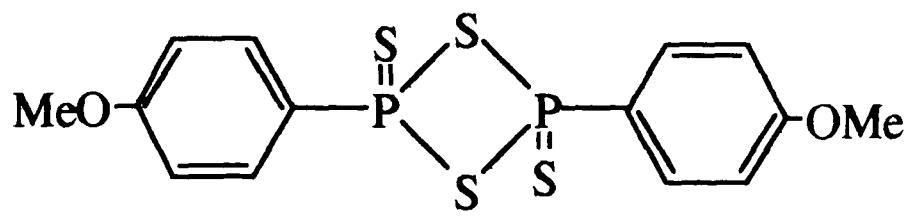
The central ring is distorted from a regular geometry. The carbon-carbon bond lengths range from 1.357(6) to 1.416(6)Å, whilst the internal angles range from 115.3(4) to 123.6(4)°. This is attributed to the attempted minimization of the steric interactions between the chlorine atom and S(2), and O(2) of the nitro group and S(1), resulting in the elongation of the C(1)-C(2) and C(4)-C(5) bond lengths to 1.416(6) and 1.405(6)Å respectively.

The only other notable feature of the structure is the position adopted by the rings of the phenylthio groups, which are essentially coplanar to each other. This orientation is adopted to reduce any steric interaction between the rings.

4.2.3 Synthesis of $[4\text{-}NO_2\text{-}OC_6H_3O][S]P[C_6H_4\text{-}4\text{-}OMe]$

2,4-bis(4-methoxyphenyl)-1,3-dithia-2,4-diphosphetane-2,4-disulphide (Lawesson's Reagent, Figure 4.3) is a widely used reagent for the conversion of carbonyls to thiocarbonyl compounds[13] and recently was found to convert alcohols to the corresponding thiols[11].

Figure 4.3 Lawesson's Reagent



Refluxing a toluene solution of 4-nitrocatechol and Lawesson's Reagent gave a pale yellow solid upon removal of the solvent. Repeated recrystallizations from a toluene-diethyl ether solvent mixture afforded an air-sensitive white crystalline solid. The infra-red spectrum does not show any sulphur-hydrogen stretching modes, but very strong phosphorus-oxygen stretching modes were observed at 1267(vs), 1255(vs) and 1233(vs) cm^{-1}. The ^1H solution

n.m.r spectra revealed the presence two different aromatic rings and a methoxy group. In order to determine the structure of this compound, a single crystal X-ray diffraction study was undertaken.

4.2.4 X-ray Crystallographic Analysis of [4-NO_2-OC_6H_3O][S]P[C_6H_4-4-OMe]

Colourless crystals of [4-NO_2-OC_6H_3O][S]P[C_6H_4-4-OMe] were grown by slow diffusion of hexane into a toluene solution of the compound. The data collection and stucture solution were carried out by Dr. Harry Powell of this laboratory.

A single crystal of dimensions 0.21 x 0.21 x 0.48 mm was mounted in a glass capillary and transferred to the goniometer head of an Enraf-Nonius CAD4. Final unit cell dimensions, calculated from a least-squares treatment of the angles of 24 accurately centered reflections are given in Table 4.3. 3626 reflections were collected by $\omega/2\vartheta$ scans (scan width 1.12 + 0.15tanϑ) using graphite monochromated Cu-K_α radiation, of which 2616 were considered unique and 1881 were considered observed ($I \geq 3\sigma(I)$, R_{merg}= 0.0796). An absorption correction based on azimuthal scans was applied to the data (min/max correction 2.36/3.26).

The coordinates of most of the non-hydrogen atoms were determined by direct methods (SIR). All remaining non-hydrogen atoms were located from a difference Fourier synthesis. Hydrogen atoms were included in geometrically idealized positions. All non-hydrogen atoms were refined with anisotropic temperature factors in the final cycles of full matrix least-squares refinement. The hydrogen atoms were assigned a common isotropic temperature factor which was refined to a final value of 0.096Å^2. Refinement converged with R = 0.0495 and R_w = 0.0449.

Table 4.4 and Appendix 6 contain the structural data for [4-NO_2-OC_6H_3O][S]P[C_6H_4-4-OMe], whilst Figure 4.4 shows the main structural features.

Table 4.3 Structural Details for $[4\text{-}NO_2\text{-}OC_6H_3O][S]P[C_6H_4\text{-}4\text{-}OMe]$

Compound	$C_{13}H_{10}NO_5PS$
Molecular Weight	323.26
Space Group	$P2_1/c$
Cell Dimensions	a 11.551(3)Å α 90°
	b 9.253(1)Å β 94.59(2)°
	c 13.250(4)Å γ 90°
Cell Volume	1411.5 $Å^3$
Z	4
Density	1.521 g cm^{-3}
Linear Absorption Coefficient	32.968 cm^{-1}
Radiation	Cu-K_α
Standard Reflections	-13, 13; -1, 11; -1, 16
Decay of Standards	< 1%
2ϑ Range	0-69°
Number of Parameters Varied	191
R	0.0495
R_w	0.0449
Goodness of Fit	1.65

Table 4.4 Selected Bond Lengths (Å) and Angles (°) for [4-NO_2-OC_6H_3O][S]P[C_6H_4-4-OMe]

Atoms	Distance	Atoms	Distance
C(1)-C(2)	1.409(5)	C(1)-C(6)	1.373(5)
C(1)-P(1)	1.761(4)	C(2)-C(3)	1.369(6)
C(3)-C(4)	1.385(6)	C(4)-C(5)	1.381(5)
C(4)-O(1)	1.354(5)	C(5)-C(6)	1.382(5)
C(7)-C(8)	1.367(5)	C(7)-C(12)	1.370(5)
C(7)-O(2)	1.387(5)	C(8)-C(9)	1.392(6)
C(9)-C(10)	1.366(6)	C(9)-N(1)	1.468(6)
C(10)-C(11)	1.380(6)	C(11)-C(12)	1.387(6)
C(12)-O(3)	1.372(4)	C(13)-O(1)	1.421(5)
C(13)-O(1)	1.421(5)	N(1)-O(4)	1.241(6)
N(1)-O(5)	1.222(6)	O(2)-P(1)	1.639(3)
O(3)-P(1)	1.647(3)	P(1)-S(1)	1.898(2)

Atoms	Angle	Atoms	Angle
C(6)-C(1)-C(2)	118.7(4)	P(1)-C(1)-C(2)	119.9(3)
P(1)-C(1)-C(6)	121.4(3)	C(3)-C(2)-C(1)	119.8(4)
C(4)-C(3)-C(2)	120.4(4)	C(5)-C(4)-C(3)	120.5(4)
O(1)-C(4)-C(3)	115.9(4)	O(1)-C(4)-C(5)	123.6(4)
C(6)-C(5)-C(4)	118.8(4)	C(5)-C(6)-C(1)	121.8(4)
C(12)-C(7)-C(8)	122.2(4)	O(2)-C(7)-C(8)	125.6(4)
O(2)-C(7)-C(12)	112.2(3)	C(9)-C(8)-C(7)	114.5(4)
C(10)-C(9)-C(8)	124.9(4)	N(1)-C(9)-C(8)	118.6(5)
N(1)-C(9)-C(10)	116.4(5)	C(11)-C(10)-C(9)	119.2(5)
C(12)-C(11)-C(10)	117.1(4)	C(11)-C(12)-C(7)	122.1(4)
O(3)-C(12)-C(7)	112.7(4)	O(3)-C(12)-C(11)	125.3(4)
O(4)-N(1)-C(9)	115.5(5)	O(5)-N(1)-C(9)	120.0(5)
O(5)-N(1)-O(4)	124.5(5)	C(13)-O(1)-C(4)	118.3(4)
P(1)-O(2)-C(7)	109.7(2)	P(1)-O(3)-C(12)	109.9(3)
O(2)-P(1)-C(1)	106.5(2)	O(3)-P(1)-C(1)	105.0(2)
O(3)-P(1)-O(2)	95.0(1)	S(1)-P(1)-C(1)	116.4(1)
S(1)-P(1)-O(2)	115.0(1)	S(1)-P(1)-O(3)	116.5(1)

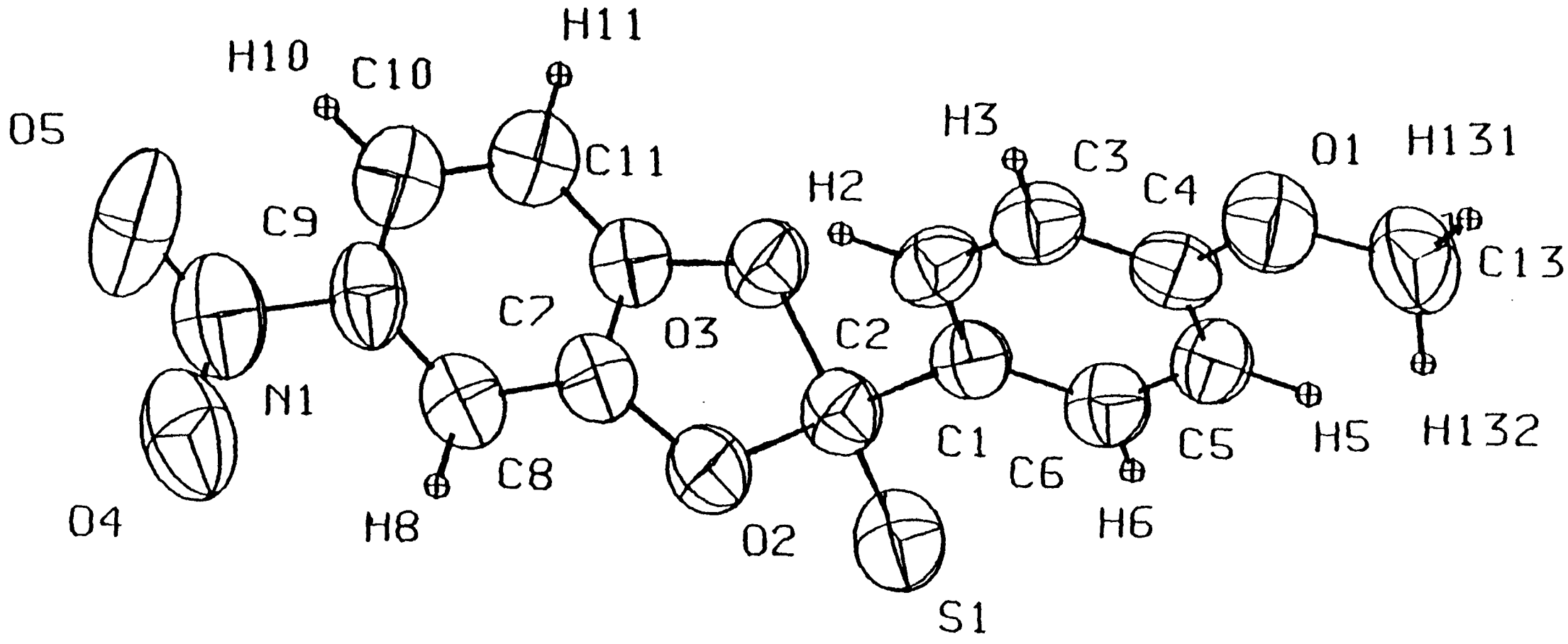


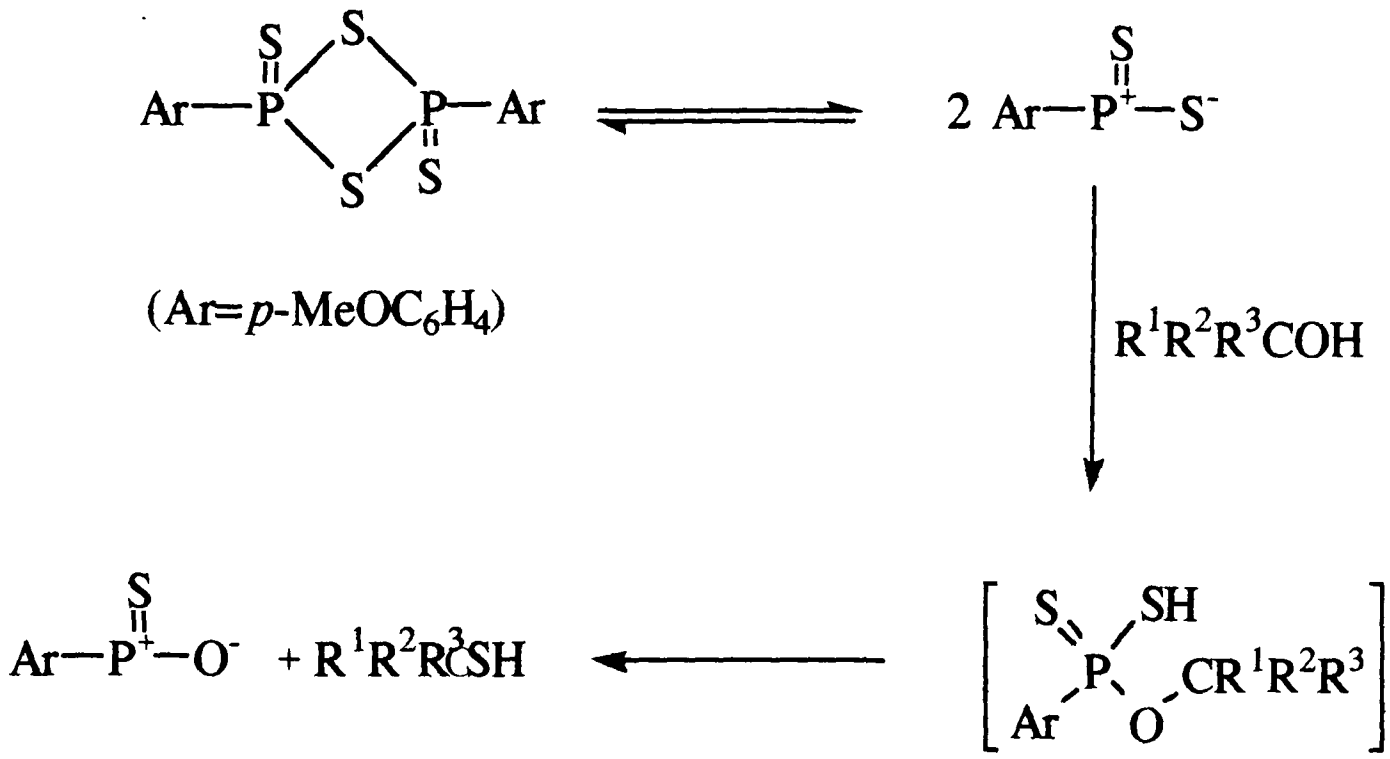
Figure 4.4 The Molecular Structure of [4-NO_2-OC_6H_3O][S]P[C_6H_4-4-OMe]

[4-NO_2-OC_6H_3O][S]P[C_6H_4-4-OMe] crystallizes in the space group $P2_1/c$. The structure consists of a central phosphorus atom bonded to a sulphur atom, a *p*-methoxyphenyl group and is chelated by a 4-nitrocatecholate group.

Thiophosphoryls $[RO]_2P[S][R]$, have been known for some years[14]. Most are liquids, but one crystal structure has been reported for the non-systemic insecticide and neurotoxin[15] [4-NO_2-C_6H_4O][EtO]P[S][Ph][16,17].

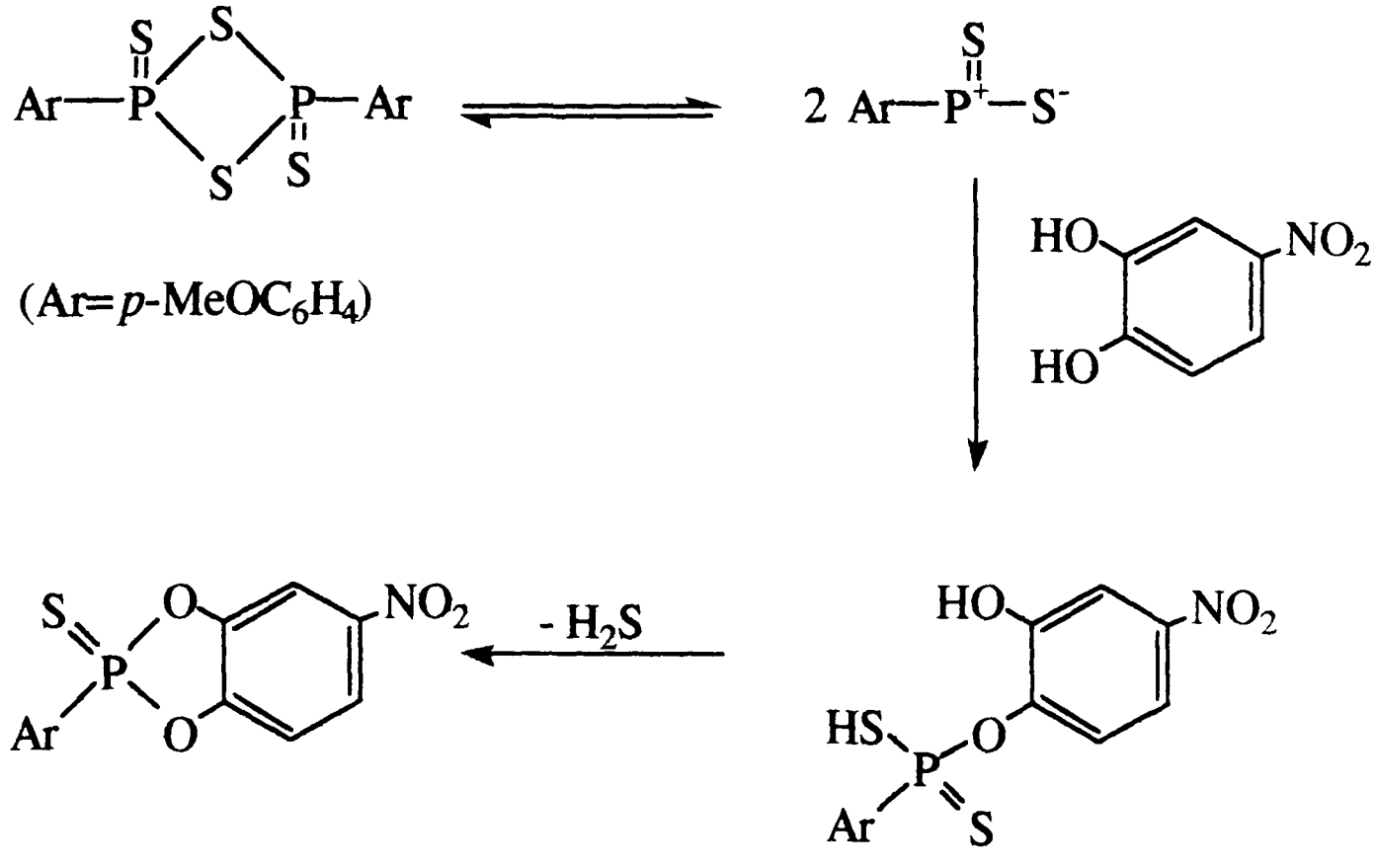
The coordination about phosphorus in [4-NO_2-OC_6H_3O][S]P[C_6H_4-4-OMe] can be described as distorted tetrahedral. The departure from the normal coordination geometry of phosphorus(V) compounds is due to the small bite angle of the catecholate ligand (O(2)-P(1)-O(3) 95.01(1)°). The rest of the angles about phosphorus in [4-NO_2-OC_6H_3O][S]P[C_6H_4-4-OMe] (O(2)-P(1)-C(1) 106.5(2), O(3)-P(1)-C(1) 105.0(2), S(1)-P(1)-C(1) 116.4(1), S(1)-P(1)-O(2) 115.0(1) and S(1)-P(1)-O(3) 116.5(1)°) are close to the expected values. The angles about phosphorus in [4-NO_2-C_6H_4O][EtO]P[S][Ph] range from 100.3 to 115.7°. The phosphorus-ligand bond lengths found in [4-NO_2-OC_6H_3O][S]P[C_6H_4-4-OMe] (P(1)-C(1) 1.761(4), P(1)-O(2) 1.639(3), P(1)-O(3) 1.647(3) and P(1)-S(1) 1.898(2)Å), are in agreement with those found for [4-NO_2-C_6H_4O][EtO]P[S][Ph] (P-C 1.794, P-O 1.588, 1.605 and P-S 1.914Å).

The isoation of [4-NO_2-OC_6H_3O][S]P[C_6H_4-4-OMe] allows us to comment on the possible reaction sequence which results when Lawesson's Reagent is added to a vicinal diol. Nishio[11], has suggested the following mechanistic scheme for the formation of thiols from alcohols using Lawesson's Reagent i.e.



Alcohols react with a dipolar species of Lawesson's Reagent, which is thought to be present in solution[18], giving a thiophosphoric acid intermediate. This is follwed by P-SH addition to the O-CR_3 carbon atom, followed by O-CR_3 bond cleavage to give the thiol.

The synthesis of [4-NO_2-OC_6H_3O][S]P[C_6H_4-4-OMe] must involve the formation of an analogous thiophosphoric intermediate which then loses H_2S to give [4-NO_2-OC_6H_3O][S]P[C_6H_4-4-OMe] i.e,



4.3 Preparation of Tin(II)-Nitrogen Heterocyles

The tin(II)-nitrogen compounds reported in the literature have been summarized in Tables 1.10 and 1.11 of Chapter 1. A number of tin(II)-nitrogen heterocycles[19-23] have already been synthesized using the standard techniques outlined in Chapter 2. As with tin(II)-oxygen and sulphur compounds, tin(II)-nitogen compounds are acutely sensitive to the steric requirements of substituent groups, changing their structure, their coordination number at tin, molecularity and chemical reactivity with the size of the attached ligands. Zuckerman[21] has shown that intensely coloured tin(II)-nitrogen compounds are monomeric, and sensitive to hydrolysis and oxidation, whilst colourless derivatives show evidence of association or chelation, and are stable with respect to hydrolysis and oxidation. The intense colours are suggested to be due to the loss of tin-nitrogen bridging, or solvate formation in monomeric compounds. Corroboration comes from an X-ray diffraction study of orange $Sn[N^tBu]_2SiMe_2$[24], which is monomeric in solid and solution, whilst the *iso*-propyl derivative is white and dimeric in solution and in the solid state.

4.3.1 Synthesis of $Sn[NH\text{-}C_6H_4NH]$

Like its oxygen and sulphur analogues, $Sn[NH\text{-}C_6H_4NH]$ was synthesized by hydrogen transfer between a tin(II) compound and the ligand. Freshly sublimed tetrakis(dimethylamido)ditin(II) was dissolved in benzene and added to a benzene solution of 1,2-phenyldiamine. The reaction was immediate and the purple-red highly crystalline solid formed was found to be highly air sensitive, giving an insoluble yellow-white solid. $Sn[NH\text{-}C_6H_4NH]$ also undergoes decomposition when exposed to protic sovents, abstracting hydrogen to give the free diamine. The stoichiometry was confirmed by elemental analyses. Infra-red spectroscopy showed nitrogen-hydrogen stretching modes at 3386(vs), 3365(vs) and 3319(vs) cm^{-1}, and a tin-nitrogen stretching mode at 543(br,s) cm^{-1}.

The colour of $Sn[NH\text{-}C_6H_4NH]$ and its instability towards air oxidation, suggests that under the criteria outlined above, $Sn[NH\text{-}C_6H_4NH]$ which does not contain any bulky

substituents, is most probably monomeric in the solid state. Unfortunately, the lack of stability of Sn[NH-C_6H_4NH] in solution meant its chemical reactivity could not be explored.

4.3.2 Synthesis of Sn[NH-4-NO_2-C_6H_3NH]

To reduce the likeli hood of decomposition of tin(II)-nitrogen heterocycles upon exposure to protic solvents, it was decided to try and reduce the nucleophilicity of the nitrogen lone pairs by the addition of an electron-withdrawing nitro substituent to the aromatic ring. As well as having the effect of reducing the basicity of the nitrogen atoms towards proton abstraction, such a compound would allow direct comparison with the analogous tin(II)-oxygen compound, $\{Sn[O\text{-}4\text{-}NO_2\text{-}C_6H_3O][OC_4H_8]\}_n$ described in Chapter 2.

Tetrakis(dimethylamido)ditin(II) was dissolved in benzene and added to 4-nitro-1,2-phenylenediamine in benzene. The reaction gave a dark red solid and elemental analyses were consistent with the stochiometry Sn[NH-4-NO_2-C_6H_3NH]. The infra-red spectrum showed a nitrogen-hydrogen stretching mode at 3351(vbr, vs) cm^{-1} and a tin-nitrogen stretching mode at 549(br, s) cm^{-1}. Sn[NH-4-NO_2-C_6H_3NH] is also sensitive to air-oxidation and decomposes to the parent diamine in protic solvents. The decomposition was slower than that of Sn[NH-C_6H_4NH], taking minutes rather than seconds, but was still too rapid to allow its chemistry to be studied in detail.

4.5 Summary

A number of tin(II)-sulphur heterocycles were synthesized but their chemical reactivities were found to be low due to their polymeric solid state stuctures. The reaction between Sn[SC_6H_4S] and N,N,N',N'-tetramethylethylenediamine (TMEDA), gave a soluble adduct, Sn[SC_6H_4S]TMEDA. Attempts were then made to synthesize bidentate sulphur ligands containing electron-withdrawing substituents.

A number of tin(II)-nitogen heterocycles were also synthesized. Their intense colours and their instability towards air oxidation indicated that they were monomeric in the solid-state. Unfortunately, their lack of stability in solution meant that their chemical reactivities could not be studied.

4.6 References

1. P. Hobein, R. Rösler and M. Veith, *Z. Naturforsch.*, 1989, **44b**, 1067.
2. P. B. Hitchcock, M. F. Lappert, B. J. Samways and E. L. Weinberg, *J. Chem. Soc., Chem. Commun.*, 1983, 1492.
3. P. G. Harrison and S. R. Stobart, *Inorg. Chim. Acta,* 1973, 7, 306.
4. W. D. Honnick and J. J. Zuckerman, *Inorg. Chem.*, 1978, **17**, 1978.
5. G. Freyberger, M. Moll and D. Sellmann, *Z. Naturforsch.*, 1989, **44b**, 1015.
6. J. L. Wardell, *The Chemistry of the Thiol Group*, 163, ed. S. Patai, Wiley, London, 1974.
7. E. E. Gilbert, *Sulfonation and Related Reactions*, 62, Interscience Publishers, Inc., New York, 1965.
8. (a) A. Ferretti, *Org. Synth.*, **42**, 54.
   (b) R. Adama, A. Ferretti and W. Reifschneider, *ibid.*, **42**, 22.
9. J. Campbell, *J. Org. Chem.*, 1964, **29**, 1830.
10. M. Mirani and K. Steliou, *J. Am. Chem. Soc.*, 1982, **104**, 3104.
11. T. Nishio, *J. Chem. Soc., Chem. Commun.*, 1989, 205.
12. C. C. Price and G. W. Stacy, *J. Am. Chem. Soc.*, 1946, **68**, 498.
13. M. P. Cava and M. I. Levinson, *Tetrahedron*, 1985, **41**, 5061.
14. L. C. Thomas, *The Identification of Functional Groups in Organophosphorus Compounds*, Academic Press, 1974.
15. H. Ohkawa, *Bull. Environ. Toxicol.*, 1977, **18**, 534.
16. R. K. D. Purnanand, *Synthesis*, 1983, 731.
17. M. R. Gifkins, *Cryst. Struct. Commun.*, 1980, **9**, 571.

18. R. Kraemer, J. P. Majoral and J. Navech, *Tetrahedron Lett.*, 1883, **24**, 5885.

19. P. G. Harrison and J. J. Zuckerman, *Inorg. Chem. Nucl. Lett.*, 1969, **5**, 545.

20. C. D. Schaeffer and J. J. Zuckerman, *J. Am. Chem. Soc.*, 1974, **96**, 7160.

21. P. J. Corvan and J. J. Zuckerman, *Inorg. Chim. Acta*, 1979, **34**, L255.

22. C. Stader and B. Wrackmeyer, *Z. Naturforsch.*, 1988, **43b**, 706.

23. M. Veith, *Angew. Chem. Int. Ed. Engl.*, 1975, **14**, 263.

24. M. Veith, *Z. Naturforsch.*, 1978, **33b**, 1.

Chapter 5

Preparation and Second Harmonic Generation Properties of Tris(catecholato)tin(IV) Compounds

5.1 Introduction

The preceding Chapters have dealt with the syntheses and properties tin(II)-catecholate and related compounds. This Chapter will describe the synthesis of a number of tin(IV)-catecholate compounds and an analysis of their second harmonic generation optical properties.

5.1.1 Second Harmonic Generation[1]

Non-linear optics (NLO) is concerned with the effects observed when electromagnetic radiation interacts with matter, and how the phase and frequency of that radiation is altered. The non-linear optical effect known as second harmonic generation (SHG) is concerned with the ability of NLO active materials to alter the frequency of the incident radiation, the output frequency being twice that of the incident radiation. Such materials have been most usefully employed when used with single frequency, coherent radiation sources such as lasers, allowing cheap low frequency, high power infra-red lasers to "pump" a non-linear solid and produce a laser of twice the imput frequency at low cost.

In linear optics, the electric field incident on the molecule, $\underline{E}$ is exactly in phase with the incident radiation.

$$\underline{P}(\omega_0) = \varepsilon_0 \chi \underline{E}(\omega_0)$$

Where $\underline{P}(\omega_0)$ is the polarization response at ω_0, the frequency of the incident light. ε_0 is the dielectric constant tensor, and is dependent upon the refractive index of the medium, of susceptibility χ, $\varepsilon_0\chi$ giving the size of the induced dipole moment.

In a non-linear molecular system, an incident electric field induces a dipole moment $\underline{P}$, where:

$$\underline{P}(\omega_0) = \underline{P} + \alpha\underline{E} + \beta\underline{E}^2 + \gamma\underline{E}^3 + \delta\underline{E}^4 + ...$$

α, β and γ are the polarizability, the first hyperpolarizability and the second hyperpolarizability respectively. It is the β and γ terms which lead to non-linear behaviour. Non-linear optical effects are generally observed in solid samples and the expression is modified accordingly:

$$\underline{P}(\omega_0) = \varepsilon_0\{\chi^1\underline{E}(\omega_1) + \chi^2\underline{E}(\omega_1)\underline{E}(\omega_2) + \chi^3\underline{E}(\omega_2)\underline{E}(\omega_3) + ...\}$$

This gives the sums and differences in the induced field, where χ^i is the i^{th} order non-linear optical susceptibility.

The polarizability is also dependent upon the symmetry of the molecule. Consider the electric field in the x-direction, E_x

$$E_x = E_0 \cos \omega_0 t$$

and

$$P_{(x)}(\omega_0) = \varepsilon_0\{\chi^1{}_{(x^2)}\, E_0 \cos \omega_0 t + \chi^2{}_{(x^3)}\, E_0{}^2 \cos^2 \omega_0 t + ...\}$$

$$= \varepsilon_0\{\chi^1{}_{(x^2)}\, E_0 \cos \omega_0 t + 1/2\chi^2{}_{(x^3)}\, E_0{}^2 (1 + \cos 2\omega_0 t) + ...\}$$

If the material is centrosymmetric, only the odd harmonics would be produced. For non-centosymmetric materials with large values of E_0, the second term in the polarizability expression becomes important. Thus $P_{(x)}$ contains a term with an oscillation of $2\omega_0$, a doubling of the incident frequency. It is therefore the second term, the second order non-linear optical susceptibility χ^2, which is resposible for Second Harmonic Generation.

To observe SHG the incident electric field, E_0 has to be large, such as that that produces a laser beam. The solid being studied must be crystallographically non-centrosymmetric and have a large second order hyperpolarizability. Furthermore, the material must not absorb at $2\omega_0$, otherwise there would be little observed SHG activity.

Since SHG efficiency is dependent upon the size of the molecular constant β, the factors which can influence its value are important[2]. Molecules with large β-values generally contain low-lying charge transfer bands and large changes in the dipole moments associated with these transitions[3-5]. For organic molecules[2,6] these conditions are met by derivatives of aromatic molecules with strategically placed donor and acceptor substituents. The conjugated π-system itself increases β and the donor and acceptor groups make mesomeric contributions to the dipole moment.

These molecular properties are of little importance if the macroscopic structure is cenrtosymmetric. Centrosymmetric crystallization is favoured by polar molecules in order to maximize intermolecular attractive forces[7], but may be overcome by careful molecular modifications[4,8,9]. A non-centrosymmetric crystal structure is encouraged by the presence of enantiomers which crystallize with no inversion centre[10].

Only recently have coordination and organometallic compounds begun to be studied as possible NLO materials[11-14]. The metal centre is used as an anchorage for donor-acceptor, conjugated organic ligands forming a large dipole moment across the molecule. The thermal stability of such compounds is also usually high. This is an important physical characteristic necessary for potential SHG materials, as they must be able to survive the effects of repeated laser heating.

Tris(catecholato)tin(IV) compounds were thought to be potentially good SHG materials because of their ability fulfil many of the requirements outlined above. A wide range

of catecholate ligands are available, with either electron-donating or electron-withdrawing substituents, allowing the creation of a large dipole moment across the molecule. Such compounds would have a high resistance to air and heat degradation. The use of three bidentate groups around an octahedral tin(IV) centre also allows the possible synthesis of pure enantiomers, resulting in the formation of non-centrosymmetric crystal lattices.

5.2 Synthesis of Tris(catecholato)tin(IV) Compounds

Although there is considerable literature on the reactions of *o*-quinones or catechols with transition metal ions, the corresponding reactions with main group metals have not been widely studied[15-22]. Only two tris(catecholato)tin(IV) compounds have been characterized, both were the unexpected products of reactions designed to make alternative compounds. $[(OC_6Cl_4O)_3Sn][HTMEDA]_2$[18] was formed when $(OC_6Cl_4O)_2SnCl_2$was added to indium(I) chloride in the presence of TMEDA, whilst $[(OC_6H_4O)_3Sn][NHEt_3]_2$[21] was produced by the reaction of phenylstannoic acid with catechol in the presence of triethylamine and 2,2-dimethoxypropane.

Since no standard synthetic procedures existed for tris(catecholato)tin(IV) compounds, three methods were devised for the formation of compounds containing either the same, $[L_3Sn]^{2-}$, or a mixture of ligands, $[L_2L'Sn]^{2-}$.

For $[L_3Sn]^{2-}$ complexes, the reaction between tin(IV) chloride, three molar equivalents of ligand and six molar equivalents of triethylamine gave the required product in high yield i.e.

$$3LH_2 + 6Et_3N + SnCl_4 \longrightarrow [L_3Sn][NHEt_3]_2 + 4Et_3NHCl$$

This was the method used for the synthesis of $[(OC_6H_4O)_3Sn][NHEt_3]_2$, $[(O\text{-}4\text{-}NO_2\text{-}C_6H_3O)_3Sn][NHEt_3]_2$ and $[(O\text{-}3\text{-}MeO\text{-}C_6H_3O)_3Sn][NHEt_3]_2$.

For $[L_2L'Sn]^{2-}$ complexes, a dihalo-precursor, $LSnX_2$ was first synthesized. This was then mixed with equimolar amounts of the two ligands, LH_2 and $L'H_2$ in the presence of triethylamine i.e.

$$LH_2 + L'H_2 + 4Et_3N + LSnX_2 \longrightarrow [L_2L'Sn][NHEt_3]_2 + 2Et_3NHCl$$

The procedure used to synthesize $LSnX_2$ was dependent upon whether the ligand was an *o*-quinone or a catechol. For *o*-quinones, $LSnX_2$ may be prepared by direct reaction between the ligand and tin(II) halides (see method A). With catechols, the compounds $LSnX_2$ were synthesized by oxidative addition of the corresponding tin(II) heterocycle by iodine (see method B).

method A $\quad L + SnX_2 \longrightarrow LSnX_2$

method B $\quad LSn + I_2 \longrightarrow LSnI_2$

Method A was used in the synthesis of $[(OC_6Cl_4O)_2Sn(OC_6H_4O)][NHEt_3]_2$, $[(OC_6Cl_4O)_2Sn(OC_6H_3\text{-}4\text{-}NO_2\text{-}O)][NHEt_3]_2$ and $[(OC_6Cl_4O)_2Sn(OC_6H_3\text{-}3\text{-}OMe\text{-}O)][NHEt_3]_2$, whilst method B was used in the synthesis of $[(OC_6H_4O)_2Sn(OC_6H_3O\text{-}NO_2\text{-}4)][NHEt_3]_2$, $[(OC_6H_4O)_2Sn(OC_6H_3O\text{-}OMe\text{-}3)][NHEt_3]_2$, $[(OC_6H_4O)_2Sn(OC_6Cl_4O)][NHEt_3]_2$, $[(O\text{-}4\text{-}NO_2\text{-}C_6H_3O)_2Sn(OC_6H_4O)][NHEt_3]_2$, $[(O\text{-}4\text{-}NO_2\text{-}C_6H_3O)_2Sn(OC_6H_3\text{-}3\text{-}OMe\text{-}O)][NHEt_3]_2$, $[(O\text{-}4\text{-}NO_2\text{-}C_6H_3O)_2Sn(OC_6Cl_4O)][NHEt_3]_2$, $[(O\text{-}3\text{-}MeO\text{-}C_6H_3O)_2Sn(OC_6H_4O)][NHEt_3]_2$, $[(O\text{-}3\text{-}MeO\text{-}C_6H_3O)_2Sn(OC_6H_3\text{-}4\text{-}NO_2\text{-}O)][NHEt_3]_2$ and $[(O\text{-}3\text{-}MeO\text{-}C_6H_3O)_2Sn(OC_6Cl_4O)][NHEt_3]_2$.

The stoichiometries of the compounds were confirmed by elemental analyses and solution ^1H n.m.r spectroscopy, whilst infra-red spectroscopy confirmed the absence of bands associated with the oxygen-hydrogen stretching mode of the catechol and the C=O stretching mode of the *o*-quinone.

To confirm the oxidation state and coordination geometry of the tin atom, samples were sent for ^{119}Sn Mössbauer analysis. The spectrum for $[(O\text{-}4\text{-}NO_2\text{-}C_6H_3O)_3Sn][NHEt_3]_2$ is shown in Figure 5.1.

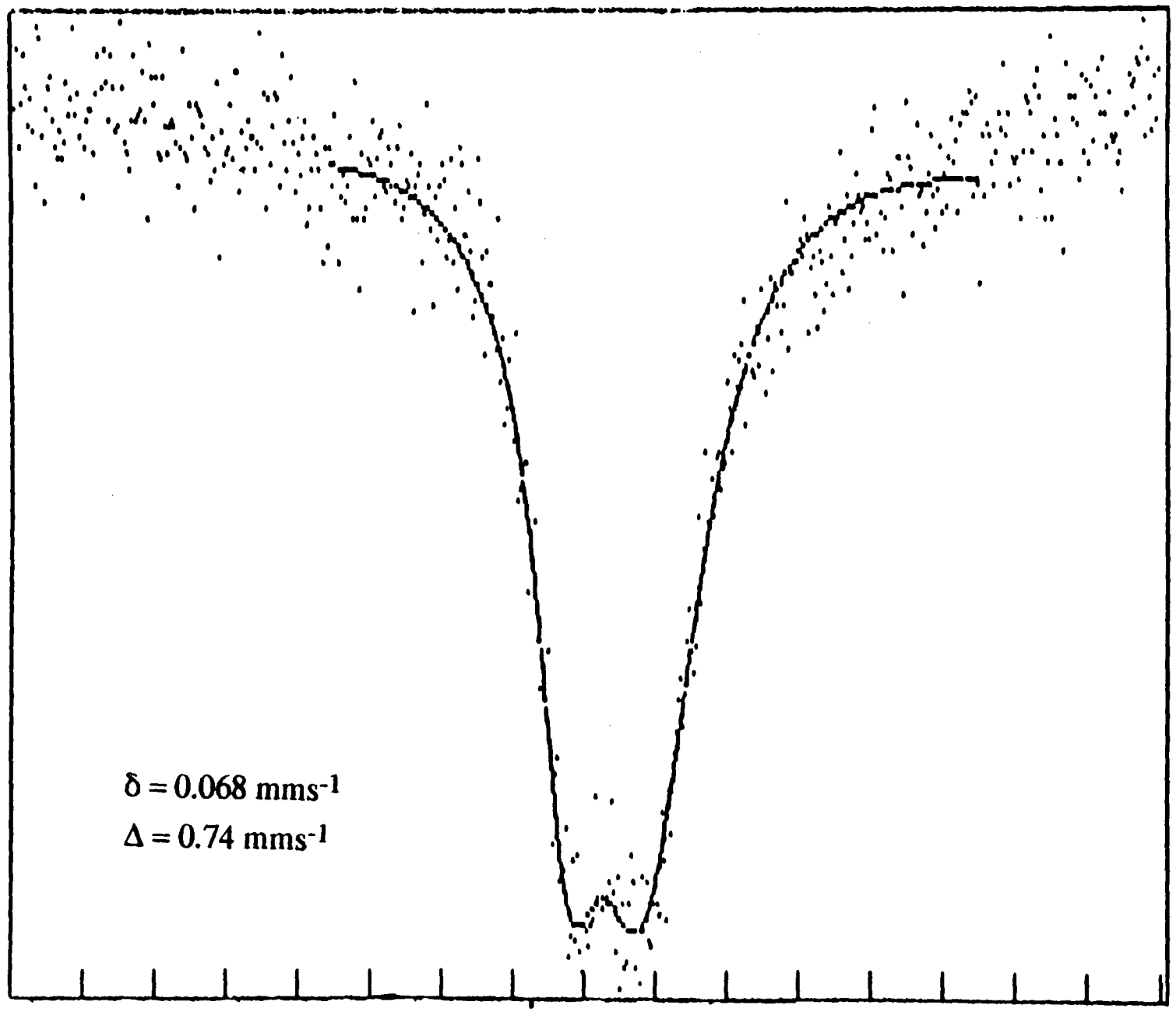


Figure 5.1 ^{119}Sn Mössbauer Spectrum for $[(O\text{-}4\text{-}NO_2\text{-}C_6H_3O)_3Sn][NHEt_3]_2$

The isomer shift, δ for $[(O\text{-}4\text{-}NO_2\text{-}C_6H_3O)_3Sn][NHEt_3]_2$ of 0.07 mms^{-1} is clearly in the range associated with tin(IV) compounds. The shift lies at the low end of the range due to the reduction in electron density, resulting from the tin atom being bonded to electronegative oxygen atoms. Since cubic symmetry (tetrahedral or octahedral arrangement of identical attached atoms) results in a zero-field gradient, the small quadrupole splitting Δ, of 0.74 mms^{-1} for $[(O\text{-}4\text{-}NO_2\text{-}C_6H_3O)_3Sn][NHEt_3]_2$ shows that there is only a small departure from an idealised octahedral geometry. This agrees with a coordination number of six for the tin atom and the occurrence of a slight distortion due to presence of bidentate ligands.

Contrary to previous reports[18,21] the triethylammonium tris(catecholato)tin(IV) salts are soluble in a wide range of polar solvents. ^1H and $^{13}C\text{-}\{^1H\}$ n.m.r spectroscopy shows them to be simple salts in solution.

5.3 Second Harmonic Generation Properties of Tris(catecholato)tin(IV) Compounds

The non-linear optical properties of tris(catecholato)tin(IV) compounds (see Table 5.1) were determined using powdered samples by the modified Kurtz powder method[23]. The sources used were a low power (less than 0.5mW) Nd/YAG laser of wavelength 1064 nm and a Nd/YAG laser Raman Shifted to 1.9 μm. The laser was attenuated using a series of calibrated neutral optical density filters. The silica cell containing the sample was irradiated at right angles to the incident beam and was located at the centre of a concave mirror which collected all the reflected light. The reflected light was then passed through an interference filter centred at 532nm (B.W. = 2 nm). The intensity of the second harmonic frequency was detected by a photomultiplier tube. The amplified anode signal was measured with a summing oscilloscope. Each measurement was the average of 64 pulses, ensuring that the pulse to pulse variation was removed. The sample signals were compared to those from graded (100 micron) reference samples. To avoid any ambiguity, the test was repeated with a different laser power and a new measurement taken. If the relationship between the two measurements was second order, with respect to the incident power, then the signal was presumed to be truly the second

harmonic. SHG measurements were carried out by Curt Lamberth and Dr. Yan-Yong Yang of this laboratory.

Table 5.1 Measured Second Harmonic Signals at 1064 nm and 1.9 μm Fundamental Laser Wavelengths Relative to Urea

Compound $[L_2L'Sn]^{2-}$		Colour	λ (nm)	SHG	
L^{2-}	L'^{2-}		(solvent thf)	1064nm	1.9μm
$[OC_6H_4O]$	$[OC_6H_4O]$	white	-	0.40	0.00
$[OC_6H_4O]$	$[O\text{-}4\text{-}NO_2\text{-}C_6H_3O]$	golden-yellow	415, 295, 271(sh)	0.28	0.17
$[OC_6H_4O]$	$[O\text{-}3\text{-}MeO\text{-}C_6H_3O]$	white	-	0.19	0.12
$[OC_6H_4O]$	$[OC_6Cl_4O]$	red-brown	297	0.07	0.05
$[O\text{-}4\text{-}NO_2\text{-}C_6H_3O]$	$[O\text{-}4\text{-}NO_2\text{-}C_6H_3O]$	yellow-orange	396, 323	1.33	0.44
$[O\text{-}4\text{-}NO_2\text{-}C_6H_3O]$	$[OC_6H_4O]$	yellow-orange	399	0.14	0.71
$[O\text{-}4\text{-}NO_2\text{-}C_6H_3O]$	$[O\text{-}3\text{-}MeO\text{-}C_6H_3O]$	orange	389	0.00	0.00
$[O\text{-}4\text{-}NO_2\text{-}C_6H_3O]$	$[OC_6Cl_4O]$	orange-brown	396, 305	0.00	0.00
$[O\text{-}3\text{-}MeO\text{-}C_6H_3O]$	$[O\text{-}3\text{-}MeO\text{-}C_6H_3O]$	white	-	0.01	0.03
$[O\text{-}3\text{-}MeO\text{-}C_6H_3O]$	$[OC_6H_4O]$	white	-	0.08	0.00
$[O\text{-}3\text{-}MeO\text{-}C_6H_3O]$	$[O\text{-}4\text{-}NO_2\text{-}C_6H_3O]$	yellow	417, 293, 271(sh)	0.14	0.32
$[O\text{-}3\text{-}MeO\text{-}C_6H_3O]$	$[OC_6Cl_4O]$	brown-green	287	0.00	0.00
$[OC_6Cl_4O]$	$[OC_6Cl_4O]$	white	-	0.00	0.00
$[OC_6Cl_4O]$	$[OC_6H_4O]$	tan-brown	312, 302	0.00	0.00
$[OC_6Cl_4O]$	$[O\text{-}4\text{-}NO_2\text{-}C_6H_3O]$	red-brown	396, 306	0.00	0.00
$[OC_6Cl_4O)$	$[O\text{-}3\text{-}MeO\text{-}C_6H_3O]$	tan-brown	313, 302	0.00	0.00

The majority of compounds show essentially zero SHG effects, these include all compounds containing the 3,4,5,6-tetrachlorocatecholate ligand. This is probably due to their crystallization in centrosymmetric space groups which result in a cancellation of the bulk

susceptibility effects. An anomalous result was seen for $[(OC_6H_4O)_3Sn][NHEt_3]_2$ at 1064 nm which shows an SHG effect of 0.40 x urea. This was despite the fact that it crystallized in the centrosymmetric space group[21], $P2_1/n$. Such an effect has been observed previously and was attributed to either the co-crystallization of centric and non-centric modifications or surface effects[24].

A number of compounds do show significant SHG effects. They can be divided into three distinct classes. The first group contains those compounds which showed a greater SHG effect at 1064 nm than at 1.9 μm. This class consists of $[(OC_6H_4O)_2Sn(OC_6H_3O\text{-}NO_2\text{-}4)][NHEt_3]_2$ and $[(O\text{-}4\text{-}NO_2\text{-}C_6H_3O)_3Sn][NHEt_3]_2$. Analysis of their electronic solution spectra showed no significant absorption at 532 nm, a harmonic of the incident laser frequency, the SHG effect was therefore strongly favoured. This was not the case for the second class of compound which showed stronger SHG at 1.9 μm. For $[(O\text{-}4\text{-}NO_2\text{-}C_6H_3O)_2Sn(OC_6H_4O)][NHEt_3]_2$ and $[(O\text{-}3\text{-}MeO\text{-}C_6H_3O)_2Sn(OC_6H_3\text{-}4\text{-}NO_2\text{-}O)][NHEt_3]_2$ tailing of their electronic spectra into the 532 nm region was observed, thus reducing their NLO properties at 1064 nm. The third class of compound shows an equal SHG effect at 1064 nm and 1.9 μm. $[(OC_6H_4O)_2Sn(OC_6H_3O\text{-}OMe\text{-}3)][NHEt_3]_2$ was the only compound to show this behaviour.

The most dramatic SHG effect was shown by $[(O\text{-}4\text{-}NO_2\text{-}C_6H_3O)_3Sn][NHEt_3]_2$, which has a value of 1.33 x urea at 1064 nm. In order to better understand its structure in the solid-state, a single crystal X-ray diffraction study was undertaken.

5.3.1 X-ray Crystallographic Analysis of $[(O\text{-}4\text{-}NO_2\text{-}C_6H_3O)_3Sn][NHEt_3]_2$

Bright yellow crystals of $[(O\text{-}4\text{-}NO_2\text{-}C_6H_3O)_3Sn][NHEt_3]_2$, were grown by slow diffusion of diethyl ether into a methanol solution of the compound. The data collection and stucture solution were carried out by Dr. Jonathan Machell of this laboratory.

A single crystal of dimensions 0.2 x 0.2 x 0.3 mm was mounted in a glass capillary under nitrogen and transferred to the goniometer head of an Enraf-Nonius CAD4 diffractometer. Final unit cell dimensions, calculated from a least-squares treatment of the

angles of 24 accurately centred reflections are given in Table 5.2. 4688 reflections were collected by $\omega/2\vartheta$ scans (scan width 0.80 + 0.35tanϑ) using graphite monochromated Mo-K_α radiation, of which 1257 were considered unique and observed ($I \geq 3\sigma(I)$, R_{merg}= 0.0558). These were corrected for Lorentz and polarization effects and an absorption correction was applied (min/max correction 1.00/1.07).

The structure was solved by routine Patterson, direct methods (SHELXS), Fourier methods and full-matrix, least squares refinement of all the non-hydrogen atoms, followed by DIFABS and spherical absorption corrections. The tin and oxygen atoms were converted to having anisotropic thermal perameters, whilst all hydrogen atoms were generated geometrically. On application of a Cebyshev weighting scheme (coefficients 9.845, -13.768, 8.313, -4.405), the model converged at R = 0.0626, R_w= 0.0699.

Table 5.3 and Appendix 7 contain the structural data for $[(O\text{-}4\text{-}NO_2\text{-}C_6H_3O)_3Sn][NHEt_3]_2$ whilst Figures 5.2 and 5.3 show the main structural features.

Table 5.2 Structural Details for $[(O\text{-}4\text{-}NO_2\text{-}C_6H_3O)_3Sn][NHEt_3]_2$

Compound	$C_{30}H_{41}N_5O_{12}Sn$
Molecular Weight	780.35
Space Group	Pbca
Cell Dimensions	a 13.655(3)Å α 90°
	b 18.299(6)Å β 90°
	c 36.030(1)Å γ 90°
Cell Volume	7003 Å^3
Z	8
Density	1.48g cm^{-3}
Linear Absorption Coefficient	7.94 cm^{-1}
Radiation	Mo-K_α (λ = 0.71069Å)
Standard Reflections	-7 2 5; 0 0 14; 0 6 7
Decay of Standards	22%
2ϑ Range	2-40°
Number of Parameters Varied	228
R	0.0626
R_w	0.0699
Goodness of Fit	1.15
F(000)	3200
Residual Electron Density	0.51 e$^-$/Å^3

Table 5.3 Selected Bond Lengths (Å) and Angles (°) for $[(O\text{-}4\text{-}NO_2\text{-}C_6H_3O)_3Sn][NHEt_3]_2$

Atoms	Distance	Atoms	Distance
Sn(1)-O(1)	2.01(2)	Sn(1)-O(2)	2.06(1)
Sn(1)-O(3)	2.07(1)	Sn(1)-O(4)	2.10(1)
Sn(1)-O(5)	2.09(1)	Sn(1)-O(6)	2.04(1)
O(1)-C(1)	1.34(2)	O(2)-C(6)	1.34(2)
O(3)-C(12)	1.30(2)	O(4)-C(7)	1.29(2)
O(5)-C(13)	1.29(2)	O(6)-C(18)	1.30(2)

Atoms	Angle	Atoms	Angle
O(2)-Sn(1)-O(1)	80.7(5)	O(3)-Sn(1)-O(1)	169.0(5)
O(3)-Sn(1)-O(2)	91.7(5)	O(4)-Sn(1)-O(1)	89.6(5)
O(4)-Sn(1)-O(2)	94.9(6)	O(4)-Sn(1)-O(3)	83.0(5)
O(5)-Sn(1)-O(1)	89.7(5)	O(5)-Sn(1)-O(2)	169.2(5)
O(5)-Sn(1)-O(3)	94.8(6)	O(5)-Sn(1)-O(4)	171.7(5)
O(6)-Sn(1)-O(1)	94.8(6)	O(6)-Sn(1)-O(2)	92.7(5)
O(6)-Sn(1)-O(3)	93.5(6)	O(6)-Sn(1)-O(4)	171.7(5)
O(6)-Sn(1)-O(5)	83.0(6)	C(1)-O(1)-Sn(1)	113.7(12)
C(6)-O(2)-Sn(1)	111.4(10)	C(12)-O(3)-Sn(1)	108.7(13)
C(7)-O(4)-Sn(1)	106.3(12)	C(13)-O(5)-Sn(1)	108.8(13)
C(18)-O(6)-Sn(1)	109.4(13)	O(8)-N(1)-O(7)	120.5(20)

Figure 5.2 Molecular Structure of $[(O\text{-}4\text{-}NO_2\text{-}C_6H_3O)_3Sn][NHEt_3]_2$

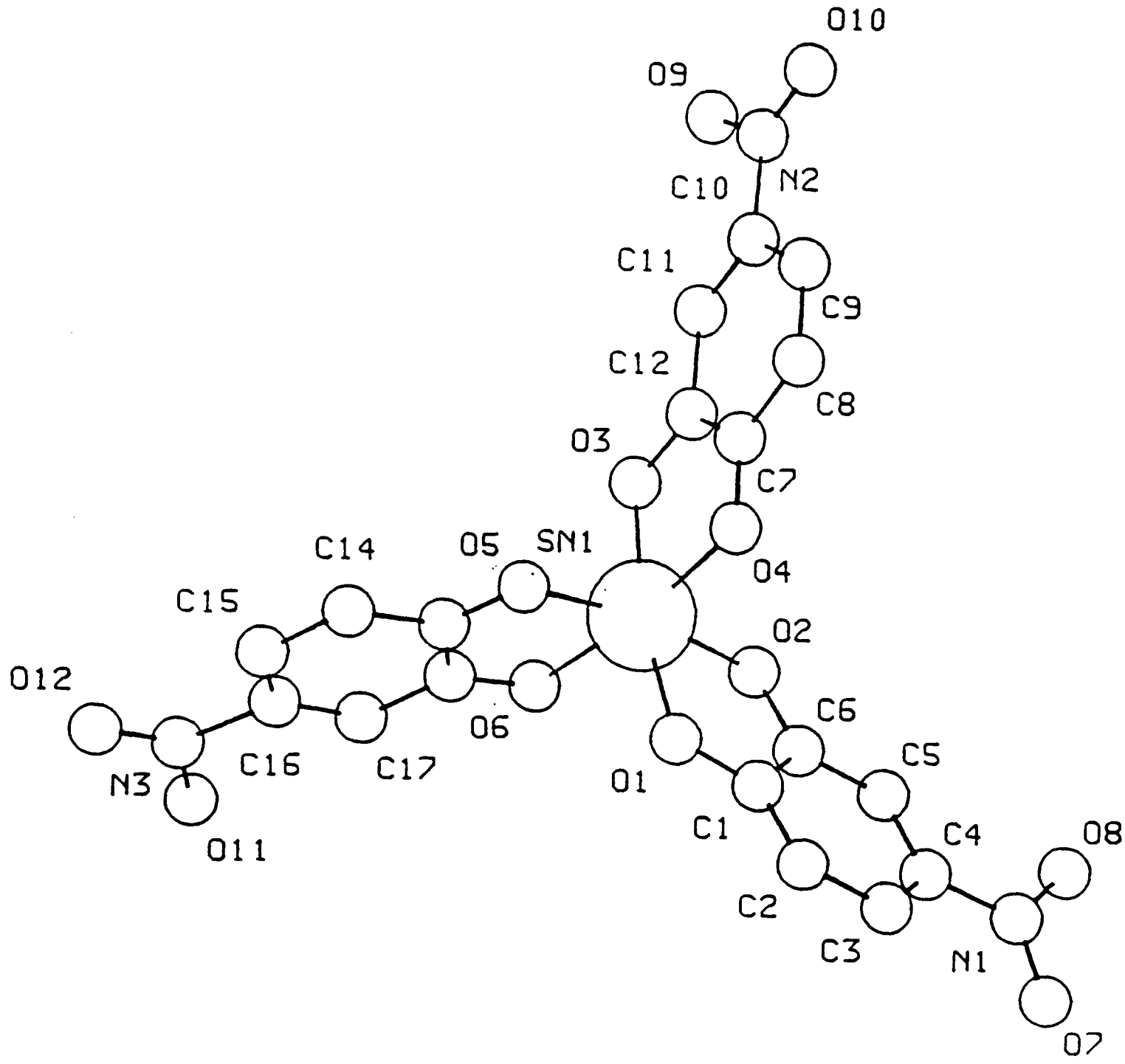
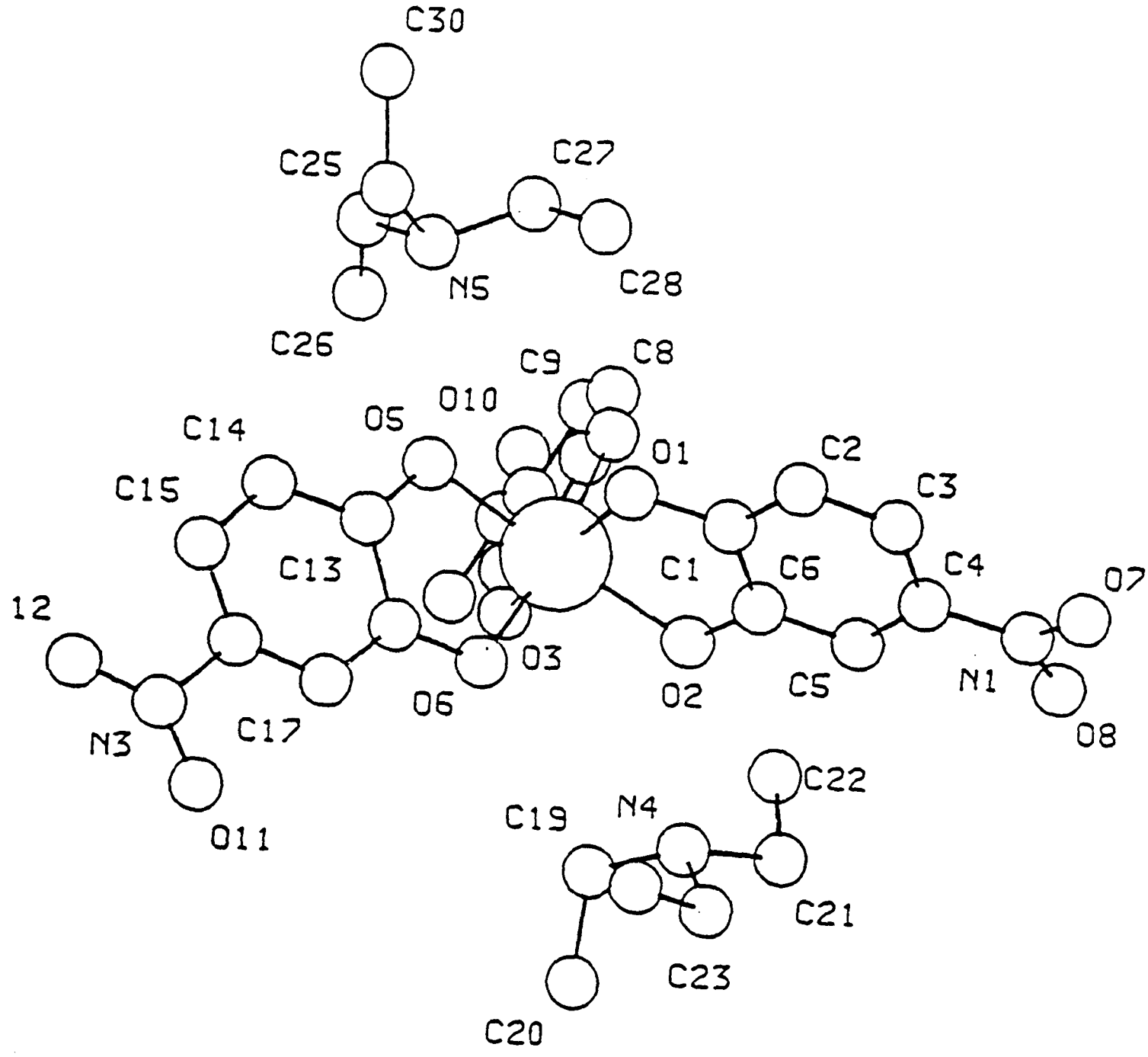


Figure 5.3 Structure of $[(O\text{-}4\text{-}NO_2\text{-}C_6H_3O)_3Sn][NHEt_3]_2$ Showing Close, Hydrogen Bonded Contacts Between Anion and Cations



The structure consists of anions of $[Sn(OC_6H_3\text{-}4\text{-}NO_2\text{-}O]^{2-}$ and cations of $[Et_3NH]^+$. The compound crystallizes in the non-centrosymmetric space group Pbca. The cations and anion are not well-separated and there is clear evidence of hydrogen-bonding between the nitrogen atoms of the triethylammonium cations and the nearest ligated oxygen atoms, with distances O(2)-N(4) 2.79Å and O(5)-N(5) 2.83Å. Hydrogen-bonding has been observed in other tris(catecholato)tin(IV) compounds. In $[(OC_6H_4O)_3Sn][NHEt_3]_2$[21] $[(OC_6Cl_4O)_3Sn][HTMEDA]_2$[18], evidence for hydrogen-bonding was shown by the lengthening of one of the tin-oxygen bonds to 2.086(4)Å. In $[(OC_6Cl_4O)_3Sn][HTMEDA]_2$[18] hydrogen-bonding occurs between the cations and two of the chlorine atoms in the anion, with a nitrogen-chlorine distance of 2.626Å. The inceased stability of $[(OC_6Cl_4O)_3Sn][HTMEDA]_2$ was also attributed to hydrogen-bonding in the crystals.

The coordination geometry around the tin atom in $[(O\text{-}4\text{-}NO_2\text{-}C_6H_3O)_3Sn][NHEt_3]_2$ is approximately octahedral. The oxygen-tin-oxygen angles involving oxygen atoms of the same catechol ligand are 80.7(5), 83.0(5) and 83.0(6)°. The other, smaller angles range from 89.6(5) to 98.4(5)°. The larger angles are 169.0(5), 169.2(5) and 171.7(5)°. This distortion is observed in other metal catechol complexes and is due to the small bite angle of the catecholate ligand. In bis(3,5-di-t-butylcatecholato)tin-1,10-phenanthroline[22] the corresponding angles are 82.6(3) and 83.6(3)°, in $[(OC_6Cl_4O)_3Sn][HTMEDA]_2$ they are 81.7(1) and 81.1(2)° and in $[(OC_6H_4O)_3Sn][NHEt_3]_2$ they are 81.5(2) and 83.3(3)°.

The tin-oxygen bond lengths in $[(O\text{-}4\text{-}NO_2\text{-}C_6H_3O)_3Sn][NHEt_3]_2$ vary between 2.01(2) and 2.10(1)Å and are typical of those reported for other tin(IV) complexes. In bis(3,5-di-t-butylcatecholato)tin-1,10-phenanthroline the tin-oxygen bond lengths lie in the range 1.995(8) to 2.019(8)Å, in $[(OC_6Cl_4O)_3Sn][HTMEDA]_2$ they lie between 2.051(3) and 2.079(3)Å and in $[(OC_6H_4O)_3Sn][NHEt_3]_2$, they lie between 2.049(5) and 2.086(4)Å. Unlike $\{Sn[O\text{-}4\text{-}NO_2\text{-}C_6H_3O][OC_4H_8]\}_n$ (see section 2.3.4), there is no apparent effect of position relative to the nitro group upon the tin-oxygen bond lengths in $[(O\text{-}4\text{-}NO_2\text{-}C_6H_3O)_3Sn][NHEt_3]_2$. The the tin-oxygen bond lengths *meta* to the nitro group have the values 2.06(1), 2.07(1) and 2.04(1)Å and those *para* to the nitro group have the values 2.01(2), 2.10(1) and 2.09(1)Å.

5.4 Summary

An outline has been given of the basis for non-linear optical properties, especially their second harmonic generation (SHG) effects. The molecular and solid state criteria required to observe a significant SHG effect were then discussed and the ability of tris(catecholato)tin(IV) compounds to fulfil these requirements was noted.

Reaction schemes for the synthesis of a wide range of tris(catecholato)tin(IV) compounds were then outlined, and the preparation and chemical properties of the tris(catecholato)tin(IV) compounds prepared are discussed.

The non-linear optical properties of a wide range of tris(catecholato)tin(IV) compounds were then tested at 1064 nm and 1.9 μm. A number were found to have a significant SHG effect, especially $[(O\text{-}4\text{-}NO_2\text{-}C_6H_3O)_3Sn][NHEt_3]_2$, which has an SHG effect 1.33 x urea. The solid state structure of $[(O\text{-}4\text{-}NO_2\text{-}C_6H_3O)_3Sn][NHEt_3]_2$ was then studied by single crystal X-ray crystallography. This showed that the molecule crystallizes in the non-centrosymmetric space group Pbca and has the anticipated octahedral geometry.

5.5 References

1. D. S. Chemla and J. Zyss, *Nonlinear Optical Properties of Organic Molecules and Crystals*, Academic Press, Orlando, 1987, Vol. 1 and 2 and references therein.
2. A. Azema, Y. Y. Cheng, K. Jain and R. Twieg, *Chem. Phys. Lett.*, 1982, **92**, 208.
3. D. S. Chemla and J. L. Oudar, *J. Chem. Phys.*, 1977, **66**, 2664.
4. A. F. Garito, G. F. Lipscomb and R. S. Narang, *J. Chem. Phys.*, 1981, **75**, 1509.
5. A. F. Garito and K. D. Singer, *J. Chem. Phys.*, 1981, **75**, 3572.
6. D. Bloor and R. A. Hann, *Organic Materials for Nonlinear Optics*, The Royal Society of Chemistry, London, 1989.
7. D. Y. Curtin and I. C. Paul, *Chem. Rev.*, 1981, **81**, 525.

8. J. L. Bernstein, C. G. Bethea, B. F. Levein, R. T. Lynch and C. D. Thurmond, *J. Appl. Phys.*, 1979, **50**, 2523.

9. D. S. Chemla, J. F. Nicoud and J. Zyss, *J. Chem. Phys.*, 1981, **74**, 4800.

10. R. J. Hierle and J. L. Oudar, *J. Appl. Phys.*, 1977, **48**, 2699.

11. J. A. Bandy, D. Bloor, M. L. H. Green, P. V. Kolinsky, S. R. Marder and M. E. Thompson, *Nature (London)*, 1987, **330**, 360.

12. A. G. Anderson, D. F. Eaton, W. Tam and Y. Wang, *J. Am. Chem. Soc.*, 1987, **109**, 1886.

13. W. Tam and J. C. Calabrese, *Chem. Phys. Lett.*, 1988, **144**, 79.

14. C. Lamberth, D. M. P. Mingos and D. M. Murphy, *J. Chem. Soc., Dalton Trans.*, submitted.

15. V. K. Andrä and H. R. Hoppe, *Z. Anorg. Allg. Chem.*, 1975,**413**, 97.

16. I. S. Belostotskaya, N. N. Bubnov, V. V. Ershov, M. I. Kabachnik, A. I. Prokof'ev, T. I. Prokof'eva and S. P. Solodovnikov, *Dokl. Akad. Nauk SSR*, 1979, **245**, 195.

17. G. I. Latorre, L. Perello and L. Soto, *Synth. React.Inorg. Met.-Org. Chem.*, 1984, **14**, 981.

18. T. A. Annan, R. K. Chadha, D. G. Tuck and K. D. Watson, *Can. J. Chem.*, 1987, **65**, 2670.

19. G. Cerveau, C. Chuit, R. J. P. Corriu and C. Reye, *Organometallics*, 1988, **7**, 786.

20. A. Boudin, G. Cerveau, C. Chuit, R. J. P. Corriu and C. Reye, *Organometallics*, 1988, **7**, 1165.

21. V. Chandrasekhar, R. O. Day, J. M. Holmes, R. R. Holmes, A. C. Sau and S. Shafieezad, *J. Am. Chem. Soc.*, 1988, **110**, 1168.

22. T. A. Annan, R. K. Chadha, B. R. McGarvey, A. Ozarowski and D. G. Tuck, *J. Chem. Soc., Dalton Trans.*, 1989, 439.

23. S. K. Kurtz and T. T. Perry, *J. Appl. Phys.*, 1968, **39**, 3798.

24. J. A. Bandy, D. Bloor, H. E. Bunting, M. H. Garcia, M. L. H. Green, R. J. Jones, P. V. Kolinsky, S. R. Marder and M. E. Thompson, *Organic Materials. Nonlinear Optics*, The Royal Society of Chemistry, Special Publication, **69**, London, 1989, p 225.

Chapter 6

Experimental Details

6.1 General

Reactions were routinely carried out using standard Schlenk line procedures under an atmosphere of pure, dry nitrogen and using dry oxygen-free solvents.

Microanalyses of air-stable compounds were carried out by Mr. M. Gascoyne and his staff of this laboratory. Air-sensitive samples were handled by Analytical Laboratories, D-5250 Engelskirchen, Germany.

Infra-red spectra were recorded as cesium iodide discs, or Nujol mulls on cesium iodide plates using a Pye-Unicam SP2000 or a Perkin-Elmer 1710 FT spectrometer.

^{119}Sn Mössbauer spectra were measured at 80K using a constant acceleration microprocessor Mössbauer spectrometer and a $Ba^{119m}SnO_3$ γ-source. The experimental errors in the isomer shifts and quadrupole splittings were ±0.05 mms^{-1}.

Solution electronic spectra were recorded on a Perkin-Elmer 552 UV-visible spectrophotometer, using either a 1mm or 10mm quartz cell. All extinction coefficients are reported as log ε_{max} except where otherwise indicated.

Electron Impact (EIMS) and Fast Atom Bombardment (FABMS) Mass Spectra were carried out by the SERC Mass Spectroscopy Service Centre, University College of Swansea.

^{19}F n.m.r spectra were recorded using a Bruker AM-250 spectrometer operating at 235.5MHz referenced externally to $CFCl_3$.

The following n.m.r. spectra were recorded using a Bruker WM-300 spectrometer.

Isotope	Operating Frequency (MHz)	Reference
^{1}H	299.96	TMS
^{11}B	96.2	$BF_3.Et_2O$
^{13}C	75.47	solvent (internal)
^{31}P	121.50	$PO(OMe)_3/D_2O$
^{117}Sn	106.95	$SnMe_4$
^{119}Sn	111.81	$SnMe_4$
^{195}Pt	64.50	Na_2PtCl_6/D_2O

X-ray diffraction data were collected on an Enraf-Nonius CAD4F diffractometer at ambient temperature in the Chemical Crystallography Laboratory, Oxford. The data was processed on the Chemical Crystallography VAX computer. The programmes used and the sources of scattering factor data are given in reference 1.

The following compounds were prepared by standard literature methods.

Compound	Reference
$Sn[OMe]_2$	2
$PtCl_2[dppe]$	3
$Pt[C_2H_4][PPh_3]_2$	4
$Pt[PPh_3]_3$	5
$RhCl[CNR]_3$ (R = xylyl)	6
Ph_3PAuCl	7
PhSCu	8
$Sn[NMe_2]_2$	9
$Sn[OC_6H_4O]$	10

6.2 Experimental Details Relevant to Chapter 2

6.2.1 Synthesis of Sn[O-3, 5-$^{t}Bu_2$-C_6H_2O]

3, 5-Di-*tert*-butylcatechol (3.53g, 15.8 mmol) was dissolved in tetrahydrofuran (10 cm^3) and added with stirring to tin(II) methoxide (2.86g, 15.8 mmol) in tetrahydrofuran (20 cm^3). After stirring at room temperature for twenty four hours the solid residue was isolated, washed with tetrahydrofuran (2 x 20 cm^3) and diethyl ether (20 cm^3), then dried *in vacuo*. The white solid was insoluble in all common solvents. Yield: 5.10g (95%). M.pt. >300°C. (Found C, 49.81; H, 6.07; Sn, 34.46. $C_{14}H_{20}O_2Sn$ requires C, 49.60; H, 5.90; Sn, 35.05%); ν(SnO) at 544(s) cm^{-1}.

6.2.2 Synthesis of Sn[aden]

(-)Adenosine (1.00g, 3.76 mmol) and tin(II) methoxide (0.68g, 3.76 mmol) were stirred in tetrahydrofuran (25 cm^3) for twenty four hours. The solid residue was isolated, washed with tetrahydrofuran (2 x 20 cm^3) and diethyl ether (20 cm^3), then dried *in vacuo*. The off-white solid was insoluble in all common solvents. Yield: 1.24g (87%). M.pt. 210°C (decomp.). (Found C, 32.11; H, 3.12; N, 16.97; Sn, 28.4. $C_{10}H_{11}N_5O_4Sn$ requires C, 31.27; H, 2.96; N, 18.24; Sn, 30.93%). ^{119m}Sn: δ 3.09 mms^{-1}, Δ 2.03 mms^{-1}.

6.2.3 Synthesis of Sn[O-3-MeO-C_6H_3O]

3-Methoxycatechol (1.50g, 10.7 mmol) was dissolved in tetrahydofuran (10 cm^3) and added with stirring to tin(II) methoxide (1.93g, 10.7 mmol) in tetrahydrofuran (20 cm^3). After stirring at room temperature for twenty four hours the solid residue was isolated, washed with tetrahydrofuran (2 x 20 cm^{-3}) and diethyl ether (20 cm^3), then dried *in vacuo*. The white solid was insoluble in all common solvents except sparingly in dimethyl sulphoxide.Yield: 2.64g (96%). M.pt. 240°C (decomp.). (Found C, 32.54; H, 2.36; Sn, 45.91. $C_7H_6O_3Sn$ requires C, 32.72; H, 2.34; Sn, 46.24%); ν(SnO) at 544(s) cm^{-1}. N.m.r.: ^1H (d_6-dmso), δ 6.35-6.16 (m, 3H, arom.) and 3.70 p.p.m. (s, 3H, OMe).

6.2.4 Synthesis of $Sn[OC_6Cl_4O][OC_4H_8]$

Tetrachloro-*o*-benzoquinone (2.59g, 11.1 mmol) was dissolved in tetrahydrofuran (10 cm^3) and added with stirring to tin(II) methoxide (2.00g, 11.1 mmol) in tetrahydrofuran (20 cm^3). The resulting reaction was slightly exothermic, and was stirred until it had cooled to room temperature. After stirring for a further thirty minutes, the solid residue was isolated, washed with tetrahydrofuran (2 x 20 cm^3) and diethyl ether (20 cm^3), then dried *in vacuo*. The pale yellow solid was found to be insoluble in all common solvents except dimethlyformamide. Yield: 4.36g (93%). M.pt. 192°C (decomp.). (Found C, 27.04; H, 1.94; Cl, 31.10. $C_{10}H_8Cl_4O_3Sn$ requires C, 27.48; H, 1.83; Cl, 32.52%); ν(SnO) at 500m cm^{-1}. N. m. r.: ^{13}C-{^1H} (dmf/D_2O), δ 148.8, 119.4, 117.5 (arom.) and 68.2, 26.2 p.p.m. (thf); ^{117}Sn-{^1H} (dmf/D_2O), δ -332.3 p.p.m.

6.2.5 Synthesis of $\{Sn[O\text{-}4\text{-}NO_2\text{-}C_6H_3O][OC_4H_8]\}_n$

4-Nitrocatechol (0.57g, 2.9 mmol) was dissolved in tetrahydrofuran (10 cm^3) and added with stirring to tin(II) methoxide (0.55g, 2.9 mmol) in tetrahydrofuran (20 cm^3). After stirring at room temperature for four hours, solvent was removed *in vacuo*, and product was extracted by hot tetrahydrofuran. Crystallization began upon cooling and was aided by the addition of a small amount of hexane (10 cm^3) as co-solvent. The bright yellow crystals formed were isolated, washed with hexane (2 x 10 cm^3) and dried *in vacuo*. The product was found to be soluble in tetrahydrofuran, acetone, methanol, ethanol, acetonitrile, dimethyl sulphoxide and sparingly in water. The product is stable in air for up to eight hours after which the colour changed from bright yellow to orange-red. Recrystallization by slow diffusion of hexane into a tetrahydrofuran solution gave crystals of $\{Sn[O\text{-}4\text{-}NO_2\text{-}C_6H_3O][OC_4H_8]\}_n$ suitable for X-ray crystallography. Yield: 0.96g (76%). M.pt. 178°C (decomp.). (Found: C, 34.44; H, 3.16; N, 4.12; Sn, 34.61. $C_{10}H_{11}NO_5Sn$ requires C, 34.91; H, 3.20; N, 4.07; Sn, 34.53%). (Mol. wt_{calc}= 272 for $Sn[O\text{-}4\text{-}NO_2\text{-}C_6H_3O]$; Mol. wt_{meas}= 298); ν(NO_2) at 1323(br,vs) and 1268(br,vs) cm^{-1}, ν(SnO) at 550m cm^{-1}. ^{119m}Sn: δ 3.49 mms^{-1}, Δ 2.33 mms^{-1}. λ (MeOH) 374 and 427 nm. N.m.r.: ^1H (d_6-dmso), δ 7.48 (dd, ^3J(H-H) 8.8, ^4J(H-

H) 3.1, 1H, arom.), 7.22 (d, ^{4}J(H-H) 3.1, 1H, arom.), 6.50 (d, ^{3}J(H-H) 8.8, 1H, arom.), 3.60 (m, 4H, thf) and 1.76 p.p.m. (m, 4H, thf); ^{13}C-{^{1}H} (CD_3OD), δ 116.5, 114.4, 110.2 (arom.), 68.5 and 26.1 p.p.m. (thf); ^{117}Sn-{^{1}H} (CH_3OH/D_2O), δ -452.3 p.p.m.

6.3 Experimental Details Relevant to Chapter 3

6.3.1 Synthesis of $SnI_2[O\text{-}4\text{-}NO_2\text{-}C_6H_3O][OC_4H_8]_2$

Iodine (0.38g, 1.50 mmol) was dissolved in tetrahydrofuran (10 cm^3) and added dropwise with stirring to $\{Sn[O\text{-}4\text{-}NO_2\text{-}C_6H_3O][OC_4H_8]\}_n$ (0.52g, 1.50 mmol) in tetrahydrofuran (20 cm^3). After stirring at room temperature for one hour, the reaction mixture was filtered and solvent volume reduced to 15 cm^3 *in vacuo*. Hexane was added as co-solvent, giving bright orange-brown crystals. Yield: 0.71g (71%). (Found: C, 25.74; H, 2.96; N, 2.14; I, 38.15; Sn, 17.36. $C_{14}H_{19}NO_6I_2Sn$ requires C, 25.09; H, 2.83; N, 2.09; I, 37.90; Sn, 17.73%). N.m.r.: ^{1}H (d_6-acetone), δ 7.69-6.65 (m, 3H, arom.), 3.72-3.60 (m, 8H, thf) and 1.83-1.75 p.p.m. (m, 8H, thf); ^{13}C-{^{1}H} (d_6-acetone), δ 118.5, 117.7, 116.2 (arom.), 68.1 (thf) and 26.1 p.p.m. (thf); ^{119}Sn-{^{1}H} (d_6-acetone), δ 69.5 p.p.m.

6.3.2 Synthesis $\{[Et_3BzN][SnCl(O\text{-}4\text{-}NO_2\text{-}C_6H_3O)]\}_n$

$\{Sn[O\text{-}4\text{-}NO_2\text{-}C_6H_3O][OC_4H_8]\}_n$ (0.18g, 0.51 mmol) was dissolved in tetrahydrofuran (20 cm^3) and added with stirring to benzyltriethylammonium chloride (0.12g, 0.51 mmol) in tetrahydrofuran (20 cm^3). After stirring at room temperature for three hours solvent was removed *in vacuo*. Extraction with methanol, followed by crystallization from methanol-diethyl ether afforded orange crystals. Single crystals suitable for X-ray crystallography were grown by the slow diffusion of diethyl ether into a methanol solution. Yield: 0.17g (68%). (Found: C, 45.50; H, 5.08; Cl, 7.60; N, 5.33. $C_{19}H_{25}ClN_2O_4Sn$ requires C, 45.65, H, 5.00; Cl, 7.10; N, 5.61%); ν(Sn-Cl) at 389(s) cm^{-1}. N.m.r.: ^{1}H (CD_3OD), δ 7.53 (s, 6H, C_6H_5), 7.59-6.63 (m, 3H, arom.), 4.47 (s, 2H, Bz CH_2), 3.24 (q, $^3J_{HH}$ 7.3Hz, 6H, $\underline{CH}_2$-CH_3), and 1.42 p.p.m. (t, $^3J_{HH}$ 7.3Hz, 9H, CH_2-$\underline{CH}_3$); ^{13}C-{^{1}H} (CD_3OD), δ 133.9,

132.2, 130.8 (Bz arom.), 116.9, 113.9, 109.5 (arom.), 53.9 (Bz CH_2), 50.2 and 8.3 p.p.m. (Et); ^{119}Sn-{^1H} (CD_3OD), δ -294.3 p.p.m.

6.3.3 Synthesis of $[Et_3NH][SnCl(O\text{-}C_6Cl_4O)]$

Tetrachloro-*o*-benzoquinone (2.00g, 8.13 mmol) was dissolved in tetrahydrofuran (10 cm^3) and added dropwise with stirring to tin(II) chloride (1.54g, 8.13 mmol) in tetrahydrofuran (20 cm^3). After stirring at room temperature for ten minutes, triethylamine (1.65g, 8.26 mmol) and methanol (2 cm^3, an excess) were added. After stirring for a further thirty minutes, and standing for two hours, the supernatant liquid was collected and combined with subsequent tetrahydrofuran washings (4 x 10 cm^3) of the solid residue. Solvent was then removed *in vacuo* and the residue crystallized from tetrahydrofuran-diethyl ether giving a cream microcrystalline solid. Yield: 2.32g (57%). (Found: C, 29.32; H, 3.52; Cl, 34.98; N, 2.79. $C_{12}H_{16}Cl_5NO_2Sn$ requires C, 28.67; H, 3.19; Cl, 35.34; N, 2.79); ν(SnCl) at 395(m) cm^{-1}. N.m.r.: ^1H (d_6-acetone), δ 3.09 (q, $^3J_{HH}$ 6.9Hz, 6H, CH_2) and 1.22 p.p.m. (t, $^3J_{HH}$ 6.9Hz, 9H, CH_3); ^{13}C-{^1H} (d_6-acetone), δ 120.5, 118.0, 116.9 (arom.), 41.9 and 9.2 p.p.m. (Et); ^{117}Sn-{^1H} (acetone/D_2O), δ -515.0 p.p.m.

6.3.4 Synthesis of $Sn[NH_2CH_2CH(Me)H_2N][O\text{-}4\text{-}NO_2\text{-}C_6H_3O][OC_4H_8]$

1, 2-Diaminopropane (0.11g, 1.46 mmol) was dissolved in tetrahydrofuran (15 cm^3) and added dropwise with stirring to $\{Sn[O\text{-}4\text{-}NO_2\text{-}C_6H_3O][OC_4H_8]\}_n$ (0.50g, 1.46 mmol) in tetrahydrofuran (20 cm^3). After stirring at room temperature for one hour, the solution was filtered, and solvent and any unreacted 1,2-diaminopropane were then removed *in vacuo*. Crystallization from tetrahydrofuran-diethylether afforded an orange microcrystalline solid. Yield: 0.53g (82%). (Found: C, 36.55; H, 5.02; N, 10.01. $C_{13}H_{21}N_3O_5Sn$ requires C, 37.34; H, 5.02; N, 10.05%); ν(NH) at 3281(vs) and 3141(s) cm^{-1}. N.m.r.: ^1H (CD_3OD), δ 7.57-6.89 (m, 3H, arom.), 3.74-3.70 (m, 4H, thf), 3.05 (q, $^3J_{HH}$ 6.2Hz, 1H, CH), 2.82-2.60 (m, 2H, CH_2), 1.86 (d, $^3J_{HH}$ 6.2Hz, 3H, CH_3) and 1.72-1.68 p.p.m. (m, 4H, thf); ^{13}C-{^1H} (CD_3OD), δ 116.9, 113.9, 109.6 (arom.), 69.2, 26.8 (thf), 48.9 (CH_2) and 19.3 p.p.m. (CH_3).

6.3.5 Synthesis of $F_3B.Sn[O\text{-}4\text{-}NO_2\text{-}C_6H_3O][OC_4H_8]$

A solution of boron trifluoride etherate (0.15g, 1.05 mmol) in tetrahydrofuran (20 cm^3) was added dropwise with stirring to $\{Sn[O\text{-}4\text{-}NO_2\text{-}C_6H_3O][OC_4H_8]\}_n$ in tetrahydrofuran (0.36g, 1.05 mmol). After stirring for thirty minutes at room temperature, solvent, and any unreacted boron trifluoride etherate were removed *in vacuo* . Crystallization from tetrahydrofuran-diethyl ether afforded pale yellow crystals which were moisture sensitive and stable only in tetrahydrofuran solution. Yield: 0.38g (87%). (Found: C, 29.87; H, 2.82; N, 3.23. $C_{10}H_{11}BF_3NO_5Sn$ requires C, 29.16; H, 2.67; N, 3.40%); FABMS: (NOBA matrix), M^+ 411 (M^+_{calc} 411). N.m.r.: ^1H (d_8-thf), δ 7.98−6.68 p.p.m (m, arom.); $^{11}B\text{-}\{^1H\}$ (d_8-thf), δ 0.05 p.p.m.; $^{19}F\text{-}\{^1H\}$ (d_8-thf), δ −148.9 p.p.m.; $^{117}Sn\text{-}\{^1H\}$ (thf/D_2O), δ -727.1 p.p.m.(s, 1393Hz at 1/2- height).

6.3.6 Synthesis of $\{(OC)_3W.Sn[(O\text{-}4\text{-}NO_2\text{-}C_6H_3O)(OC_4H_8)]\}_2$

$\{Sn[O\text{-}4\text{-}NO_2\text{-}C_6H_3O][OC_4H_8]\}_n$ (0.49g, 1.42 mmol) was dissolved in tetrahydrofuran (30 cm^3) and added with stirring to freshly prepared $W(CO)_5$(thf) (0.56g, 1.42 mmol) in tetrahydrofuran (20 cm^3). After stirring at 60°C for three hours, the reaction was allowed to cool to room temperature. After filtering, solvent was removed *in vacuo* and crystallization from tetrahydrofuran-diethyl ether afforded a red-orange microcrystalline solid. Yield: 0.36g (45%). (Found: C, 25.18; H, 1.74; N, 2.69; Sn, 17.93; W, 29.14. $C_{26}H_{22}N_2O_{16}Sn_2W_2$ requires C, 25.51; H, 1.80; N, 2.29; Sn, 19.41; W, 30.06%); ν(CO) (thf), at 2068(m), 1977(m), 1940(vs) and 1932(vs) cm^{-1}. FABMS: (NOBA matrix), M^+ 1080 (M^+_{calc} $\{[OC]_3W.Sn[O\text{-}4\text{-}NO_2\text{-}C_6H_3O]\}_2$ 1080). N.m.r.: ^1H (d_6-acetone), δ 7.73-6.98 (m, 3H, arom.), 3.62 (m, 4H, thf), and 1.80 p.p.m. (m, 4H, thf); $^{13}C\text{-}\{^1H\}$ (thf/D_2O), δ 196.1, 191.1 ($^1J_{CW}$ 128Hz, CO), 115.8, 113.8, 109.7 (arom.), 46.8 and 8.1 p.p.m. (thf); $^{117}Sn\text{-}\{^1H\}$ (thf/D_2O), δ -166.0 p.p.m.

6.3.7 Synthesis of $[Et_4N][Pt(dppe)(SnCl_3)_3]$

Tin(II) chloride (0.44g, 2.28 mmol) was added with stirring to $PtCl_2(dppe)$ (0.76g, 1.14 mmol) in dichloromethane (20 cm^3). After stirring at room temperature for thirty minutes, tetraethylammonium chloride (0.21g, 1.14 mmol) and a further molar equivalent of tin(II) chloride were added. As soon as reaction mixture became clear, the red-orange solution was filtered and solvent volume reduced *in vacuo*. Addition of acetonitrile and cooling to -20°C afforded red-orange plates suitable for study by X-ray crystallography. The product was found to be unstable in solution decomposing to $PtCl_2(dppe)$. Yield: 0.61g (38%). (Found: C, 28.37; H, 3.05; Cl, 25.36; N, 0.92. $C_{34}H_{44}Cl_9NP_2PtSn_3$ requires C, 28.96; H, 3.12; Cl, 22.68; N, 0.99%); ν(SnCl) at 359(m), 287(m) and 266(br, m) cm^{-1}. N.m.r.: $[Et_4N][Pt(dppe)(SnCl_3)_3]$ decomposes in solution. N.m.r. details are given in Section 3.5.4.3.

6.3.8 Synthesis of $\{PtH[PPh_3]_3\}\{[\mu_2\text{-}O][\mu_2\text{-}OH][Sn(O\text{-}4\text{-}NO_2\text{-}C_6H_3O)]_2\}$

(a) $\{Sn[O\text{-}4\text{-}NO_2\text{-}C_6H_3O][OC_4H_8]\}_n$ (0.40g, 1.17 mmol) was dissolved in tetrahydrofuran (25 cm^3) and added with stirring to bis(triphenylphosphine)platinum-ethylene (0.88g, 1.17 mmol) in tetrahydrofuran (20 cm^3). After stirring at room temperature for one hour, the reaction mixture was filtered and solvent removed *in vacuo*. The dark-red residue was washed with toluene (2 x 20 cm^3) and dried. Crystallization from tetrahydrofuran-hexane afforded a dark-red microcrystalline solid. Yield: 0.58g (32%). (Found: C, 47.62; H, 3.34; N, 1.79; Pt, 12.91; Sn, 16.01. $C_{60}H_{53}N_2O_{10}P_3PtSn_2$ requires C, 48.44; H, 3.56; N, 1.88; Pt, 13.12; Sn, 15.97%); ν(SnO) at 522(vs) cm^{-1}. FABMS: (NOBA matrix), M^+ 982 (M^+_{calc} 982); M^- 577 (M^-_{calc} 577). N.m.r.: ^1H (d_6-acetone), δ -5.71 p.p.m. (AB_2XM spin system, $^2J_{HP(cis)}$ 12.6Hz, $^2J_{HP(trans)}$ 160Hz, 1H, hydride); $^1H\text{-}\{^{31}P\}$ (d_6-acetone), δ -5.71 p.p.m. ($^1J_{HPt}$ 777Hz); $^{31}P\text{-}\{^1H\}$ (d_6-acetone) (218K), δ 20.63 (d, $^2J_{PP}$ 19Hz, $^1J_{PPt}$ 2819Hz, 2P) and 19.62 p.p.m. (t, $^2J_{PP}$ 19Hz, $^1J_{PPt}$ 2218Hz, 1P); $^{117}Sn\text{-}\{^1H\}$ (acetone/D_2O), δ -455.0 p.p.m.

(b) When the reaction was repeated using tris(triphenylphosphine)platinum and two equivalents of $\{Sn[O\text{-}4\text{-}NO_2\text{-}C_6H_3O][OC_4H_8]\}_n$, the same product was obtained (yield 75%).

6.3.9 Synthesis of $\{RhCl[CNC_8H_9]_3[\mu_2\text{-}Sn(O\text{-}4\text{-}NO_2\text{-}C_6H_3O)]\}_2$

$\{Sn[O\text{-}4\text{-}NO_2\text{-}C_6H_3O][OC_4H_8]\}_n$ (0.44g, 1.27 mmol) was dissolved in tetrahydrofuran (25 cm^3) and added dropwise with stirring to $RhCl[CNC_8H_9]_3$ (0.67g, 1.27 mmol) in tetrahydrofuran (15 cm^3). After stirring at room temperature for two hours, solvent was removed *in vacuo*. Extraction with tetrahydrofuran gave an intense red-green dichroic solution, crystallisation beginning upon addition of diethyl ether. Recrystallization from dichloromethane-diethyl ether afforded dark red crystals. Yield: 0.95g (93%). (Found: C, 48.95; H, 3.76; Cl, 4.95; N, 6.68. $C_{66}H_{60}Cl_2N_8O_8Rh_2Sn_2$ requires C, 49.30; H, 3.73; Cl, 4.42; N, 6.97%); ν(CN) at 2170(s), 2144(vs) and ν(RhCl) at 305(m) cm^{-1}. λ_{max} 326(4123) and 404(1520) nm. N.m.r.: ^1H ($CDCl_3$), δ 7.74-6.81 (m, 6H, arom.), 7.28-6.72 (m, 18H, xylyl arom.), 2.40 (s, 12H, CH_3), 2.19 (s, 6H, CH_3), 2.15 (s, 12H, CH_3) and 2.12 p.p.m. (s, 6H, CH_3); $^{117}Sn\text{-}\{^1H\}$ (CH_2Cl_2/D_2O), δ -561.4 p.p.m. (t, $^1J_{SnRh}$ 472Hz).

6.3.10 Synthesis of $[Au_4(PPh_3)_4(\mu_2\text{-}SnCl_3)_2]$

Triphenylphosphinegold chloride (0.54g, 1.08 mmol) was added with stirring to $\{Sn[O\text{-}4\text{-}NO_2\text{-}C_6H_3O][OC_4H_8]\}_n$ (0.19g, 0.54 mmol) in tetrahydrofuran (40 cm^3). After stirring at 55°C for three hours, the reaction mixture was hot filtered and solvent removed *in vacuo*. Extraction with acetone, and crystallization from acetone-toluene afforded golden-yellow octahedral crystals suitable for study by X-ray diffraction. Yield: 0.09g (7%); ν(SnCl) at 312(br, m) cm^{-1}. N.m.r.: $^{31}P\text{-}\{^1H\}$ (CH_2Cl_2/D_2O), δ 56.86 p.p.m.

6.4 Experimental Details Relevant to Chapter 4

6.4.1 Synthesis of $Sn[SC_6H_4S]$

1,2-Benzenedithiol (2.00g, 14.1 mmol) was dissolved in tetrahydofuran (20 cm^3) and added with stirring to tin(II) methoxide (2.43g, 14.1 mmol) in tetrahydrofuran (20 cm^3). After stirring at room temperature for four hours, the supernatant liquid was removed and the precipitate washed with tetrahydrofuran (4 x 10 cm^3) and diethyl ether (2 x 10 cm^3), then dried *in vacuo*. The cream solid was found to be sparingly soluble in dimethyl sulphoxide. Yield: 3.36g (92%). (Found: C, 27.92; H, 1.58; S, 24.52. $C_6H_4S_2Sn$ requires C, 27.83; H, 1.55; S, 24.74%); ν(SnS) 314(s) cm^{-1}. ^{119m}Sn: δ 3.44 mms^{-1}, Δ 1.72 mms^{-1}. N.m.r.: ^1H (d_6-dmso), δ 7.42-7.38 (m, 2H, arom.) and 6.79-6.75 p.p.m. (m, 2H, arom.); ^{13}C-{^1H} (d_6-dmso), δ 130.2 and 122.0 p.p.m.(arom).

6.4.2 Synthesis of $Sn[SC_6H_4S]$TMEDA.

To a slurry of $Sn[SC_6H_4S]$ (0.20g, 0.79 mmol) in tetrahydrofuran (25 cm^3) was added with stirring a solution of N,N,N',N'-tetramethylethylenediamine (TMEDA, 0.09g, 0.79 mmol) in tetrahydrofuran (10 cm^3). After stirring at roon temperature for two hours the reaction mixture was filtered and solvent and any unreacted TMEDA were removed *in vacuo*. Crystallization from tetrahydrofuran-diethyl ether afforded a cream crystalline solid. Yield: 0.25g (87%). (Found: C, 37.87; H, 5.27; N, 7.30; S, 16.54. $C_{12}H_{20}N_2S_2Sn$ requires C, 38.43; H, 5.34; N, 7.47; S, 17.08%); ν(SnS) at 319(s) cm^{-1}. N.m.r.: ^1H (d_6-dmso), δ 7.39 (dd, $^3J_{HH}$ 5.8Hz, $^4J_{HH}$ 3.4Hz, 2H, arom.), 6.75 (dd, $^3J_{HH}$ 5.8Hz, $^4J_{HH}$ 3.4Hz, 2H, arom.), 2.45 (s, 4H, CH_2) and 2.21 p.p.m. (s, 12H, CH_3); ^{13}C-{^1H} (d_6-dmso), δ 147.1, 130.2, 122.0 (arom), 57.0 (CH_2) and 15.4 p.p.m. (CH_3); ^{117}Sn (d_6-dmso), δ -335.4 p.p.m.

6.4.3 Synthesis of 3-nitro-4,6-bis(phenylthio)chlorobenzene

Cuprous phenylmercaptide (5.82g, 33.72 mmol) was added to a solution of 1,2-dichloro-4,5-dinitrobenzene (2.00g, 8.43 mmol) in pyridine (10 cm^3) and quinoline (100 cm^3). After

stirring under reflux for three hours, the reaction mixture was allowed to cool to about 100°C. The rection mixture was then added with stirring to a mixture of ice (750g) and concentrated hydrochloric acid (200 cm^3). After stirring at room temperature for two hours, the aqueous solution was decanted off and extracted with diethyl ether (3 x 100 cm^3). The diethyl ether extract was then added to the residue and stirred for ten minutes. The residue was then extracted with further portions of diethyl ether (2 x 100 cm^3) and also with toluene (4 x 50 cm^3). The extracts were then combined and washed with 10% hydrochloric acid (2 x 50 cm^3), water (50 cm^3) and concentrated ammonia (2 x 50 cm^3). After a final wash with water (50 cm^3), the solution was dried over anhydrous potassium carbonate. The solution was then filtered and solvent volume reduced *in vacuo* to approximately 30 cm^3. Chromatography on a silica gel column, with toluene as elutant, afforded a bright orange band. The volume of solvent was reduced *in vacuo* and addition of hexane afforded an orange crystalline solid. Yield: 1.67g (53%). (Found: 57.63; H, 3.30; Cl, 9.79; N, 3.81; S, 17.10. $C_{18}H_{12}ClNO_2S_2$ requires C, 57.83; H, 3.21; Cl, 9.50; N, 3.75; S, 17.13%). EIMS: M^+ 373 (M^+_{calc} 373). λ_{max} 291(sh) and 339 nm.

6.4.4 Synthesis of [4-NO_2-OC_6H_3O][S]P[C_6H_4-4-OMe]

4-Nitrocatechol (1.00g, 6.45 mmol) was added to a solution of [2,4-bis(4-methoxyphenyl)-1,3-dithia-2,4-diphosphetane-2,4-disulphide] (Lawesson's Reagent, 2.61g, 6.45 mmol) in toluene (100 cm^3). After refluxing at 110°C for thirty minutes the reaction mixture was hot filtered and allowed to cool to room temperature. The mixture was filtered giving a pale yellow supernatant. Solvent was removed *in vacuo* and repeated crystallizations from a toluene-diethyl ether mixture eventually afforded an air sensitive white crystalline solid. Single crystals suitable for X-ray crystallography were grown by the slow diffusion of hexane into a toluene solution. Found: C, 48.47; H, 3.15; N, 4.30. $C_{13}H_{10}NO_5PS$ requires C, 48.30; H, 3.10; N, 4.33%. ν(PO) at 1267(vs), 1255(vs) and 1233(vs) cm^{-1}. N.m.r.: ^1H (C_6D_6), δ 7.63 (app dd, $^3J_{HH}$ 8.9Hz, 2H, arom (OMe).), 7.40 (s, 1H, arom (NO_2).), 7.38 (d, $^3J_{HH}$ 8.3Hz, 1H, arom (NO_2).), 6.46 (app dd, $^3J_{HH}$ 8.9Hz, arom (OMe).), 6.21 (d, $^3J_{HH}$ 8.3Hz, 1H, arom (NO_2).) and 3.04p.p.m. (s, 3H, CH_3).

6.4.5 Synthesis of $Sn[NH\text{-}C_6H_4NH]$

Tetrakis(dimethylamido)ditin(II) (1.30g, 6.28 mmol) was dissolved in benzene (25 cm^3) and added dropwise with stirring to a solution of 1,2-phenylenediamine (0.07g, 6.28 mmol) in benzene (20 cm^3). After stirring at room temperature for fifteen minutes the supernatant liquid was removed, the residue washed with benzene (2 x 10 cm^3) and dried *in vacuo*. The purple-red crystalline solid was found to be highly air sensitive and decomposes in protic solvents. Yield: 1.38 (98%). M.pt. 220°C (decomp.). (Found: C, 31.87; H, 2.82; N, 12.36; Sn, 52.67. $C_6H_6N_2Sn$ requires C, 32.04; H, 2.67; N, 12.46; Sn, 52.83%); ν(NH) at 3386(vs), 3365(vs) and 3319(vs) cm^{-1}; ν(SnN) at 543(br,s) cm^{-1}.

6.4.6 Synthesis of $Sn[NH\text{-}4\text{-}NO_2\text{-}C_6H_3NH]$

Tetrakis(dimethylamido)ditin(II) (4.34g, 20.96 mmol) was dissolved in benzene (25 cm^3) and added dropwise with stirring to 4-nitro-1,2-phenylenediamine (0.07g, 6.28 mmol) in benzene (60 cm^3). After stirring at room temperature for twenty four hours the supernatant liquid was removed, the residue washed with benzene (2 x 20 cm^3) and dried *in vacuo*. The air sensitive dark red solid was found to decompose in protic solvents. M.pt. >300°C. Found: C, 25.61; H, 1.99; N, 15.44; Sn, 43.70. $C_6H_5N_3O_2Sn$ requires C, 26.69; H, 1.85; N, 15.57; Sn, 44.01%); ν(NH) at 3351(vbr, vs) cm^{-1}; ν(SnN) at 549(br,s) cm^{-1}.

6.5 Experimental Details Relevant to Chapter 5

6.5.1 Synthesis of $[Sn(OC_6H_4O)_3[NHEt_3]_2$

Catechol (2.00g, 18.0 mmol) and triethylamine (3.67g, 36.0 mmol) were dissolved in tetrahydrofuran (15 cm^3) and added with stirring to a solution of tin(IV) chloride (1.58g, 6.0 mmol) in tetrahydrofuran (25 cm^3). The reaction was exothermic, and the mixture was stirred until it had cooled to room temperature. The white solid isolated was washed with methanol (3 x 15 cm^3) and dried *in vacuo*. Crystallization from dichloromethane-diethyl ether afforded a white crystalline solid. Yield 2.94g (76%). (Found: C, 55.86; H, 6.89; N, 4.47; Sn,

17.00. $C_{30}H_{44}N_2O_6Sn$ requires C, 55.66; H, 6.80; N, 4.33; Sn, 18.35%); ^{119m}Sn: δ 0.041 mms^{-1}, Δ 0.701 mms^{-1}. N.m.r.: ^1H (CD_2Cl_2), δ 6.58-6.44 (m, 12H, arom.), 3.30 (q, $^3J_{HH}$ 7.3Hz, 12H, $\underline{CH_2}$-CH_3), 1.56 (s, 2H, NH) and 1.23 p.p.m (t, $^3J_{HH}$ 7.3Hz, 18H, CH_2-$\underline{CH_3}$); ^{13}C-{^1H} (CD_2Cl_2), δ 151.2, 117.3, 113.8 (arom.) and 46.0, 8.1 p.p.m (Et); ^{119}Sn-{^1H} (CD_2Cl_2), δ 353.5 p.p.m.

6.5.2 Synthesis of $[Sn(O\text{-}4\text{-}NO_2\text{-}C_6H_3O)_3][NHEt_3]_2$

4-Nitrocatechol (0.75g, 4.84 mmol) and triethylamine (0.98g, 9.61 mmol) were dissolved in tetrahydrofuran (10 cm^3) and added with stirring to a solution of tin(IV) chloride (0.42g, 1.61 mmol) in tetrahydrofuran (25 cm^3). After stirring at room temperature for two hours, the reaction mixture was filtered and the residue washed with tetrahydrofuran (2 x 10 cm^3). The solvent washings and supernatant liquid were combined and solvent removed *in vacuo*. Crystallization from methanol-diethyl ether afforded a yellow-orange highly crystalline solid. Recrystallization by slow diffusion of diethyether into a methanol solution gave crystals of $[(O\text{-}4\text{-}NO_2\text{-}C_6H_3O)_3Sn][NHEt_3]_2$ suitable for X-ray crystallography. Yield: 1.41g (89%). M.pt. 202°C (decomp.). (Found: C, 45.87; H, 5.23; N, 8.79; Sn, 14.77. $C_{30}H_{41}N_5O_{12}Sn$ requires C, 46.05; H, 5.24; N, 8.95; Sn, 15.18%); ν(C-NO_2) at 1573(s) and 1328(vs) cm^{-1}. ^{119m}Sn: δ 0.068 mms^{-1}, Δ 0.740 mms^{-1}. λ (thf) 396 and 323 nm. N.m.r.: ^1H (CD_3OD), δ 7.60-7.51 (m, 6H, arom.), 6.72-6.68 (m, 3H, arom.), 4.91 (s, 2H, NH), 3.18 (q, $^3J_{HH}$ 7.3Hz, 12H, $\underline{CH_2}$-CH_3), and 1.28 p.p.m (t, $^3J_{HH}$ 7.3Hz, 18H, CH_2-$\underline{CH_3}$); ^{13}C-{^1H} (CD_3OD), δ 116.8, 113.8, 109.5 (arom.) and 9.55 p.p.m (Et).

6.5.3 Synthesis of $[Sn(O\text{-}3\text{-}MeO\text{-}C_6H_3O)_3][NHEt_3]_2$

Procedure as for 6.5.2. Quantities used: 3-methoxycatechol 0.50g (3.57 mmol), triethylamine 0.72g (7.14 mmol) and tin(IV) chloride 0.31g (1.19 mmol). Recrystallization from methanol-diethylether afforded a white highly crystalline solid. Yield: 0.82g (94%). (Found: C, 53.17; H, 7.02; N, 3.66. $C_{33}H_{50}N_2O_9Sn$ requires C, 53.75; H, 6.78; N, 3.80%); N.m.r.: ^1H (CD_3OD), δ 6.38-6.25 (m, 9H, arom.), 4.89 (s, 2H, NH), 3.16 (q, $^3J_{HH}$ 7.2Hz, 12H,

$\underline{CH_2}$-CH_3), and 1.17 p.p.m (t, $^3J_{HH}$ 7.3Hz, 18H, CH_2-$\underline{CH_3}$); ^{13}C-{^1H} (CD_3OD), δ 116.7, 109.8, 103.7 (arom.) and 47.73, 9.55 p.p.m (Et).

6.5.4 Synthesis of $[Sn(OC_6H_4O)_2(OC_6H_3O\text{-}NO_2\text{-}4)][NHEt_3]_2$

Iodine (0.51g, 2.00 mmol) was dissolved in tetrahydrofuran (15 cm^3) and added with stirring to a suspension of $[OC_6H_4O]Sn$ (0.45g, 2.00 mmol) in tetrahydrofuran (15 cm^3). After stirring at room temperature for one hour, a solution containing catechol (0.22g, 2.00 mmol), 4-nitrocatechol (0.31g, 2.00 mmol) and triethylamine (0.81g, 8.00 mmol) in tetrahydrofuran (25 cm^3) was added dropwise with stirring. The reaction mixture was stirred at room temperature for a further two hours, solvent removed *in vacuo*, and the product extracted by cold tetrahydrofuran (4 x 10 cm^3). Concentration of the solution and addition of diethyl ether afforded a golden-yellow microcrystalline solid. Yield: 1.30g (93%). (Found: C, 51.41; H, 5.95; N, 6.02. $C_{30}H_{43}N_3O_8Sn$ requires C, 52.05; H, 6.22; N, 6.08%); ν(C-NO_2) at 1587(m) and 1328(vs) cm^{-1}. λ (thf) 415, 295 and 271(sh) nm. N.m.r.: ^1H (CD_3OD), δ 7.57-7.48 (m, 3H, NO_2-arom.), 6.67-6.41 (m, 8H, arom.), 4.93 (s, 2H, NH), 3.13 (q, $^3J_{HH}$ 6.6Hz, 12H, $\underline{CH_2}$-CH_3), and 1.21 p.p.m (t, $^3J_{HH}$ 6.6Hz, 18H, CH_2-$\underline{CH_3}$).

6.5.5 Synthesis of $[Sn(OC_6H_4O)_2(OC_6H_3O\text{-}OMe\text{-}3)][NHEt_3]_2$

Procedure as for 6.5.4. Quantities used: Iodine (0.40g, 1.56 mmol), $[OC_6H_4O]Sn$ (0.35g, 1.56 mmol), catechol (0.17g, 1.56 mmol), 3-methoxycatechol (0.22g, 1.56 mmol) and triethylamine (0.63g, 6.24 mmol). Extraction with acetone and crystallization from acetone-diethyl ether afforded a white microcrystalline solid. Yield: 0.64g (60%). (Found: C, 54.62; H, 6.88; N, 3.90. $C_{31}H_{46}N_2O_7Sn$ requires C, 54.97; H, 6.80; N, 4.14%). N.m.r.: ^1H (d_6-dmso), δ 6.36-6.23 (m, 8H, arom.), 6.21-6.09 (m, 3H, MeO-arom.), 3.65 (s, 3H, O-$\underline{CH_3}$), 3.14 (q, $^3J_{HH}$ 7.2Hz, 12H, $\underline{CH_2}$-CH_3), 2.10 (s, 2H, NH) and 1.16 p.p.m (t, $^3J_{HH}$ 7.2Hz, 18H, CH_2-$\underline{CH_3}$).

6.5.6 Synthesis of $[Sn(OC_6H_4O)_2(OC_6Cl_4O)][NHEt_3]_2$

Procedure as for 6.5.4. Quantities used: Iodine (0.55g, 2.14 mmol), $[OC_6H_4O]Sn$ (0.49g, 2.14 mmol), catechol (0.17g, 1.56 mmol), tetrachloro-*o*-benzoquinone (0.53g, 2.14 mmol) and triethylamine (0.87g, 8.56 mmol). Extraction with acetone and crystallization from acetone-diethyl ether afforded a dark red-brown microcrystalline solid. Yield: 1.42g (84%). (Found: C, 44.60; H, 5.19; Cl, 17.53; N, 4.42. $C_{30}H_{40}Cl_4N_2O_6Sn$ requires C, 45.88; H, 5.09; Cl, 18.10; N, 3.57%). λ (thf) 297 nm. N.m.r.: ^1H (d_6-acetone), δ 6.65-6.36 (m, 8H, arom.), 3.31 (q, $^3J_{HH}$ 7.0Hz, 12H, $\underline{CH_2}$-CH_3), 2.09 (s, 2H, NH) and 1.35 p.p.m (t, $^3J_{HH}$ 7.2Hz, 18H, CH_2-$\underline{CH_3}$).

6.5.7 Synthesis of $[Sn(O\text{-}4\text{-}NO_2\text{-}C_6H_3O)_2(OC_6H_4O)][NHEt_3]_2$

4-Nitrocatechol (0.19g, 1.20 mmol), catechol (0.13g, 1.20 mmol) and triethylamine (0.37g, 4.82 mmol) were dissolved in tetrahydrofuran (20 cm^3) and added with stirring to $I_2Sn[O\text{-}4\text{-}NO_2\text{-}C_6H_3O][OC_4H_8]_2$ (0.81g, 1.20 mmol) in tetrahydrofuran (25 cm^3). After stirring at room temperature for four hours solvent was removed *in vacuo*. Extraction with acetonitrile and crystallization from acetonitrile-diethyl ether afforded a yellow-orange microcrystalline solid. (Found: C, 48.18; H, 5.62; N, 7.68. $C_{30}H_{42}N_4O_{10}Sn$ requires C, 48.86; H, 5.70; N, 7.60%); ν(C-NO_2) at 1580(m), 1575(m) and 1325(vs) cm^{-1}. λ (thf) 399 nm. N.m.r.: ^1H (CD_3OD), δ 7.62-7.58 (m, 4H, NO_2-arom.), 7.57-7.50 (m, 2H, arom.), 6.72-6.63 (m, 2H, arom.), 6.50-6.41 (m, 2H, NO_2-arom.), 4.92 (s, 2H, NH), 3.25 (q, $^3J_{HH}$ 6.7Hz, 12H, $\underline{CH_2}$-CH_3) and 1.31 p.p.m (t, $^3J_{HH}$ 6.7Hz, 18H, CH_2-$\underline{CH_3}$).

6.5.8 Synthesis of $[Sn(O\text{-}4\text{-}NO_2\text{-}C_6H_3O)_2(OC_6H_3\text{-}3\text{-}OMe\text{-}O)][NHEt_3]_2$

Procedure as for 6.5.7. Quantities used: $SnI_2[O\text{-}4\text{-}NO_2\text{-}C_6H_3O][OC_4H_8]_2$ (0.89g, 1.33 mmol), 4-nitrocatechol (0.21g, 1.33 mmol), 3-methoxycatechol (0.19g, 1.33 mmol) and triethylamine (0.54g, 5.32 mmol). Extraction with tetrahydrofuran and crystallization from tetrahydrofuran-diethyl ether afforded an orange microcrystalline solid. (Found: C, 47.60; H, 5.90; N, 6.72. $C_{31}H_{44}N_4O_{11}Sn$ requires C, 48.52; H, 5.74; N, 7.30%); ν(C-NO_2) at 1587(m), 1570(s) and 1319(br, vs) cm^{-1}. λ (thf) 389 nm. N.m.r.: ^1H (CD_3OD), δ 7.60-7.42

(m, 4H, NO_2-arom.), 6.72-6.65 (m, 2H, MeO-arom.), 6.45-6.40 (m, 2H, NO_2-arom.), 6.33-6.27 (m, 1H, MeO-arom.), 4.90 (s, 2H, NH), 3.75 (s, 3H, O$\underline{CH_3}$), 3.17 (q, $^3J_{HH}$ 7.3Hz, 12H, $\underline{CH_2}$-CH_3) and 1.25 p.p.m (t, $^3J_{HH}$ 7.3Hz, 18H, CH_2-$\underline{CH_3}$).

6.5.9 Synthesis of $[Sn(O\text{-}4\text{-}NO_2\text{-}C_6H_3O)_2(OC_6Cl_4O)][NHEt_3]_2$

Procedure as for 6.5.7. Quantities used: $SnI_2[O\text{-}4\text{-}NO_2\text{-}C_6H_3O][OC_4H_8]_2$ (0.71g, 1.06 mmol), 4-nitrocatechol (0.16g, 1.06 mmol), tetrachloro-*o*-benzoquinone (0.26g, 1.06 mmol) and triethylamine (0.64g, 6.36 mmol). Extraction with tetrahydrofuran and crystallization from tetrahydrofuran-diethyl ether afforded a dark orange-brown solid. (Found: C, 41.06; H, 4.35; Cl, 15.87; N, 6.22. $C_{30}H_{38}Cl_4N_4O_{10}Sn$ requires C, 41.16; H, 4.34; Cl, 16.23; N, 6.40%); ν(C-NO_2) at 1572(m) and 1341(vs) cm^{-1}. λ (thf) 396 and 305 nm. N.m.r.: ^1H (d_6-acetone), δ 7.89 (dd, $^3J_{HH}$ 8.8Hz, $^4J_{HH}$ 2.8Hz, 2H, NO_2-arom.), 7.74 (d, $^4J_{HH}$ 2.8Hz, 2H, NO_2-arom.), 7.14 (d, $^3J_{HH}$ 8.8Hz, 2H, NO_2-arom.), 3.48 (q, $^3J_{HH}$ 7.3Hz, 12H, $\underline{CH_2}$-CH_3), 2.88 (s, 2H, NH) and 1.40 p.p.m (t, $^3J_{HH}$ 7.3Hz, 18H, CH_2-$\underline{CH_3}$).

6.5.10 Synthesis of $[Sn(O\text{-}3\text{-}MeO\text{-}C_6H_3O)_2(OC_6H_4O)][NHEt_3]_2$

Procedure as for 6.5.4. Quantities used: Iodine (0.68g, 2.68 mmol), $Sn[O\text{-}3\text{-}MeO\text{-}C_6H_3O]$ (0.69g, 2.68 mmol), catechol (0.30g, 2.68 mmol), 3-methoxycatechol (0.38g, 2.68 mmol) and triethylamine (1.09g, 10.72 mmol). After washing with acetone (4 x 10 cm^3), crystallization from methanol-diethyl ether afforded a white microcrystalline solid. Yield: 0.92g (49%). (Found: C, 54.19; H, 7.25; N, 3.62. $C_{32}H_{48}N_2O_8Sn$ requires C, 54.34; H, 6.79; N, 3.96%). N.m.r.: ^1H (d_6-dmso), δ 6.32-6.04 (m, 10H, arom.), 3.61 (s, 6H, O-$\underline{CH_3}$), 3.10 (q, $^3J_{HH}$ 7.2Hz, 12H, $\underline{CH_2}$-CH_3), 2.09 (s, 2H, NH) and 1.15 p.p.m (t, $^3J_{HH}$ 7.2Hz, 18H, CH_2-$\underline{CH_3}$).

6.5.11 Synthesis of $[Sn(O\text{-}3\text{-}MeO\text{-}C_6H_3O)_2(OC_6H_3\text{-}4\text{-}NO_2\text{-}O)][NHEt_3]_2$

Procedure as for 6.5.10. Quantities used: Iodine (0.38g, 1.48 mmol), $Sn[O\text{-}3\text{-}MeO\text{-}C_6H_3O]$ (0.38g, 1.48 mmol), 4-nitrocatechol (0.23g, 1.48 mmol), 3-methoxycatechol (0.20g, 1.48 mmol) and triethylamine (0.60g, 5.92 mmol). Extraction with tetrahydrofuran and

crystallization from tetrahydrofuran-diethyl ether afforded a bright yellow microcrystalline solid. (Found: C, 50.59; H, 6.44; N, 5.62. $C_{32}H_{47}N_3O_{10}Sn$ requires C, 51.08; H, 6.25; N, 5.58%); ν(C-NO_2) at 1585(m), 1568(m) and 1378(s) cm^{-1}. λ (thf) 417, 293 and 271(sh) nm. N.m.r.: ^1H (d_6-dmso), δ 7.46-6.09 (m, 9H, arom.), 3.62 (s, 6H, O-$\underline{CH_3}$), 3.11 (q, $^3J_{HH}$ 7.2Hz, 12H, $\underline{CH_2}$-CH_3), 2.09 (s, 2H, NH) and 1.14 p.p.m (t, $^3J_{HH}$ 7.2Hz, 18H, CH_2-$\underline{CH_3}$).

6.5.12 Synthesis of $[Sn(O\text{-}3\text{-}MeO\text{-}C_6H_3O)_2(OC_6Cl_4O)][NHEt_3]_2$

Procedure as for 6.5.10. Quantities used: Iodine (0.23g, 0.91 mmol), Sn[O-3-MeO-C_6H_3O] (0.23g, 0.91 mmol), tetrachloro-*o*-benzoquinone (0.22g, 0.91 mmol), 3-methoxycatechol (0.13g, 0.91 mmol) and triethylamine (0.37g, 3.64 mmol). Extraction with tetrahydrofuran and crystallization from tetrahydrofuran-diethyl ether afforded a brown-green solid. (Found: C, 44.61; H, 4.93; Cl, 16.26; N, 3.07. $C_{32}H_{44}Cl_4N_2O_8Sn$ requires C, 45.46; H, 5.21; Cl, 16.81; N, 3.31%); λ (thf) 287 nm. N.m.r.: ^1H (d_6-dmso), δ 6.74-6.67 (m, 2H, MeO-arom.), 6.35-5.92 (m, 4H, MeO-arom.) 3.63 (s, 6H, O-$\underline{CH_3}$), 3.11 (q, $^3J_{HH}$ 7.1Hz, 12H, $\underline{CH_2}$-CH_3), 2.09 (s, 2H, NH) and 1.15 p.p.m (t, $^3J_{HH}$ 7.1Hz, 18H, CH_2-$\underline{CH_3}$).

6.5.13 Synthesis of $[Sn(OC_6Cl_4O)_2(OC_6H_4O)][NHEt_3]_2$

Tin(II) chloride (0.39g, 2.03 mmol) was dissolved in tetrahydrofuran (30 cm^3) and added with stirring to tetrachloro-*o*-benzoquinone (0.50g, 2.03 mmol) in tetrahydrofuran (15 cm^3). After stirring at room temperature for twenty minutes, a solution containing tetrachloro-*o*-benzoquinone (0.50g, 2.03 mmol), catechol (0.22g, 2.03 mmol) and triethylamine (1.24g, 12.18 mmol) in tetrahydrofuran (20 cm^3) was added dropwise with stirring. The reaction mixture was stirred at room temperature for a further two hours, solvent removed *in vacuo*, and the product extracted with methanol (4 x 15 cm^3). Concentration of the solution and addition of hexane afforded a tan brown solid. Yield: 0.54g (30%). (Found: C, 39.36; H, 3.74; Cl, 30.74; N, 2.97. $C_{30}H_{36}Cl_8N_2O_6Sn$ requires C, 39.06; H, 3.77; Cl, 30.61; N, 3.02%). λ (thf) 313 and 302 nm. N.m.r.: ^1H (d_6-acetone), δ 6.63-6.42 (m, 4H, arom.), 4.15 (s, 2H, NH), 3.38 (q, $^3J_{HH}$ 7.0Hz, 12H, $\underline{CH_2}$-CH_3), and 1.31 p.p.m (t, $^3J_{HH}$ 7.0Hz,

18H, CH_2-$\underline{CH}_3$); ^{13}C-{^1H} (d_6-acetone), δ 151.3, 150.4, 124.7 (Cl_4-arom.), 118.0, 116.9, 114.5 (arom.), 47.4 and 9.2 p.p.m. (Et).

6.5.14 Synthesis of $[Sn(OC_6Cl_4O)_2(OC_6H_3\text{-}4\text{-}NO_2\text{-}O)][NHEt_3]_2$

Procedure as for 6.5.13. Quantities used: Tin(II) chloride (0.39g, 2.03 mmol), tetrachloro-*o*-benzoquinone (2 x 0.50g, 4.06 mmol), 4-nitrocatechol (0.32, 2.03 mmol) and triethylamine (1.24g, 12.18 mmol) Extraction with methanol and crystallization from methanol-diethyl ether afforded a red-brown solid. (Found: C, 37.88; H, 3.26; Cl, 28.87; N, 4.48. $C_{30}H_{35}Cl_8N_3O_8Sn$ requires C, 37.20; H, 3.62; Cl, 29.34; N, 4.34%); ν(C-NO_2) at 1524(s) and 1379(s) cm^{-1}. λ (thf) 396 and 306 nm. N.m.r.: ^1H (d_6-acetone), δ 7.89 (dd, $^3J_{HH}$ 8.8Hz, $^4J_{HH}$ 2.7Hz, 2H, NO_2-arom.), 7.74 (d, $^4J_{HH}$ 2.7Hz, 2H, NO_2-arom.), 7.14 (d, $^3J_{HH}$ 8.8Hz, 2H, NO_2-arom.), 3.52 (q, $^3J_{HH}$ 7.1Hz, 12H, $\underline{CH}_2$-CH_3), 2.91 (s, 2H, NH) and 1.38 p.p.m (t, $^3J_{HH}$ 7.1Hz, 18H, CH_2-$\underline{CH}_3$); ^{13}C-{^1H} (d_6-acetone), δ 151.3, 147.9, 144.2 (Cl_4-arom.), 120.9, 118.1, 117.5, 112.6 (NO_2-arom.), 48.0 and 9.3 p.p.m. (Et).

6.5.15 Synthesis of $[Sn(OC_6Cl_4O)_2(OC_6H_3\text{-}3\text{-}OMe\text{-}O)][NHEt_3]_2$

Procedure as for 6.5.13. Quantities used: Tin(II) chloride (0.39g, 2.03 mmol), tetrachloro-*o*-benzoquinone (2 x 0.50g, 4.06 mmol), 3-methoxycatechol (0.29, 2.03 mmol) and triethylamine (1.24g, 12.18 mmol) Extraction with methanol and crystallization from methanol-diethyl ether afforded a tan brown solid. Yield: 1.40g (72%); (Found: C, 40.20; H, 4.08; Cl, 29.42; N, 3.43. $C_{31}H_{38}Cl_8N_2O_7Sn$ requires C, 39.05; H, 3.99; Cl, 29.81; N, 2.94%). λ (thf) 313 and 302 nm. N.m.r.: ^1H (d_6-acetone), δ 6.47-6.24 (m, 3H, MeO-arom.), 3.31 (s, 3H, O-$\underline{CH}_3$), 3.22 (q, $^3J_{HH}$ 7.3Hz, 12H, $\underline{CH}_2$-CH_3), 2.05 (s, 2H, NH) and 1.23 p.p.m (t, $^3J_{HH}$ 7.3Hz, 18H, CH_2-$\underline{CH}_3$); ^{13}C-{^1H} (d_6-acetone), δ 151.6, 148,2, 139.3 (Cl_4-arom.), 150.2, 118.0, 116.9, 109.1, 102.4 (MeO-arom.), 55.8 (OMe), 47.1 and 9.5 p.p.m. (Et).

6.6 References

1. (a) J. R. Carruthers, *CRYSTALS User Manual*, Oxford University Computing Centre 1975;

   (b) K. Davies, *CHEMGRAF User Manual*, Chemical Crystallography Laboratory, Oxford 1981;

   (c) *International Tables for X-Ray Crystallography*, **4**, 99, Kynoch Press, 1974.
2. H. M. Haendler and J. S. Morrison, *J. Inorg. Nucl. Chem.*, 1967, **29**, 393.
3. M. P. Brown, *J. Chem. Soc., Dalton Trans.*, 1977, 951.
4 J. L. Spencer, *Inorg. Synth.*, 1976, **19**, 213.
5. F. Cariati, G. La Monica and R. Ugo, *Inorg. Synth.*, 1968, **11**, 105.
6. K. Aoki, Y. Yamamoto and H. Yamazaki., *Inorg. Chem.*, 1979, **18**, 1681.
7. F. Caviati, L. Malatesta, L. Naldini and G. Simonetta., *Coord. Chem. Rev.*, 1966, **1**,255.
8. R. Adams, A. Ferretti and W. Reifschneider, *Org. Synth.*, **42**, 22.
9. P. Foley and M. Zeldin, *Inorg. Chem.*, 1975, **14**, 2264.
10. A. J. Bearden, H. S. Marsh and J. J. Zuckerman, *Inorg. Chem.*, 1966, **5**, 1260.

Appendices

Appendix 1

Atomic Parameters for $\{Sn[O\text{-}4\text{-}NO_2\text{-}C_6H_3O][OC_4H_8]\}_n$

Appendix 1.1 Final Anisotropic Thermal Parameters ($Å^2$) for $\{Sn[O\text{-}4\text{-}NO_2\text{-}C_6H_3O][OC_4H_8]\}_n$

Atom	U(11)	U(22)	U(33)	U(23)	U(13)	U(12)
Sn(1)	0.0321(2)	0.0288(2)	0.0372(2)	0.0108(2)	0.0057(2)	0.0057(2)
C(1)	0.0328(36)	0.0284(32)	0.0280(33)	0.0096(26)	0.0016(26)	0.0027(27)
C(2)	0.0336(35)	0.0225(29)	0.0347(35)	0.0095(25)	0.0059(29)	0.0032(27)
C(3)	0.0276(35)	0.0372(35)	0.0363(36)	0.0137(29)	0.0028(30)	0.0083(27)
C(4)	0.0357(37)	0.0286(32)	0.0362(37)	0.0127(28)	0.0000(31)	0.0030(29)
C(5)	0.0320(36)	0.0302(33)	0.0340(35)	0.0120(27)	-0.0014(29)	-0.0012(28)
C(6)	0.0282(34)	0.0425(37)	0.0248(32)	0.0148(27)	0.0016(27)	0.0024(29)
C(7)	0.0515(55)	0.1090(84)	0.0547(57)	0.0133(55)	0.0044(47)	0.0303(57)
C(8)	0.0708(80)	0.1908(157)	0.0558(68)	-0.0051(80)	-0.0044(61)	0.0224(92)
C(9)	0.1179(127)	0.2292(200)	0.0757(89)	-0.0653(105)	-0.0105(86)	0.0720(133)
C(10)	0.0707(75)	0.1845(139)	0.0523(61)	0.0155(73)	-0.0027(56)	0.0636(86)
O(1)	0.0321(25)	0.0417(26)	0.0378(25)	0.0184(21)	0.0100(21)	0.0086(21)
O(2)	0.0354(26)	0.0282(23)	0.0451(27)	0.0152(20)	0.0166(22)	0.0048(20)
O(3)	0.0822(48)	0.0633(38)	0.0977(50)	0.0550(37)	0.0407(41)	0.0209(36)
O(4)	0.0538(40)	0.0958(51)	0.1241(61)	0.0754(48)	0.0475(41)	0.0253(37)
O(5)	0.0477(34)	0.0773(40)	0.0385(30)	0.0026(28)	-0.0023(26)	0.0126(31)
N(1)	0.0453(40)	0.0531(39)	0.0597(42)	0.0363(33)	0.0167(33)	0.0090(33)

Appendix 1.2 Final Fractional Coordinates and Isotropic Temperature Factors (Å x 10^4) for $\{Sn[O\text{-}4\text{-}NO_2C_6H_3O][OC_4H_8]\}_n$

Atom	x/a	y/b	z/c	U(iso) or U(equiv)
Sn(1)	0.2188(9)	0.3813(5)	0.4188(5)	326
C(1)	0.4275(11)	0.6642(7)	0.3726(6)	301
C(2)	0.2313(11)	0.6991(7)	0.4172(6)	299
C(3)	0.1596(11)	0.8317(8)	0.4116(7)	329
C(4)	-0.2765(12)	0.9306(7)	0.3602(6)	333
C(5)	0.4667(11)	0.8942(7)	0.3174(6)	322
C(6)	0.5475(11)	0.7616(8)	0.3206(6)	303
C(7)	-0.1700(16)	0.3944(13)	0.1593(9)	666
C(8)	-0.2519(21)	0.2818(19)	0.0269(11)	950
C(9)	-0.0744(25)	0.2183(22)	-0.0090(13)	1134
C(10)	0.1191(19)	0.2801(17)	0.0911(10)	810
O(1)	0.4950(8)	0.5359(5)	0.3847(4)	350
O(2)	0.1167(8)	0.5955(5)	0.4604(4)	331
O(3)	0.5201(12)	1.1125(7)	0.2565(7)	625
O(4)	0.7689(11)	0.9715(8)	0.2332(8)	639
O(5)	0.0582(10)	0.3819(7)	0.1948(5)	544
N(1)	0.5933(11)	1.0003(8)	0.2656(7)	447
H(31)	0.0296(11)	0.8658(8)	0.4492(7)	519(229)
H(41)	0.2344(12)	0.9602(7)	0.3519(6)	876(315)
H(61)	0.6930(11)	0.7243(8)	0.2751(6)	468(212)

Appendix 1.3 Short Intermolecular Contacts (Less Than 3.6Å)

Sn(1)-C(1)	3.10	(i)	Sn(1)-O(1)	2.43	(i)
Sn(1)-O(2)	2.61	(ii)	Sn(1)-O(3)	3.54	(iii)
C(2)-O(3)	3.51	(iv)	C(3)-C(5)	3.54	(iv)
C(3)-N(1)	3.45	(iv)	C(3)-O(4)	3.52	(v)
C(4)-C(4)	3.59	(iv)	C(4)-C(5)	3.47	(iv)
C(4)-O(4)	3.34	(v)	C(7)-O(1)	3.53	(v)
C(7)-O(3)	3.53	(vi)	C(9)-O(4)	3.53	(vii)
O(1)-O(1)	2.82	(i)	O(1)-O(2)	3.32	(i)
O(2)-O(2)	2.56	(ii)			

(i)	1-x, 1-y, 1-z
(ii)	-x, 1-y, 1-z
(iii)	x, y-1, z
(iv)	1-x, 2-y, 1-z
(v)	x-1, y, z
(vi)	x-1, y-1, z
(vii)	1-x, !-y, -z

Appendix 2

Atomic Parameters for $\{[Et_3BzN][ClSn(O\text{-}4\text{-}NO_2\text{-}C_6H_3O)]\}_n$

Appendix 2.1 Final Anisotropic Thermal Parameters ($Å^2$) for $\{[Et_3BzN][ClSn(O\text{-}4\text{-}NO_2\text{-}C_6H_3O)]\}_n$

Atom	U(11)	U(22)	U(33)	U(23)	U(13)	U(12)
Sn(1)	0.0320(2)	0.0316(2)	0.0332(2)	-0.0005(2)	0.0134(1)	-0.0009(2)
Cl(1)	0.0512(8)	0.0474(9)	0.0365(7)	-0.0070(7)	0.0086(6)	-0.0035(8)
O(1)	0.0372(20)	0.0237(18)	0.0344(20)	0.0001(16)	0.0166(17)	0.0028(16)
O(2)	0.0317(19)	0.0312(19)	0.0296(20)	0.0029(16)	0.0087(16)	0.0062(16)
O(3)	0.0913(42)	0.0797(39)	0.0935(42)	0.0330(35)	0.0567(36)	0.0493(34)
O(4)	0.0657(34)	0.1060(46)	0.1071(44)	0.0165(38)	0.0639(35)	0.0170(33)
C(1)	0.0300(27)	0.0255(26)	0.0218(25)	-0.0049(21)	0.0081(21)	-0.0044(22)
C(2)	0.0296(27)	0.0348(32)	0.0262(28)	-0.0005(23)	0.0034(23)	-0.0003(24)
C(3)	0.0299(28)	0.0398(33)	0.0309(29)	-0.0075(27)	0.0087(23)	-0.0012(26)
C(4)	0.0351(28)	0.0566(36)	0.0317(27)	-0.0007(33)	0.0152(23)	-0.0109(33)
C(5)	0.0364(31)	0.0463(35)	0.0302(30)	0.0054(27)	0.0096(25)	-0.0021(27)
C(6)	0.0295(26)	0.0335(35)	0.0257(26)	-0.0010(23)	0.0086(21)	-0.0012(23)
C(7)	0.0487(34)	0.0445(35)	0.0182(27)	0.0029(26)	0.0060(25)	0.0074(29)
C(8)	0.0513(37)	0.0713(48)	0.0634(43)	0.0173(42)	0.0270(34)	0.0040(40)
C(9)	0.0347(31)	0.0422(34)	0.0401(35)	0.0072(28)	0.0055(26)	-0.0011(27)
C(10)	0.0596(45)	0.0601(46)	0.0785(51)	0.0291(42)	0.0338(41)	0.0122(38)
C(11)	0.0302(28)	0.0541(37)	0.0381(31)	0.0087(33)	0.0017(23)	-0.0004(31)
C(12)	0.0408(36)	0.0587(43)	0.0533(41)	0.0078(35)	0.0061(31)	0.0188(33)
C(13)	0.0399(31)	0.0445(38)	0.0299(29)	-0.0096(27)	0.0026(24)	-0.0032(27)
C(14)	0.0433(33)	0.0355(32)	0.0241(27)	-0.0068(25)	0.0062(24)	0.0032(26)
C(15)	0.0490(36)	0.0352(34)	0.0402(34)	-0.0008(26)	0.0178(28)	-0.0058(27)
C(16)	0.0594(39)	0.0385(38)	0.0379(33)	0.0046(27)	0.0131(30)	0.0037(30)
C(17)	0.0496(35)	0.0448(35)	0.0562(38)	0.0013(37)	0.0151(30)	0.0113(37)
C(18)	0.0609(44)	0.0574(44)	0.0654(46)	-0.0031(38)	0.0352(39)	0.0037(37)
C(19)	0.0541(39)	0.0489(39)	0.0436(36)	0.0097(31)	0.0220(31)	0.0059(32)
N(1)	0.0279(23)	0.0377(25)	0.0242(22)	0.0000(9)	-0.0006(18)	-0.0006(19)
N(2)	0.0362(29)	0.0647(37)	0.0534(34)	-0.0056(30)	0.0169(27)	0.0026(27)

Appendix 2.2 Final Fractional Coordinates and Isotropic Temperature Factors (Å x 10^4) for $\{[Et_3BzN][ClSn(O\text{-}4\text{-}NO_2\text{-}C_6H_3O)]\}_n$

Atom	x/a	y/b	z/c	U(iso) or U(equiv)
Sn(1)	0.2325(2)	0.1546(5)	0.2708(2)	320
Cl(1)	0.3433(9)	0.3281(2)	0.3931(9)	459
O(1)	0.3307(2)	-0.0225(4)	0.2732(2)	303
O(2)	0.2783(2)	0.2684(5)	0.1822(2)	312
O(3)	0.5728(4)	-0.2165(7)	0.2045(4)	692
O(4)	0.5773(3)	-0.0405(8)	0.1077(4)	707
C(1)	0.3726(3)	0.0309(6)	0.2251(3)	256
C(2)	0.4395(3)	-0.0580(7)	0.2201(3)	315
C(3)	0.4765(3)	0.0060(8)	0.1650(3)	336
C(4)	0.4496(3)	0.1575(9)	0.1168(3)	379
C(5)	0.3836(3)	0.2465(8)	0.1231(4)	376
C(6)	0.3436(3)	0.1874(7)	0.1761(3)	300
C(7)	0.3551(4)	-0.2509(8)	0.5083(3)	351
C(8)	0.4240(4)	-0.1404(10)	0.5013(4)	582
C(9)	0.2909(4)	-0.4185(8)	0.5898(4)	403
C(10)	0.2875(4)	-0.4849(10)	0.6724(5)	589
C(11)	0.4466(3)	-0.3563(9)	0.6579(4)	412
C(12)	0.4691(4)	-0.5253(9)	0.6273(4)	499
C(13)	0.3453(4)	-0.1188(8)	0.6409(4)	386
C(14)	0.2642(4)	-0.0236(8)	0.5943(3)	339
C(15)	0.2584(4)	0.1055(7)	0.5341(4)	406
C(16)	0.1827(4)	0.1938(8)	0.4927(4)	453
C(17)	0.1161(4)	0.1609(9)	0.5138(4)	502
C(18)	0.1197(4)	0.0303(9)	0.5725(5)	567
C(19)	0.1947(4)	-0.0594(9)	0.6135(4)	468
N(1)	0.3593(3)	-0.2841(6)	0.5994(3)	310
N(2)	0.5467(3)	-0.0889(8)	0.1589(4)	497
H(21)	0.4581(3)	-0.1660(7)	0.2634(3)	500
H(41)	0.4760(3)	0.1595(9)	0.0745(3)	500
H(51)	0.3687(3)	0.3512(8)	0.0856(4)	500
H(71)	0.3009(4)	-0.1998(8)	0.4786(3)	500
H(72)	0.3491(4)	-0.3744(8)	0.4787(3)	500
H(81)	0.4788(4)	-0.1660(10)	0.5228(4)	500
H(82)	0.4407(4)	-0.0272(10)	0.5454(4)	500
H(83)	0.3774(4)	-0.1176(10)	0.4133(4)	500
H(91)	0.2467(4)	-0.3514(8)	0.5527(4)	500
H(92)	0.3080(4)	-0.5435(8)	0.5609(4)	500
H(101)	0.2694(4)	-0.4069(10)	0.7156(5)	500
H(102)	0.2440(4)	-0.5879(10)	0.6624(5)	500
H(103)	0.3443(4)	-0.5375(10)	0.7128(5)	500
H(111)	0.4818(3)	-0.2781(9)	0.6435(4)	500
H(112)	0.4359(3)	-0.3485(9)	0.7100(4)	500
H(121)	0.5242(4)	-0.5495(9)	0.6621(4)	500
H(122)	0.4315(4)	-0.6245(9)	0.6312(4)	500
H(123)	0.4625(4)	-0.5224(9)	0.5708(4)	500
H(131)	0.3492(4)	-0.1493(8)	0.7052(4)	500
H(132)	0.4001(4)	-0.0418(8)	0.6514(4)	500
H(151)	0.2898(4)	0.1275(7)	0.4997(4)	500
H(161)	0.1801(4)	0.2765(8)	0.4515(4)	500
H(171)	0.0593(4)	0.2341(9)	0.4886(4)	500
H(181)	0.0761(4)	0.0620(9)	0.5989(5)	500
H(191)	0.1958(4)	-0.1522(9)	0.6645(4)	

Appendix 2.3 Short Intermolecular Contacts (Less Than 3.6Å)

Anion-anion

Sn(1)-Cl(1)	3.57	(i)	Sn(1)-O(1)	2.70	(ii)
Sn(1)-O(2)	3.10	(i)	Sn(1)-C(1)	3.43	(ii)
Cl(1)-O(1)	3.41	(ii)	O(1)-O(2))	2.79	(i)

Anion-cation

O(2)-C(7)	3.13	(ii)	O(3)-C(10)	3.39	(iii)
O(3)-C(13)	3.54	(iv)	O(3)-C(18)	3.57	(v)
O(3)-C(19)	3.49	(v)	O(4)-C(10)	3.37	(v)
O(4)-C(17)	3.50	(vi)	C13-N(2)	3.53	(iv)

Cation-cation

C(8)-C(8)	3.41	(iv)	C(9)-C(16)	3.56	(vii)
C(10)-C(19)	3.52	(i)			

(i)	1/2-x, y-1/2, 1/2-z
(ii)	1/2-x, y+1/2, 1/2-z
(iii)	1-x, -1-y, 1-z
(iv)	1-x, -y, 1-z
(v)	1/2+x, -1/2-y, z-1/2
(vi)	1/2+x, 1/2-y, z-1/2
(vii)	x, y-1, z

Appendix 3

Atomic Parameters for $Au_4(PPh_3)_4(\mu_2\text{-}SnCl_3)_2$

Appendix 3.1 Final Anisotropic Thermal Parameters ($Å^2$) for $Au_4(PPh_3)_4(\mu_2\text{-}SnCl_3)_2$

Atom	U(11)	U(22)	U(33)	U(23)	U(13)	U(12)
Au(2)	0.0403(2)	0.0397(2)	0.0393(2)	-0.0013(1)	-0.0052(1)	-0.0069(1)
Au(3)	0.0407(2)	0.0390(2)	0.0450(2)	-0.0018(1)	0.0131(1)	0.0083(1)
Sn(1)	0.0323(3)	0.0727(5)	0.0798(5)	0.0240(4)	0.0004(3)	-0.0029(3)
Cl(1)	0.1060(2)	0.0700(2)	0.1090(3)	-0.0090(2)	0.0090(2)	-0.0060(2)
Cl(2)	0.1190(3)	0.0580(2)	0.1040(3)	0.0030(2)	0.0100(2)	0.0140(2)
Cl(3)	0.0830(2)	0.1380(3)	0.1020(3)	0.0430(2)	0.0320(2)	-0.0100(2)
P(2)	0.0540(1)	0.0410(1)	0.0430(1)	0.0010(1)	-0.0030(1)	-0.0070(1)
P(3)	0.0510(1)	0.0440(1)	0.0460(1)	-0.0040(1)	0.0130(1)	0.0090(1)
C(211)	0.0620(6)	0.0460(5)	0.0540(6)	0.0040(4)	-0.0030(5)	-0.0120(4)
C(212)	0.0960(9)	0.0700(7)	0.0630(7)	-0.0060(6)	-0.0120(6)	-0.0340(7)
C(213)	0.1300(1)	0.0900(1)	0.1000(1)	-0.0160(8)	-0.0020(9)	-0.0570(9)
C(214)	0.1300(1)	0.1000(1)	0.1600(2)	-0.0200(1)	0.0100(1)	-0.0900(1)
C(215)	0.1100(1)	0.1100(1)	0.1200(1)	0.0200(1)	0.0300(1)	-0.0400(1)
C(216)	0.1000(1)	0.0680(8)	0.0910(9)	0.0010(7)	-0.0020(8)	-0.0260(7)
C(221)	0.0730(7)	0.0560(6)	0.0470(6)	-0.0100(5)	0.0020(5)	-0.0200(5)
C(222)	0.1050(9)	0.0670(7)	0.0440(6)	0.0030(5)	-0.0170(6)	0.0140(6)
C(223)	0.1600(2)	0.0900(1)	0.0800(1)	-0.0000(8)	-0.0300(1)	0.0200(1)
C(224)	0.2000(2)	0.0800(1)	0.0600(1)	0.0080(8)	-0.0300(1)	-0.0400(1)
C(225)	0.1900(2)	0.1200(1)	0.0580(9)	-0.0140(9)	0.0300(1)	-0.0800(1)
C(226)	0.0990(9)	0.0800(8)	0.0650(7)	0.0080(6)	-0.0030(7)	-0.0210(7)
C(231)	0.0650(6)	0.0500(5)	0.0400(5)	-0.0060(4)	0.0000(4)	0.0090(4)
C(232)	0.1000(1)	0.0510(6)	0.0790(8)	-0.0050(6)	-0.0040(7)	0.0140(6)
C(233)	0.1000(1)	0.0690(8)	0.1000(1)	0.0030(7)	0.0010(8)	0.0250(8)
C(234)	0.0820(9)	0.1000(1)	0.0900(1)	-0.0080(8)	0.0070(7)	0.0440(8)
C(235)	0.0570(7)	0.1000(1)	0.0900(1)	-0.0170(8)	0.0040(6)	0.0020(7)
C(236)	0.0520(6)	0.0710(7)	0.0810(8)	-0.0190(6)	0.0060(5)	-0.0020(5)
C(311)	0.0600(6)	0.0670(6)	0.0520(6)	0.0120(5)	0.0210(5)	0.0210(5)
C(312)	0.1020(9)	0.0800(8)	0.0470(6)	0.0040(5)	0.0240(6)	0.0150(7)
C(313)	0.1400(1)	0.1000(1)	0.0650(8)	0.0170(7)	0.0340(9)	0.0200(1)
C(314)	0.1200(1)	0.2400(2)	0.1200(2)	0.0700(2)	0.0800(1)	0.0200(2)
C(315)	0.1000(1)	0.3500(4)	0.1000(1)	0.0500(2)	0.0400(1)	-0.0800(2)
C(316)	0.0900(1)	0.1800(2)	0.1000(1)	0.0200(1)	0.0100(8)	-0.0400(1)
C(321)	0.0660(6)	0.0380(5)	0.0550(6)	0.0060(4)	0.0110(5)	0.0120(4)
C(322)	0.1030(9)	0.0660(7)	0.0460(6)	0.0080(5)	0.0170(6)	0.0190(6)
C(323)	0.1200(1)	0.0720(8)	0.0770(8)	0.0210(7)	0.0250(8)	0.0470(8)
C(324)	0.1400(1)	0.0760(9)	0.0840(9)	0.0250(7)	0.0280(9)	0.0440(8)
C(325)	0.1300(1)	0.0780(9)	0.0900(1)	-0.0100(7)	0.0170(8)	0.0510(8)
C(326)	0.1070(9)	0.0680(7)	0.0520(6)	0.0010(5)	0.0150(6)	0.0370(6)
C(331)	0.0510(5)	0.0420(5)	0.0450(5)	-0.0080(4)	0.0090(4)	-0.0030(4)
C(332)	0.0570(6)	0.0660(6)	0.0660(7)	0.0030(5)	0.0000(5)	-0.0030(5)
C(333)	0.0600(7)	0.0790(8)	0.0860(8)	0.0080(6)	-0.0030(6)	0.0120(6)
C(334)	0.0610(7)	0.0960(9)	0.0670(7)	-0.0130(6)	0.0050(6)	-0.0090(7)
C(335)	0.0760(8)	0.0620(7)	0.0969(9)	-0.0130(6)	0.0160(7)	-0.0270(6)
C(336)	0.0690(7)	0.0580(6)	0.0600(7)	-0.0050(5)	0.0130(5)	0.0010(5)

Appendix 3.2 Final Fractional Coordinates and Isotropic Temperature Factors (Å x 10^4) for $Au_4(PPh_3)_4(\mu_2\text{-}SnCl_3)_2$

Atom	x/a	y/b	z/c	U(iso) or U(equiv)
Au(2)	0.4465(2)	0.1934(2)	0.1985(2)	393
Au(3)	0.4479(2)	0.2887(2)	0.2896(2)	396
Sn(1)	0.3171(3)	0.2550(4)	0.2279(4)	555
Cl(1)	0.2558(2)	0.1922(2)	0.1391(2)	928
Cl(2)	0.2621(2)	0.3591(2)	0.2019(2)	893
Cl(3)	0.2491(2)	0.2222(2)	0.3122(2)	951
P(2)	0.4508(1)	0.1096(1)	0.1193(1)	457
P(3)	0.4590(1)	0.3713(1)	0.3719(1)	452
C(211)	0.3885(1)	0.0433(1)	0.1147(1)	528
C(212)	0.3696(6)	0.0060(6)	0.0568(6)	699
C(213)	0.3220(8)	-0.0436(7)	0.0569(8)	900
C(214)	0.2922(9)	-0.0578(8)	0.1100(1)	983
C(215)	0.3087(8)	-0.0221(8)	0.1674(9)	1032
C(216)	0.3570(7)	0.0297(6)	0.1709(7)	832
C(221)	0.4407(1)	0.1469(1)	0.0358(1)	553
C(222)	0.3777(7)	0.1684(5)	0.0108(5)	654
C(223)	0.3670(1)	0.2009(8)	-0.0505(8)	1015
C(224)	0.4210(1)	0.2116(8)	-0.0849(8)	995
C(225)	0.4850(1)	0.1894(9)	-0.0626(7)	959
C(226)	0.4950(7)	0.1546(6)	0.0011(6)	787
C(231)	0.5325(1)	0.0670(1)	0.1298(1)	504
C(232)	0.5377(7)	-0.0031(6)	0.1242(6)	742
C(233)	0.6012(8)	-0.0323(7)	0.1308(7)	864
C(234)	0.6584(7)	0.0051(7)	0.1395(7)	823
C(235)	0.6547(6)	0.0749(7)	0.1449(7)	819
C(236)	0.5919(5)	0.1054(6)	0.1403(6)	654
C(311)	0.4238(1)	0.3502(1)	0.4485(1)	545
C(312)	0.4557(7)	0.3665(6)	0.5113(5)	694
C(313)	0.4279(9)	0.3504(7)	0.5686(7)	921
C(314)	0.3660(1)	0.3150(1)	0.5600(1)	1140
C(315)	0.3350(1)	0.3000(1)	0.4990(1)	1230
C(316)	0.3663(7)	0.3137(9)	0.4437(8)	1092
C(321)	0.4175(1)	0.4499(1)	0.3449(1)	504
C(322)	0.4071(6)	0.4637(6)	0.2775(5)	654
C(323)	0.3758(7)	0.5233(6)	0.2544(7)	781
C(324)	0.3578(8)	0.5694(7)	0.2999(7)	862
C(325)	0.3703(8)	0.5571(7)	0.3673(7)	858
C(326)	0.4002(6)	0.4967(6)	0.3903(5)	665
C(331)	0.5480(1)	0.3913(1)	0.4015(1)	447
C(332)	0.5906(5)	0.3394(6)	0.4294(5)	629
C(333)	0.6559(6)	0.3522(6)	0.4512(6)	733
C(334)	0.6801(6)	0.4169(7)	0.4544(6)	724
C(335)	0.6381(6)	0.4680(6)	0.4316(6)	716
C(336)	0.5712(6)	0.4559(5)	0.4050(5)	615
C(996)	0.0000(1)	0.2130(1)	0.2500(1)	127
C(997)	0.0580(2)	0.2630(2)	0.2690(2)	127
C(998)	0.0580(2)	0.3200(2)	0.2670(2)	127
C(999)	0.0000(1)	0.3530(3)	0.2500(1)	127
H(212)	0.3891(6)	0.0176(6)	0.0165(6)	123
H(213)	0.3121(8)	-0.0706(7)	0.0167(8)	123
H(214)	0.2575(9)	-0.0925(8)	0.1070(1)	123
H(215)	0.2867(8)	-0.0337(8)	0.2063(9)	123
H(216)	0.3691(7)	0.0555(6)	0.2115(7)	123
H(222)	0.3402(7)	0.1604(5)	0.0364(5)	123
H(223)	0.3220(1)	0.2167(8)	-0.0689(8)	123
H(224)	0.4140(1)	0.2367(8)	-0.1265(8)	123
H(225)	0.5220(1)	0.1966(9)	-0.0895(7)	123
H(226)	0.5392(7)	0.1366(6)	0.0184(6)	123

H(232)	0.4972(7)	-0.0305(6)	0.1150(6)	123
H(233)	0.6055(8)	-0.0809(7)	0.1285(7)	123
H(234)	0.7027(7)	-0.0161(7)	0.1433(7)	123
H(235)	0.6955(6)	0.1021(7)	0.1516(7)	123
H(236)	0.5882(5)	0.1539(6)	0.1439(6)	123
H(312)	0.4991(7)	0.3896(6)	0.5146(5)	123
H(313)	0.4490(9)	0.3620(7)	0.6132(7)	123
H(314)	0.3440(1)	0.3060(1)	0.5990(1)	123
H(315)	0.2920(1)	0.2760(1)	0.4970(1)	123
H(316)	0.3474(7)	0.2966(9)	0.4001(8)	123
H(322)	0.4205(6)	0.4310(6)	0.2459(5)	123
H(323)	0.3674(7)	0.5326(6)	0.2068(7)	123
H(324)	0.3364(8)	0.6111(7)	0.2835(7)	123
H(325)	0.3582(8)	0.5907(7)	0.3987(7)	123
H(326)	0.4087(6)	0.4873(6)	0.4379(5)	123
H(332)	0.5742(5)	0.2934(6)	0.4219(5)	123
H(333)	0.6861(6)	0.3158(6)	0.4676(6)	123
H(334)	0.7266(6)	0.4260(7)	0.4731(6)	123
H(335)	0.6550(6)	0.5138(6)	0.4355(6)	123
H(336)	0.5417(6)	0.4926(5)	0.3878(5)	123

Appendix 4

Atomic Parameters for $[Et_4N][(dppe)Pt(SnCl_3)_3]$

Appendix 4.1 Final Anisotropic Thermal Parameters ($Å^2$) for $[Et_4N][(dppe)Pt(SnCl_3)_3]$

Atom	U(11)	U(22)	U(33)	U(23)	U(13)	U(12)
Pt(1)	0.0347(8)	0.0389(7)	0.0347(8)	0.0006(8)	0.0002(8)	-0.0012(7)
Sn(1)	0.0603(18)	0.0457(14)	0.0511(18)	-0.0080(13)	0.0028(14)	0.0006(13)
Sn(2)	0.0421(15)	0.0494(15)	0.0485(16)	0.0038(13)	0.0044(14)	-0.0070(13)
Sn(3)	0.0526(17)	0.0518(16)	0.0528(18)	0.0105(14)	-0.0034(15)	0.0018(13)
P(1)	0.0439(61)	0.0341(50)	0.0372(59)	-0.0040(49)	-0.0059(52)	0.0003(43)
P(2)	0.0418(59)	0.0364(52)	0.0374(60)	-0.0018(50)	-0.0053(51)	-0.0073(43)
Cl(1)	0.1575(112)	0.0500(61)	0.1233(94)	-0.0269(64)	0.0390(86)	-0.0335(72)
Cl(2)	0.0820(80)	0.1018(80)	0.1632(122)	-0.0226(84)	-0.0102(79)	0.0287(67)
Cl(3)	0.1713(11)	0.1052(85)	0.0629(75)	-0.0426(67)	-0.0081(79)	0.0209(84)
Cl(4)	0.0828(79)	0.0862(67)	0.0638(71)	-0.0049(58)	0.0169(61)	-0.0058(54)
Cl(5)	0.0754(68)	0.0523(57)	0.0957(81)	0.0143(57)	0.0028(60)	-0.0062(52)
Cl(6)	0.0657(75)	0.1282(83)	0.0645(76)	0.0137(66)	-0.0260(58)	-0.0117(62)
Cl(7)	0.0576(65)	0.1023(75)	0.1057(87)	0.0198(72)	0.0041(60)	0.0279(61)
Cl(8)	0.0845(73)	0.1044(73)	0.0512(66)	0.0001(59)	-0.0193(59)	-0.0032(62)
Cl(9)	0.0855(72)	0.0734(64)	0.0888(81)	0.0256(62)	-0.0065(64)	-0.0169(58)

Appendix 4.2 Final Fractional Coordinates and Isotropic Temperature Factors (Å x 10^4) for $[Et_4N][(dppe)Pt(SnCl_3)_3]$

Atom	x/a	y/b	z/c	U(iso) or U(equiv)
Pt(1)	0.1151(7)	0.6816(6)	0.3676(4)	360
Sn(1)	0.0808(1)	0.7963(1)	0.4063(7)	515
Sn(2)	-0.0212(1)	0.6136(1)	0.3894(6)	459
Sn(3)	0.0746(2)	0.7595(1)	0.3109(7)	516
P(1)	0.2207(5)	0.6496(4)	0.4067(2)	377
P(2)	0.1655(5)	0.5888(4)	0.3313(2)	377
Cl(1)	0.1390(7)	0.9080(5)	0.3898(3)	893
Cl(2)	-0.0543(7)	0.8380(6)	0.4088(4)	1059
Cl(3)	0.1103(8)	0.8040(5)	0.4681(3)	930
Cl(4)	-0.0875(6)	0.6522(5)	0.4436(3)	753
Cl(5)	-0.0008(5)	0.4891(4)	0.4056(3)	710
Cl(6)	-0.1457(6)	0.5948(6)	0.3568(2)	762
Cl(7)	-0.0527(5)	0.8174(5)	0.3094(3)	804
Cl(8)	0.0595(6)	0.7094(5)	0.2527(3)	744
Cl(9)	0.1591(6)	0.8587(5)	0.2938(3)	782
Cl(10)	-0.0484(9)	0.5708(7)	0.1888(4)	1506(51)
Cl(11)	0.1141(11)	0.5194(9)	0.1723(5)	2069(70)
Cl(12)	0.0090(20)	0.1093(17)	0.4371(9)	1911(125)
Cl(13)	-0.1396(28)	0.1047(23)	0.4373(13)	1129(155)
Cl(14)	-0.0964(36)	0.1009(31)	0.4721(18)	1732(238)
C(1)	0.2902(16)	0.5939(15)	0.3806(7)	380(85)
C(2)	0.2397(16)	0.5401(14)	0.3584(8)	384(87)
C(3)	0.1938(20)	0.5919(18)	0.4453(9)	590(103)
C(4)	0.2359(22)	0.5288(20)	0.4561(10)	834(126)
C(5)	0.2064(23)	0.4856(19)	0.4848(11)	816(119)
C(6)	0.1421(21)	0.5104(18)	0.5022(9)	619(104)
C(7)	0.1005(22)	0.5666(20)	0.4967(11)	893(104)
C(8)	0.1279(21)	0.6077(17)	0.4649(9)	631(99)
C(9)	0.2845(19)	0.7179(17)	0.4238(9)	561(101)
C(10)	0.3238(23)	0.7115(20)	0.4603(11)	866(131)
C(11)	0.3812(27)	0.7675(22)	0.4683(11)	1032(136)
C(12)	0.3976(23)	0.8256(23)	0.4497(11)	0128(136)
C(13)	0.3744(23)	0.8283(19)	0.4126(10)	846(114)
C(14)	0.3111(23)	0.7735(19)	0.4039(10)	796(123)
C(15)	0.0944(15)	0.5196(13)	0.3142(7)	221(75)
C(16)	0.0210(19)	0.5365(16)	0.2966(8)	547(98)
C(17)	-0.0266(19)	0.4829(18)	0.2825(9)	619(102)
C(18)	-0.0030(21)	0.4150(19)	0.2838(9)	713(111)
C(19)	0.0662(22)	0.3924(17)	0.3006(9)	698(108)
C(20)	0.1196(21)	0.4477(18)	0.3132(9)	732(108)
C(21)	0.2255(15)	0.6197(14)	0.2931(7)	286(81)
C(22)	0.2324(19)	0.5752(16)	0.2604(9)	547(100)
C(23)	0.2783(22)	0.5994(20)	0.2308(10)	760(113)
C(24)	0.3206(24)	0.6592(21)	0.2333(11)	915(136)
C(25)	0.3193(24)	0.7024(21)	0.2630(12)	947(139)
C(26)	0.2726(18)	0.6801(17)	0.2906(8)	503(90)
C(27)	0.0085(37)	0.4986(30)	0.1822(15)	1887(243)
C(28)	-0.3144(34)	0.8930(33)	0.3940(15)	1685(214)
C(29)	-0.2528(36)	0.9366(28)	0.4109(15)	1696(216)
C(30)	-0.3954(40)	0.7835(36)	0.3726(18)	2046(261)
C(31)	-0.3981(37)	0.7204(34)	0.3515(16)	1967(264)
C(32)	-0.2799(36)	0.7567(30)	0.4085(19)	1749(241)
C(33)	-0.3219(43)	0.7567(30)	0.4085(19)	2225(283)
C(34)	-0.2535(35)	0.8109(30)	0.3477(17)	1750(220)
C(35)	-0.2754(38)	0.8576(32)	0.3137(18)	2078(262)
N(1)	-0.3111(23)	0.8087(21)	0.3802(10)	1153(122)

Appendix 4.3 Short Intermolecular Contacts (Less Than 3.6Å)

Anion-anion					
Cl(1)-C(2)	3.34	(i)	Cl(4)-C(11)	3.60	(ii)
Cl(6)-C(23)	3.46	(iii)	Cl(6)-C(24)	3.56	(iii)
Anion-cation					
Cl(7)-C(34)	3.58	(iv)	Cl(5)-C(28)	3.53	(vii)
Anion-solvent					
Cl(12)-C(10)	3.60	(v)	Cl(14)-C(5)	3.60	(vi)
Cl(7)-C(27)	3.41	(vii)			
Cation-solvent					
Cl(13)-C(29)	2.91	(vii)			

(i)	1/2-x, y+1/2, z
(ii)	x-3/2, 1/2-y, 1-z
(iii)	x-3/2, y, -z-1/2
(iv)	-x-1/2, y+1/2, z
(v)	x-1, y, z
(vi)	-x, 1-y, 1-z
(vii)	x, y, z

Appendix 5

Atomic Parameters for 3-Nitro-4,6-bis(phenylthio)chlorobenzene

Appendix 5.1 Final Anisotropic Thermal Parameters ($Å^2$) for 3-Nitro-4,6-bis(phenylthio)chlorobenzene

Atom	U(11)	U(22)	U(33)	U(23)	U(13)	U(12)
S(1)	0.0366(7)	0.0479(8)	0.0515(8)	0.0058(6)	0.0135(6)	0.0025(6)
S(2)	0.0489(8)	0.0558(9)	0.0581(9)	0.0160(7)	0.0147(7)	0.0108(6)
Cl(1)	0.096(1)	0.0595(9)	0.092(1)	0.0024(8)	0.046(1)	0.0065(8)
N(1)	0.035(3)	0.057(3)	0.043(3)	-0.001(2)	0.016(2)	-0.003(2)
O(1)	0.055(2)	0.084(3)	0.066(2)	-0.020(2)	0.002(2)	-0.007(2)
O(2)	0.040(2)	0.070(3)	0.066(3)	0.013(2)	0.007(2)	0.005(2)
C(1)	0.051(3)	0.042(3)	0.051(3)	0.003(3)	0.031(3)	0.004(3)
C(2)	0.040(3)	0.039(3)	0.044(3)	0.006(2)	0.023(3)	0.004(2)
C(3)	0.032(3)	0.046(3)	0.043(3)	0.001(2)	0.017(2)	-0.002(2)
C(4)	0.030(3)	0.043(3)	0.038(3)	0.004(2)	0.019(2)	0.002(2)
C(5)	0.031(3)	0.052(3)	0.034(3)	0.005(2)	0.016(2)	0.000(2)
C(6)	0.037(3)	0.052(4)	0.043(3)	-0.006(2)	0.020(3)	-0.006(2)
C(11)	0.037(3)	0.038(3)	0.049(3)	0.001(2)	0.019(3)	-0.004(2)
C(12)	0.048(3)	0.055(3)	0.052(3)	-0.004(3)	0.028(3)	-0.000(3)
C(13)	0.046(3)	0.063(3)	0.063(4)	-0.007(3)	0.029(3)	-0.013(3)
C(14)	0.058(4)	0.081(4)	0.057(4)	-0.016(3)	0.022(3)	-0.019(3)
C(15)	0.081(4)	0.105(5)	0.061(4)	-0.025(4)	0.045(4)	-0.026(4)
C(16)	0.064(4)	0.084(4)	0.068(4)	-0.006(3)	0.046(3)	-0.015(3)
C(21)	0.035(3)	0.060(3)	0.038(3)	0.020(2)	0.012(2)	0.007(2)
C(22)	0.048(3)	0.080(4)	0.064(4)	0.016(3)	0.030(3)	0.008(3)
C(23)	0.045(3)	0.101(5)	0.076(4)	0.021(4)	0.027(3)	-0.010(3)
C(24)	0.062(4)	0.091(5)	0.049(3)	0.004(3)	0.018(3)	-0.025(3)
C(25)	0.078(4)	0.091(4)	0.050(3)	0.001(3)	0.035(3)	-0.011(4)
C(26)	0.047(3)	0.086(4)	0.054(3)	0.013(3)	0.027(3)	-0.009(3)

Appendix 5.2 Final Fractional Coordinates and Temperature Factors (Å x 10^4) for 3-Nitro-4,6-bis(phenylthio)chlorobenzene

Atom	x/a	y/b	z/c	U(equiv)
S(1)	0.46806(6)	0.1862(1)	0.33100(8)	504
S(2)	0.65056(7)	-0.2399(1)	0.52484(9)	595
Cl(1)	0.53240(9)	-0.4214(1)	0.3725(1)	858
N(1)	0.3639(2)	-0.0332(5)	0.1936(3)	488
O(1)	0.3220(2)	-0.1173(4)	0.1408(3)	763
O(2)	0.3502(2)	0.0818(4)	0.1826(2)	654
C(1)	0.5146(3)	-0.2573(5)	0.3618(3)	479
C(2)	0.5680(2)	-0.1693(4)	0.4303(3)	420
C(3)	0.5523(2)	-0.0371(5)	0.4186(3)	434
C(4)	0.4862(2)	0.0158(4)	0.3433(3)	376
C(5)	0.4355(2)	-0.0762(5)	0.2775(3)	403
C(6)	0.4494(2)	-0.2100(5)	0.2873(3)	460
C(11)	0.5486(2)	0.2533(4)	0.4318(3)	447
C(12)	0.6127(3)	0.2704(5)	0.4405(3)	532
C(13)	0.6727(3)	0.3330(5)	0.5159(4)	585
C(14)	0.6685(3)	0.3794(6)	0.5821(4)	687
C(15)	0.6055(4)	0.3637(6)	0.5723(4)	760
C(16)	0.5454(3)	0.2997(6)	0.4995(4)	658
C(21)	0.7029(2)	-0.1030(5)	0.5940(3)	454
C(22)	0.7641(3)	-0.0656(6)	0.6024(4)	639
C(23)	0.8089(3)	0.0343(7)	0.6619(5)	720
C(24)	0.7914(3)	0.0985(6)	0.7108(4)	696
C(25)	0.7293(4)	0.0640(6)	0.7008(4)	725
C(26)	0.6856(3)	-0.0375(6)	0.6437(4)	599

Appendix 6

Atomic Parameters for [4-NO_2-OC_6H_3O][S]P[C_6H_4-4-OMe]

Appendix 6.1 Final Anisotropic Thermal Parameters ($Å^2$) for [4-NO_2-OC_6H_3O][S]P[C_6H_4-4-OMe]

Atom	U(11)	U(22)	U(33)	U(23)	U(13)	U(12)
C(1)	0.0459(20)	0.0600(24)	0.0661(24)	-0.0042(20)	0.0035(17)	-0.0032(18)
C(2)	0.0555(22)	0.0719(28)	0.0732(28)	-0.0137(24)	0.0075(20)	0.0055(20)
C(3)	0.0600(25)	0.0692(29)	0.0837(30)	-0.0049(25)	0.0032(22)	0.0130(21)
C(4)	0.0613(24)	0.0568(25)	0.0698(27)	-0.0004(22)	-0.0046(21)	-0.0020(20)
C(5)	0.0524(21)	0.0697(27)	0.0637(25)	0.0001(21)	0.0070(18)	0.0034(20)
C(6)	0.0484(21)	0.0671(26)	0.0740(27)	-0.0037(22)	0.0048(19)	0.0033(19)
C(7)	0.0499(21)	0.0669(27)	0.0666(25)	0.0127(22)	0.0013(18)	0.0033(19)
C(8)	0.0513(22)	0.0736(29)	0.0794(29)	0.0163(24)	0.0003(20)	0.0033(20)
C(9)	0.0481(22)	0.0987(36)	0.0706(28)	0.0265(28)	0.0092(20)	0.0072(24)
C(10)	0.0707(28)	0.1018(39)	0.0697(30)	0.0055(28)	0.0015(23)	0.0085(27)
C(11)	0.0653(26)	0.0856(33)	0.0687(28)	0.0007(25)	-0.0026(21)	0.0011(24)
C(12)	0.0526(22)	0.0721(29)	0.0623(25)	0.0062(22)	0.0001(19)	0.0008(20)
C(13)	0.1071(37)	0.0951(39)	0.0965(35)	0.0319(32)	0.0201(30)	0.0091(32)
N(1)	0.0574(25)	0.1387(46)	0.1022(35)	0.0261(34)	0.0035(24)	-0.0049(27)
O(1)	0.0852(21)	0.0876(23)	0.0867(22)	0.0187(19)	0.0095(17)	0.0207(18)
O(2)	0.0581(16)	0.0726(19)	0.0777(19)	-0.0054(16)	0.0075(14)	-0.0147(14)
O(3)	0.0592(16)	0.0829(20)	0.0695(18)	-0.0129(16)	0.0110(13)	-0.0146(15)
O(4)	0.0745(24)	0.1338(36)	0.1398(36)	0.0395(30)	0.0263(23)	-0.0009(24)
O(5)	0.0974(28)	0.2321(54)	0.0809(26)	-0.0140(33)	0.0296(21)	-0.0186(32)
P(1)	0.0501(5)	0.0685(7)	0.0667(6)	-0.0019(6)	0.0051(4)	-0.0050(5)
S(1)	0.0631(6)	0.0889(9)	0.0907(8)	0.0150(7)	0.0092(6)	0.0137(6)

Appendix 6.2 Final Fractional Coordinates and Isotropic Temperature Factors (Å x 10^4) for [4-NO_2-OC_6H_3O][S]P[C_6H_4-4-OMe]

Atom	x/a	y/b	z/c	U(iso) or U(equiv)
C(1)	0.6826(3)	0.0822(4)	0.5349(3)	566
C(2)	0.7792(3)	-0.0112(5)	0.5404(3)	651
C(3)	0.8037(4)	-0.0941(5)	0.6251(3)	693
C(4)	0.7345(3)	-0.0860(4)	0.7056(3)	624
C(5)	0.6393(3)	0.0048(4)	0.7012(3)	613
C(6)	0.6149(3)	0.0878(4)	0.6154(3)	620
C(7)	0.8051(3)	0.2160(4)	0.3090(3)	599
C(8)	0.8948(3)	0.2706(5)	0.2594(3)	659
C(9)	0.9129(3)	0.2010(6)	0.1689(3)	665
C(10)	0.8499(4)	0.0859(6)	0.1302(3)	792
C(11)	0.7592(4)	0.0343(5)	0.1816(3)	728
C(12)	0.7381(3)	0.1032(5)	0.2713(3)	618
C(13)	0.6945(4)	-0.1742(6)	0.8681(4)	945
N(1)	1.0002(4)	0.2599(6)	0.1055(4)	918
O(1)	0.7664(3)	-0.1715(4)	0.7860(2)	835
O(2)	0.7691(2)	0.2672(3)	0.3998(2)	675
O(3)	0.6500(2)	0.0698(3)	0.3308(2)	679
O(4)	1.0448(3)	0.3761(5)	0.1348(3)	1060
O(5)	1.0251(3)	0.1944(6)	0.0301(3)	1171
P(1)	0.6488(8)	0.1857(1)	0.4249(8)	610
S(1)	0.5168(9)	0.3077(1)	0.4256(9)	781
H(2)	0.8282(3)	-0.0168(5)	0.4844(3)	963(47)
H(3)	0.8699(4)	-0.1588(5)	0.6287(3)	963(47)
H(5)	0.5905(3)	0.0110(4)	0.7573(3)	963(47)
H(6)	0.5481(3)	0.1517(4)	0.6120(3)	963(47)
H(8)	0.9420(3)	0.3513(5)	0.2852(3)	963(47)
H(10)	0.8689(4)	0.0411(6)	0.0674(3)	963(47)
H(11)	0.7121(4)	-0.0467(5)	0.1561(3)	963(47)
H(131)	0.7275(4)	-0.2395(6)	0.9200(4)	963(47)
H(132)	0.6896(4)	-0.0778(6)	0.8961(4)	963(47)
H(133)	0.6174(4)	-0.2072(6)	0.8443(4)	963(47)

Appendix 7

Atomic Parameters for $[(O\text{-}4\text{-}NO_2\text{-}C_6H_3O)_3Sn][NHEt_3]_2$

Appendix 7.1 Final Anisotropic Thermal Parameters ($Å^2$) for $[(O\text{-}4\text{-}NO_2\text{-}C_6H_3O)_3Sn][NHEt_3]_2$

Atom	U(11)	U(22)	U(33)	U(23)	U(13)	U(12)
Sn(1)	0.0608(8)	0.0638(9)	0.0601(9)	-0.0000(10)	0.0044(10)	0.0005(11)
O(1)	0.0503(96)	0.0932(116)	0.0877(118)	-0.0079(89)	0.0287(80)	-0.0196(86)
O(2)	0.0687(90)	0.0852(106)	0.0584(75)	0.0268(77)	-0.0049(75)	-0.0070(91)
O(3)	0.0820(102)	0.0485(99)	0.0822(115)	-0.0147(79)	-0.0141(86)	-0.0004(79)
O(4)	0.0615(82)	0.0619(88)	0.0768(102)	0.0272(75)	-0.0221(88)	0.0011(86)
O(5)	0.0898(110)	0.0571(109)	0.0809(106)	-0.0114(79)	0.0041(84)	-0.0031(79)
O(6)	0.0614(105)	0.0674(101)	0.1108(125)	0.0032(86)	0.0263(86)	-0.0052(88)

Appendix 7.2 Final Fractional Coordinates and Isotropic Temperature Factors (Å x 10^4) for $[(O\text{-}4\text{-}NO_2\text{-}C_6H_3O)_3Sn][NHEt_3]_2$

Atom	x/a	y/b	z/c	U(iso) or U(equiv)
Sn(1)	0.0904(1)	0.6376(8)	0.3879(5)	614
O(1)	0.1548(10)	0.5846(8)	0.4421(5)	674
O(2)	0.2347(9)	0.6485(8)	0.3674(4)	661
O(3)	0.0441(10)	0.7073(7)	0.3345(5)	669
O(4)	0.0882(10)	0.73347)	0.4291(5)	599
O(5)	-0.0467(11)	0.6085(7)	0.4150(5)	738
O(6)	0.0711(10)	0.5462(7)	0.3472(6)	741
O(7)	0.6106(12)	0.5829(9)	0.4622(6)	903(50)
O(8)	0.5908(14)	0.6612(9)	0.4063(6)	1090(57)
O(9)	-0.0635(15)	0.9466(11)	0.2741(8)	1340(71)
O(10)	-0.0519(14)	1.0219(13)	0.3345(8)	1382(71)
O(11)	-0.1124(17)	0.3306(12)	0.2948(8)	1542(83)
O(12)	-0.2584(19)	0.3380(13)	0.3294(8)	1597(82)
N(1)	0.5565(14)	0.6137(10)	0.4356(7)	795(63)
N(2)	-0.0396(17)	0.9618(14)	0.3157(9)	1181(78)
N(3)	-0.1750(20)	0.3619(15)	0.3189(9)	1258(80)
N(4)	0.2906(15)	0.6431(12)	0.2718(7)	986(62)
N(5)	-0.1165(13)	0.6617(9)	0.5034(6)	752(55)
C(1)	0.2529(17)	0.5905(11)	0.4423(7)	586(59)
C(2)	0.3134(15)	0.5658(11)	0.4774(8)	626(59)
C(3)	0.4118(17)	0.5738(10)	0.4751(7)	660(57)
C(4)	0.4529(1)	0.6058(11)	0.4361(7)	574(59)
C(5)	0.3955(12)	0.6318(10)	0.3995(6)	499(49)
C(6)	0.2959(13)	0.6239(10)	0.4012(6)	463(53)
C(7)	0.0585(13)	0.7850(11)	0.4011(7)	519(59)
C(8)	0.0505(14)	0.8572(12)	0.4179(8)	746(63)
C(9)	0.0159(15)	0.9133(13)	0.3932(8)	802(67)
C(10)	-0.0082(15)	0.9010(12)	0.3464(8)	664(62)
C(11)	0.0054(16)	0.8343(12)	0.3237(8)	722(69)
C(12)	0.0388(15)	0.7734(12)	0.3518(8)	617(62)
C(13)	-0.0764(15)	0.5503(11)	0.3933(8)	642(57)
C(14)	-0.1701(17)	0.5194(13)	0.4003(8)	809(71)
C(15)	-0.2014(18)	0.4570(13)	0.3765(8)	860(75)
C(16)	-0.1379(17)	0.4286(13)	0.3443(8)	760(70)
C(17)	-0.0487(15)	0.4533(12)	0.3348(8)	653(62)
C(18)	-0.0140(17)	0.5176(12)	0.3565(7)	656(63)
C(19)	0.2071(21)	0.6528(16)	0.2433(9)	1178(96)
C(20)	0.2230(26)	0.6502(18)	0.1904(9)	1752(143)
C(21)	0.3686(22)	0.7088(15)	0.2679(12)	1365(118)
C(22)	0.3250(30)	0.7796(24)	0.2881(15)	1923(170)
C(23)	0.3427(30)	0.5753(19)	0.2641(15)	1936(168)
C(24)	0.2865(23)	0.5063(18)	0.2802(12)	1350(112)
C(25)	-0.1971(24)	0.7148(18)	0.4889(12)	1565(135)
C(26)	-0.1896(21)	0.7526(16)	0.4455(11)	1165(97)
C(27)	-0.0404(21)	0.6978(17)	0.5290(11)	1333(109)
C(28)	0.0408(23)	0.6565(18)	0.5411(11)	1665(138)
C(29)	-0.1605(22)	0.6065(16)	0.5328(10)	1292(107)
C(30)	-0.1940(20)	0.6154(15)	0.5832(9)	1288(104)
H(21)	0.2820(15)	0.5422(11)	0.5057(8)	600
H(31)	0.4558(17)	0.5555(10)	0.5010(7)	600
H(51)	0.4281(12)	0.6569(10)	0.3721(6)	600
H(81)	0.0694(14)	0.8660(12)	0.4519(8)	600
H(91)	0.0105(15)	0.9632(13)	0.4074(8)	600
H(111)	-0.0065(16)	0.8290(12)	0.2887(8)	600
H(141)	-0.2146(17)	0.5441(13)	0.4236(8)	600

H(151)	-0.2668(18)	0.4341(13)	0.3823(8)	600
H(171)	-0.0059(15)	0.4266(12)	0.3116(8)	600
H(191)	0.1801(21)	0.7018(16)	0.2519(9)	600
H(192)	0.1582(21)	0.6141(16)	0.2514(9)	600
H(201)	0.1937(26)	0.6155(18)	0.1871(9)	500
H(202)	0.1967(26)	0.6927(18)	0.1720(9)	600
H(203)	0.2944(26)	0.6443(18)	0.1835(9)	600
H(211)	0.4277(22)	0.6957(15)	0.2872(12)	600
H(212)	0.3883(22)	0.7173(15)	0.2340(12)	600
H(231)	0.4015(30)	0.5782(19)	0.2853(15)	600
H(232)	0.3643(30)	0.5707(19)	0.2302(15)	600
H(251)	-0.2007(24)	0.7537(18)	0.5139(12)	600
H(252)	-0.2602(24)	0.6871(18)	0.4881(12)	600
H(271)	-0.0664(21)	0.7190(17)	0.5594(11)	600
H(272)	-0.0145(21)	0.7380(17)	0.5083(11)	600
H(281)	0.0286(23)	0.6026(18)	0.5389(11)	500
H(282)	0.0627(23)	0.6662(18)	0.5746(11)	600
H(283)	0.0956(23)	0.6675(18)	0.5186(11)	600
H(291)	-0.1106(22)	0.5666(16)	0.5350(10)	600
H(292)	-0.2181(22)	0.5889(16)	0.5141(10)	600
H(301)	-0.1696(20)	0.6563(15)	0.5890(9)	500
H(302)	-0.2671(20)	0.6176(15)	0.5845(9)	600
H(303)	-0.1698(20)	0.5780(15)	0.6064(9)	600

Appendix 7.3 Short Intermolecular Contacts (Less Than 3.6Å)

Cation-anion

O(1)-C(28)	3.44	(i)	O(1)-C(29)	3.57	(ii)
O(2)-C(19)	3.50	(i)	O(2)-C(21)	3.51	(i)
O(2)-C(22)	3.49	(i)	O(2)-C(23)	3.51	(i)
O(2)-N(4)	2.79	(i)	O(3)-C(19)	3.53	(i)
O(4)-C(27)	3.37	(i)	O(4)-C(28)	3.50	(i)
O(5)-C(25)	3.51	(i)	O(5)-C(26)	3.39	(i)
O(5)-C(27)	3.59	(i)	O(5)-N(5)	2.83	(i)
O(6)-C(24)	3.57	(i)	O(8)-C(20)	3.38	(v)
O(9)-C(24)	3.58	(vii)	O(10)-C(20)	3.38	(vii)
O(12)-C(20)	3.52	(x)	O(12)-C(22)	3.58	(x)
C(8)-C(30)	3.53	(xi)			

Anion-anion

O(9)-O(12)	3.50	(vi)	O(7)-C(2)	3.37	(iii)
O(7)-C(3)	3.38	(iii)	O(8)-O(10)	3.29	(iv)
O(9)-C(17)	3.42	(vii)	O(10)-N(1)	3.33	(viii)
O(10)-C(4)	3.51	(viii)	O(10)-C(5)	3.45	(viii)
O(12)-N(2)	3.59	(ix)	O(12)-C(10)	3.42	(ix)
O(12)-C(11)	3.38	(ix)			

(i)	x, y, z
(ii)	-x, 1-y, 1-z
(iii)	1-x, 1-y, 1-z
(iv)	1/2-x, y-1/2, z
(v)	1/2+x, y, 1/2-z
(vi)	-1/2-x, y+1/2, z
(vii)	-x, y+1/2, z
(viii)	1/2-x, 1/2+y, z
(ix)	-1/2-x, y-1/2, z
(x)	-x, y-1/2, 1/2-z
(xi)	1/2+x, 3/2-y, 1-z